Selection of Aptamers for Human Serum Albumin and its Glycated Form

Daniel Malcolm Wilkinson

A thesis submitted in partial fulfilment of the requirement for the degree of Doctor of Philosophy
Chemistry, Imperial College London

Declaration of Originality

I declare that the work within this thesis is my own unless otherwise stated. All work that is not my own has been appropriately referenced.

Copyright Declaration

Acknowledgments

It's been a long journey, one which would have been a lot more stressful, less insightful, less interesting without the people around me. I would first and foremost like to thank my supervisor Tony Cass who has supported throughout this PhD, thank you for offering me this opportunity Tony and thank you for providing your invaluable knowledge which has aided me throughout. I'd also like to thank my secondary supervisor Sylvain Ladame who's advice was always available.

I'd like to thank everyone over the year's who has been part of Tony's research group who have assisted me both academically and in life. Particularly I'd like to thank Thao Le, Christopher Johnson and Sanjiv Sharma for their help throughout and who's experience and knowledge was always welcome. I'd like to thank Antony Smith and everyone else at Lifescan Scotland who on my visits to and interactions with, were always friendly and welcoming. The knowledge gained on my trips to Lifescan Scotland was insightful and enabled me to look beyond my lab work and see how thoughts and processes about patient use were vital in even the early stages of research. Thank you to Lifescan Scotland and the EPSRC who funded this PhD.

This PhD would have not has been as enjoyable or fulfilling without an array of people. Thank you Ben M and Kerry for being wonderful friends and who made every day in the Lab a joy. Thank you everyone in the CDT, who we spent numerous nights, conferences and training days away together, many of them I won't easily forget. Thank you in particular to Ben T and Markus who made life at Imperial that much more enjoyable.

Thank you to my parents, grandma's and brother who have always assisted me in any way I've ever needed. Mum and dad your support through my childhood and into early adult life has made me believe anything is achievable. Thank you Grandmas, your love and support over the years has always been vital. Ryan thank you for being a awesome brother and always reminding me of the important things in life.

Finally I'd like to thank Beckie, my soon to be Wife, who has helped me pull through the dark times when I was Ill and always motivated and inspired me to do better than I did the day before. Without your humour, love and care I can honestly say I wouldn't of been able to get where I am today. Thank you Beckie for everything .

Thank you all.

Abstract

Diabetes prevalence is increasing above and beyond what can be attributed to population growth as reduced physical activity and increased sugar in people's diets is leading to an epidemic that is pushing healthcare systems to breaking point. While therapeutic treatments remain limited for diabetes patients, measurement and management of their glycemic status can prove beneficial. Glucose and HbA1C are currently utilised to manage diabetes in the short and long term respectively. However, problems with the accuracy of the HbA1c in certain diabetes patients, particularly those with renal problems and/or anaemia make it not ideal in all situations. Additionally its half life of 2-3 months make it slow to respond to glycemic changes.

Measurement of human serum albumin may be beneficial in both filling the gap between glucose and HbA1c and being less susceptible to interferents. HSA has a half life of between 2-3 weeks and like haemoglobin is readily glycated. Any changes in glycated HSA will demonstrate changes in a patient's glycemic status over the preceding weeks instead of months like HbA1c. Additionally it has been demonstrated to be a better representation of glucose levels in certain patient groups.

The relative lack of GHSA testing in the clinic comes down to the cost, complexity and lack of specificity of current techniques. A simple test is needed which can determine the GHSA/HSA ratio of a patient more accurately then current techniques while at a cost that is viable for restrained healthcare budgets.

Within this thesis the selection and subsequent testing of aptamers to HSA and early stage glycated HSA (GHSA) is demonstrated.

Abbreviations

- ACV - Alternating Current Voltammetry
- AGE - Advanced Glycation End products
- BB- Binding Buffer
- CV - Cyclic Voltammetry
- DNA - Deoxyribonucleic acid
- DPV - Differential Pulse Voltammetry
- EIS - Electrochemical Impedance Spectroscopy
- ELONA - Enzyme Linked Oligonucleotide Assay
- fH_20 - 0.2µm filtered deionised water
- GHSA - early stage Glycated Human Serum Albumin
- HbA1C - Glycated Haemoglobin
- HSA - Human Serum Albumin
- NGS - Next Generation Sequencing
- PDGF - Platelet- Derived Growth Factor
- SELEX - Systematic Evolution of Ligands by Exponential enrichment
- ss - Single strand
- SWV - Square Wave Voltammetry

Contents

Figures

Chapter 1

Introduction

1 Introduction

The incidence of diabetes is continuing to increase despite the best efforts of governments, healthcare providers and charities. Recent figures (2014) by the World Health Organisation show that 422 million adults live with diabetes, an increase from 108 million in 1980 (1). Only some of this increase can be attributed to worldwide population growth which grew from approximately 4.5 billion in 1980 to approximately 7.2 billion in 2014, an increase of 60% . Whereas the prevalence of diabetes in this period rose 391%. When looking at the age standardised prevalence, we see it has almost doubled from 4.7% to 8.7% in the same time period.

With no known cure for either type 1 of type 2 diabetes on the immediate horizon, current medical efforts are being directed towards the management of the disease. With better control and understanding of a patient's diabetic levels, complications can be avoided. Currently there are two key markers that can be monitored to help patients manage their disease, glucose and glycated haemoglobin. The detection of glucose and glycated haemoglobin is used to both diagnose a patient with diabetes and aid in the management of the disease. Glucose with its biological half life of 90 minutes is a perfect indicator of a patient's diabetic status over the preceding few hours, while glycated haemoglobin with its half life of 3 months acts as a long term indicator of how a patient is managing their glucose over weeks and months. Glucose is currently monitored using a disposable cheap enzyme biosensor used by the patients themselves. Since its inception in 1962 glucose biosensors have risen to dominate the global biosensor market (2). Although far removed technologically from that first research by Clark and Lyons, the basic principle of a glucose specific enzyme immobilised in a membrane still holds true with modern devices. Glycated haemoglobin however, is not as conveniently detected and is often monitored by an array of lab based techniques, each with advantages and disadvantages (3).

Due to the difficulties and cost involved in monitoring glycated haemoglobin through lab based testing, it is done infrequently. A more portable and rapid detection system that can monitor a

patient's medium to long-term diabetic levels is needed. While monitoring glycated haemoglobin is useful, it is known to inaccurately reflect glycemic status in particular patient groups, notably chronic kidney and dialysis patients, additionally its half-life is long enough that any changes in a patient's diabetic levels appear slowly (3–6). Another protein that is readily glycated, less susceptible to misrepresentation (in certain patient groups) and has a half-life between glucose and glycated haemoglobin is needed. Human serum album fits this criteria, it has a half-life of 3 weeks, is the most abundant protein in blood plasma and is readily glycated. To monitor human serum albumin a sensing mechanism had to be determined. Aptamers (single stranded DNA) were considered perfect for this role, with the ability to select them against a range of targets, the low cost of producing them once they have been selected and the ease with which you can modify them with signal generating components. Aptamers were generated by SELEX, specific strands were selected by NGS before aptamers were tested with ELONA. Finally electrochemistry was utilised as a means to prototype an aptamer based sensor.

1.1 Diabetes

1.1.1 Overview

Diabetes is a chronic disease that occurs when the pancreas is no longer able to make insulin, or when the body cannot make good use of the insulin it produces. These two different types are commonly categorised as Type 1 or Type 2 respectively. A third type of diabetes that arises in pregnant woman is referred to as gestational diabetes, here the insulin is not as effective as it otherwise should be.

The cost of diabetes both for the NHS and healthcare providers around the world is ever increasing, this has been driven mainly by the increasing prevalence of diabetes. As of 2014, the number of people with diabetes within the UK has risen to 3.3 million (7), which is more than double the 1.4 million people with diabetes in 1996 (8). Diabetes within the financial year 2012/2013 (Most recent available) accounts for 9.3 % of the total cost of prescriptions and 4.3 % of total items within the

NHS (9). By 2025 an estimated 5 million people will have diabetes within the UK (7) and by 2035, an estimated 592 million people globally (10).

Patients with type 2 diabetes within the UK account for 90% of all diabetic cases and of all diabetic patients, men comprise 56%(7). While prevalence of Type 2 diabetes peaks in older populations, 80.9% of all diabetic patients within England and Wales and 82.8% of patients within Scotland (11,12) are between 40 and 79. An increase in prevalence of Type 2 diabetes is being observed in younger patients, the first reported cases were in 2000 amongst overweight girls between 9 and 16 (13). Large variances in prevalence based on ethnicity are also observed; Black and Asian ethnicities showing a higher prevalence of diabetes than white ethnic groups (14). The rising prevalence amongst all ages, ethnicities and genders shows no sign of slowing and the medical community needs to look at quicker and cheaper ways of studying the long term health of its diabetes patients.

While ethnicity and genes can affect the incidence of diabetes, the leading risk factor with Type 2 diabetes is obesity. Around 90% of patients diagnosed with type 2 diabetes are obese (15). Obesity is on the rise and is major risk factor for a range of diseases. Worldwide, the prevalence of obesity in men increased from 28.8% in 1980 to 36.9% in 2013, while woman saw an increase from 29.8 to 38.0% over the same period (16).

There are multiple risk factors that can affect the chance of a patient becoming diabetic and multiple complications created by a patient being diabetic. The most common complication of diabetes is cardiovascular disease, 52% of Type 2 diabetic patients die due to cardiovascular complications including myocardial infarction and stroke (17). High quality and cost effective long term monitoring of a patient's diabetes is needed to minimise or prevent these complications.

1.1.2 Glucose and Insulin

1.1.2.1 Introduction

Glucose is a small molecule (molecular formula $C_6H_{12}O_6$) that is a vital energy source for the body and plays several key roles. Maintaining a correct concentration in the body is vital as extremes of circulating glucose can be devastating. Glucose concentrations typically fall between 4 and 6 mmol/l when fasting and below 7.8 mmol/l 90 minutes after eating (18,19). Deviations from this may indicate diabetes; further tests, generally the testing of glycated haemoglobin levels can give more clarity, typically over 6.0% glycation indicates diabetes(20). Insulin is a 5.8 kD protein that plays a key role in glucose regulation, it controls the uptake of glucose into the cells. Diabetes affects this ability either preventing insulin production (Type 1) or making the body unable to utilise it correctly (Type 2).

1.1.2.2 Roles in the body

The body needs glucose to work, it can be obtained through a variety of food sources and can be generated in the body from a range of different sources. Guidelines by NICE recommend a daily intake of 10.9 MJ and 8.7 MJ for men and woman respectively, while muscles under maximum strain can vastly increase the energy needs of the body (21).

If glucose is not immediately utilised then it can be stored in a variety of ways, mainly it is deposited by the liver via a process known as glycogenesis. Here the liver combines glucose into the larger molecular weight glycogen molecules, which are stored in chains. When the body needs glucose from its reserves, the glycogen undergoes a process called Glycogenolysis that generates glucose which can easily be transported around the body. Glycogenolysis can also occur in skeletal muscular tissues but the glucose generated can only be used in the muscle tissues.

After all glycogen deposits are filled then the glucose is stored as fat by being converted into fatty acids and then triglycerides. Storage of glucose by formation of triglycerides is unlimited but the

generation of glucose from these deposits is not readily achieved. There are two know ways of generating glucose from triglycerides. One is Lipolysis that takes place in the adipose tissue, triglycerides are turned into fatty acids which the muscles then utilise as energy. A second means of generating glucose from triglyceride deposits is gluconeogenesis which again takes place in the adipose tissue and generates glycerol which is then transported to the liver where it can be used in the generation of glucose. Gluconeogenesis covers a range of reactions that result in the generation of glucose, one other being the conversion of amino acids into glucose via the liver. The kidneys are also able to generate small amount of glucose by gluconeogenesis but their most useful function is removing dangerously high levels of glucose from the body. Glucose concentrations above 10 mmol/l in the blood can't be absorbed and are excreted in the urine. Finally, glucose can be generated from lactate which is created under anaerobic conditions, the lactate once again is transported to the liver where glucose can be generated that is transported around the body (22).

While the liver, skeletal muscle and kidneys all help in the regulation of glucose levels within the body, the pancreas and specifically the pancreatic islets of Langerhans is where some of the most important glucose management systems are located. The pancreatic islets of Langerhans compose 1-2% of the total pancreas volume and are made up of five endocrine cell types. The two most important are the alpha and beta cells. The alpha cells produce glucagon that stimulates glucose mobilisation via glycogenolysis. While the beta cells produce insulin that inhibits glucagon secretion as well as stimulating the uptake of glucose within the body.

Insulin has a range of roles within the body that all result in the control of glucose levels. A key mechanism is to regulate the uptake of glucose into cells. Insulin receptors on the surface of cells respond upon the binding of insulin by a range of different mechanisms, one being the translocation of the glucose transporter protein family from the cytosol to the cell surface. Here the glucose transporter promotes the transportation of glucose into the cell where it is utilised.

1.1.2.3 Role in Diabetes

The ability of insulin to regulate glucose levels becomes severely diminished when a person has diabetes mellitus. Diabetes is a range of different diseases that can cause a variety of problems in the body. In type 1 diabetes the pancreas doesn't produce any insulin or produces mutated unusable insulin and as such the body can't respond to increasing glucose levels. One cause of no insulin production can be a viral infection that results in the destruction of the beta cells by an autoimmune response. Other problems in type 1 results from either mutations in the insulin hormone itself or mutations in the insulin creation pathway. In both these cases the only way to treat the patient is to provide insulin via injection.

In type 2 diabetes defects with insulin receptors on cells or with the intracellular pathways that are activated by insulin means the body cannot effectively utilise insulin. This degraded insulin efficiency means patients are most effectively treated by control of their glucose intake. Whether it's type 1 or type 2 the effect on the body can be devastating as glucose accumulates in the blood stream while cells become starved of nutrients, often referred to as 'starvation in the midst of plenty'. As the body believes it's starving it stimulates gluconeogenesis with glucose being generated from amino or fatty acids, this pumps even more glucose into the blood stream and the effect becomes amplified. As these amino and fatty acids are being utilised a diabetic patient can undergo weight loss as their body is desperately trying to provide the energy it believes isn't being provided.

Fat deposits begin to be utilised to generate glucose, triglycerides deposits are mobilised and transported to the liver where it responds by generating glucose but also ketones and ketoacids, these ketoacids lower the pH of the blood which can cause a life threatening situation referred tp as ketoacidosis.

Mentioned above are the immediate effects of complications caused by the inefficiency of either insulin use or its production but the long-term complications can be devastating. Whether it's

diabetic neuropathy (23), nephropathy (kidney disease) (24), hypertension (25) or cardiovascular disease (26) the need to monitor the long term effects of diabetes is vital.

Diabetes can have long lasting and devastating effect on the body, this manifests in many ways, one being the glycation of proteins; the non-enzymatic addition of glucose or a glucose intermediate to a primary or secondary amine groups on proteins like Human serum albumin.

1.1.2.4 How is Glucose measured?

Glucose can be measured in a variety of ways, commonly by utilising an enzyme to generate an electrochemical signal upon glucose binding. Although this basic principle remains unchanged in modern glucose sensors, the devices have evolved dramatically since their inception. Glucose sensors are some of the cheapest and most reliable sensors available, which combined with the growing incidence of diabetes, have allowed glucose sensors to dominate the global biosensor market. Clark and Lyons developed the first glucose biosensor in 1962 that utilised glucose oxidase to generate gluconic acid and hydrogen peroxide from glucose and oxygen, the consumption of oxygen was monitored by a reductive measurement at a platinum cathode (2). Since its inception, the electrochemical glucose sensor has gone through distinct changes often referred to as first, second and third generation. First generation sensors relied on enzymes that interacted with oxygen and glucose; this meant both could be a limiting factor where only glucose would preferably be These oxygen glucose reactions generated hydrogen peroxide; which was often measured with a platinum electrode around 0.6 V against a silver/silver chloride electrode, a key limitation of this technique was that the presence of O_2 or H_20_2 could generate a false positive. Another problem with these first generation devices was the voltage range they operated in. At 0.6 V a significant number of interferents like uric acid are also active, this interference problem was mitigated by a variety of approaches (27) but can only truly solved with a change in mediators that operate outside of the electro active window of said interferents which we saw with the birth of second-generation sensors.

The main disadvantage of first generation glucose biosensors was their reliance on oxygen as an electron acceptor. Second generation glucose sensors aimed to solve this. Synthetic mediators were developed that could transfer electrons from the flavin adenine dinucleotide within the glucose oxidase to the electrode. A range of mediators were developed that all provided improvements over the previous generation (28,29), ferrocene became one of the most popular, with it and its derivatives still utilised today (30). Mediated glucose sensors now dominate the commercial market and can be seen in the vast majority of single use strip based technology. Third generation sensors are relatively new, the technology has yet to settle and as such no known commercial sensors currently exist. Third generation sensors aim to remove the mediator and by utilising the correct electrode material promote electron transfer directly from the enzyme(28).

1.1.3 Human Serum Albumin (HSA)

Monitoring a patient's diabetes by the measurement of HbA1C and glucose does not always produce a clear picture of the disease. Along with haemoglobin an array of proteins are glycated within the body, one of the most abundant and easily glycated is human serum albumin. The regular measurement of both a patient's glycated HSA and non glycated HSA could generate information of a patient's midterm diabetic status that is difficult to obtain from Hba1C and glucose. HSA has a shorter half life (2-3 weeks) than HbA1C (3-4 months) (31–36) allowing for changes to be observed more rapidly; it is also seen as a more accurate reflection of glucose status in anaemia and/or patients with kidney disease and is believed to competitively inhibit glycation of less abundant proteins (31,37,38). Additionally it is abundant enough that any changes in glycated HSA concentrations will be representative of the whole body. Up to 20% but typically below 10% of HSA in the plasma of healthy humans is glycated while in diabetic patients this ratio is often around 30% but in extreme cases has been known to reach 94% (39–42).

Unmodified HSA is mainly synthesized in the liver and plays many vital roles within the body. Unmodified it has a molecular weight of 66.7 kDa. Its concentration in blood plasma ranges between

35 and 50 g/l making it the most abundant protein in the blood comprising around 50% of protein in healthy individuals (43). The protein consists of 585 amino acids and 17 disulphide bonds arranged in a single polypeptide chain. The structure consists of no β- sheets but about 67% is made of α-helices and according to the crystal structures it occupies a volume of about 500 nm^3 (32,44).

HSA's main physiological process is to regulate osmotic pressure, however it additionally performs many other physiological and pharmacological processes including regulating blood pH, transportation of solutes like hormones or drugs, mediating lipid metabolism, toxin removal and it works as both an anti-inflammatory and antioxidant (38,39,45). Drugs are known to bind to two main regions, referred to as Sudlow binding sites I and II. Named after the work of Sudlow et al who discovered the sites by monitoring the displacement of fluorescent probes by a range of drugs including Warfarin (46,47).

Both sites bind to an array of compounds, Sudlow I the larger site of the two has a more flexible structure and tends to bind larger molecules like bilbriubin and more generally hetereocyclic compounds or dicarboxylic acids; it is also referred to as the warafin - azapropazone site (38,43,44). Sudlow II is known to bind to aromatic compounds like ibuprofen and indole-containing compounds like tryptophan(48). It is often referred to as the indole-benzodiazepine site(38,43,44).

Additionally HSA contains 35 cysteine residues that all except for Cys-34 form disulfide bridges . 70% to 80% of Cys-34 sites on HSA in healthy humans is reduced, it is an important free radical scavenger and is additionally known to bind an array of compounds (49,50).

1.1.4 Glycation

Glycation is a process by which sugars, particularly glucose, are added in a non-enzymatic process to primary or secondary amine groups. This can occur to a range of compounds including but not limited to proteins, hormones and enzymes.

On HSA glycation is possible across 59 lysine, 6 argine residues, Cys-34 and the N terminus of the polypetide chain. Glycation is a multistage process and can be broadly divided into early stage glycation and advanced stage glycation (AGE) (Figure 1). Early stage usually occurs within the first 2 weeks of a reaction, where AGE products are usually formed after 1-2 months (45,51). Of the array of sites, the majority of the glycation is believed to take place at Lys- 525 and is believed to account for 30% -50% of overall glycation(52,53). Other Lysine sites including Lys 199, 281 and 489 are also believed to be significant glycation sites and are believed to be involved so readily due the close proximity of basic amino acids (38,52,53). While comparatively less in number Arg-410 and Cys-34 also appear to be significant sites for glycation, particularly formation of AGE (54,55).

Early stage glycation involves the nucleophilic attack of glucose with amine group to form what is known as a Schiff base. This Schiff base is unstable and needs to undergo further rearrangement to form a stable ketoamine, commonly referred to as fructosamine. This fructosamine can then react with numerous other compounds to form over 30 advanced stage glycations (AGE) (Figure 1).

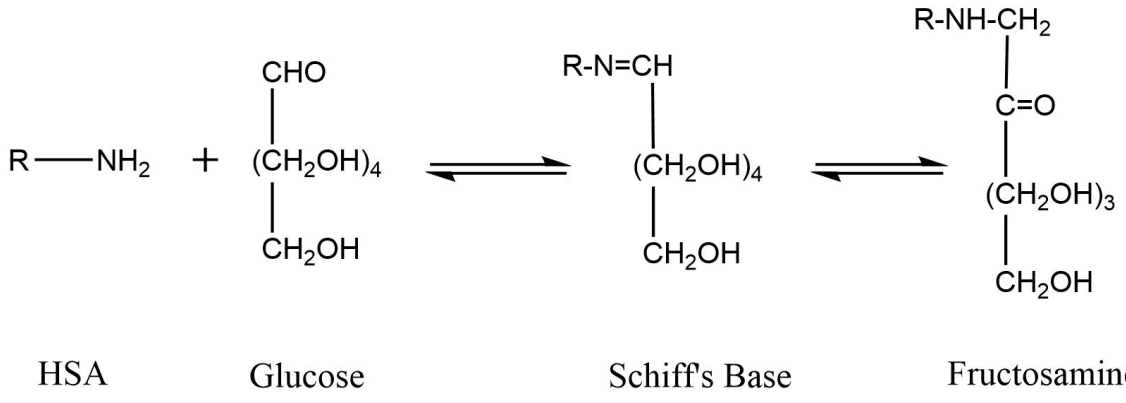

Figure 1 : The modification of HSA by the non enzymatic addition of glucose

As HSA has a half life of between two and three weeks, only a small minority of glycated HSA will be AGE glycated. As such the measurement of fructosamine modified HSA could prove more clinically relevant in measuring changes in medium term glycation. However, significant research has still

been directed towards AGE and the effect they have in the long term complications relating to diabetes (56–58).

1.1.5 The need for detection of glycated human serum albumin

The current diabetes measurement landscape is based around two main analytes, glucose and HbA1C. Short term glucose measurements make it difficult to determine long term trends (59). The Fremantle Diabetes study in 2007 demonstrated that in an observational trial with 1,280 patients, no survival benefit was identified from patients who performed self monitoring of their glucose. While other groups and papers have pointed to benefits of self monitoring of glucose, a 2005 review of six randomised controlled trials determined that self monitoring of glucose in type 2 patients led to a 0.39% reduction compared to control groups (60). Additionally a meta analysis in 2010 of 3,270 non insulin controlled type 2 diabetes patients in Canada concluded that self monitoring of blood glucose resulted in a modest but statistically significant reduction in HbA1c (61). While one paper highlights limitations with the education of patients in self monitoring of glucose as a defining factor rather than the technology itself (62). The majority of literature points towards the benefits of self monitoring of glucose, however the uncertainty over the exact benefit and the additional non conforming patients who do not self monitor make it difficult to determine overall benefits for a healthcare system.

What appears more clear is the benefit a reduction in HbA1c has on patient outcomes. 3642 patients were observed in 23 hospital based clinics across England, Scotland and Wales. It was observed that for each 1% reduction in mean HbA1c a 21% reduction in death (95% confidence interval; 15% to 27%, $P < 0.0001$) was observed along with substantial reductions in rates of myocardial infarction (14% reduction, 95%CI: 8% to 21%, $P<0.0001$)and micro vascular complications (37% reduction, 95%CI: 33% to 41%, $P<0.0001$) (63).

Recent research casts doubt on the effectiveness of HbA1c in certain patient groups including patients with chronic kidney disease, patients on haemodialysis and patients with anaemia;

measurement of glycated HSA in these patient groups was shown to more accurately reflect glycemic status.

A study of 25 diabetic patients on haemodialysis comparing glycated albumin, HbA1c and plasma glucose demonstrated that glycated albumin was a better measure to estimate glycemic control than HbA1c(37). Multiple larger studies demonstrated similar outcomes. One in 519 diabetic patients undergoing peritoneal (n=55) and haemodialysis (n=415, 49 patients were used as a control) demonstrated that HbA1c significantly underestimated glycemic control compared with glycated HSA (64).Two other studies with 258 and 538 diabetic patients undergoing haemodialysis also highlighted HbA1c underestimation of glycemic levels(34,65). The benefits of glycated HSA measurements in patient with renal disease can be related to shortened red cell survival times. The utilisation of erythropoietin injections in patients suffering anaemia related complications from chronic kidney disease will cause younger erythrocytes to enter circulation, ones that have yet to be glycated. This combined with lower red blood cell survival could create artificially low HbA1C levels (6,34). Glycated HSA on the other hand is believed to not correlate with erythropoietin dose, total HSA concentration (changes in total HSA concentration do not affect the glycated HSA/HSA ratio) or haemoglobin concentration (65).

1.1.6 Measurement of Glycated HSA and HbA1c

A range of techniques exist for measuring glycated human serum albumin, commonly affinity column, colorimetric, enzyme linked or immunoassay based. Boronate immunoassay utilises a column which includes a boronate like phenylboronic acid that interacts with the glucose moieties on a glycated protein. This separates glycated and non-glycated compound, after which their concentrations and/or structures can be analysed by optical or mass spectroscopy.

Colorimetric assays such as nitroblue tetrazolium (NBT) rely on a colour change which can be measured, in this case the ability of fructosamine to reduce NBT which can be measured as a change in absorbance at 530 nm (66). Immunoassays like ELISA, which utilise antibodies to capture the

desired target and linked enzyme that produces a colourmetric response have demonstrated their ability to detect glycated human serum albumin accurately (67).

Enzymatic detection of HSA and GHSA is a well developed technique, commonly utilised is Lucica GA-L test (Asahi Kasei Pharmaceutical Corporation, Japan) (68). Utilising a protease, the glycated human serum albumin is hydrolysed to glycated amino acids. These are then oxidised by ketoamine oxidase, this reaction produces hydrogen peroxide along with amino acids and glucosone. The hydrogen peroxide is coupled to a dye that generates a blue-purple pigment upon reaction, which is measured using a spectrophotometer. This technique has been demonstrated as one of the most effective current techniques and is not effected by high concentrations of bilirubin, triglycerides, glucose, ascorbic acid, hemoglobin and human serum γ gobulins (6,34,39,65,69–73). Separately HSA concentration is generally measured using the bromo-cresol blue method and the ratio of non glycated to glycated is compared.

1.2 Aptamers

1.2.1 Overview

Aptamers are single strands of DNA or RNA and can form an array of structural conformations that can allow them to bind to a range of targets. Two separate labs in 1990 created what we now know of and understand as aptamers(74,75). Tuerk and Gold coined the term SELEX (Systematic Evolution of Ligands by Exponential enrichment) and showed an RNA aptamer could be selected against T4 DNA Polymerase while Ellington and Szostak who coined the term aptamers presented RNA aptamers binding to a variety of organic dyes. Both these groups showed by utilising a vast random library of single stranded RNA and running these through cycles of selection, separation and amplification that they could generate specific strong binders to their chosen target. This repeat process of selection, separation and then amplification is referred to as SELEX and generation of both DNA and RNA aptamers has been regularly achieved (Figure 2).

Many variants of SELEX exist but typically it requires generating a library of single stranded DNA/RNA that has a random nucleotide sequence flanked by two defined regions. This random region is typically around 40 nucleotides in length but can be up to 100 and as low as 20. The defined regions flanking the random region tend to be shorter and are required in amplification of the strands via polymerase chain reaction. The library will contain vast numbers of aptamers and depending on length of the random region and concentration, each is often an individual sequence. Typically between 10^{13} and 10^{15} strands exist in a pool. Individual strands in a library can be calculated by taking the number of monomer units, in this case 4 nucleotides and performing an exponentiation where the exponent is the length of the random region, if we assume this is 40 then the maximum individual strands is about 10^{24}. However this is significantly more than the practically viable, if we consider the average weight of a DNA base pair is 650 g/mol, then a single base would be 325 g/mol. If we take an aptamer length of 40 we can assume that it's total weight would be 130000 g/mol. Number of copies can be calculated by:

*Number of copies (NC) = (ng*Avogadro's Number)/(Length * $1x10^9$*325)*

If we assume a weight of 100000ng (100ug)

*NC = (100000 * 6.022 $x10^{23}$)/(40 * $1x10^9$*325)*

NC= 4.63 $x10^{15}$

In this example case we have about 10^{15} individual strands, without utilising unrealistic amounts of aptamer it is not practically possible to hit the theoretical limit. As such any library only samples a small part of the entire variations possible. However, depending on conditions, further mutations are brought in when the aptamer library undergoes polymerase chain reactions in the amplification stage of SELEX. This can be both a positive, as it can introduce mutations that are beneficial but equally mutations could occur which have a negative effect on binding.

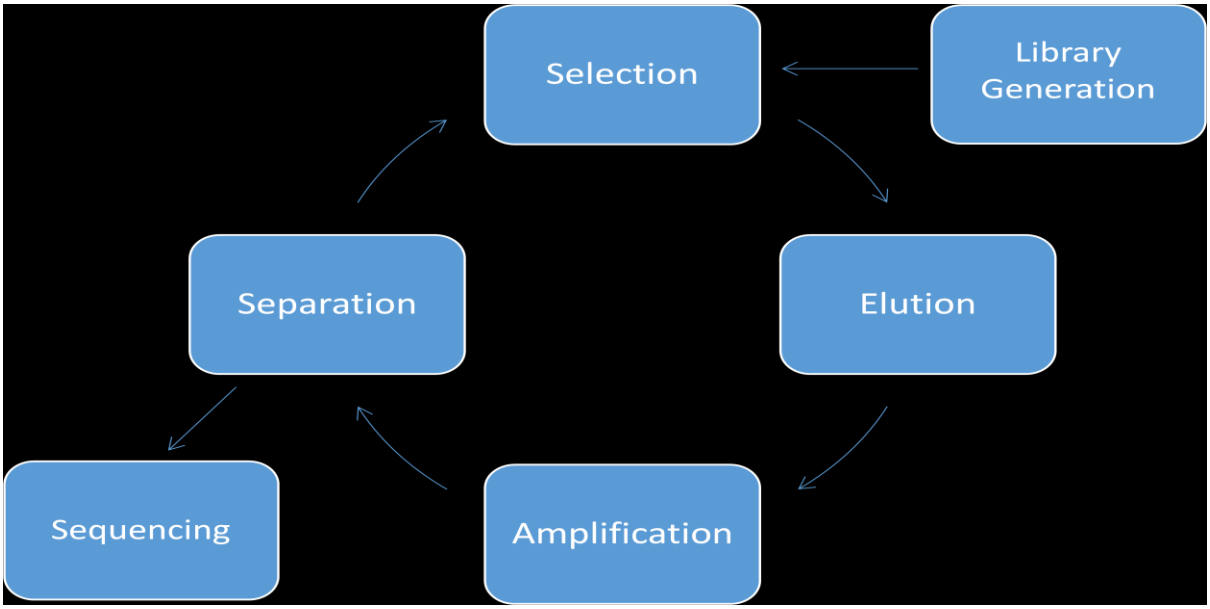

Figure 2 : Typical SELEX process

The random central region is flanked by two defined sequence regions, typically between 10 and 20 bases in length. These regions are utilised as primer attachment points. This allows the aptamers to be amplified and then later separated.

1.2.2 SELEX

One of the key drivers that allowed SELEX to take off is that the cost to not just sequence but also synthesise oligonucleotides has dropped dramatically over the years and can be seen as the main factor which has aided their use. The price per base for oligo synthesis is now in the cents(76).

Current synthesis techniques are often based on phosphoramidite monomers. Phosphoramidite monomers is in essence a standard nucleotide surrounded by an array or protection groups. These protection groups are there to prevent unwanted side reactions and to push the oligo synthesis in the desired direction.

Since the inception of SELEX as a technique, many different methods have been developed (77–80). While methods may vary the procedure is generally the same across all techniques. A simple overview of the workflow can be seen in Figure 2. Initially an aptamer library is generated. This

library is then selected against a target, the target can be immobilised, free in solution, in a simple or complex medium .

Medium conditions including salt, pH or temperature maybe taken into consideration. Next the aptamers which have bound need to be carefully eluted, making sure they are separated from any non binders. Commonly this is carried out with magnetic beads, affinity columns or membrane filters. Once the binding aptamers have been selected they need to be amplified, this is carried out through polymerase chain reaction (PCR). As this creates double stranded DNA, strands need to be separated with the forward strands being retained, an effective way is utilising magnetic bead tagged primers. Once amplified strands have been separated, they are then reselected against the target. The process then repeats, typically for between 8 and 15 rounds, with later rounds introducing higher stringency, so only the most effective binders remain in the final pool. Once the final pool has been achieved. They are sequenced, historically this was performed by cloning, a small number (30-50) of clone containing aptamers are sequenced. These are then compared and analysed. Recently Next Generation Sequencing has become more prevalent, instead of sequencing 30-50 aptamers, the entire library is sequenced. This produces millions of sequences and allows for a more in depth look at sequence distribution across the library. This allows for reduced selection rounds to be performed notably reducing PCR mutations and overall costs. The utilisation of NGS has been driven by cost, to sequence a genome in 2001 would have cost approximately $100m, where today it is around about £1k(81). With smaller libraries like those generated from SELEX costing half that.

Of the selection methods nitrocellulose membrane filtration is one of the most common, its ease and speed of use make it ideal in certain applications. Originally it was developed in 1968 by Pristoupil and Kramlova as a means to separate RNA from proteins(82). As the target proteins get caught in the membrane, any non binders will simply wash through.

Although easy to use, nitrocellulose membrane filtration has its limitations, it has been commonly utilised for RNA aptamers and will not work with small targets (77,83–85) Another commonly utilised technique is sepharose columns. The aptamers and target are allowed to bind in solution before the aptamer/protein complex is selectively absorbed into the matrix, any unbound aptamers will wash through (80).

A different approach is the utilisation of affinity surfaces, where the protein or target molecule is immobilised on a surface. This approach allows for smaller targets to be utilised, however, matching immobilisation chemistry is needed and similar to other techniques, one has to be aware of any potential binding to the affinity surface (85–87).

The choice of selection and elution technique is based on the target of choice. Human serum albumin has a thiol group at cys-34 that can be utilised to anchor the protein to a column. Unmodified HSA typically has a reduced free thiol in around 70% of the molecules and while GHSA will have less reduced thiol at cys-34, it should still retain significant free thiol (88).

1.3 Aptamer sensing systems

An advantage of aptamers over antibodies or enzymes is not just to do with their ability to be selected to a range of targets. The ability to easily modify them with an array of tags, whether fluorescent or electrochemical make them ideal in sensing systems. Herein we lay out the different approaches to developing an aptamer sensing system

1.4 Electrochemical sensor systems

Electrochemical aptamer sensors provide many advantages over other detection techniques, herein we outline the benefits of electrochemical techniques based on their sensing mechanism. We discuss how various electrochemical techniques, modifications and solution conditions affect the aptasensor performance. We will review sensors that involve measuring direct structural changes that subsequently allow for a change in current, capacitance or resistance between a redox probe

tagged aptamer strand and an electrode(89–91). Then we'll move onto aptamer tagged enzyme sensors (92,93) before finally discussing sensors that rely on dissociation of either aptamer strand or target (94–96). The five main electrochemical techniques utilized in the literature include cyclic voltammetry(CV), differential pulse voltammetry (DPV), square wave voltammetry (SWV), alternating current voltammetry (ACV), electrochemical impedance spectroscopy(EIS). A brief description of the techniques can be found at the end of this section

1.4.1 Direct measurement of aptamer binding involving covalently bound redox probes.

Aptamers are readily chemically modified by electrochemical labels(97,98). The ability to add a redox probe into a sensing structure allows for direct measurement of structural changes. Electrochemical aptasensors tend to fall into two distinct categories, 'signal on' and 'signal off'. 'Signal on' is the preferred method of binding for two key reasons. 'Signal off' can never achieve more than a 100% signal gain and 'signal off' mechanisms are more susceptible to false positives(99,100). All the sensors within this sub section employ a variation of the beacon structure, where one end of the aptamer is bound to an electrode and the other end is labelled with a redox tag. Binding of the aptamer and its target will promote a structural change that moves the redox marker, changing its accessibility to the electrode.

Xiao (90) compared a 'signal on' mechanism to a previous 'signal off' mechanism utilising the same thrombin binding DNA aptamer and the same redox probe (methylene blue) (99).The 'signal off' sensor consists of a 5' prime immobilised 32 base thrombin aptamer (extended 15 base aptamer with binding sequence at 3' end). The 'signal on' mechanism consists of the same 15 base aptamer (immobilised at 5' end) extended to 27 bases and part hybridised to another oligonucleotide with methylene blue (MB) at its 5' end ; upon thrombin binding the oligo partly separates from the thrombin aptamer and the MB strand physically approaches the electrode surface, producing an electronic signal. Both sensors were analysed using ACV with thrombin as a target and MB as the covalently bound redox label. Looking at signal gain across both a 53% improvement in signal from

the 7% of the 'signal off' to the 60% of the 'signal on' at 19nM is observed. Interestingly the 'signal off' mechanism shows a larger linear range. While the 'signal on' mechanism saturates around 100nM, the 'signal off' mechanism showed linearity up to the highest tested concentration of 768nM with the same aptamer. A possible reason for the decrease in thrombin aptamer range is potentially due to the new sensor configuration. The 'signal on' mechanism required a modified version of the well know 15-mer thrombin aptamer to partly dehybridise from a complimentary strand that contains the MB tag. This breaking of the strands is no doubt unfavourable and will decrease the affinity of the aptamer to its target; the increased signal gain observed is just a result of the 'signal on' mechanism.

Thrombin aptamer electrode surface concentrations for both sensors were different, with the 'signal off' sensor; electrodes were incubated with 0.1uM thrombin aptamer compared to 0.8uM in the 'signal on'. Based on work done by White (101) we know that an increase in aptamer surface concentration is not always beneficial to the sensor performance due to steric hindrance effects and individual aptamers have varying density sweet spots. Thus it is difficult to determine without further data what effect this would have on the two sensors.

The two most commonly used labels are ferrocene and methylene blue. Successful studies have been demonstrated with ferrocene tagged aptamer systems(102–104),however ferrocene shares a positive redox potential with many serum constituents such as ascorbic and uric acid. . Ferapontova (105)highlighted this and showed a significant decrease in theophylline ferrocene tagged RNA aptamer response in serum using CV, EIS and DPV. Aptamer systems utilizing MB which has a negative operating potential have shown good results in serum(106,107).

Lai (106) demonstrated the use of MB tagged DNA aptamer in the detection of PDGF aptamer using ACV and further noted the effect ionic concentrations and pH had on their system. PDGF has been show to be dependent on $Mg2^{+}$ and $Ca2^{+}$ concentrations(108) and it was noted that the PDGF aptamer produced higher background current in serum. This was attributed to a higher

concentration of these two divalent cations producing folding in the aptamer even when no target was present. The redox potential shifted more negatively in the slightly alkaline serum, MB's reduction is dependent on pH and thus the serum would have caused a shift. This paper highlights the problems that can be expected when aptamers which are selected in specific buffers are utilised in other conditions.

This is furthermore not just a case of choosing one redox probe over another, as MB has shown to be less sensitive when used with RNA aptamers (109). Choice of redox probe will fully depend on the aptamer and situation it is utilised in.

The packing and arrangement of aptamers is of particular importance to their performance when you are observing changes in redox tagged aptamer structures. White(101)compared the ACV performance of MB covalently bound DNA aptamers at different aptamer surface concentrations. A cocaine aptamer demonstrated Kd values ranging from 327 $\pm$ 64uM to 101 $\pm$ 8uM based on packing density alone, the lowest packing density of 1.6 x 10^{12} molecules/cm^2 produced the lowest Kd of 101 uM which compares favourably with the solution phase Kd of 100uM (110). Thrombin aptamer showed optimal performance at a higher probe density of around 7 x 10^{12} molecules/cm^2. Unfortunately Kd values for the thrombin aptamer were not given. And thus it cannot be readily compared to other thrombin systems.

1.4.2 Direct measurement of aptamer binding using solution diffusing redox systems based on electrostatic repulsion.

The alteration of surface charge via aptamer-target binding allows for modifications in the electrostatic interaction of redox tags with the aptamer conjugate. These changes can be monitored and utilised as a sensor.

Rodriguez (111) showed alterations in surface charge caused by binding of a target to a DNA aptamer could allow for diffusible redox probes to more readily access the electrode. The basic principle being the negatively charged aptamer backbone electrostatically repelled the redox probe,

in this case $[Fe(CN)_6]^{3-/4-}$. Binding of the target then causes a positive surface charge to dominate allowing a decrease in electron transfer resistance measured by Faradaic EIS. This is opposite to what is commonly seen by others(112–114) who see an increase in electron transfer resistance upon binding of the target. This is due to the target lysozyme having a relatively high pI of 11 (115) which at physiological pH, will cause it to be positively charged. The charge on the protein is often ignored and needs to be more carefully considered when studying target-aptamer interactions. Careful choice of the redox probe is also important as it needs to interact with the surface charges in the desired manner.

Arguments can be made that electrostatic aptamer systems are more susceptible to changes in solution conditions then other systems. Hianik (91) demonstrated with CV and DPV changes in pH above and below pH 7 for a DNA thrombin aptamer can drastically effect its sensitivity and dynamic range. While this is mostly attributed to changes in the thrombin aptamer structure, some of this effect will arise from changes in the amount of MB (the redox maker used) electrostatically bound at these varying pHs. Increase in NaCl concentration also demonstrated a significant degradation in the sensor performance as a result of increased ionic strength effecting electrostatic attraction and repulsion.

Cheng (116) utilize a CV based system for electrostatically bound aptamers. A significant decrease is observed in the Kd value of the electrode bound lysozyme aptamers (610 $\pm$ 46nM) compared to Kd values obtained from solution measurements (31nM) demonstrated by Cox(117). This decrease could arise from steric hindrances formed at the electrode surface, the use of the relatively insensitive CV or could be a result of the 'signal off' mechanism. Here we see further evidence that for any suitable discussion of electrochemical aptasensors and their sensitivity, the Kd values of the sensor in action need to obtained and studied.

Li (118)demonstrated a DNA EIS aptamer immobilized on gold nanoparticles who were in turn immobilized on glassy carbon. The blockage of $[Fe(CN)_6]^{3-/4-}$ was demonstrated. Kd values of

between 4.2nM and 15nM for two thrombin aptamers was observed. This is close to the value in solution for this thrombin aptamer (0.5nM) (119). Demonstrating the thiol modification to the thrombin aptamer that allows immobilization on the gold nanoparticle surface has minimal detrimental effect on binding.

1.4.3 Enzymatic tagging

The ease at which aptamers can be labelled has allowed the use of well characterized sensing structures to be utilised alongside aptamers. Enzyme biosensors have been utilised by electrochemists for many years with the glucose sensor being the most recognized (120). Mir (92) compared three DNA aptamer enzyme systems using DPV. Sensor 1 involved monitoring the aptamer bound thrombin enzymatic turnover, sensor 2 sandwich assay involving horseradish peroxidase (HRP) labelled secondary aptamer and finally sensor 3 a thrombin down HRP aptamer detection. Sensors 2 and 3 provided the best thrombin response, while sensor 1 showed a 60 fold detection speed increase over an ELONA method that was demonstrated. It was noted the use of all sensors in more complex serums solutions could prove problematic and push the sensor out of a clinically viable range. Similar results were demonstrated by Tan (93)and Deng (121)utilising glucose/glucose oxidase for signal amplification and Ikebukuro (122) utilising pyrroquinoline quinine glucose dehydrogenase ((PQQ)GDH). However, neither would be suited to serum analysis due to background glucose concentrations.

1.4.4 Configurational changes caused by binding

Configurational changes often revolve around ‘signal off’ mechanisms, commonly dissociation of a tagged hybridised strand or competition displacement of a tagged target. DNA/RNA strand dehybridisation is often an unfavourable reaction even in the presence of aptamer target. The effect this has on the Kd is rarely noted. There are cases where the dissociation of one structure allows for a ‘signal on’ mechanism that provide similar advantages to other ‘signal on’ mechanisms. Lu (123) demonstrates a ‘signal on’ sensing technique involving the dissociation of the aptamer strand and

the retention of a redox tagged ssDNA that folds upon itself allowing for an increase in current. This technique could be generalized across many aptamers and within the same paper has been show to work with ATP and thrombin, giving detection limits of 10nM and 2nM respectively.

Measuring changes in surface capacitance or resistance when not in the presence of redox tags is based on ideas brought over from antibody sensing, where label free systems are desired as tagging of antibodies can prove problematic. As aptamers are readily labelled, the development of these types of systems is not needed. Li (124) highlight this by their measurement of adenosine based on changes in impedance resulting from the dehybridzation of a surface bound adenosine aptamer after target binding. A relatively high detection limit of 0.1uM and linear range between 0.5 and 160uM is observed, the linearity of 4 points is also open for debate and more data would be needed. This high detection limit can be attributed to a high background noise from the dynamic surface chemistry thus small changes in this would be difficult to detect.

Chakraborty (125) demonstrated the effect immobilization of sensing structure via the 3' or 5' end had on sensor performance of a DNA adenosine aptamer measured by SWV and CV. 3' end immobilization was beneficial and saw a 25% -30 % signal gain over its 5' counterpart. This will be aptamer dependent and vary based on aptamer structure. Kd values of 127 $\pm$ 24 uM were reported for the 3' immobilised aptamer, unfortunately no Kd data was provided for the 5' aptasensor. An increase in Kd value of the aptamer when compared to solution free aptamer (6 $\pm$ 3 uM) was observed (87).

1.5 Electrochemical techniques

Cyclic Voltammetry (CV) involves measuring current over a potential range and switching the direction of the scan at a certain potential, current is then measured in the opposite direction of the original scan before the scan direction again switches at the other end of the potential range and proceeds in the original direction. This 'sweeping' as it is often referred to may be repeated several times as changes in the system are observed. This technique is often used when a redox couple is

present in the system, as changes in the positioning or accessibility of the redox probe to the working electrode are detectable as peak current changes (126–128).

Differential pulse voltammetry (DPV) much like square wave voltammetry is utilized as it allows the reduction in charging current and thus a reduction in detection limit. The technique involves linearly ramping the potential by imposing constant potential pulses at set times, current is measured just before a pulse, a certain amount of wait time is allowed (pulse width) and then the current is measured just before the end of the pulse. This wait time allows for the decay of the charging current. The difference between the current before and after the pulse is measured and plotted against potential (128).

Square wave voltammetry (SWV) is commonly seen as one of the most sensitive techniques . Much like DPV it involves the application of a potential ramp and applying a small pulse of constant amplitude to it. Unlike DPV SWV can be seen as applying a symmetrical double pulse, one in the direction of the scan (forward) direction and one in the reverse, this results in a square wave been superimposed on a potential staircase. Each current measurement is taken at the end of the individual pulses. A difference current is plotted against potential. This technique provides the excellent background noise suppression of DPV, as charging currents are allowed to decay, while an increased sensitivity is noted due to the recording of both forward and backwards currents. Finally the technique allows for vastly improved speeds over other techniques as the increased samples taken allows for increased frequency while maintaining its sensitivity. The scan speed is inherently related to the reciprocal square wave frequency where in DPV it is related to the pulse width. Thus a SWV scan can occur in a matter of seconds compared to other techniques(128,129).

Electrochemical impedance spectroscopy (EIS) is often utilized due to its high sensitivity but due to the complexity in understanding impedance it is often not correctly analysed. EIS technique involves the application of regular small AC amplitudes. The impedance can then be observed over a wide range of AC frequencies. Significant information can be obtained on the system including resistance

and capacitance. Often problems arise when trying to fit the data to equivalent circuits and often greatly simplified versions are used(128,130).

1.6 Enzyme-linked oligonucleotide assay (ELONA)

1.6.1 ELISA

ELISA (enzyme-linked immunosorbent assay) technology is well know and a vital part of clinical diagnostics today. It was invented in 1971 by Engvall and Perlmann (131) to detect immunoglobulin G and is now widely used both in research and clinical applications. It relies on the principle that a range of antibodies or antigens will passively adsorb on a surface, often in the case of ELISA a polystyrene plate. Once an antigen/antibody is surface immobilised a combination of specific antibodies/antigens and enzymes are used to generate a signal. This signal manifests as a colour change that is proportional to the amount of antigen and antibody that are bound to one another. This colour change can easily be read by a plate reader and recorded as an absorbance, fluorescence or chemiluminescence signal.

As the antigen or antibody are bound to the solid surface of a plate they can be readily washed, allowing for removal of low binding or non-specifically bound products. Most antibodies or antigens are suitable for passive adsorption to a polystyrene plate allowing for a range of systems to be quantified. The small sample volume and large sample number allows for numerous experiments to be run in parallel, with the most common plate sizes being the 96 (360ul max per well) and 384 (120ul max per well) well plates. This is essential for immunochemistry as varying conditions and concentrations often need to be tested. There are 4 main types of ELISA; direct, indirect, sandwich and competition. Direct ELISA (Figure 3) falls into two categories, antibody labelled and antigen labelled. In both cases direct implies a direct conjugation of the enzyme with either the antibody or antigen depending on which is being utilised as the signal generator. The antibody or antigen that isn't labelled is passively adsorbed to the surface and the other labelled component will bind to this.

The majority of diagnostic tests require the detection of the antigen within a complex sample like blood, as such antibody labelled ELISA is predominantly used in these situations.

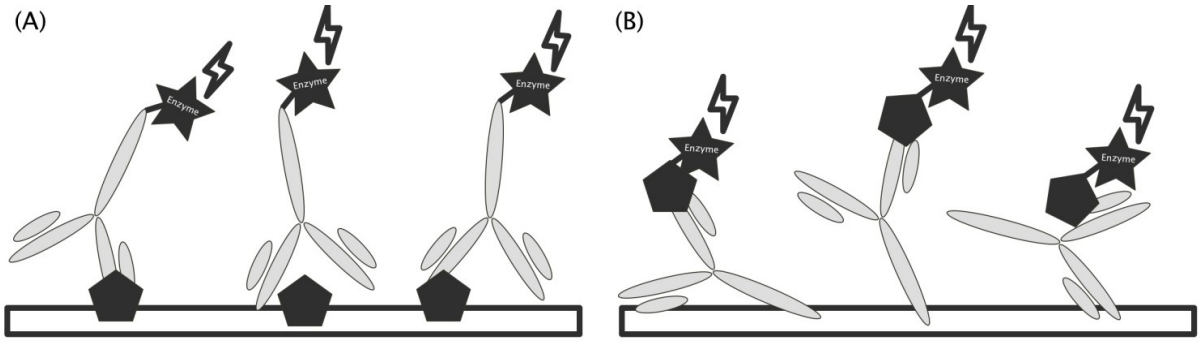

Figure 3: Direct antibody labelled ELISA. (A)Antigen is passively adsorbed onto the well surface. (B) Antibody is passively adsorbed onto the well surface.

Indirect ELISA involves the passive adsorption of the antigen to the surface. An antibody that is specific to that antigen will bind followed by a labelled antibody that is specific to the antigen bound antibody (Figure 4). Sandwich ELISA requires an immobilised antibody on the surface that binds the antigen, while another labelled antibody binds to another part of the antigen (Figure 5). Competitive ELISA requires the simultaneous addition of two or more antibodies/antigens (Figure 5). This is useful for determining the specificity of a binding pair and if a competing antibody or antigen will affect the binding.

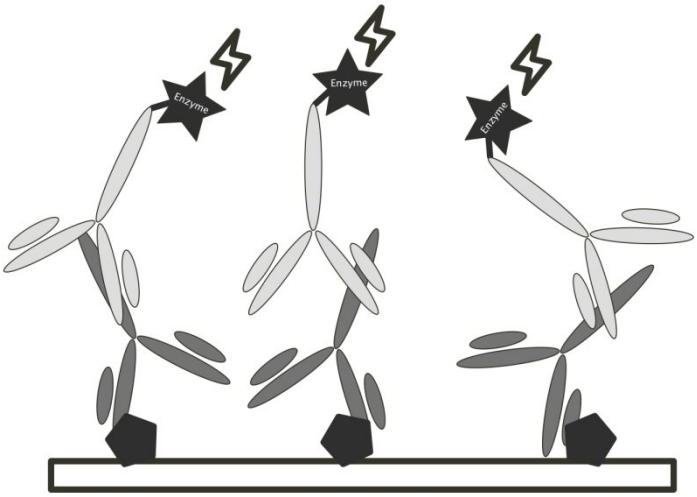

Figure 4: Indirect ELISA

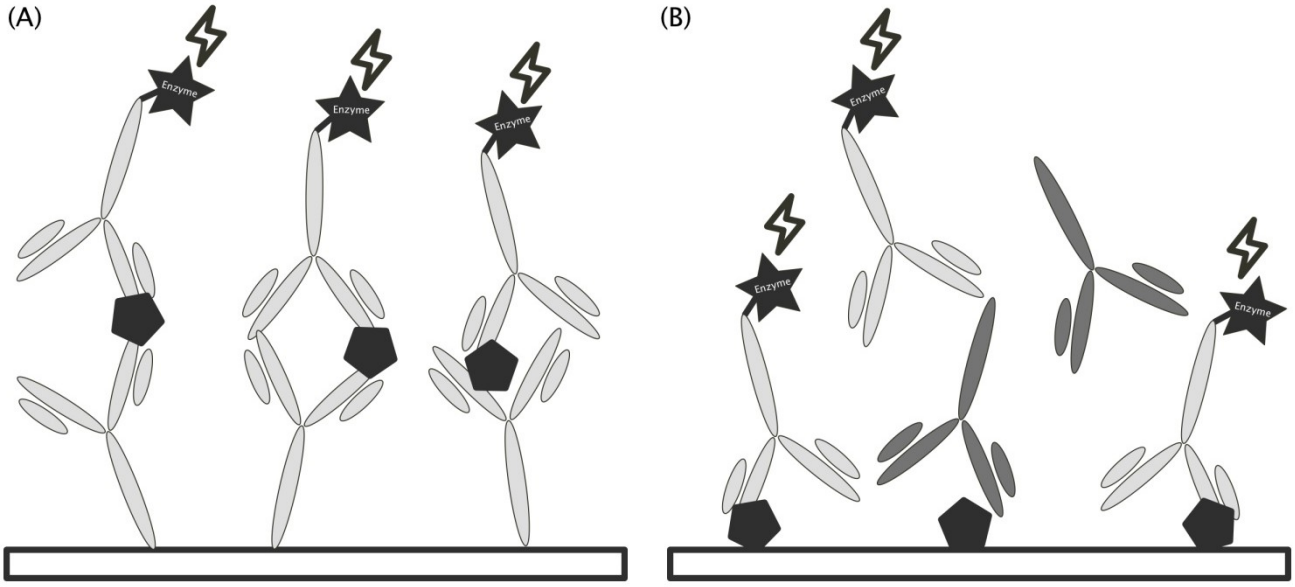

Figure 5: (A): Sandwich ELISA. (B): Competitive ELISA

1.6.2 ELONA (enzyme-linked oligonucleotide assay)

In 1996 Romig et al (132) adapted the ELISA for use with oligonucleotides to detect vascular endothelial growth factor (VEGF). Using a capture monoclonal antibody and a fluorescein tagged

oligonucleotide they created a sandwich assay. Since then other versions of the assay have been developed and ELONA is now a widely utilised technique.

Herein we utilised a direct ELONA assay, where the HSA or glycated HSA was immobilised on the surface of a polystyrene plate and a biotin tagged oligonucleotide was directly bound to it. The sample was then incubated with streptavidin conjugated Horseradish peroxidase before a substrate of 3,3',5,5'-Tetramethylbenzidine (TMB) was incubated with the sample. This causes a visible colour change, which is quenched by 1mM Sulphuric Acid after 5 minutes. The solutions are then measured at 480nm and absorbance is recorded.

1.7 The effect of experimental conditions on aptamer response

While the focus of this thesis is on ELONA and electrochemical aptamer systems we will also briefly review some other techniques in the context of how solution conditions, immobilisation, amplification techniques and sensing mechanism have on the response of aptamers.

1.7.1 Solution conditions

Salt and temperature variations have been demonstrated to have a range of effects on aptamer binding. Utilising isothermal titration calorimetry (ITC) (a useful technique for determining Kd values of aptamers target interactions in solution), Kuo (133) observed the effects temperature and NaCl concentrations had on Kd value of a DNA aptamer to streptavidin. Increasing NaCl concentration from 140 mM to 350 mM saw a reduction in Kd value at all temperatures; for example at 23^0C a decrease from 99.70 to 32.47 nM was observed. Kanakraj (134) demonstrated a similar effect with a DNA aptamer to VEGF using ITC. Increasing NaCl concentrations from 50 mM to 250 mM resulted in a decline in all of the tested VEGF aptamers, one aptamer's Kd value declined from 15.2 $\pm$ 2.3 nM to 77.4 $\pm$ 26.6 nM. This was highlighted further still by a study from Potty (135) who using ITC and fluorescence anisotropy demonstrated increasing NaCl concentrations had a detrimental effect on Kd values for both a DNA and RNA aptamer to lysozyme. The DNA aptamer demonstrated a change of 198 $\pm$ 41 nM (25^0C) at 0 mM NaCl concentration to 2796 $\pm$ 135 nM (25^0C) at 50mM NaCl

concentration. These three papers highlight the negative effect increasing NaCl concentration has on aptasensor performance. This same effect can also be observed with cocaine aptamers (136) ,VEGF (137) and L-tyrosinamide aptamers (138).

One of the earliest fluorescent aptamer techniques demonstrated was the use of an aptamer beacon with a fluorescent tag and quencher (139). A Kd of 10 nM was observed for the thrombin aptamer. Effect of various ions was demonstrated, increases in both KCl and $MgCl_2$ prove detrimental to sensor performance at any level. Both are seen to stabilize the duplex form of the aptamer beacon making it unfavourable to bind thrombin. $MgCl_2$ has shown to be detrimental in a cocaine DNA aptasensor based on a beacon fluorescent quenching structure. Positive results were demonstrated in serum but corrections have to be made to account for background fluorescence (110).

FRET (fluorescence resonance energy transfer) has often been utilised for studying aptamer binding, it involves the emission of fluorescence signal when one molecule (donor) is close enough (2-10nm) to its pair (acceptor) to excite it. To avoid labelling the target protein various novel methods have been demonstrated (140–142). The effect solution conditions have on DNA PDGF aptamer sensitivity have been observed by Vicens (108). Increasing concentrations of Ca^{2+}, Mg^{2+}, K^{+} and Na^{+} all resulted in quenching of the fluorescence signal that in turn lowers the detection limit. It was noted that the relevant levels of ions in their cell culture medium would only result in minimal quenching of the fluorescence. PDFG aptasensor performance in low levels or blood serum have been observed(143).

Potty (137) studied the effects buffer solution had on VEGF DNA aptamer Kd. Aptamer VEGF Kd in PBS + 5mM $MgCl_2$ was more than twice (1066.4 $\pm$ 198 nM) that of PBS alone (403.6 $\pm$ 66.6 nM). While PBS alone demonstrated approximately a 200 fold increase on the Kd observed in 20mM Tris (1.9 +1.0 nM). Li (144) demonstrated the addition of Na+ resulted in a decrease in affinity from 1.3 $\pm$ 0.2 nM (0mM Na^{+}) to 17 + 1.5 mM (150 mM Na^{+}) for a DNA angiogenin aptamer. While Zou (145) observed the negative effect increasing Mg^{2+} concentration has on a DNA lysozyme aptamer.

Solution conditions not including salt concentrations can additionally alter Kd values. Kang (146) presented a Kd of 11uM for DNA aptamer to cocaine, however acetonitrile (common solvent for cocaine standards) reduces the affinity of cocaine for its DNA aptamer. Acetonitrile concentrations below 2% resulted in a kd values ranging from 11 to 22 uM, while those over 3% saw Kd values of more than 200 uM.

We are consistently observing that solution conditions have an important part to play in aptamer binding. Of note is that an increase in ionic concentration has a negative effect on aptamer performance. As the majority of these systems are to be utilised in serum, initial aptamer selections need to be performed in conditions that as closely resemble serum as possible.

1.7.2 Immobilisation of aptamers

Utilising fluorescent anisotropy (147,148), McCauley (149) demonstrated a multianalyte aptasensor containing a DNA aptamer for thrombin, and three RNA aptamers for the cancer markers basic fibroblast growth factor (bFGF), inosine monophosphate dehydrogenase II (IMPDH II) and vascular endothelial factor (VEGF). Experiments were performed on DNA thrombin aptamer to determine the effect surface immobilisation had on its Kd. The Kd for the surface immobilised thrombin aptamer was favorable (15 nM) in comparison with the solution phase aptamer (26 nM). As all measurements were taken in bacterial cell lysate, RNA aptamers degraded quickly so Kds were unobtainable. Fluorescence anisotropy has also been demonstrated to be a viable detection method for leukemia cells in whole blood (150).

In a cantilever system, Kang (146) demonstrated the use of DNA aptamer for cocaine detection, demonstrating a linear dependence of surface stress on bound/ unbound aptamer cocaine complexes up to 90% of bound target. Surface stress between 9-51 mN/m was observed over cocaine range of 25-500 uM. It was noted that binding of cocaine caused an expansion in the aptamer coated surface, possibly due to a decrease in free surface area and subsequently increased repulsion between neighbouring aptamers.

The use of a more complex cantilever system has recently been described. Nagai (151) demonstrated the use of an electrochemically controlled cantilever. This allows for control of the surface charge density by an applied potential. L-argininamide was used as a DNA aptamer target, advantages arose as it was demonstrated it could electrochemically modify the amount of ions at the surface of the cantilever, allowing for highly reproducible results.

Zhai (152) demonstrated the effect surface immobilisation of an RNA aptamer to the target inflammatory marker Lipocalin-2 has on Kd. Interestingly an increase in Kd is observed from the data obtained via filter binding assay, a shift is observed from 340 nM to 70 nM for the cantilever sensor. This was attributed to close packing of the cantilever surface potentially stabilizing the aptamer structure and the recapturing of dissociated proteins by neighbouring aptamer strands. Aptamer cantilever detection systems have typically focused on novel targets and have been utilised with Oxytetracycline (153), hepatitis C virus (154), Taq DNA polymerase (Kd=15 pM) (155).

1.7.3 Signal generation and amplification

Detection of low mass molecules has always been proved problematic, especially for fluorescent techniques; often amplification of the binding event is needed. Liu (156) demonstrates the use of graphene oxide as a mass amplifier to enhance fluorescence anisotropy signal in a DNA ATP aptasensor, however problems arose with selectivity of the system in human serum. Quantum dots in a DNA H1N1 aptasensor (157) and the use of single stranded DNA binding protein for a DNA adenosine aptamer (158) both showed amplification.

Quartz crystal microbalance works on the principle that addition of material to a resonating QC will alter its frequency (159–161) Limitations of the technique revolve around its ability to detect lower mass targets; however with aptamers being readily modified this can be altered. Dong (162)demonstrated the addition of a gold nanoparticle to a complimentary oligonucleotide (bound to a theophylline aptamer) increased the detection limit to 8.2 nM compared without gold nanoparticles (120nM). Interestingly the aptamer strands which did not include the gold

nanoparticle showed a higher affinity (27 nM) than those that did (526 nM), potentially due to steric hindrance associated with the added gold nanoparticles.

Similar amplification using gold nanoparticles has also been demonstrated by Chen (100) for the detection of thrombin. The sensor takes advantage of the two available DNA thrombin aptamers to provide a sandwich assay. The first aptamer is immobilized on the QC, while the secondary aptamer is conjugated to a gold nanoparticle that provides amplification. This technique is not transferable to many other proteins due to needing two separate aptamers that bind to two separate sites on the same protein.

Mass based techniques are susceptible to large background signals from non specific inferences resulting from the mass of various contaminants in a sample. This is usually countered by utilising a reference QCM that does not bind said target. Another method is the complete removal of bound aptamer-target complex from solution via magnetic tagging of the aptamer strands before measuring the purified aptamers on the QCM system (163) This has the added benefit of allowing aptamer target binding in solution which often shows a lower Kd.

Nutiu (164) demonstrate the effect tagging the aptamer has on Kd value. The majority of techniques require labelling of the aptamer to enable sensing; here we see the addition of a fluorescent molecule and a quenching molecule. Thrombin DNA aptamer demonstrated an increase in Kd from 200 nM (119) to 400 nM, while ATP aptamer saw a increase from 6 uM (87) to 600 uM . The original ATP Kd value referenced was from solution measurements while the original thrombin aptamer was radioactively tagged. Both changes demonstrate the differences in Kd values commonly observed when labelling aptamers.

1.7.4 Towards a universal assay

A tantalizing promise of aptamers over antibodies has been the possibility of creating universal systems where any aptamer can be utilised. Due to the ease at which they can be modified, sensing structures can be built around them. There are few systems that exist where this bares truth. One

possible approach is the modification of a microarray format with aptamers. Lee (165) demonstrated this with a fibre optic thrombin aptamer microarray, while a decent Kd of 300nM was observed, fluorescent tagging of the thrombin protein was needed to run a competition assay against untagged thrombin. This makes it a technique that is not readily transferable between targets.

Kong (166) has demonstrated an impressive sensing platform that has potential to be used with a wide array of aptamers. It relies on solution free aptamers semi hybridized to semi complimentary strands, SYBR Green I dye is added to the system and will bind dsDNA. Importantly SYBR Green I dye has a week fluorescent signal in solution and when bound to ssDNA, while a strong signal is observed upon binding with dsDNA. The addition of target causes dehybridization and a quenching in fluorescent signal. DNA aptamers for both ATP and thrombin showed good selectivity and detection ranges. No Kd was provided, it would be interesting to see how the response of the aptamers are affected by the complementary strands. The system was only tested in buffer; more complex samples may prove problematic for the dye. Other novel fluorescent intensity ATP aptamer systems have also been demonstrated (140,167).

1.8 Overview of thesis

Within this thesis, the creation of aptamers to both HSA and early stage glycated HSA (GHSA) has been carried out through systematic evolution of ligands by exponential enrichment (SELEX). The challenges involved in this are discussed including the need to carefully control SELEX conditions. The sequencing and analysis of these aptamer libraries was undertaken by next generation sequencing (NGS) where 27 HSA aptamers and 20 GHSA aptamers were selected for experimental analysis. The resulting aptamers have been experimentally tested with enzyme linked oligonucleotide assay (ELISA), where careful selection of buffer and blocking conditions were key to understanding aptamer binding. Finally a selection of aptamers that demonstrated positive responses with ELONA were tested electrochemically. Both cyclic voltammetry and square wave

voltammetry were utilised in this analysis. The combined ELONA and electrochemical data highlighted a range of aptamers to both HSA and GHSA.

Chapter 2

Methods and Techniques

2 Methods and techniques

Within this chapter we lay out the methods and techniques utilised for selecting and testing HSA and GHSA aptamers. This includes the selection of aptamers through SELEX (Chapter 2.1), the analysis of the aptamer library utilising NGS computational techniques (Chapter 2.2), before the experimental examination of the aptamers utilising ELONA (Chapter 2.3) and Electrochemistry (Chapter 2.4). While the main protocols are defined in this section, modifications were made at times as described in the results chapter (Chapter 3).

2.1 Experimental: SELEX

2.1.1 Equipment and materials

The following equipment and materials were utilised:

- SulfoLink immobilisation kit for proteins (Thermo Scientific. Product Code 44995). Contents include:
    - SulfoLink Column, 5 × 2mL, 6% cross linked beaded agarose supplied as a 50% slurry in storage buffer (10mM EDTA-Na, 0.05% NaN_3, 50% glycerol) Binding Capacity: ≥ 5mg reduced human IgG/mL of resin
    - SulfoLink Coupling Buffer, 500mL, 50mM Tris, 5mM EDTA-Na; pH 8.5
    - Wash Solution, 120mL, 1.0 M NaCl, 0.05% NaN_3
    - L-Cysteine•HCl, 100mg
- Human Serum Albumin (HSA) (Sigma A3782)
- Glycated Human Serum Albumin (GHSA) (Sigma A8301)
- Streptavidin MagneSphere Paramagnetic Beads (Promega Z5481)
- Desalting columns.
    - Illustra NAP 5/25 columns (GE Healthcare 17-0853-01/17-0852-01)
    - G-25 PD 10 column (GE Healthcare 17-0851-01)
- Ethanol (Sigma E7023)
- Sodium Acetate (Sigma W302406)

- PBS (Sigma P4417)
- $MgCl_2$ (Sigma M8266)
- Filtered water
- PCR Thermocycler
- Electrophoresis tank and power supply
- TAE Buffer (Made from Tris -acetate (Sigma: T1258) and EDTA (E9884))
- PCR Nucleotide mix including 10x PCR buffer and DNTPs (Promega C1141)
- Taq Polymerase (New England Bio labs: M0480s)
- Blue/Orange Loading Dye, 6x (Promega G1881)
- Forward and reverse primers including both unmodified and biotin modified reverse primer. Extended forward and reverse primers. (Custom order from IDT)
- DNA Library (76 bases in length with random 40 base pair centre flanked by two 18 base pair primer regions) (Custom order from IDT)
- SYBR Gold nucleic acid gel stain (Invitrogen S11494)
- Gel Imager
- Nanodrop 100
- 25bp DNA ladder (Promega - G4511)
- QIAquick gel extraction kit (Qiagen - 28704)
- QIAquick PCR purification kit (Qiagen - 28104)
- Glycine HCL (Sigma- G2879)

2.1.2 Immobilisation of HSA/GHSA on column (Instructions taken from Sulfolink Immobilisation kit and have been slightly adapted)

Perform all column centrifugations at 1,000 × *g* for 1 minute using a 15mL collection tube unless otherwise stated. Do not allow the resin to become dry at any time.

Binding buffer is PBS + $MgCl_2$ 10mM pH 7.4

1. Suspend the SulfoLink Resin by end-over-end mixing. To avoid drawing air into the column, sequentially remove the top cap and then the bottom tab. Centrifuge the column to remove the storage buffer.
2. Add 2mL of Coupling Buffer and centrifuge. Repeat with an additional 2mL Coupling Buffer. Replace the bottom cap.
3. Add 2mL of HSA/GHSA at 20mg/ml protein to the SulfoLink Column.
4. Replace the bottom and top cap and mix by rocking or end-over-end mixing at room temperature for 15 minutes.
5. Place the column upright and incubate at room temperature for 30 minutes without mixing.
6. Sequentially remove top and bottom column caps, place column into a new tube and centrifuge to collect non-bound protein.
7. Save the flow-through and determine the coupling efficiency on the Nanodrop while continuing the blocking steps. Determine the coupling efficiency by comparing the protein concentrations of the non-bound fraction to the starting concentration. To calculate the concentration of the unbound protein on the nanodrop you need the molecular weight (MW) and molar extinction coefficient (ε). For HSA the MW is 66,500 and ε is 36,500 $M^{-1}cm^{-1}$. The same MW and ε was utilised for GHSA as it closely correlates.
8. Wash the column with at least 2mL of Wash Solution and centrifuge. Repeat this wash three times.
9. Wash the column with 2mL of Coupling Buffer and centrifuge. Repeat this step once.

2.1.3 Block non specific binding sites

1. Replace the bottom cap. Add 15.8 mg L-Cysteine•HCl to 2mL of Coupling Buffer (50 mM

cysteine). Apply the cysteine solution to the column and replace the top cap.

2. Mix for 15 minutes at room temperature. Incubate the reaction without mixing for 30 minutes.

3. Sequentially remove the top and bottom caps and allow column to drain.

4. If not preparing for storage then jump straight to Affinity Purification point 3.

5. Prepare for storage by pipetting in 4ml of binding buffer and store at -4^{0}C upright.

2.1.4 Affinity Purification

1. Remove HSA bound column from fridge if it was stored and allow it to warm up to room temperature.

2. Centrifuge out storage buffer

3. Equilibrate column with 6ml of binding buffer

4. Take aptamer library from previous round or fresh aptamer library and incubate with column as described in point a/b. Equilibrate column with 2ml of binding buffer and just as the top of the column becomes dry put the lid on the bottom of the column and add the 2ml solution of aptamer. Cap the top.

    a. Fresh Library – 20ul of 100uM aptamer stock in 2 ml of binding buffer. Working concentration of library is 1uM.

    b. Library from previous round. Comes as 1ml. Dilute in 1ml of binding buffer for a total of 2ml.

5. Invert the column end over end for 15 minutes and then leave to stand upright for 45 minutes at room temperature.

6. Remove top and bottom caps, place column in a 15ml collection tube and centrifuge.

7. Without changing collection tube centrifuge a further 1ml of binding buffer.

   Optional step: As the rounds progress the stringency of washing will need to be increased to remove aptamers with low binding affinity. To increase stringency 2ml batches of binding buffer are used.

8. Collection of bound aptamer. Elute protein with 2ml of elution buffer (glycine HCL at pH 2.86) into a 15ml collection tube containing 100ul 1M Sodium phosphate at pH8.75. Before centrifugation quickly invert 2ml of elution buffer in column over and over to ensure thorough mixing. Open caps and centrifuge.

9. Without changing collection tube add 1ml glycine HCL at pH 2.86 and centrifuge . Should have roughly 3ml of solution in 15ml collection tube that contains your aptamers. Place to one side until you reach desalting of aptamer solution instructions.

10. Change collection tubes and add 6ml of binding buffer to the column as quickly as possible. This will allow the column to equilibrate to physiological conditions and avoid damage to the HSA/gHSA from prolonged exposure to acidic conditions.

11. Store column containing HSA/gHSA in binding buffer with 20% ethanol. Add 6ml and store in fridge upright.

Desalting of aptamer solution

1. Wash PD-10 column with 10ml of filtered water.

2. Take the 3ml of bound aptamer left over from earlier and add to the column. Allow to flow under gravity

3. Immediately start taking 500ul fractions. Follow the 3ml of bound aptamer with 7ml of fH_2O. Collect a total of 20 fractions.

4. Measure the eluted solutions on the Nanodrop to determine at what stage the aptamers are

eluted.

5. The aptamer solution may be too low to measure. If this is the case we know from past experiments that the aptamer starts appearing after 6 fractions (3ml).

Desalting of aptamer solution - 2nd process

GHSA aptamers were desalted with Illustria Nap-25 columns as described in the manual. The change of columns was made to try and increase retained aptamer concentration.

2.1.5 Ethanol precipitation

1. Take suitable fraction (e.g. fractions 6-17). Take each fraction (500ul) and add it to its own mix of 1250ul absolute ethanol and 100ul (Used 50ul at points as described in Chapter 3.2 and Chapter 3.4) 3M sodium acetate. Repeat this for all fractions.
2. Store tubes in -20^{0}C overnight or -80^{0}C for 2 hours
3. Spin tubes at 4^{0}C, 14,000rpm for 50 minutes.
4. Remove supernatant and add 200ul 80% ethanol to each tube.
5. Spin tubes at 4^{0}C, 14,000rpm for 20 minutes.
6. Remove supernatant and heat in a vacuum concentrator on low for 5-10 minutes. Check periodically until you have notice the liquid has evaporated.
7. Resuspend the contents of all tubes in 200ul fH_2O. That's 200ul total for all tubes, so transfer the 200ul water between all the tubes resuspending aptamer until you have a 200ul of water with all the aptamers from all the tubes in it. The aptamer should appear as white mark at the bottom of each tube, make sure to fully dissolve this back into solution, it may prove difficult so a combination of vortex and repeated pipetting may have to be utilised.

2.1.6 PCR

1. Make a PCR mix with the following components. Total volume may be altered to better suit each PCR depending on available DNA template. The PCR mix described here is the final settled mix, however this was altered throughout the SELEX round depending on circumstances. This is further expanded on in the results (Chapter 3.2).

    - 200ul aptamer library (DNA template)
    - 1400ul fH_2O
    - 400ul PCR buffer 10x
    - 25ul dNTP@10mM
    - 10ul forward primer (100uM)
    - 10ul reverse primer (biotin modified at 5' end) (100uM)

2. Take 100ul from the 2ml PCR solution created (Ensure it is fully mixed before removing 100ul from the 2ml stock)

3. Add 0.5% Taq Polymerase to 100ul solution, so add 0.5ul of Taq.

4. Setup 9 PCR tubes (500ul) with 1ul of blue/orange loading dye. Label 1 through 9.

5. Prepare separate 500ul PCR tube with 1ul of blue/orange loading dye and 3ul of 25bp DNA ladder . This is your marker.

6. Input the following PCR program into Thermocycler.

    1. T=95^0C 3 minutes
    2. T=95^0C 30 seconds
    3. T=51^0C 30 seconds
    4. T=72^0C 30 seconds
    5. Go to 2 repeat twice

6. Go to 2 repeat 8.

7. This PCR protocol was altered at times to reflect the requirements of the SELEX, most notably in Chapter 3.4.

8. Run PCR with tube containing 100ul PCR mix and 0.5% Taq polymerase

9. The PCR program will perform three rounds of thermo cycling before pausing. At this stage the user removes 6ul of solution from the 100ul trial PCR tube and places it in the tube 1, mixing it thoroughly with the blue/orange loading dye. The user then resumes the machine and repeats this process until the 9 separate tubes have been filled with PCR mix from the various rounds. Tube 9 should represent 27 cycles.

2.1.7 Gel Electrophoresis

1. While the PCR is running prepare an agarose gel. 1.5g Agarose in 50ml 1X TAE buffer for a 3% Gel. Heat in microwave at 560W for 2 minutes or until buffer is clear.

2. Take a gel cassette and seal off both ends with tape. Pour in agarose liquid. Place a 10 space comb in and allow to set. Once set remove the 10 space comb and the tape.

3. Prepare an electrophoresis tank until it's partially full with 1x TAE buffer. The buffer should immerse the electrophoresis tank electrodes.

4. Place the cassette containing the set agarose gel into the electrophoresis tank such that is equidistant from the cathode and anode. The cassette should be placed such that the wells within the cassette left by the comb are nearest the cathode. Note: This is so samples placed into these wells move towards the anode through the remaining agarose gel. If the gel was placed the other way round with the wells nearest the anode, the samples would move off the gel and be lost.

5. Take the marker tube and pipette 4ul of the fully mixed solution into the first lane of the

immersed agarose gel within the electrophoresis tank. Then take the 9 samples collected from the trial PCR and subsequently pipette each sample into the remaining lanes.

6. Connect up the electrodes and run the gel for 1 hour at 200V and 400mA.

7. Once the hour is complete disconnect the electrodes and remove the gel and cassette from the tank. Utilising a small box that can hold the gel, prepare 10ul of Syb Gold in 70ml of 1x TAE buffer and decant it into the box. Remove the gel from the cassette that supports it and place the gel in the box containing the 70 ml mix of 1x TAE buffer and Syb gold. Leave for 1 hour in the dark.

8. Remove the gel from the solution and place on a cassette. Image the gel using a gel imaging system.

9. Observe the PCR bands and determine based on the intensity, width and location of the bands the correct number of PCR rounds to perform. Narrow intense bands are preferred as they indicate a product that is both high in concentration and well defined. Broadening of a bands indicates truncation/elongation have arisen as the molecular weights are not where they should be.

10. Carry out full PCR for the number of rounds determined by the trial PCR.

2.1.8 Separation of double stranded DNA

1. Take 2 tubes of streptavidin magnetic beads and remove the solutions and mix them together in a 2ml PCR tube.

2. Place the tube in a magnetic holder and wait until the beads have visibly collected on the inside of the tube nearest the magnet. Remove the supernatant and discard it.

3. Wash the leftover magnetic beads in binding buffer three times. Each time using the magnetic holder to retain the beads.

4. Add the PCR product to the magnetic beads only. No additional buffer
5. Constantly inverting the solution incubate the mixture for 1 hour.
6. Place the tube in a magnetic holder and wait until the beads have visibly collected on the inside of the tube nearest the magnet. Remove the supernatant and discard it.
7. Wash the leftover magnetic beads in binding buffer three times. Each time using the magnetic holder to retain the beads.
8. Resuspend the beads in filtered distilled water.
9. Mix the solution well and split the beads into 10 different tubes. Use 500ul PCR tubes and put 100ul in each.
10. Heat the tubes for 95^0C for 5 minutes
11. Recombine the solutions into one 1ml solution.
12. Place the tube in a magnetic holder and wait until the beads have visibly collected on the inside of the tube nearest the magnet. Remove the supernatant and KEEP IT
13. Solution should now contain single stranded DNA ready for the next round of SELEX. The solution concentration was checked on a Nanodrop 1000 utilizing the Nucleic acids feature set to single stranded DNA . If the concentration is too low then a further PCR round can be performed to increase it before proceeding to the next SELEX round.

2.2 Next Generation Sequencing (NGS)

2.2.1 Next Generation Sequencing (NGS) Overview

Next Generation Sequencing (NGS) was performed externally by GATC using the Illumina HiSeq 2500 platform with its sequencing by synthesis (SBS) technology, specifically paired-end sequencing. NGS involves three key steps:

1. Library preparation

2. Cluster generation

3. Sequencing

Library preparation involves the separation of the dsDNA and the ligation of Illumina primers to both the 5' and 3' ends of each ssDNA fragment. The DNA is sequenced in a flow cell, on the surface of this flow cell there are two different immobilised ssDNA populations (OL1 and OL2). OL1 is complimentary to the ligated Illumina primer at the 5' end and OL2 is the identical sequence to the primer that has been ligated at the 3' end of the ssDNA fragments.

The adapted ssDNA fragments are flown into the cell and they hybridise to OL1. Utilising a DNA polymerase the immobilised ssDNA undergoes second strand synthesis and the original forward strand is removed by denaturing the surface bound dsDNA, this leaves the reverse strand on the surface.

This reverse strand now has a complementary sequence to OL2 at its 3' end. This is a result of the Illumina ligated primer that was identical to OL2 now presenting its reverse form.

The strands are now clonally amplified into clusters to boost the observed signal when sequencing. This is done by bridge amplification. The strands are now able to hybridise to this OL2 creating a bridge due to the anchoring of the ssDNA at both it's 5' and 3' end. This is then made double stranded by a polymerase, forming a double stranded bridge anchored to the surface of the flow cell at both ends.

The bridge is denatured, resulting in two separate but complimentary strands that are both anchored to the surface. Amplification can now occur again and again, generating clusters of fragments. Once amplification has occurred the reverse strands are cleaved and washed away.

The 3' ends are now blocked and a sequencing primer is hybridised to the end. DNA strands are then sequenced by the addition of fluorescently tagged nucleotides which compete to bind to each base.

When the correct one binds the nucleotide is read by a laser with the colour informing the system of which base has bound. The fluorescent tag is then removed as well as the blocker which prevented the next nucleotide binding. This process is then repeated until a whole DNA strand has been sequenced. This process is run in parallel to millions of other DNA clusters. Allowing for the sequencing of the entire library. This sequencing technique is referred to as sequencing by synthesis.

2.2.2 Preparation of DNA library for Next Generation Sequencing (NGS)

Upon completion of the SELEX rounds the DNA library needs to be modified and checked to ensure it is of sufficient quality for NGS.

The Illumina HiSeq 2500 which was utilized for sequencing requires that the DNA library used for sequencing be:

- At least 100 bases in length
- > 500ng per sample
- > 10ng/ml
- Double stranded
- OD 260/280 > 1.8
- OD 260/230 > 1.9
- Dissolved in RNAse-, DNAse- and protease free water or Tris HCl buffer (pH 8-8.5)
- Free of impurities like denaturants, detergents and biological macromolecules.

Creation of elongated double stranded DNA

Following a similar setup as before single stranded DNA from the final round of SELEX was PCR amplified to form both double stranded DNA, elongated it and increase its concentration. The main difference from PCR performed in the SELEX rounds is here we utilize longer extended primers with

no biotin modification on the reverse primer.

The 72^0C elongation PCR step that was removed from some of the SELEX PCRs returned here as there was concern that full extension of the dsDNA would not occur without it.

Following PCR protocol was used:

1. T=95^0C 3 minutes
2. T=95^0C 30 seconds
3. T=51^0C 30 seconds
4. T=72^0C 10 seconds
5. Go to 2 repeat twice
6. Sound 2
7. Press enter
8. Go to 2 repeat 8.

PCR Mix

- 1ml aptamer in filtered water
- 600ul filtered water
- 400ul 5x buffer
- 25ul dNTP @ 10mM
- 15ul extended forward primer at 100uM
- 15ul extended reverse primer at 100uM

1. Run the PCR trial and the gel electrophoresis as already stated in section 2.1.6 and 2.1.7. Upon studying the Gel, the DNA band should have shifted from around 80bp to 100bp.

2. After completion of trial PCR, run the full sample PCR.

3. Next ethanol precipitate the PCR sample to concentrate it.

2.2.3 PCR cleanup

Used both Qiagen QIAquick PCR purification kit and Qiagen QIAquick Gel extraction kit. Originally the Gel extraction kit was utilised but the decision was made to change to the PCR purification kit as the typical DNA recovery was higher at between 90-95% compared with 70-80% for the Gel extraction kit. The Gel extraction kit also typically only removed oligonucleotides below 10 bases where the PCR purification kit removed any below 40 bases which in principle should mean better removal of unbound primers. The Gel extraction kit and PCR purification kit recover oligonucleotides over 70bp and 100bp respectively. As our DNA strands should be 104 bases in length this change of kits would not prove problematic.

Manufacture protocols were followed for both and DNA samples were eluted in RNAse-, DNAse- and protease free water. Elution volumes were kept to a minimum to retain the highest DNA concentration possible. Typical elution volumes were between 30ul and 50ul.

2.2.4 Quality check of DNA

The elongated DNA that resulted from the extended primer PCR, ethanol precipitation and finally cleanup was analysed spectroscopically on a Nanodrop 1000.

The following criteria was checked:

- > 500ng per sample
- > 10ng/ml
- OD 260/280 > 1.8
- OD 260/230 > 1.9

If the sample met the above criteria it was ready for NGS, however if it failed any of the criteria it

was amplified and cleaned up until it met said criteria.

2.2.5 Next Generation Sequencing (NGS) Analysis

After the DNA library has been sequenced, analysis of that data is required to identify potential aptamers that bind to your target. This is a complex procedure and often requires trialling several different techniques to identify potential aptamers that bind to your target. While analysis of genomic data has become routine with specific solutions built for it, analysis of aptamer libraries has until very recently relied on custom solutions built from non-aptamer specific software. This is starting to change in the last couple of years as a range of groups have started publishing software packages that are built for aptamer selection.

For the initial analysis of the HSA NGS data a range of packages that were not specifically tailored for aptamer detection but for more general DNA analysis were utilised. At the time more tailored aptamer software was either not available or limited in scope. There are a variety of ways to search for aptamers within a library but the most common and still most reliable approach is to look for consensus sequences, while certain groups believe searching for consensus structures along with predicted structures also has its benefits. However, it is still unknown how predicted structures translate to binding and aptamers that do not show certain predicted structures should not be readily ignored.

Before looking for consensus sequences, NGS data needs to be quality checked and controlled to ensure the data set that finally get analysed only contains the sequences you are interested in. FastQC is a UNIX based software that allows for a range of parameters to be analysed. Upon completion of each step of analysis it is prudent to return to FastQC to determine the effect on the overall quality of the data.

The vast majority of NGS data analysis took place on the Imperial College London bioinformatics server farm and I would like to thank James Abbot for his knowledgeable help. The data was

analysed within the UNIX, Mac and Windows operating systems. Multiple different software packages were trialled and are summarised below.

2.2.5.1 Software package summaries:

- **Clustal Omega** (168)-Utilises guide trees to generate alignments from multiple sequences. Originally developed for use in protein alignments can also be utilised in DNA alignments
- **MAFFT**(169) - Alignment program for multiple sequences that utilises fast Fourier transforms to identify homologous regions. The use of simple scoring based system allows for quicker calculations and thus shorter alignment times than most other packages.
- **FastQC** (170)- Checks data set, highlighting a range of parameters giving the user an idea of the quality of their data. Parameters include but are not limited to sequence quality scores, base quality scores, average length, base content, duplication levels and kmer content.
- **discard_seqs** - Trim primers and remove homogenous base regions. Custom code was created by Dr James Abbott of the Bioinformatics Support Service, Imperial College London.
- **Jalview** (171) - View alignments created by MAFFT and Clustal Omega.
- **FASTX_Toolkit** (172) - A collection of tools that enable the user to perform a range of techniques including but not limited to clipping, trimming and quality analysis.
- **Fastaptamer** (173) - A sequence alignment program that is specifically built for aptamer alignments. As simpler search algorithms are utilised that exclude family trees, alignment time is significantly faster than MAFFT or Clustal Omega.
- **Cutadapt** (174)- Utilised in trimming primers off DNA sequences. Any sequence can be specified.

2.2.5.2 Method 1: HSA analysis by MAFFT, Clustal Omega and Jalview

Specific NGS aptamer analysis packages were not available when initially studying the HSA NGS data, as such a packages specific to genomic analysis were tested. Ultimately MAFFT and Clustal Omega were utilised to analyse the data.

Initially the data was analysed to determine its quality using FastQC. The data was then analysed using FastQC after each quality control step to determine the overall effect on data quality. FastQC produces a range of metrics that can help determine the quality of the sample (Chapter 3.5.1.1). Various workflows were trialled but eventually it settled on the below process.

1. FastQC

   fastqc -i /location/Inputfile.fastq -o /location/Outputfile.fastq

2. Remove reverse strands using discard_seqs . DISCARD specifies the output file to look for at the beginning of a strand, for example the start of the 5' reverse strand GATT. All strands starting with GATT are removed.

   discard_seqs --in /location/Inputfile.fastq --/location/Outputfile.fastq --discard PATTERN

3. FastQC

   fastqc -i /location/Inputfile.fastq -o /location/Outputfile.fastq

4. Remove aptamers containing homogenous sections of nucleotides above 4 using discard_seqs. Where the number after --homo specifies the retention of aptamers with homogenous regions of n size, for example if 4 was selected then any strands with 5 or more repeating bases would be removed.

   discard_seqs --in /location/Inputfile.fastq --/location/Outputfile.fastq -- homo (n)

5. FastQC

fastqc -i /location/Inputfile.fastq -o /location/Outputfile.fastq

6. Clip forward primers with cutadapt. Where *--front* ADAPTOR defines the known primer region that will be cut from the 5' end. The forward region CATGACCTAGTAGTAAGCATCCGCTGGTTGAC was searched for and clipped. but additionally based on observations in the raw data that many strands started with an N instead of a C, strands containing NATGACCTAGTAGTAAGCATCCGCTGGTTGAC were also searched for and clipped.

   cutadapt --front ADAPTOR - o /location/Outputfile.fastq /location/Inputfile.fastq

7. FastQC

   fastqc -i /location/Inputfile.fastq -o /location/Outputfile.fastq

8. Clip reverse primers with cutadapt. Where *--adapter* ADAPTOR defines the known primer region that will be cut from the 3' end. The reverse region GATCTTGGACCCTGCGAACGATCATCTGAATC was searched for and clipped. It is to be noted that the region needs to be defined from the 5' end as that is the direction the program reads in.

   cutadapt --adapter ADAPTOR -o /location/Outputfile.fastq /location/Inputfile.fastq

9. FastQC

   fastqc -i /location/Inputfile.fastq -o /location/Outputfile.fastq

10. Removal of strands not 40 bases in length utilsing the fastx_toolkit, particularly the fastx_trimmer/ fastx_clipper. Fastx_clipper will remove strands below set limit, fastx_trimmer above. -Q33 defines that Illumina encoding is utilised and not Sanger encoding.

    fastx_trimmer -l 40 -Q33 -i /location/Inputfile.fastq -o /location/Outputfile.fastq

fastx_clipper -l 40 -Q33 -i /location/Inputfile.fastq -o /location/Outputfile.fastq

11. FastQC

    fastqc -i /location/Inputfile.fastq -o /location/Outputfile.fastq

12. Sequence Analysis with ClustalOmega and MAFFT. Although the dataset has been reduced in size significantly by the quality control, a massive number of strands still remain. As such alignments need to be run for speed otherwise even on servers data processing can take days. For Clustal Omega *--max-guide-treeiterations* was kept to 1 to reduce processing time. While for mafft the fast processing mode *--retree 1* was selected. Slower more accurate modes were trialled but often failed due to the complexity and the size of the datasets.

    clustalo --guidetree-out/Outputguidetree.fastq --max-guide-treeiterations<1> -i /location/Inputfile.fastq -o /location/Outputfile.fastq

    mafft--retree 1 in /location/Inputfile.fastq > out /location/Outputfile.fastq

2.2.5.3 Method 2: HSA analysis and GSHA analysis with FastAptamer

NGS analysis using fastx_clipper from the fastx toolkit and FastAptamer, specifically fastaptamer_count developed by Alam et al(173). The following analysis was performed on the GHSA NGS data and for reanalysis of the HSA data.

Initially the GHSA data was analysed to determine its quality using FastQC and was again analysed using FastQC after each data analysis step to determine the overall effect on data quality. The initial analysis (Chapter 3.5.2.1)determined that unlike the HSA library Illumina primers were present in the GHSA library. While removal of the Illumina, forward and reverse primers was trialled, it was eventually determined that sequencing analysis on the whole library with the reverse strands removed was a more suitable option. The high quality of the unmodified data along with the speed of the Fastaptamer package enabled this decision. The workflow is below.

1. FastQC

   fastqc -i /location/Inputfile.fastq -o /location/Outputfile.fastq

2. Remove reverse strands using discard_seqs . DISCARD specifies the output file to look for at the beginning of a strand, for example the start of the 5' reverse strand GATT. All strands starting with GATT are removed.

   discard_seqs --in /location/Inputfile.fastq --/location/Outputfile.fastq --discard PATTERN

3. FastQC

   fastqc -i /location/Inputfile.fastq -o /location/Outputfile.fastq

4. Repeat aptamer sequences were counted with fastaptamer.

   perl fastaptamer_count –i /location/Inputfile.fastq –o/ location/Outputfile.fasta

Additionally the reverse strands were removed with fastx_clipper and ran using fastaptamer to check for differences in removal techniques .

fastx_clipper -a GATTCAGATGAT -C -Q33 --i /location/Inputfile.fastq -o /location/Outputfile.fastq

2.3 ELONA (Enzyme linked oligonucleotide assay) experimental

Once potential sequences have been selected by NGS analysis they need to be experimentally verified for their binding. ELONA enables multiple sequences at various concentrations and conditions to be tested in parallel. Throughout ELONA testing, one of the main points of contention was what and how blocking agents were utilised, due to this, the technique evolved over time. In the standard experimental protocol, the small changes are labelled alternative. Any ELONA experiments that did not fall within the main protocol are listed separately.

Plates are costar sterile non-treated polystyrene 96 well flat bottom plates.

Binding Buffer refers to PBS+ $MgCl_2$ at 10 mM, pH 7.2

2.3.1 Equipment and Materials

- Plate reader (Thermo Scientific VarioSkan Flash Multimode reader)
- Corning Costar plates (Sigma CLS3370-100EA)
- Binding buffer (10mM PBS + 10mM $MgCl_2$ pH7.4)
- Human serum albumin (HSA) (Sigma A3782)
- Glycated Human Serum Albumin (GHSA) (Sigma A8301)
- Immungoblobulin G (Sigma 56834)
- Casein (Sigma C7078-500G)
- Synblock (AbD Serotec BUF034A)
- Aptamers (Custom synthesised by Integrated DNA Technologies)
- Biotinylated primers (Custom synthesised by Integrated DNA Technologies)
- Streptavidin - Horseradish Peroxidase (SA-HRP) (GE Healthcare RPN1231-100ul)
- Tetramethylbenzidine Liquid Substrate (TMB) (CHBBCNN0717)
- Tissue paper

2.3.2 Standard preparation of ELONA plates with required protein.

Optimal plate incubation concentration is 20ug/ml for the immobilised protein of choice. Need 10 ml per plate but prepare at 15ml per plate. The following protocol is for 2 plates so a total of 30 ml.

2.3.3 HSA, GHSA and IGG preperations.

Prepare high concentrations (above 1 mg/ml) of each if storing to minimise protein unfolding. Max plate absorption concentration is 20ug/ml. 10ml is enough to fill an entire plate. Adjust solution volume accordingly for how many plates are being run.

2.3.3.1 Example protein preparation:

1. Prepare 4 mg/ml of HSA/fHSA/IGG in 5ml of Binding Buffer. Unused solution can be aliquoted and stored at -20^{0}C for future use. Avoid repeated freeze/thaw cycles as this will damage the protein.
2. Take 50ul of 4mg/ml stock in 9.95ml of Binding Buffer.
3. Now have 20ug/ml in 10 ml.
4. Incubate overnight at -4^{0}C. Typical incubation time 16 hours.
5. Incubate each well with 100ul of HSA solution.

2.3.4 Blocking of plates with Casein to prevent non-specific binding

1. First wash plates by incubating each well with 200ul of Binding Buffer and tapping them dry. Repeat this twice.
2. Through optimisation experiments (Chapter 3.7.1.2)it was determined 0.1% casein provided the perfect balance of effective blocking while still being soluble in water.
3. 50mg of casein in 50ml of Binding Buffer provides enough casein at 0.1% to block two plates at 200ul per well.
4. Incubate each well with 0.1% casein at a volume of 200ul.
5. Incubate for 2 hours at room temperature.

6. Wash plates by incubating each well with 200ul of Binding Buffer and tapping them dry onto tissue paper. Repeat this twice.

2.3.5 (Alternative): Blocking of plates with Synblock to prevent non-specific binding

1. First wash plates by incubating each well with 200ul of Binding Buffer and tapping them dry. Repeat this twice.
2. Incubate each plate in 200ul per well of SynBlock
3. Incubate for 2 hours at room temperature.
4. Wash plates by incubating each well (Use the same reservoir as the Synblock was in) with 200ul of Binding Buffer and tapping them dry. Repeat this twice.

2.3.6 Incubation with aptamers

1. Prepare aptamer solutions to required concentration with biotinylated primer (Aptamer Primer 1:1).
2. Incubate aptamer primer solution at 90^0C for 10 minutes then 45^0C for 10 minutes. This will enable aptamer primer hybridisation.
3. Incubate 100ul of aptamer solution per well for 2 hours.
4. Wash plates by incubating each well with 200ul of Binding Buffer (+0.05% Tween in Synblock alternative) and tapping them dry. Repeat this twice.

2.3.7 Binding detection utilising Streptavidin – Horseradish peroxidase (SA-HRP) and Tetramethylbenzidine Liquid Substrate (TMB)

1. Take 1ul of SA-HRP from stock and dilute in 10ml of Binding Buffer (Alternative: Dilute in 10ml Binding buffer with 0.05% Tween)
2. Incubate 100ul of SA-HRP Binding Buffer mix in each well.

3. Incubate for 40 minutes at room temperature.
4. Wash plates by incubating each well with 200ul of Binding Buffer + 0.05% Tween and tapping them dry. Repeat this twice.
5. Add 100ul of TMB per well and incubate for 5 minutes exactly. Should see a shift in the colour of the wells from colourless to blue. Time needs to be kept constant between experiments, as incubation time will have an effect on the absorbance.
6. Incubate each well with 1M H_2SO_4 which will stop the reaction
7. Measure the absorbance of the wells on a plate reader at 450nm.

2.3.8 Blocking tests including casein concentration ranges.

The benefits of casein, Synblock and no blocking agent were tested. Casein was tested at concentrations of 1%, 0.1% and 0.01%. Higher concentrations of casein were not possible as it would not dissolve in Binding Buffer. Two different methods were tested.

1. Method one was the utilisation of the blocking agent at only the blocking step (2 hour incubation).
2. Method two was the utilisation of the blocking agent at the blocking step and at subsequent washing steps.

Protocol was carried out as described by the standard protocol. No aptamers were utilised so the true background effect from the streptavidin-HRP could be observed.

2.4 Electrochemistry

2.4.1 Equipment

- Gamry reference 600. Potentiostat/Galvanostat/ZRA
- Ivium Compactstat potentiostat
- Electrode Cell and lid (IJ Cambria Scientific 012669)
- 3mm diameter gold disk electrodes (IJ Cambria Scientific 011171)
- Silver/Silver Chloride Reference Electrode (IJ Cambria Scientific 012167)
- Platinum counter electrode (IJ Cambria Scientific 012669)
- Computer running relevant potentiostat software
- 0.5M H_2SO_4 (Sigma 339741)
- Diamond polishing pads (IJ Cambria Scientific 012601)
- Alumina polishing pads (IJ Cambria Scientific 012600)
- 1um, 0.3um and 0.05um particle size polishing solutions. (IJ Cambria Scientific 012620,012621,012622)
- Ferrocene carboxylic acid (FCA)
- Sulfo -NHS (Thermo Scientific 24510)
- EDC (Thermo Scientific 22980)
- Ethanol (Sigma E7023)
- Aptamers + matching amine modified primers.
- PerfectHyb Plus Hybrization buffer (Sigma H 7033)
- Binding Buffer: PBS 10mM + $MgCl_2$ 10mM pH 7.4
- Mercaptohexanol (Sigma M3148)

2.4.2 Standard Electrochemistry Setup

Setup was a standard three electrode array with a gold disk working electrode, a platinum counter electrode and an Ag/AgCl reference electrode.

2.4.3 Basic procedure for the preparation of gold working electrodes

More detailed explanations follow this procedure.

1. Mechanically polish electrodes on diamond and alumina polishing pads with 1um, 0.3um and 0.05um polishing solutions.
2. Electrochemically polish electrodes by cycling the potential from -0.3V to +1.55V at $4Vs^{-1}$ in H_2SO_4 until Figure 6 is observed.
3. Incubate 100uM of amino group modified aptamer with 20uM FCA, 100uM EDC and 500uM Sulfo-NHS for 2 hours.
4. Add 50uM TCEP to the aptamer, FCA, EDC, Sulfo-NHS mix and incubate with the clean gold working electrode for 2 hours.
5. Run electrochemistry experiment.

2.4.4 Cleaning and preparation of electrodes

Gold electrodes need to be cleaned such that they are suitable for the immobilisation of DNA. Diamond polishing pads were utilised with 1um and 0.3um particle size polishing solutions and the electrodes were finished off with 0.05um polishing solution on Alumina pads. Each polishing cycle was done by keeping the gold rod electrodes perpendicular to the pad and moving them over the pad and appropriate polishing solutions in a figure of 8 pattern. This process was repeated 50 times at each polishing solution size. Once the mechanical polishing was complete, each electrode was sonicated in ethanol and then water for 10 minutes apiece. This ensured any particulates from the polishing solutions that may have been lodged in the gold were removed.

Next electrochemical cleaning was performed. This followed a well-known protocol for electrochemical cleaning (175,176) which involved the application of a +2V potential for 5s followed

by -0.35V for 10 seconds in 0.5M H_2SO_4. Then using cyclic voltammetry, the potential was cycled between -0.3V and +1.55V at 4V s^{-1} approximately 20 times or until a reproducible voltammogram could be observed. The H_2SO_4 solution was changed regularly between scans. To determine the cleanliness of the electrode the scan rate was dropped to 0.1V s^{-1}. At which point the typical graph for a clean gold electrode should be observed as shown in Figure 6. The single sharp reduction peak should be observed around +0.9V while the three oxidation peaks are located between +1.2 V and +1.4V.

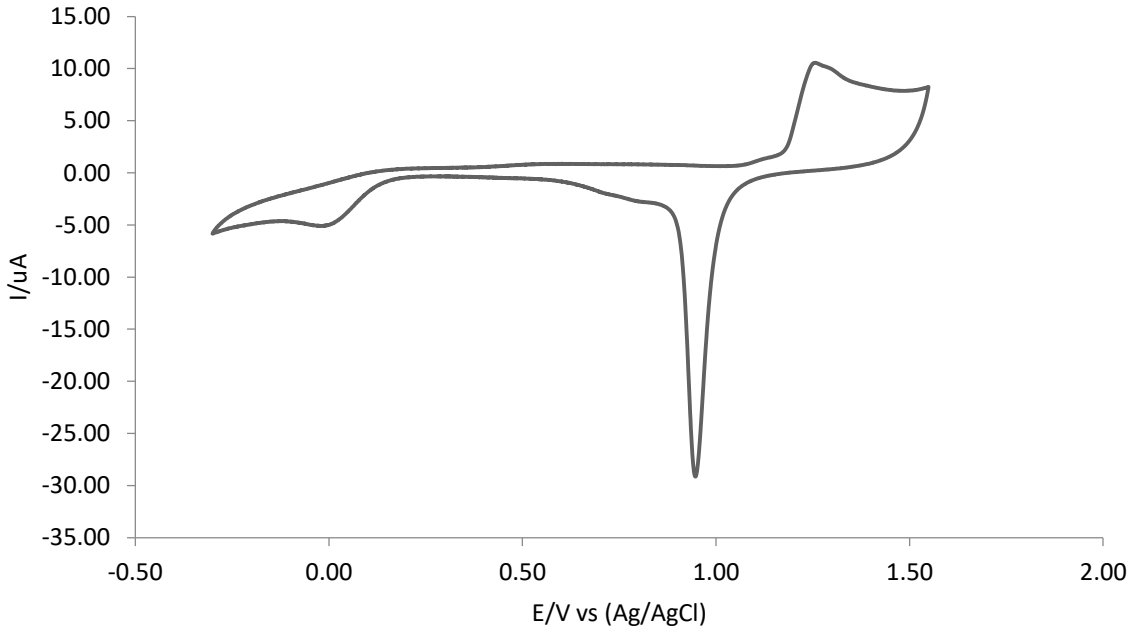

Figure 6: Cyclic Voltammetry cleaning of gold electrode in 0.5M H_2SO_4. Scan range -0.3V to 1.55V. Scan rate =0.1Vs^{-1}. Step/Interval = 0.001V. Changed H_2SO_4 solution when curve no longer progressing, typically between 10 and 20 cycles. Cycled until reached above curve. Typically between 30 and 40 scans required to reach the typical curve seen above.

2.4.5 Testing electrode electrochemistry

To check the gold disk electrodes once cleaned were working as expected an experiment involving soluble free redox probe (particularly the one attached to the aptamers) was carried out. The redox marker was ferrocene carboxylic acid (FCA), utilised because of the ease at which it can be covalently attached to aptamers with Sulfo - NHS/EDC chemistry.

Clean gold working electrode was connected in a standard three electrode setup as previously described.

Electrochemical Parameters

- Technique: Cyclic Voltammetry
- Range: 0V - 0.8V
- Scan rate: 0.5 Vs^{-1}
- Step/Interval: 0.001V

FCA was measured at 10mM, 3mM, 1mM, 300uM and 100uM. Solution volume was 5ml in each case of binding buffer (PBS 10mM + 10mM $MgCl_2$ pH 7.4)

2.4.6 Attachment of FCA to an aptamer

One of the main benefits of using aptamers over other binding motifs like antibodies is the ease at which they can be chemical modified. When utilising aptamers that are to be surface bound to an electrode and covalently attached to a redox marker one has to consider the chemistry on both the 5' and 3' ends. As the working electrode is gold, a primer was utilised that is modified at the 5' end with a thiol group. This primer was utilised instead of a modified aptamer due to savings in cost but it is realised that this may have an effect on binding, whether positive or negative. Aptamers were modified with an amino group with a 6 carbon spacer at the 5' end. Aptamers also contained a region at the 3' end that was complimentary to the thiol containing primer. Aptamer and primer were hybridised before immobilisation on to the gold electrode surface.

5' Thiol reverse primer:

/5ThioMC6-D/TTCGCAGGGTCCAAGATC
AAGCGTCCCAGGTTCTAGNNNNNNNNNNNNNNNNNNNNNNNNNNNNNNNNNNNNNNNN

Example amine modified aptamer (aptamer 3):

/5AmMC6/GATGTTCTGGCGCTACTTACTAAATATCGGCCTGTCATGGATCTTGGACCCTGCGAA

Hybridisation was carried out by utilising a 1:1 ratio of aptamer and primer in PerfectHyb Plus Hybrization buffer. Aptamers were heated for 10 minutes at 95^0C, followed by 10 minutes at 45^0C. Utilising Sulfo N-hyroxysuccinimide (Sulfo -NHS) and 1-Ethyl-3-(3-dimethylaminopropyl) carbodiimide HCl (EDC) we can crosslink a carboxylic acid with a primary amine. Hence, we can crosslink amine modified aptamer with ferrocene carboxylic acid (FCA).

For the Sulfo NHS/EDC attachment of FCA to an amine modified aptamer prepare an aptamer concentration of 100uM, FCA concentration of 20uM, EDC concentration of 100uM and Sulfo-NHS concentration of 500uM(177). Incubate all components together for 2 hours. Excess products do not need to be removed at this stage as the aptamers will be immobilised onto the surface of the gold working electrode where this excess products can be easily washed away.

2.4.7 Immobilisation of aptamers to gold working electrode

TCEP was utilised to reduce the thiol on the aptamer (93,109,178). Add 50uM TCEP to the aptamer, FCA, EDC, Sulfo-NHS mix and incubate with the cleaned gold working electrode for 2 hours. Electrodes were then washed in binding buffer and incubated for 2 hours in 10mM Mercaptohexanol to ensure blocking of the surface.

2.4.8 Electrochemical experiments

Electrochemical experiments were carried out using the aforementioned 3 electrode setup. Cyclic voltammetry (CV) and square wave voltammetry (SWV) were utilised. Experiments consisted of testing a range of aptamers against varying concentrations of analytes.

Modified electrochemical settings were often utilised depending on experiment conditions and will be outlined as such in the electrochemistry results (section 3.8). However, most experiments used the following settings.

CV settings

- Range: 0 to +0.8V

- Scan rate = 0.5Vs^{-1}
- Step/Interval = 0.001V

SWV settings

- Range:0 to +0.7V
- Step Size: 2mV
- Frequency: 100Hz
- Pulse height: 50mV

Chapter 3

Results: SELEX

3 Results

3.1 Introduction

In this chapter the selection, analysis and quantification of HSA and GHSA aptamers is noted. This comprises 4 main sections, the SELEX selection of HSA and GHSA aptamers. The analysis of the NGS sequencing data, the testing and quantification of aptamer binding utilising ELONA and the testing of an aptamer based sensor with electrochemistry.

3.2 HSA SELEX

3.2.1 Early rounds

HSA was immobilised onto the column. Measurements were taken of the HSA concentration before and after column incubation using a Nanodrop. Molecular weight was defined as 66.5 kDa and Molar extinction coefficient was 36.5k M^{-1} cm^{-1}. Total HSA concentration was 10.85mg in 2ml before incubation and 8.47mg after incubation. Based on this 21.94% of HSA bound to the column. This tallies with the data from the Ellman's reagent test which indicated 16% of HSA within the sample had a free sulfhydryl at cys-34.

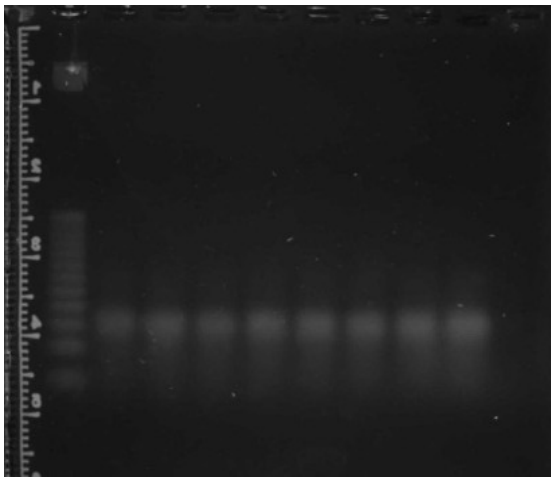

Figure 7: Electrophoresis PCR Gel. HSA SELEX round 1.

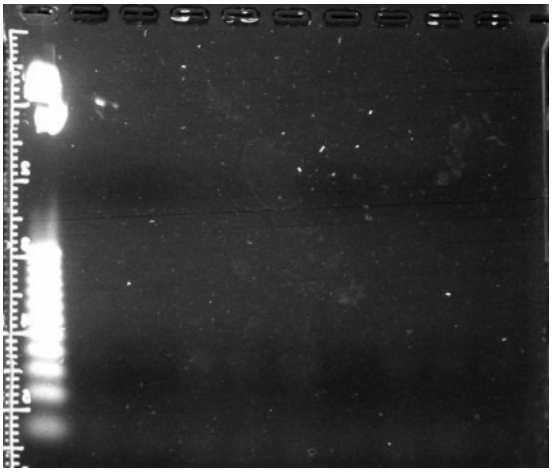

Figure 8: Electrophoresis PCR Gel. HSA SELEX round 2.

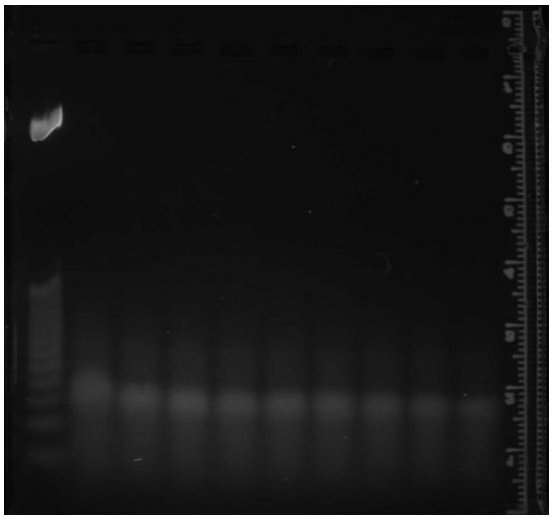

Figure 9: Electrophoresis PCR Gel. HSA SELEX round 2 + DNA starting Library.

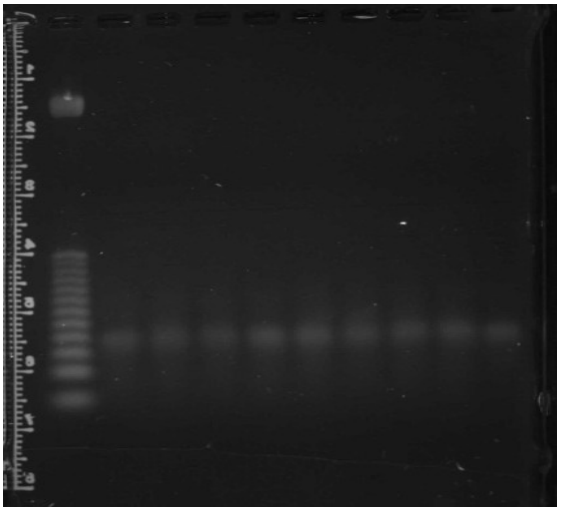

Figure 10: Electrophoresis PCR Gel. HSA SELEX round 1 New mix.

For the electrophoresis gels a 25bp DNA ladder was utilised which starts at 25bp at the bottom of the images and goes up in 25bp increments until it reaches 300bp. The broad band at the top is a 1,800bp backbone fragment; the 300bp band is generally 3 times the intensity of the lower size bands. Each band as you proceed right after the PCR ladder is three rounds of PCR, normally 9 samples are taken from the trial PCR with the 1st band (Leftmost) representing 3 rounds of PCR and the last 27 (rightmost).

In the initial trial PCR of round 1 (Figure 7) it was observed that the library was present at the correct size, however, the DNA demonstrated no amplification as the PCR rounds progressed shown by no increase in band intensity. This can be for a variety of reasons that are hard to separate. Failures could be a result of:

- Lack of aptamer binding to protein
- Loss of aptamer in the washing step
- Loss of aptamer in desalting (Not undertaken in initial rounds)
- Not enough PCR amplification due to insufficient primer of nucleotide concentrations.

Primer bands can be observed in Figure 7, however, the bands including the ladder are low in intensity, this can be attributed to too little time incubating in Sybr Gold. Original incubation time was 40 minutes. This was subsequently increased to 60 minutes. Although there was a lack of amplification, there was enough DNA present to proceed to the next round. Based on the gel, the main PCR was run 6 times (2nd band in from the left after the ladder) before moving on with the SELEX procedure.

Primer amounts were lower compared to the final protocol, the initial volumes used was 5ul (100uM) for each primer, however, these volumes were adjusted depending on the actual concentration of the stock primer (Determined by Nanodrop 1000).

Initial PCR mix:

- 200ul DNA template
- 5ul forward primer
- 5ul reverse primer
- 25ul dNTP mix @10mM
- 400ul 10x PCR buffer
- 1400ul fH_20

The ssDNA concentration after Round 1 was 6.3ng/ul which compares with 5749.9ng/ul for the DNA library (measured before the start of SELEX), this is a 99.9% reduction in total DNA. While this may seem excessive, there are still around $1.5x10^{14}$ molecules of DNA present in the sample. At this early round, many of these molecules will be unique or only number a few per group. The number of DNA molecules was calculated using the following formula and assumptions. The central 40 bases of the DNA library are random so it is difficult to know the exact molecular weight, so an assumption was made that the random region on average contained an equal distribution of all the four nucleotides.

$$\text{Number of DNA molecules} = \frac{[\text{amount of DNA(ng)} * \text{Avogadro's constant } (6.022 \times 10^{23}\ \text{mol}^{-1})]}{[\text{Molecular weight of DNA} * 1\text{x}10^{9}]}$$

Round 2 proved problematic as no aptamer appeared in the trial PCR gel. The DNA ladder was visible so it was of concern that not enough aptamer made it through the affinity purification step of the SELEX or that if aptamer was recovered it wasn't being amplified correctly. To test if there was a failure in the Trial PCR, it was rerun. Again almost no aptamer was observed (Figure 8). With this image the brightness and contrast has been increased so any potential bands can be observed. As can be seen faint bands of aptamers at the correct weight are observed. Faint primer binds can be observed indicating it is not consumed through the cycles.

To test whether there were any problems with the PCR mix (Taq polymerase or Nucleotides), original aptamer library (0.5ul at 5749.9 ng/ul) was added to the previous mix. As expected (Figure 9) the aptamers are present in each round but no amplification is apparent. Additionally we see broadening and shifting of the bands. The shifting of the bands is commonly due to the disturbance of the gel when it was running. The broadening of the bands is attributed to impurities (DNA strands that have formed complexes with other strands or failed to be synthesised to the correct length) in the starting DNA library that normally occur at too low a concentration to be visible in gels post affinity purification. As the rounds progress the ssDNA generation step using magnetic beads ensures fewer DNA contaminants remain. As a result of this later rounds have more defined aptamer bands in their trial PCR gels. Of note is the lack of amplification in the DNA library, this indicated that there were underlying issues with the PCR procedure.

At this stage it was apparent that a new PCR mix had to be created as no or very little DNA was observed in the original mix, thus recovery would have proven problematic. No previous round existed from which the DNA library could be obtained, as such the decision was made to restart the SELEX procedure with fresh reagents including DNA library, PCR mix and a new HSA column. The method and technique was identical to the previous round 1 SELEX. Figure 10 is the gel from said

SELEX round after affinity purification on a HSA column as described in Chapter 2.1. The gel is comparable to the original round 1 SELEX PCR gel (Figure 7) with amplification being of similar intensity.

The next SELEX round progressed using the DNA from round 1 under the same conditions but produced no visible DNA as was originally seen in Figure 8. Yet again the DNA ladder was present so it was apparent that a failure had occurred either in the single strand generation or with the affinity purification step. One possible answer is that the DNA from the previous round was not of a high enough concentration post PCR amplification to be retained.

The aptamer library concentration after the round 1 with the new mix (Figure 10) as measured on the Nanodrop 1000 was 10ng/ul. As this was measured post single strand generation, the affinity purification step looks culpable. The recovery of the DNA is susceptible to changes in pH, elution time and salt concentration. In these early rounds no desalting was carried out after affinity purification as there was concern that the little DNA present would also be removed. In later rounds this approach was altered.

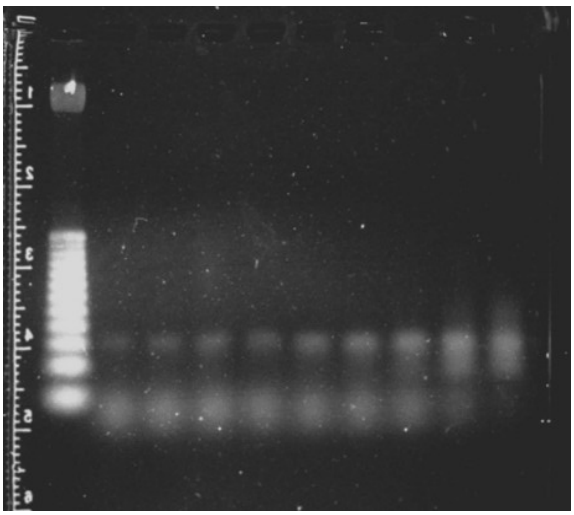

Figure 11: Electrophoresis PCR Gel. HSA round 2 combined round 1 samples.

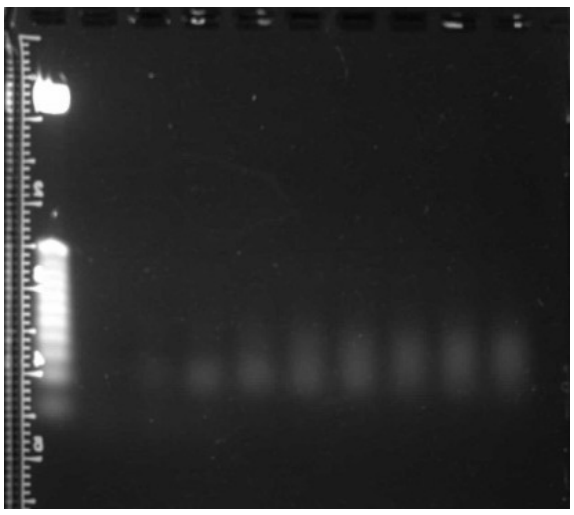

Figure 12: Electrophoresis PCR Gel. HSA round 3.

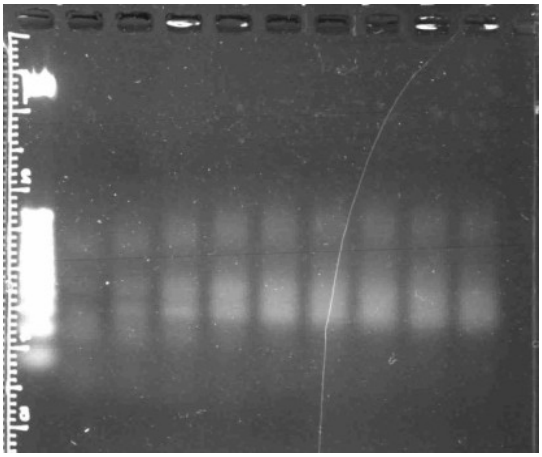

Figure 13: Electrophoresis PCR Gel. HSA round 1: New components.

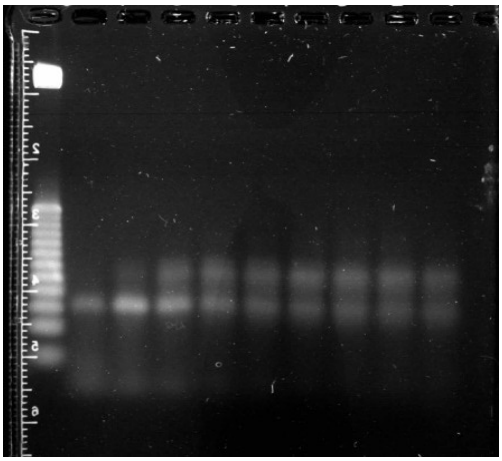

Figure 14: Electrophoresis PCR Gel. Increase primer concentration.

Saved DNA library from both the two successful round 1s were taken, combined and used as a starting point for PCR amplification. Amplification of both rounds together was to increase diversity of aptamers selected while increasing overall concentration before the next SELEX round. PCR mix was altered to reflect the smaller volumes utilised.

- 100µl 10x PCR buffer
- 2µl Forward Primer
- 2µl Reverse Primer
- 10µl DNTPs
- 15µl DNA template (Mix of the two successful round 1 selections)

After the complete initial failure of the trial PCR due to unknown circumstances , the trial PCR was performed again. The gel can be observed in Figure 11 , we can see that the DNA library is gradually amplified over the PCR cycles. Simultaneously we can see the primers decreasing in concentration, demonstrating that they are being utilised in the PCR process. The primers are particularly visible in this gel due an increase in relative concentration due to a reduction in PCR mix volume that is greater than the amount the primers volumes were reduced by. Unlike the normal PCR where the

DNA library comes in a high salt concentration solution as a result of the affinity purification, these were in just water. High salt concentrations can be problematic in PCR, , the effect of salt was tested in chapter 3.2.2.

Concentration of aptamer library post main PCR, single strand generation and ethanol precipitation was measured at 2.2 ng/µl in 500ul fH_2O. The next PCR was at standard volumes and concentrations, the resulting ssDNA after 9 rounds of PCR and the subsequent ssDNA generation was 6.1 ng/µl in 500ul fH_2O. The PCR gel (Figure 12) demonstrated broad and weak peaks. The broadening will be a result of mutations that have arisen from either excessive PCR cycles or insufficient primer concentrations. As the primer only seemed to be utilised in all PCR cycles less than expected, everything was reordered and remade. A new SELEX round was performed. Primer volumes were altered slightly and increased to 5 µl each. Figure 13 is the trial PCR gel from said PCR cycle. As can be observed the mutations have increased. The bands at more advanced PCR rounds have both broadened and split. While these want to be avoided these will be removed in the single stranded DNA generation step if the mutations include no reverse biotin primer or inaccessible biotin. However, as knowledge of what is removed isn't possible, further reduction of mutations is needed.

An additional 2 µl of forward and reverse primer were added to the PCR mix as it appeared that a lack of primer could be a cause of the mutations. There was minimal change to the mutations and the gel appeared as Figure 13.

The continuing problems with mutations and lack of amplification pointed at broader problems that had yet to be solved. One concern was that high salt concentrations were having a negative effect on the PCR. It was determined that a desalting procedure had to be introduced.

3.2.2 Removal of salt

Removed salt from aptamer solutions using PD-10 columns (GE Healthcare 17-0851-01). Columns utilised as described in the manufactures guidelines. Aptamer library was added at 500 µl followed

by 4 ml of BB/fH_2O. Fractions at 500 µl were taken so both the aptamer concentration and salt concentration could be analysed to determine at what point both were eluted. While the

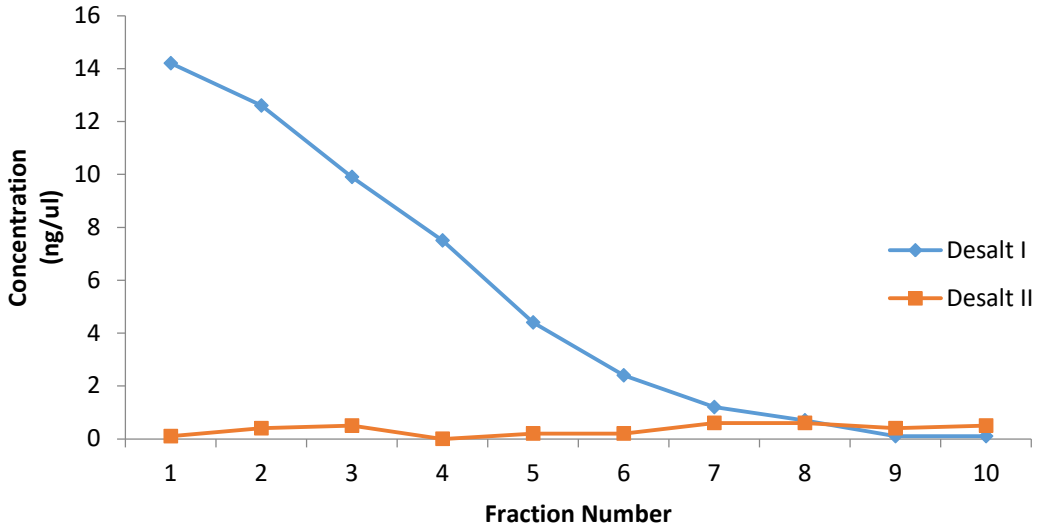

Figure 15: Plot of aliquot fraction against aptamer concentration. Desalt I was performed utilising BB as elution solution, Desalt II was performed on the same sample subsequently to Desalt I using fH20 as the elution

aptamer concentration could be directly measured on the Nanodrop 1000, salt concentration was estimated by visualisation of the salt remaining after ethanol precipitation. Typically the salt was seen to be visible around fractions 8, 9 and 10 but within this experiment the salt was visible at all fractions due to the use of BB to prepare the column. While the aptamer concentration appeared much earlier as expected. The aptamer concentration in each 500 µl fraction is plotted in Figure 15. As can be seen the aptamer concentration falls off for Desalt I as the number of fractions increases. All 10 factions were ethanol precipitated and recombined and desalted again using fH_2O as a preparation solution (Desalt II). The double desalting had a detrimental effect on aptamer concentration as demonstrated in Figure 15. Salt wasn't visible until fractions 8, 9 and 10. After recombining all fractions of Desalt II after ethanol precipitation the final concentration was 0.4 ng/µl in 200 µl. This indicated that the vast majority of aptamer had been lost. However, while the double desalting had a detrimental effect on aptamer concentration on the second pass, this experiment demonstrated on the initial pass that significant aptamer is retained, as such it was adapted in future rounds.

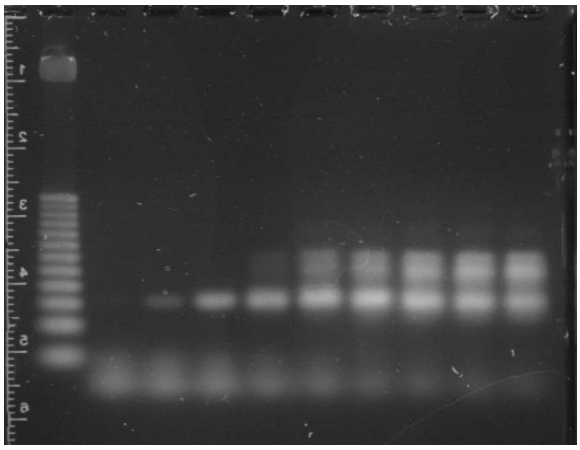

Figure 16: Electrophoresis PCR Gel. HSA round 2 increased primer volumes (8ul).

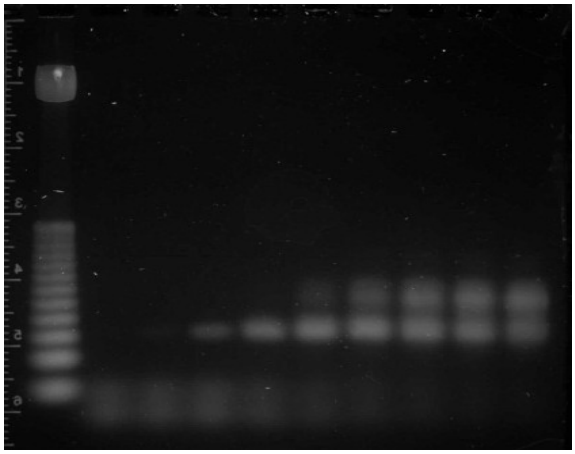

Figure 17: Electrophoresis PCR Gel. HSA round 3.

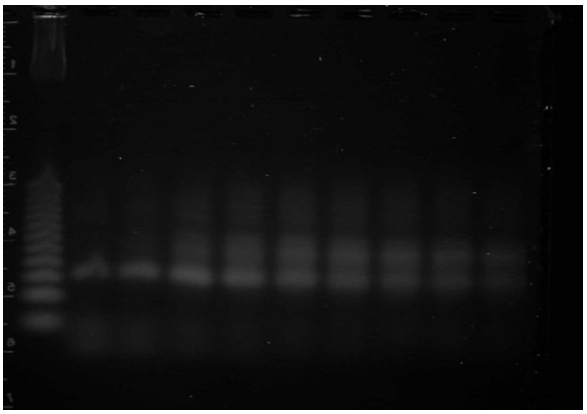

Figure 18: Electrophoresis PCR Gel. HSA round 3. 2nd round of amplification.

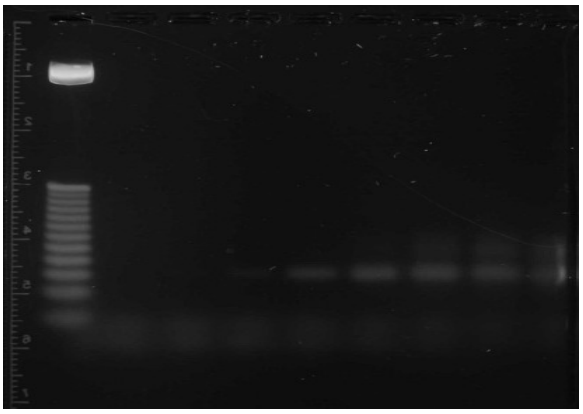

Figure 19: Electrophoresis PCR Gel. HSA round 4.

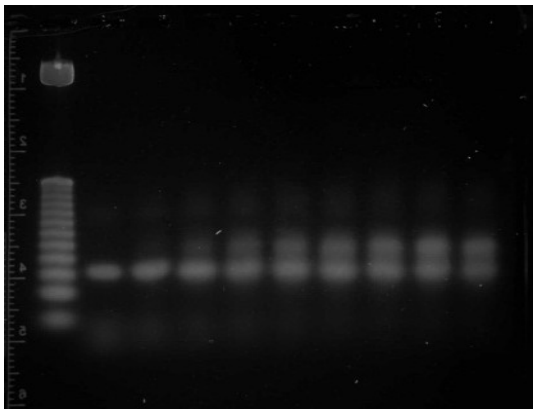

Figure 20: Electrophoresis PCR Gel. HSA round 4. 2nd round of amplification.

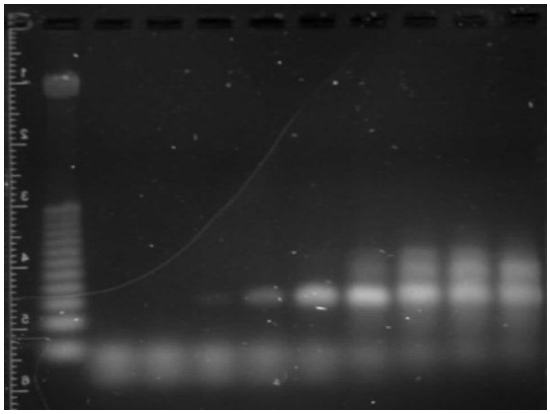

Figure 21: Electrophoresis PCR Gel. HSA round 5.

3.2.3 Continuation of rounds 1 and 2

Using what had been learnt up to this point, the SELEX process was restarted due to the vast amount of mutations that had occurred up to this point. Additionally, a new HSA affinity column was created. Starting aptamer library was combined with the two round 1 aptamer libraries and SELEX was continued. Affinity purification was undertaken and after desalting aptamer library concentration was 17 ng/µl in 200ul DNA. PCR mix volumes was also altered:

- 200 µl DNA library
- 6 µl Forward primer
- 6 µl Reverse primer
- 25 µl dNTP@10mM
- 400 µl 10x PCR Buffer
- 1400 µl fH_2O

The resulting trial PCR gel can be seen in Figure 14. We can see that at band 2, which accounts for 6 PCR cycles, we have for the first time obvious amplification, demonstrated by an increased intensity of that band. The increased primer concentration is also visible and is consumed as the PCR rounds

progress. As has been observed before but more clearly defined here is the ladder like by-products that form at approximately twice the weight of the library. This by-product formation is a known phenomenon and later work has tried to minimise this formation (179).In the next round primer concentrations were increased by a further 2 µl each to 8 µl at 100uM.

This had a positive effect on the gel and more amplification occurred before mutations arose as seen in Figure 16. End Round 2 aptamer concentration after 11 rounds of PCR was 8.1 mg/µl. At this point we had successfully finished rounds 1 and 2.

3.2.4 Rounds 3-5

Round 3 trial PCR gel can be observed in Figure 17, it demonstrates similar attributes to Figure 16 and we observe clean amplification up to 12 rounds of PCR. Concentration after this was 5.6 ng/µl in 1ml and so additional PCR amplification was undertaken. Figure 18 demonstrates the resulting trial PCR gel, multiple mutations can be observed along with smearing of the gel, most likely caused by physical movement of the gel within the electrophoresis tank. The full PCR was only run for 6 cycles to avoid mutations and 24 ng/µl of aptamer library was present after ssDNA generation. Figure 19 is the trial PCR from round 4 and while Figure 18 demonstrates the negative effects of running too many PCR cycles, we can see that by correctly picking PCR cycles that we can avoid these mutations in the next round.

Round 4 concentration was 4.5ng/µl in 1ml. Further amplification was trialled but with increased primer concentrations to determine if they were a limiting factor. Primer volumes were doubled to 16ul each. As can be seen from Figure 20, mutations arose at earlier cycles and were broader. Abundance in primer and a relative lack of DNA template could be a cause for these mutations. Due to the mutations past PCR cycle three, the full PCR was only run for this amount. After ssDNA generation, aptamer concentration was only 4.2 ng/µl in 1ml indicating a small loss from the previous amplification. As no affinity purification was performed between this amplification steps the reason for this small loss of aptamer is unknown.

Round 5 was undertaken with standard 8µl primer volumes in a 2ml PCR mix. The trial PCR gel from round 5 (Figure 21) demonstrated that the correct picking of the number of PCR cycles in the SELEX round 4 was vital in limiting mutations carried over into round 5.

3.2.5 Rounds 6-10

Round 6 proceeded without any problems and 15 cycles of PCR was undertaken to produce 5.3 ng/µl of aptamer in 1ml fH_2O (Figure 22). Round 6 trial PCR gel image was dimmer than most as reduced Sybr Gold stain was utilised due to limited resources at the time. With the start of round 7, stringency was increased. This included the addition of an additional washing step (2ml BB) in the affinity purification at step 7 of the method (Section2.1.4). The gel of the trial PCR of round 7 produced no visible aptamer but both the primers and the DNA ladder are visible as seen in Figure 23. This loss of aptamer could be a result of the increased stringency. A small amount of aptamer gets retained after each round, the aptamer that was retained from round 6 was used to restart the SELEX process.

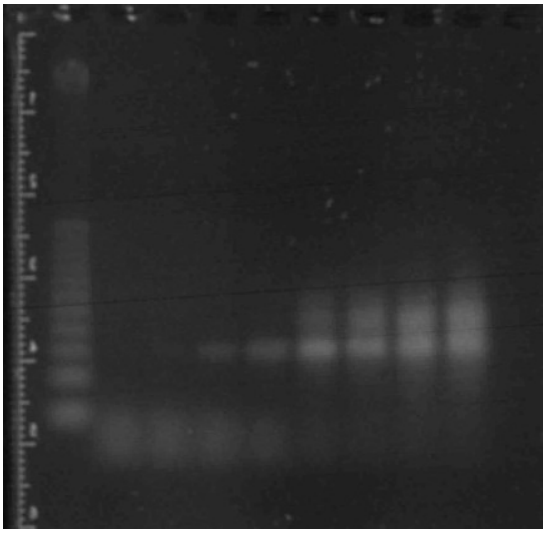

Figure 22: Electrophoresis PCR Gel. HSA round 6.

An altered PCR mix (1ml total volume) was utilised to account for the small aptamer library volume.

- 20 µl Aptamer Library
- 8 µl forward primer

- 8 µl reverse primer
- 25 µl dNTP@10mM
- 200 µl 10x PCR buffer
- 780 µl fH_2O

Aptamer concentration was 5.4 ng/µl (Figure 24). Library underwent ss generation before a further amplification round. Primers were not visible past 9 rounds of trial PCR gel, primer concentrations were doubled for the next PCR amplification round.

- 1 ml aptamer library in fH_2O from ssDNA generation
- 16 µl forward primer
- 16 µl reverse primer
- 25 µl dNTP @10mM
- 400 µl 10x PCR buffer
- 600 µl fH_2O

The trial PCR gel (Figure 25) showed multiple mutations as early as the first 3 PCR cycles but still limited primer was observed. Another trial PCR was ran with the same PCR mix but with further increased primer concentrations. Total primer volumes for both forward and reverse were 40ul each. Figure 26 demonstrates the benefit of increasing primer concentrations in this case. We see a more defined band of aptamers at the expected weight and a lower intensity of mutations at later PCR cycles compared with Figure 25. Aptamer concentration was 7.7 ng/µl in 1ml fH_2O.

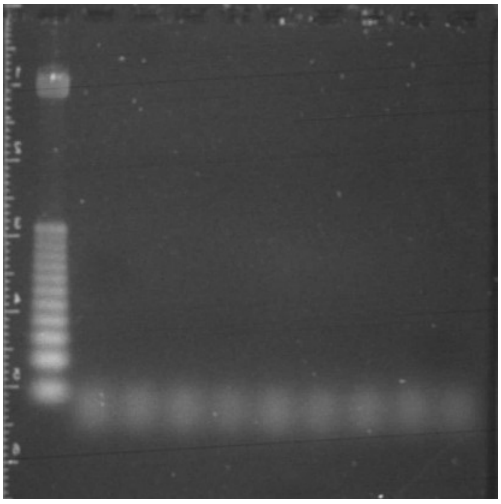

Figure 23: Electrophoresis PCR Gel. HSA round 7.

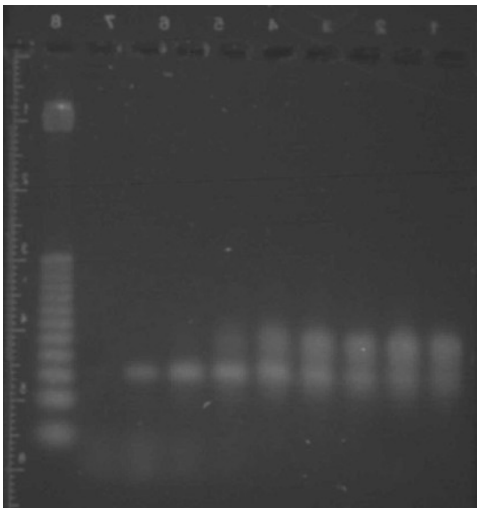

Figure 24: Electrophoresis PCR Gel. HSA round 7. Redone SELEX round.

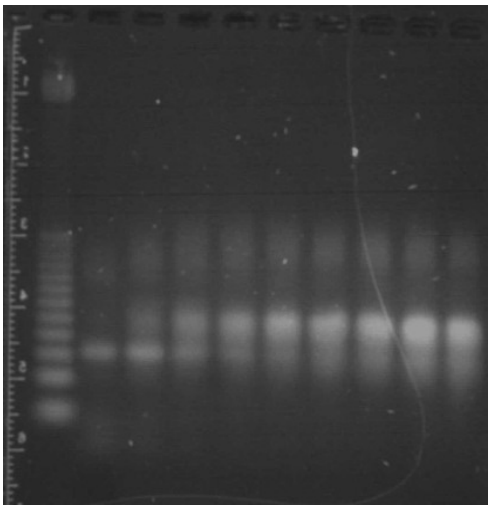

Figure 25: Electrophoresis PCR Gel. HSA round 7. 2nd round of amplification.

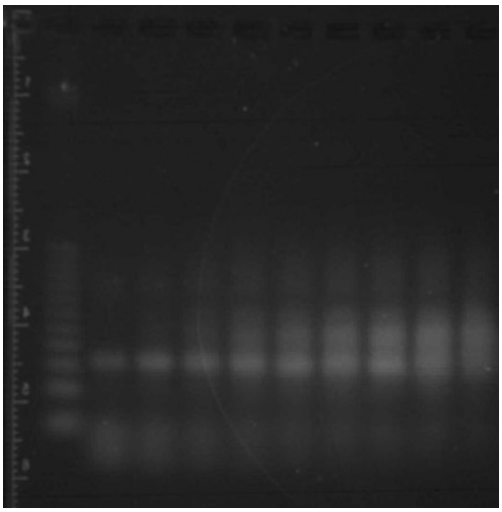

Figure 26: Electrophoresis PCR Gel. HSA round 7 2nd round of amplification with alternative primer volume (40ul).

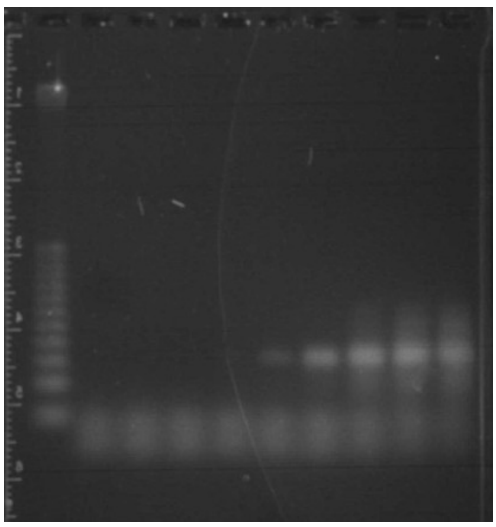

Figure 27: Electrophoresis PCR Gel. HSA round 8.

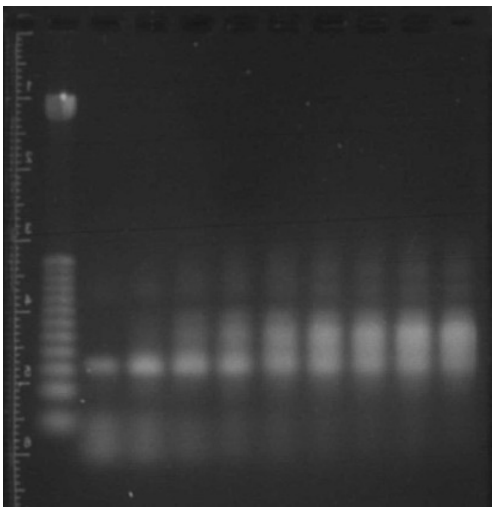

Figure 28: Electrophoresis PCR Gel. HSA round 8. 2nd round of amplification.

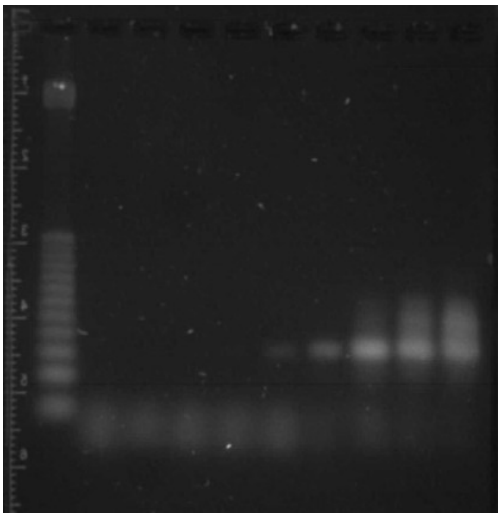

Figure 29: Electrophoresis PCR Gel. HSA round 9.

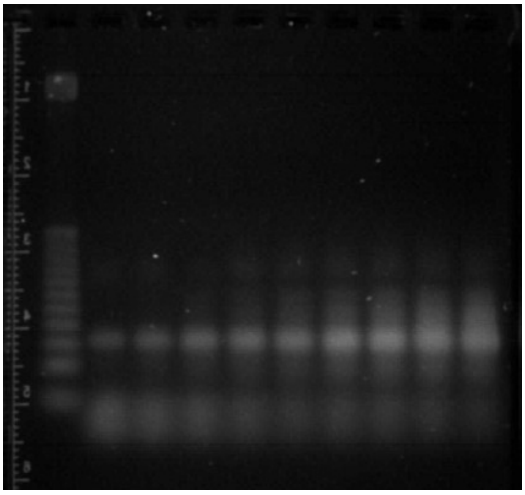

Figure 30: Electrophoresis PCR Gel. HSA round 9. 2nd round of amplification. Increased dNTP concentrations.

Start round 8. After desalting and ethanol precipitation the trial PCR gel (Figure 27) demonstrated that mutations from previous amplification were not carried through. The PCR mix was also altered to increase the relative concentrations of all components. Total PCR mix volume was 1ml. Primers were increased to 10ul each.

- 200 µl Aptamer Library
- 10 µl forward primer
- 10 µl reverse primer
- 25 µl dNTP@10mM
- 200 µl 10x PCR buffer
- 600 µl fH_2O

Aptamer library was further amplified in another round of PCR (6 cycles of PCR with main mix) (Figure 28). Final concentration at the end of round 8 was 7.2 ng/µl.

A new HSA column was created before round 9, 11.42 mg/ml of HSA was incubated with the column, HSA concentration post incubation was 3.08 mg/ml. Indicating some 73% was retained.

Round 9 followed the standard protocol with a PCR mix concentrations and volumes as in round 8. 18 cycles of PCR (Figure 29) were ran on the main mix. Aptamer concentration was 5.7ng/µl in 1ml fH_2O. Secondary amplifications of aptamer libraries have so far not generated the level of amplification that would be expected. Up to this point the focus has been on primer concentrations, it was decided to increase nucleotide (dNTP) concentration in the belief that we would see more amplification and less mutations.

The following PCR was ran:

- 1 ml Aptamer Library
- 400 µl 10x PCR buffer
- 500 µl fH_2O
- 30 µl forward
- 30 µl reverse
- 100 µl dNTP.

Figure 30 demonstrates the effect this had on the trial PCR. When compared to the additional amplification round in round 8 (Figure 28) we see that amplification can occur for more rounds before mutations occur. 12 rounds of the main PCR were run producing a final aptamer concentration of 5.8 ng/µl in 1ml fH_2O. Demonstrating almost no change in aptamer concentration. As the secondary aptamer amplification is limited and resulting in more mutations, it was removed in future SELEX rounds.

Rounds 10 and 11 proceeded with the following mix:

- 200 µl Aptamer Library
- 200 µl 10x PCR buffer
- 600 µl fH_2O

- 10 µl forward primer
- 10 µl reverse primer
- 25 µl dNTP@10mM

Rounds 10 (Figure 31) and 11 (Figure 32) proceeded without issues and generated 4.4ng/µl and 4.7ng/µl respectively of aptamer in 1ml fH_2O. A slight kink can be observed in PCR cycle 12-14 of round 10 due to an uneven agarose gel.

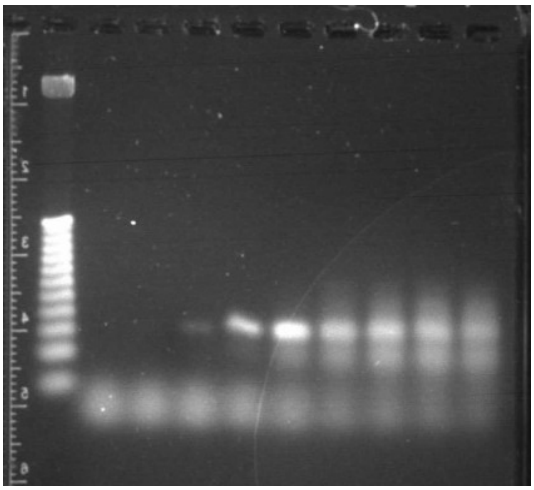

Figure 31: Electrophoresis PCR Gel. HSA round 10.

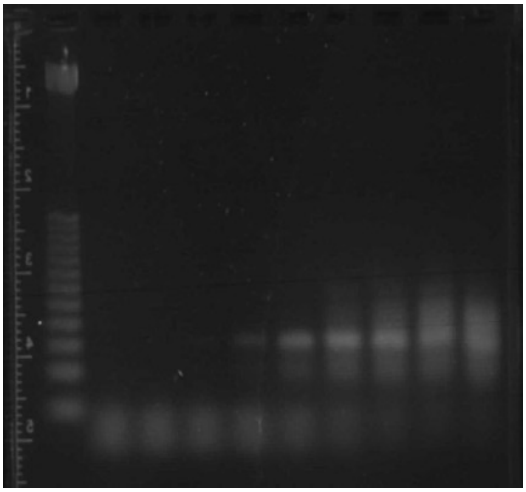

Figure 32: Electrophoresis PCR Gel. HSA round 11.

3.3 Next Generation Sequencing Sample Preparation

After the repeated failure of cloning and Sanger sequencing of the aptamer library it was determined that next generation sequencing (NGS) would be undertaken. NGS has a few innate advantages over cloning, of note is the ability to sequence every aptamer in the library compared with only a select handful with cloning. While these advantages have been well known for a while they have been out of reach of a significant portion of researchers due to cost. The cost to run NGS is now below the £500 mark which allows it to be considered for a larger range of applications.

Before NGS can be performed the aptamer library needs to be modified. The library needs to be extended and purified.

- 260/280 $\geq$ 1.8
- 260/230 $\geq$ 1.9
- Quantity = 500 ng per sample
- Concentration = 10 ng/µl
- Dissolved in RNAse-, DNAse and protease free water or Tris-HCL (pH 8.0 -8.5)
- Solution must not contain any impurities.
- Double stranded DNA above 100 bases.
- Qualitative assessment of DNA in Gel

DNA was extended from the original 76 bases to 102 by the use of extended primers in a PCR. Extended primers are below and nucleotides within the brackets highlight the aforementioned extended regions.

Extended Forward Primer 5'-(CATGACCTAGTAGT) AAGCATCCGCTGGTTGAC-3'

Extended Reverse Primer 5'-(GATTCAGATGATCG)TTCGCAGGGTCCAAGATC-3'

PCR volumes and concentrations used were:

- 100 µl aptamer library
- 10 µl forward primer (100uM stock)
- 10 µl reverse primer (100uM stock)
- 30 µl DNTP @10mM
- 300 µl fH_2O
- 100 µl 10x PCR buffer

As aptamers were to be extended it was believed that a high concentration of extended aptamers and DNTP were needed to facilitate as near complete extension of the DNA library as possible.

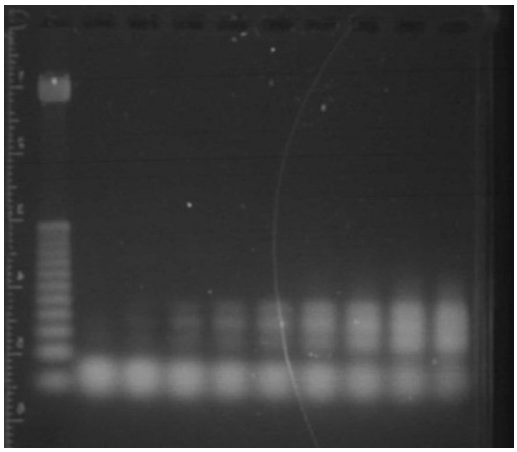

Figure 33: Electrophoresis PCR Gel. Length extension of aptamer library

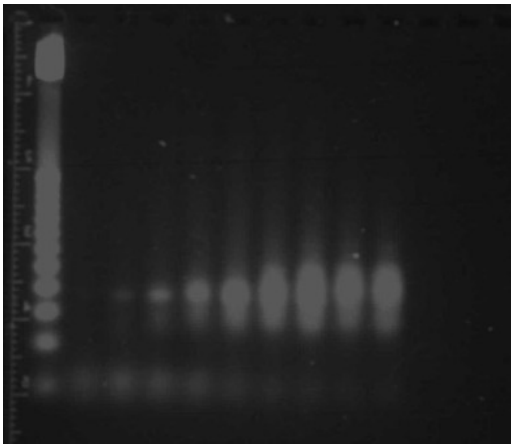

Figure 34: Electrophoresis PCR Gel. Length extension of aptamer library. Altered PCR mix.

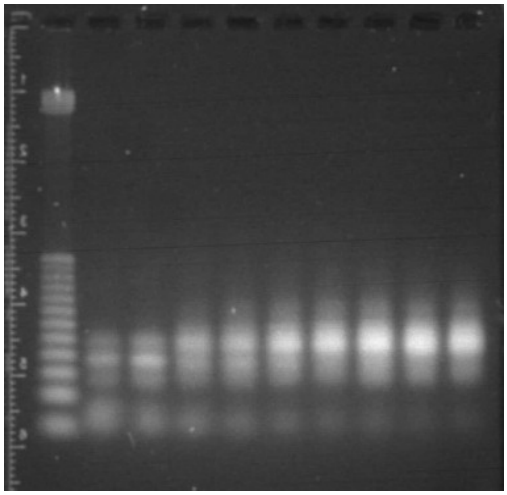

Figure 35: Electrophoresis PCR Gel. Length extension of aptamer library. 2nd round of amplification.

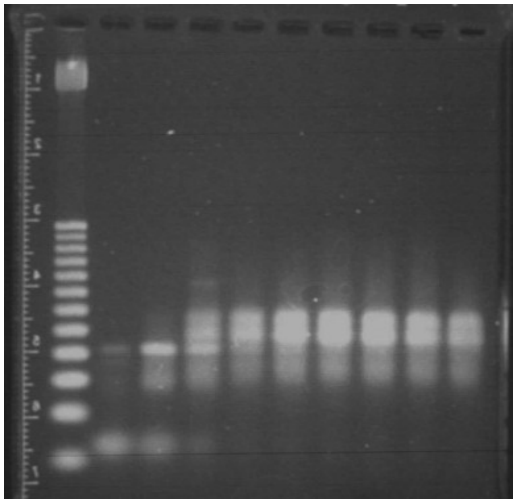

Figure 36: Electrophoresis PCR Gel. Length extension of aptamer library. New PCR mix

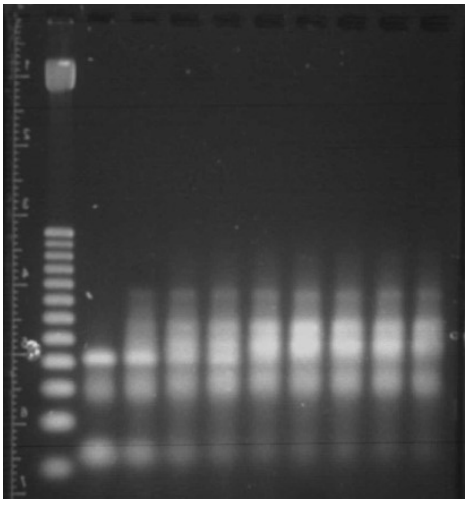

Figure 37: Electrophoresis PCR Gel. Length extension of aptamer library. 2nd round of amplification.

A high amount of mutations can be observed occurring very early in the PCR cycles (Figure 33). Too high primer concentrations may have resulted in this extremely high incidence of mutations. The original PCR mix was taken and the primer concentrations and DNTP's were diluted, aptamer library was kept consistent by increasing its volume relative to overall PCR volume.

Original aptamer PCR extension volumes and concentrations plus:

- + 400 µl PCR mix
- + 100 µl DNA library
- + 100 µl 10x PCR buffer
- +300 µl fH_2O

A trial PCR that was ran from the adapted PCR mix (Figure 34). A small gel comb (resulting in lower well volume and decreased lane spacing) was accidently utilised which resulted in the compression of the lanes. We see that 6 cycles of PCR produce an aptamer library at an increased weight that corresponds with what would be expected, 9 cycles shows further amplification with minimal mutations. A 9 cycle main PCR was ran.

QIAquick Gel extraction kit was utilised to clean up the DNA. Nanodrop concentration was 480 ng/ul for the whole PCR mix. Following the manufacture's protocol, 35ul of extended PCR mix was cleaned up and eluted in 50ul of fH_2O. The concentration of the cleaned up aptamer was 1.9ng/ul.

As this was too low the entire PCR mix of approximately 750ul (480ng/ul). 4.1ng/ul of aptamer library was eluted in 50ul. The wash off contained 407.7ng/ul of PCR components. As cleanup seemed ineffective, the entire sample was ethanol precipitated and resuspended in 50ul QIquick binding buffer. Ran the solution through the QIAquick PCR cleanup and noted a concentration of 82ng/ul in 30ul. The concentration was not sufficient to send the aptamers off for NGS, the 260/280 and 260/230 ratios also did not meet the required criteria.

The 30ul sample was further amplified and combined with 100ul of remaining DNA library. PCR mix was as follows:

- 130ul aptamer library
- 6ul forward
- 6ul reverse
- 14ul dNTP
- 130ul 10x PCR buffer
- 390ul fH_2O

At cycle 3 and 6 we can see three distinct populations not including the primers (Figure 35). The middle band of the three represents the extended aptamers with the bottom band not extended and the top band mutated. As the cycles progress past 9 we see mutations at higher weights dominate the gel.

After main PCR concentration was 346.7ng/ul. Sample was ethanol precipitated, resulting in 1533ng/ul in 100ul fH_2O. 50ul of sample was taken and cleaned up using QIAquick PCR purification. The choice of kit changed as after further investigation it was believed the PCR kit would result in a higher purity than utilising the Gel purification kit. Sample was eluted in 30ul fH_2O. Concentration was 218.7ng/ul, 260/280 = 1.89. 260/230 = 2.22.

3.3.1 Reducing mutations

Although the sample hits the quantified limits there were concerns about the levels of mutations apparent in the gel. As such a new extension and amplification procedure was performed to determine if a higher quality extended aptamer library could be generated. By keeping PCR cycles to a minimum and utilisation the PCR cleanup column mutations and impurities can be kept to a minimum while amplification can be maintained. Had retained 20ul of R11 at 4.7ng/ul which was utilised.

PCR mix

- 20ul aptamer library
- 1ul extended forward primer
- 1ul extended reverse primer
- 3ul dNTP@10 mM
- 50ul 10x PCR buffer

Unlike the normal 100ul PCR trial that is run, a 70ul trial was ran due to the volume limits on the main mix. As can been seen by Figure 36, 6 rounds produces a sharp peek with minimum broadening. Primers were visibly used up by cycle 9/12, indicating this may have been a cause of the high mutations from cycle 9 onwards. Sample was ethanol precipitated, concentration after was 498.1ng/ul in 48ul, 260/280 = 1.79. 260/230 = 2.19. After cleanup with the QIAquick PCR kit, concentration was 42 ng/ul in 30ul, 260/280 =1.82, 260/230 = 2.18. Aptamer library did not meet the required criteria. A further PCR was ran to try and further amplify the sample.

PCR mix

- 30ul aptamer library
- 3ul extended forward
- 3ul extended reverse
- 7ul dNTP@10mM
- 50ul PCR buffer
- 207ul fH_2O

Again 70ul was utilised for the trial PCR (Figure 37). Massive mutations occur from cycle 6 onwards, as such 4 cycles was utilised. Main PCR concentration post amplification was 430.7ng/ul in 230ul. Ethanol precipitation and PCR cleanup was performed. Concentration was 138.6ng/ul in 26ul fH_2O, 260/280 =1.94. 260/230 =2.17. Sample had met all quantitative and qualitative requirements after cleanup and as such the sample was used for NGS.

3.4 GHSA SELEX

With techniques learnt from the HSA aptamer selection, aptamer selection against early stage glycated HSA (GHSA) was carried out. Less total SELEX rounds were performed to reduced mutations and preferential amplification of PCR specific aptamers. With the ability to comb through the entire aptamer library with NGS it was theorised that binders could be found with less rounds.

Less total GHSA was available than HSA, 25mg of GHSA was dissolved in 2ml of coupling buffer. Initial concentration of solution as measured on a Nanodrop 1000 assuming a molecular weight of 66,500 and Molar extinction coefficient of 36,5000 was 10.46mg/ml. After immobilisation of the protein in the column, concentration of GHSA was 3.63mg/ml in the wash through. Indicating 65% was retained.

Aptamer library was prepared and concentration was 203.4ng/ul in 2ml binding buffer. In a modification to the protocol, 4ml of elution buffer (two lots of 2ml) was utilised instead of 2ml to ensure capture of all binders. Neutralisation buffer volume was increased to make sure solution was neutral as measured by pH paper. 400ul of Neutralisation buffer was utilised instead of 100ul. Unbound aptamer was measured on a Nanodrop 1000 as 55.6ng/ul in 4ml of buffer, while bound aptamer was measure as 3.7ng/ul in 4ml, representing a significant cut. After desalting on a NAP 25 column and ethanol precipitation, concentration was 107.4ng/ul in 200ul fH_20. PCR mix was:

- 200ul aptamer library
- 1400ul fH20
- 400ul PCR buffer 5x
- 25ul dNTP@ 10mM
- 10ul forward primer
- 10ul reverse primer

Two distinct bands are visible in Figure 38 indicating the potential formation of dimers as seen in HSA SELEX process. The heavier mutated band appears to be approximately twice the weight of the

correct band. An additional 10ul of both forward and reverse primer were added to the mix and the trial PCR process was repeated again. A double banding effect is still observed (Figure 39) but additionally the primer is evident as a large smear at low weight indicating further mutations have been added. After studying the literature it was discovered that one of the main causes for this observed effect was time spent at elongation temperature (72^0C) in the PCR cycle (179). Removal of this step did not fully removed the banding but instead delayed their onset. It was also observed that primer design and target had an effect on banding, both of which couldn't be altered.

The PCR protocol was adjusted so the elongation step was removed, while this will reduce the time the Taq polymerase has to synthesise complementary DNA strands it was theorised that it will still occur as the thermocycler takes time to ramp from 51^0C back to 90^0C. The following protocol was used:

1. 95^0C 3 min
2. 95^0C 30 seconds
3. 51^0C 30 seconds
4. Go to (2) repeat twice
5. Go to (2) repeat eight times

After modification of the PCR protocol, gel analysis was performed. The resulting gel image (Figure 40) demonstrated almost no change in banding compared to the previous protocol. As any mutations would potentially be removed in the single strand generation it was decided to progress. The main PCR was ran for 1 cycle (3 PCR steps) and single strand separated. Nanodrop concentration was 1.3ng/ul in 1ml fH_20. This marked the completion of round 1.

3.4.1 Round 2 - 8

A new GHSA column was created. GHSA was 25mg in 2ml . GHSA concentration before incubation was 10.51mg/ml, after incubation with the column the flow through GHSA concentration was 3.14mg/ml. Indicating a 70% retention of GHSA on the column, this was in line with the first column

created. Aptamers were incubated for 1 hour as described in chapter 2.1.4, with an initial 15 minutes of head over tail mixing. Aptamers were washed with 2ml of binding buffer instead of 1ml to increase the stringency. Once the affinity selection was completed as laid out in the methods a trial PCR was set up.

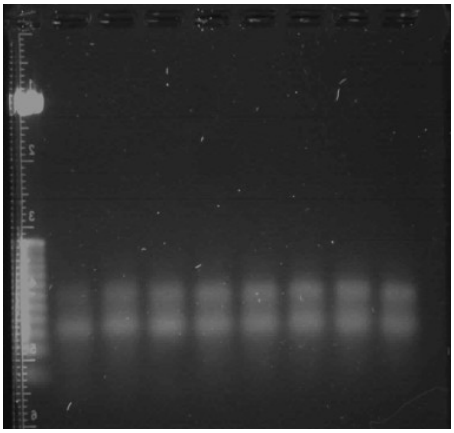

Figure 38: Electrophoresis PCR Gel. GHSA round 1.

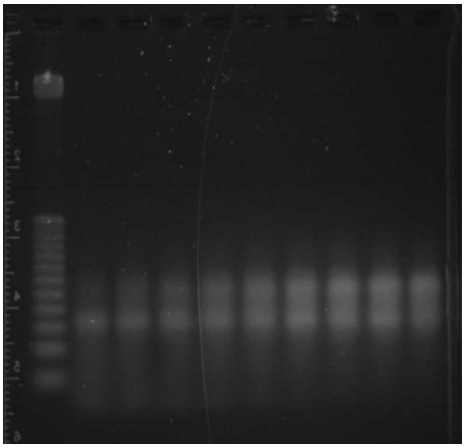

Figure 39: Electrophoresis PCR Gel. GHSA round 1. Increased primer volume (20ul).

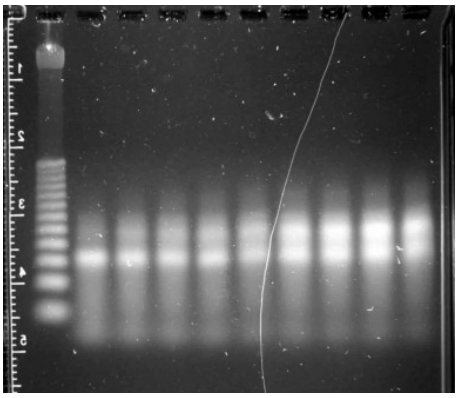

Figure 40: Electrophoresis PCR Gel. GHSA round 1. Removal of elongation step from PCR protocol.

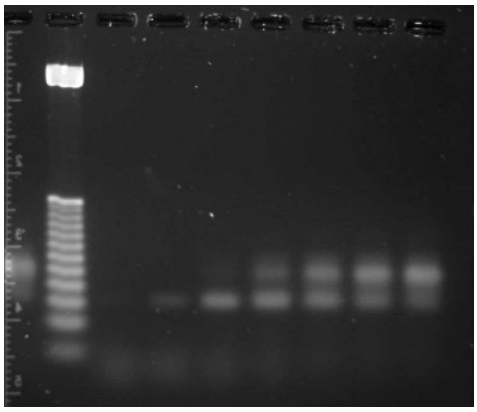

Figure 41: Electrophoresis PCR Gel. GHSA round 2.

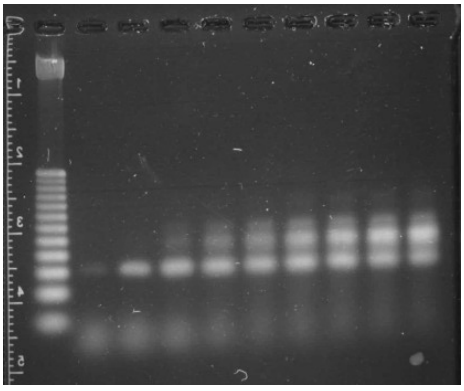

Figure 42: Electrophoresis PCR Gel. GHSA round 3

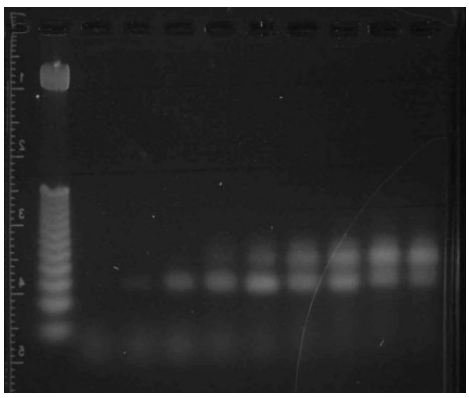

Figure 43: Electrophoresis PCR Gel. GHSA round 4.

PCR protocol was yet again run without a 72^0C elongation step.

PCR mix:

- 600ul aptamer (fH_20)
- 1000ul fH20
- 400ul pCR buffer
- 10ul forward primer
- 10ul reverse primer
- 25ul dNTP @10mM.

As demonstrated by the trial PCR gel image (Figure 41) the banding effect starts at later rounds then that seen in round 1. Concentration at the end of round 2 was 1.6ng/ul.

SELEX round 3 was carried out the same as round 2 but with a 50% increase in primer concentrations. This was done as later PCR cycles in round 2 demonstrated little primer concentration which may have aided in creating mutations. PCR mix was as follows:

- 600ul aptamer (fH_20)
- 1000ul fH20
- 400ul pCR buffer
- 15ul forward primer
- 15ul reverse primer
- 25ul dNTP @10mM.

From this point rounds progressed unchanged from protocol and unlike HSA SELEX there were no additional PCR rounds per SELEX round, this was to try and reduce PCR mutations. Aptamer library concentrations at the end of each round and PCR cycles performed can be found in Table 1. Washing stringency was increased at round 4 from 2ml of binding buffer to 4ml of binding buffer in two separate washes. New GHSA column was created at the start of round 6 with an GHSA incubation concentration of 10.47mg/ml and a flow through concentration of 3.20 mg/ml (69% retention).

3.4.2 Counter selection

As well as GHSA selection, counter selection rounds were performed at round 5 and round 7. Counter selection involved exposing the library to HSA columns and retaining the wash off (Figure 44 and Figure 46) but disposing off the binders (Figure 48 and Figure 49), this was done in an effort to find only aptamer that bind to GHSA and not both. HSA column in round 5 had a HSA incubation concentration of 12.14mg/ml with a flow through of 5.05mg/ml (58% retained). Counter selection gels containing aptamer that bound to the HSA column can be seen in Figures (Figure 48 and Figure 49). It appears that in Figure 49 we see no aptamer present but both the ladder and primer are. While this does indicate that by the 2nd counter selection round no HSA binding aptamers were present, one has to be careful with such assumption as it was discovered at a later date that the Taq polymerase may not have been working correctly and had produced a similar result in another experiment. As such it is difficult to know what concentration of HSA binding aptamers were present.

Round	PCR cycles performed	Aptamer concentration(ng/ul) in 1ml fH_20
1	3	1.3
2	8	1.6
3	6	2.0
4	9	2.0
5	12	1.5
6	7	1.9
7	12	2.0
8	21	1.2

Table 1: GHSA Aptamer library concentration of each round post desalting and ethanol precipitation.

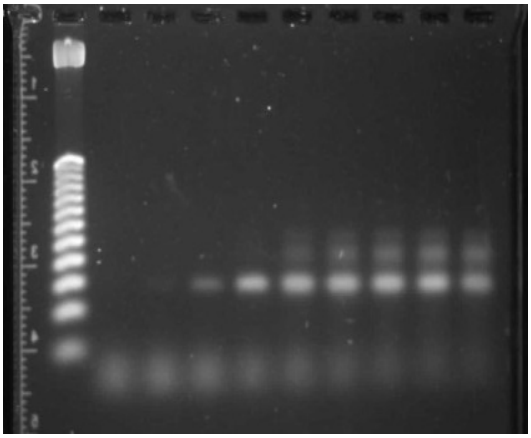

Figure 44: Electrophoresis PCR Gel of non HSA binders. GHSA counter selection round 5.

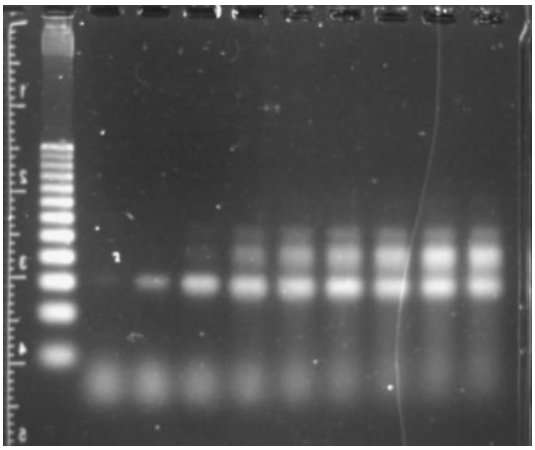

Figure 45: Electrophoresis PCR Gel. GHSA round 6.

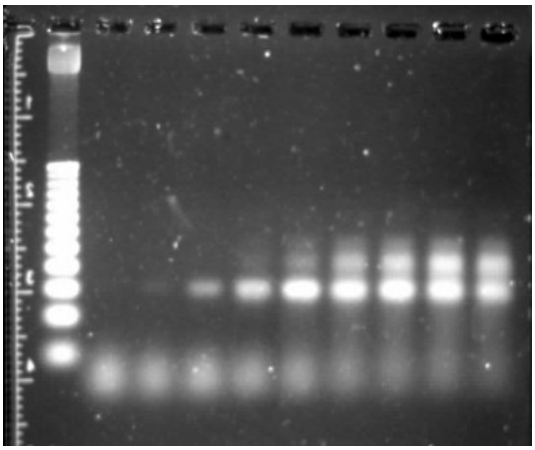

Figure 46: Electrophoresis PCR Gel of non HSA binders. GHSA counter selection round 7.

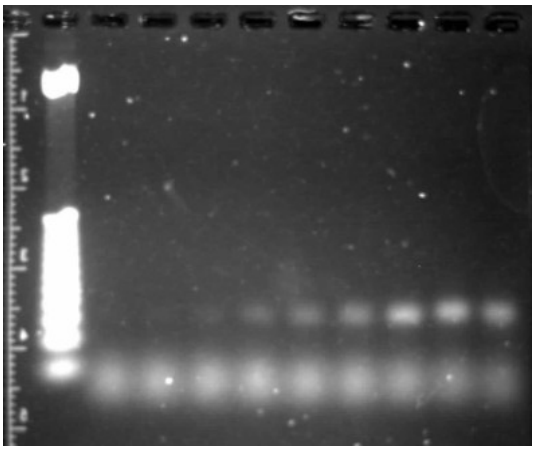

Figure 47: Electrophoresis PCR Gel. GHSA round 8

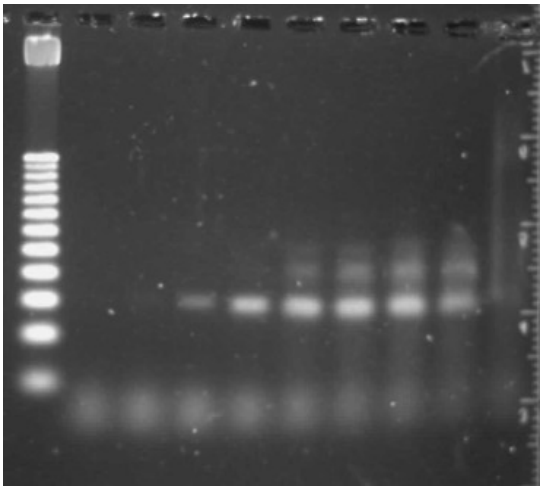

Figure 48: Electrophoresis PCR Gel of HSA binders. GHSA counter selection round 5.

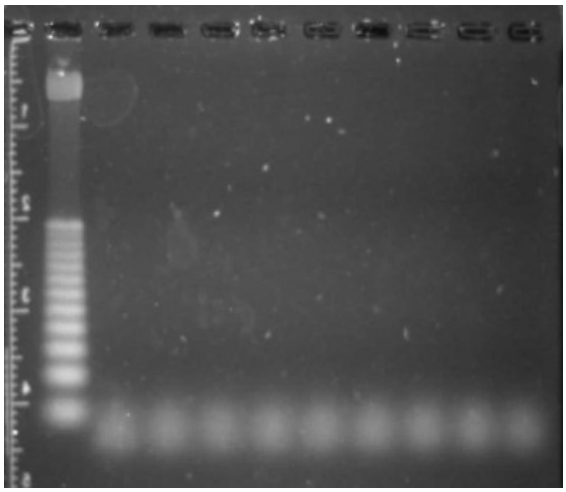

Figure 49: Electrophoresis PCR Gel of HSA binders. GHSA counter selection round 7.

3.4.3 Amplification and elongation of GHSA library in preparation for NGS

Similar to HSA aptamer generation it was decided to perform NGS on the aptamer library due to the aforementioned advantages. However, the aptamer library needs to be modified before this can occur. The library needs to be both extended and purified. The sample needs to meet the following criteria:

- 260/280 $\geq$ 1.8
- 260/230 $\geq$ 1.9
- Quantity = 500ng per sample
- Concentration = 10ng/ul
- Dissolved in RNAse-, DNAse and protease free water or Tris-HCL (pH 8.0 -8.5)
- Solution must not contain any impurities.
- Double stranded DNA above 100 bases.
- Qualitative assessment of DNA in Gel

DNA was extended from the original 76 bases to 102 by the use of extended primers in a PCR.

Extended primers are below and nucleotides within the brackets highlight the aforementioned extended regions.

Extended Forward Primer 5'-(CATGACCTAGTAGT) AAGCATCCGCTGGTTGAC-3'

Extended Reverse Primer 5'-(GATTCAGATGATCG)TTCGCAGGGTCCAAGATC-3'

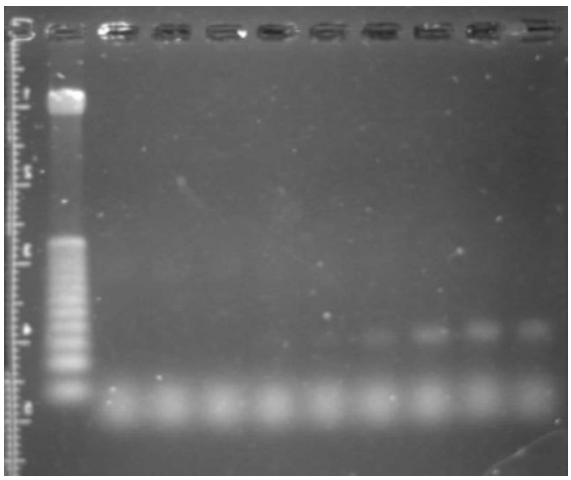

Figure 50: Electrophoresis PCR Gel amplification of GHSA library.

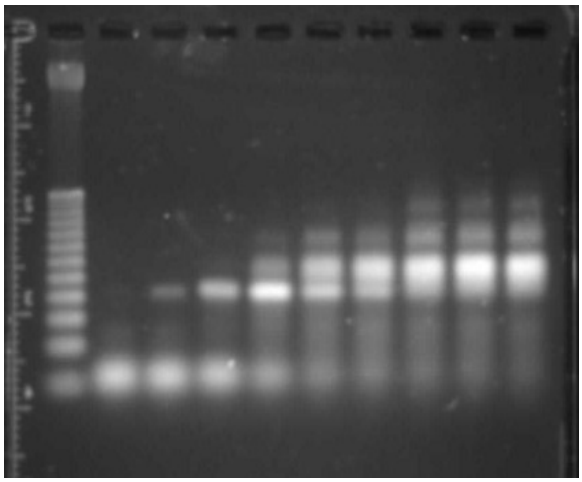

Figure 51: Electrophoresis PCR Gel. Length extension of GHSA aptamer library.

Before utilising extended primers, PCR was performed utilising the original primers to try and amplify the library. The PCR protocol previously utilised in the latter GSHA rounds which did not include the elongation step was utilised. PCR mix was as follows:

- 1ml aptamer (fH_20)
- 600ul fH20
- 400ul pCR buffer
- 15ul forward primer
- 15ul reverse primer
- 25ul dNTP @10mM.

Very small amounts of DNA were present in the trial PCR (Figure 50), based on the gel, 7 cycles were performed (24 total PCR cycles). This resulted in 1.7ng/ul of DNA in 1ml fH_20, a very small

amplification. It was hypothesised that this may be due to the removal of the elongation step from the PCR protocol. The elongation step was added back in so the PCR protocol matched the original protocol seen in the methods section. Additionally, it was decided to utilise the extended primers. The PCR mix was as before. Strong defined bands are observed indicating good amplification (Figure 51). 3 cycles were performed (9 PCR cycles) as this appeared to give the best amplification with limited mutations. It is also apparent from the gel that the extension of the library from 76 to 102 bases was successful as all the main bands appear within the 100bp range according to the ladder.

After the standard ethanol precipitation, the sample was purified utilising the Qiagen QIAquick PCR purification kit. Readings as measured on a Nanodrop 1000 were:

- Concentration: 313 ng/ul in 30ul fH_20
- 260/280 ratio: 1.87
- 260/230 ratio: 2.30

As this matched the aforementioned criteria the sample was sent off for NGS analysis.

Chapter 3.5

Results: NGS analysis

3.5 NGS analysis

3.5.1 HSA NGS analysis

3.5.1.1 Cleanup of data

Before sequencing of the data can be performed, the data needs to be cleaned up. The workflow for this can be found in section 2.2.5.2. FastQC was utilised to check the quality of the data(170).

Basic statistics

- Total sequences = 6368505
- Sequence length = 101
- 52 %GC
- Encoding : Sanger / Illumina 1.9
- Sequences flagged as poor quality = 0

At over 6 million sequences we have an abundance of data far beyond what is achievable from cloning. Of immediate note is that the average sequence length is noted as 101 bases. Theoretically we expect the aptamers to be 104 bases in length. This reduction in average length is most likely attributable to the limitations of the Illumina technology, it is well know that bases at the end are either not read or read incorrectly (180).Throughout the cleaning of data, quality scores across bases were observed. Figure 52 - Figure 57 demonstrate the effect various stages of cleaning have on the quality of the data.

Figure 52 - Figure 57 demonstrate quality (Phred) scores plotted against nucleotide position for the HSA NGS data. BoxWhisker plots are drawn, where:

- Median value = red line
- Inter-quartile range (25%-75%) = yellow box
- 10% and 90% represented by upper and lower whiskers respectively

- Mean quality = blue line

Phred scores are the probability that a given base is called incorrectly, a Phred score above 30 represents a base call accuracy of above 99.9%, while below 20 is 99% and below 10 is 90% (181,182). Phred scores are based on a range of error probabilities and have been shown to be one of the most accurate ways of determining the combined error probabilities arising from the synthesis technology(181,183).

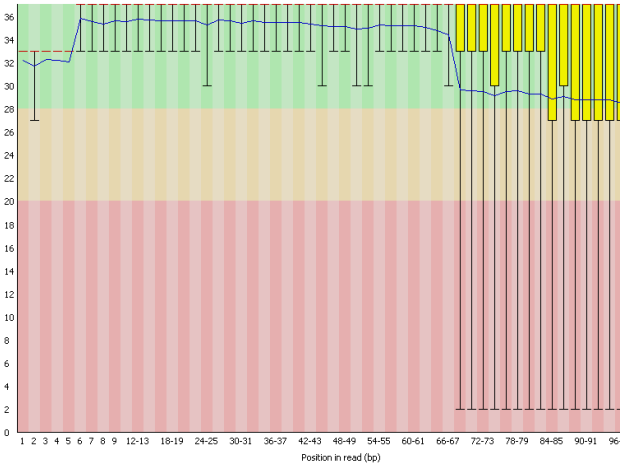

Figure 52: HSA NGS data. Quality (Phred) scores against base position. Original unmodified HSA NGS data.

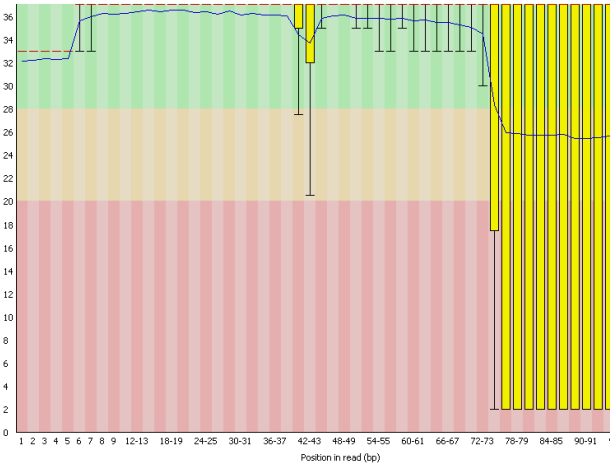

Figure 53: HSA NGS data. Quality (Phred) scores against base position. Reverse strand removed.

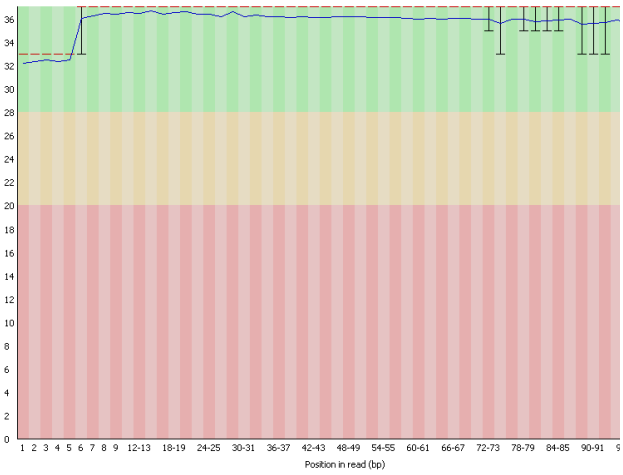

Figure 54: HSA NGS data. Quality (Phred) scores against base position. Removal of homogenous regions above 4 bases.

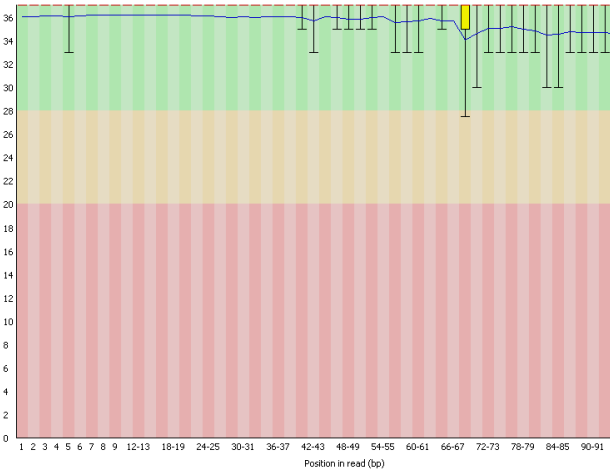

Figure 55: HSA NGS data. Quality (Phred) scores against base position. Trimming of primer regions from 5' end.

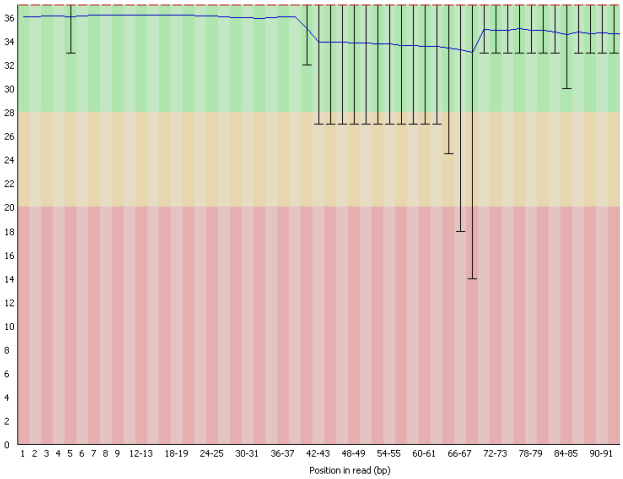

Figure 56: HSA NGS data. Quality (Phred) scores against base position. Trimming of primer regions from 3' end.

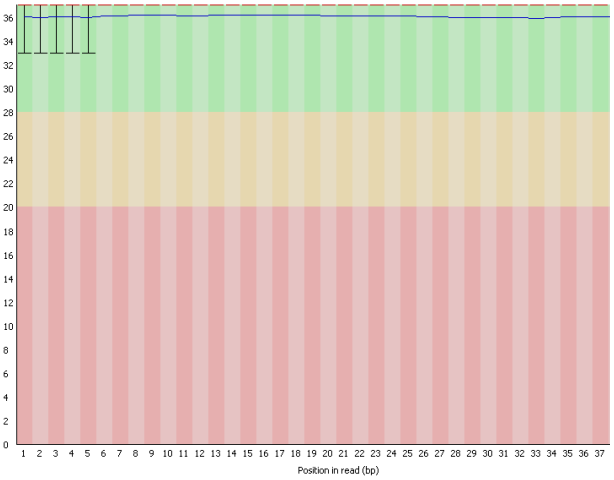

Figure 57: HSA NGS data. Quality (Phred) scores against base position. Removal of all strands that are not 40 bases in length.

We see that removal of reverse strands has a detrimental effect on two regions, the 3' end and bases between 38 and 42 (Figure 53). Sequencing chemistry degrades towards the end of a run, as can be observed in Figure 52 the original data demonstrates a reduction in Phred score the closer to the end of the run you get. While Phred scores are a calculated probability based on peak intensity of the synthesised nucleotide, the probability does not just relate to the detection sensors but also the synthesis chemistry. In areas with irregular nucleotide arrangements like large base repeat regions we can expect problems with the technology calling the right base, as overlapping signals and phasing or pre-phasing (Phasing: synthesising base not incorporated on the correct cycle. Pre-phasing: More than one base is incorporated on a cycle.) could occur with more frequency. Once the reverse strands are removed, the homogenous strands in that data set are also removed, this leaves the forward library and any mutations which did not start with the reverse strand primer. Large regions of homogenous bases (same base recurring again and again) will be a result of PCR mutations, while small mutations can be useful, long sections of the strands (especially in known primer regions as is generally the case in this data set) are unlikely to be binders and need to be removed. Additionally they are typically hard to synthesise. Any homogenous regions above 4 bases were removed; 4 was decided as the cut-off as known aptamers typically have no more then 4 base repeats in a strand and the difficulty in synthesising 5 base repeats and above is substantial.

The effect of removing entire strands that have homogenous nucleotide regions above 4 is demonstrated in Figure 54. We see all mean quality values now read above 30. The low Phred Scores between bases 38 and 42 are also removed indicating we were observing a region of unusual nucleotide chemistry, likely as a result from a large base repeat region. This region falls within the random region, so while it was removed here, in another analysis we include these aptamers to determine if this region was important for binding (Section 3.5.1.4).

Next in the cleanup process, primers were removed. Figure 55 demonstrates the clipping of 5' primer region. We see a shift of the phred scores from between 72 and 100 to 40 and 68, a 32 base

shift which equals the extended aptamer length. While the vast majority of aptamers within this library will have this primer region there will still be a significant number of aptamers which have mutated and don't include this region. This means they'll not be clipped, so any signals from above 72 will be of mutated aptamers which depending on their composition could deliver lower Phred scores. This effect is exaggerated further when we remove the 3' primer region (Figure 57). We see that Phred reads above 40 bases will now be of only mutated strands. When strands above and below 40 bases are removed (Figure 57) we observe that our random region contains bases with high quality scores. Strands above and below 40 were removed because it was reasoned that any strands that were in this size range after the removal of the primers were mutated strands that were not a representation of the SELEX process but a representation of PCR mutations. While additions or deletions of bases could result in beneficial binding, they are due to PCR mutations and could be present due to preferential amplification or repeat systematic mutations. They were removed from the dataset, however later analysis (FASTAptamer) included these to determine if any potential binders were missed.

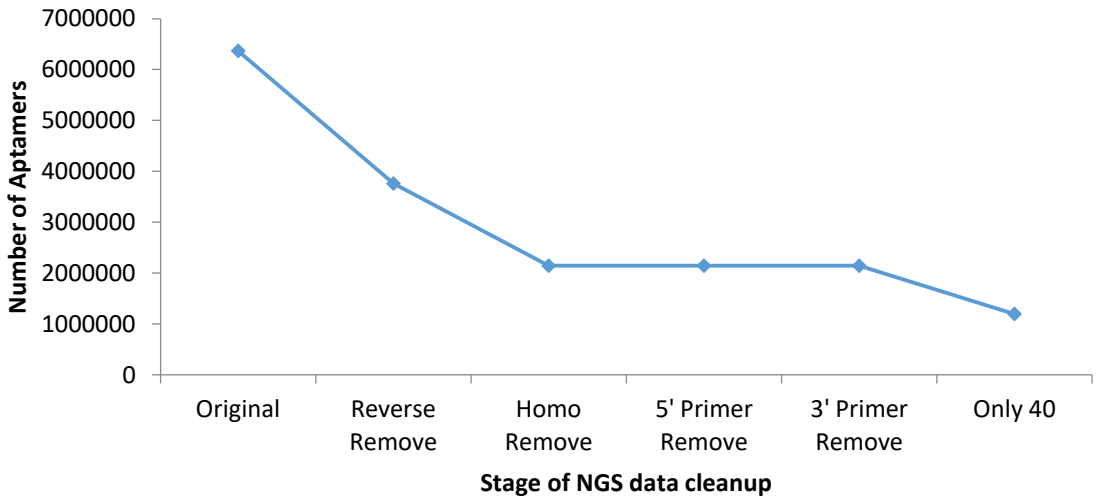

Figure 58: Changes in number of total aptamers throughout the NGS data cleanup process.

Figure 58 demonstrates how many aptamers by total volume are removed though the data cleaning process, total retained sequences of 1198028, represents 19% of the total starting volume. When only considering forward strands, the final cleaned data represents 32% of the forward strands. The reverse strands compromised 41% of the entire library. The 9% difference from the theoretical 50% can be attributed to mutated strands that are not closely related to either the forward or reverse strands.

Illumina adaptor primers were present in data. 16.44% of strands in the original unmodified data set contain Illumina Single End PCR Primer 1. Once the reverse strands were removed, 27.20% of strands contained TruSeq Adapter, Index 5.

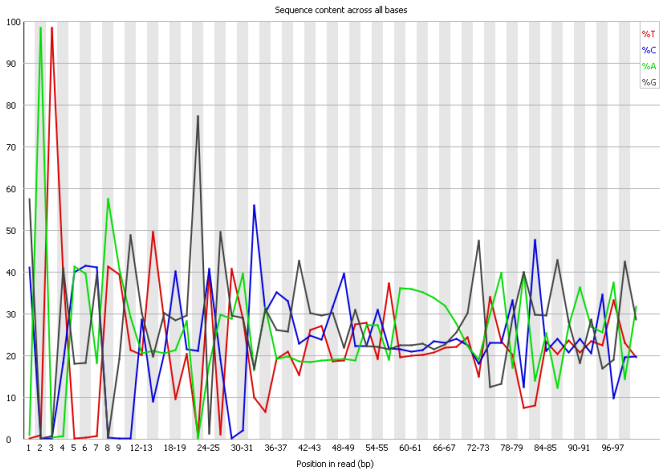

Figure 59: HSA NGS data. Plot of sequence content across all bases. Original unmodified HSA NGS data.

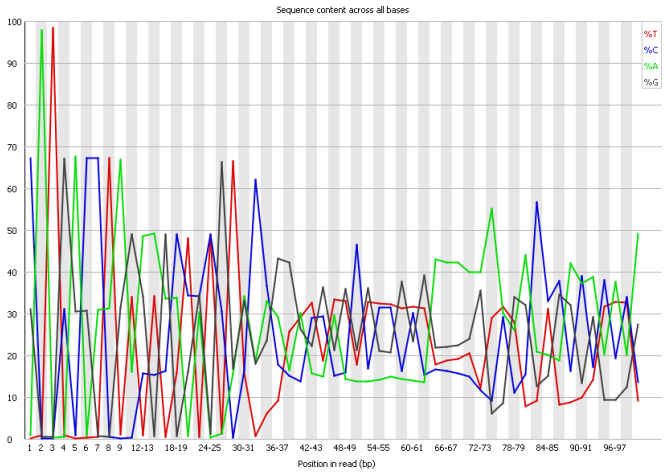

Figure 60: HSA NGS data. Plot of sequence content across all bases. Reverse strand removed.

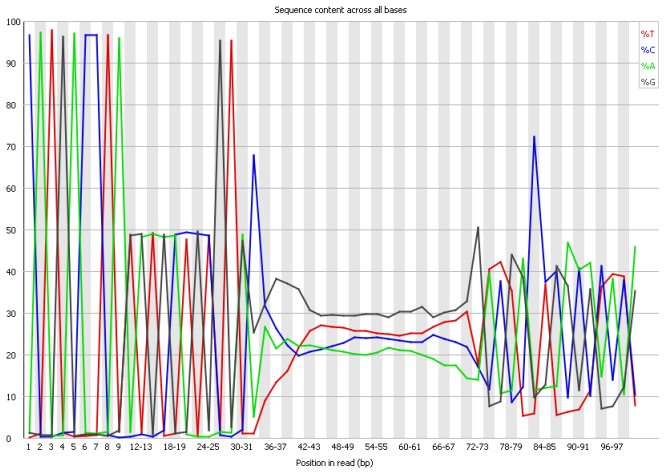

Figure 61: HSA NGS data. Plot of sequence content across all bases. Removal of homogonous regions above 4 bases.

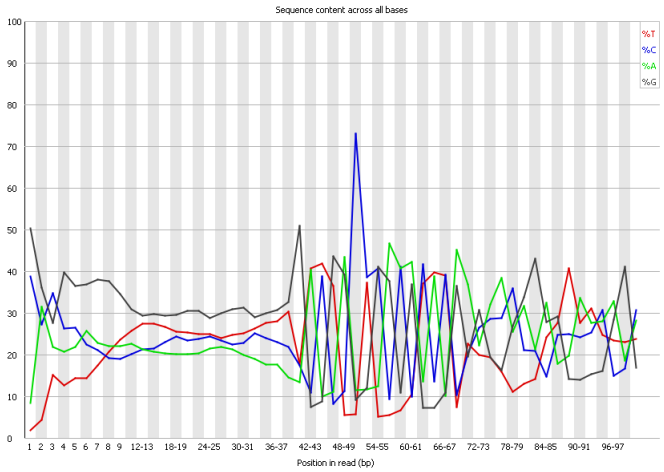

Figure 62: HSA NGS data. Plot of sequence content across all bases. Trimming of primer regions from 5' end.

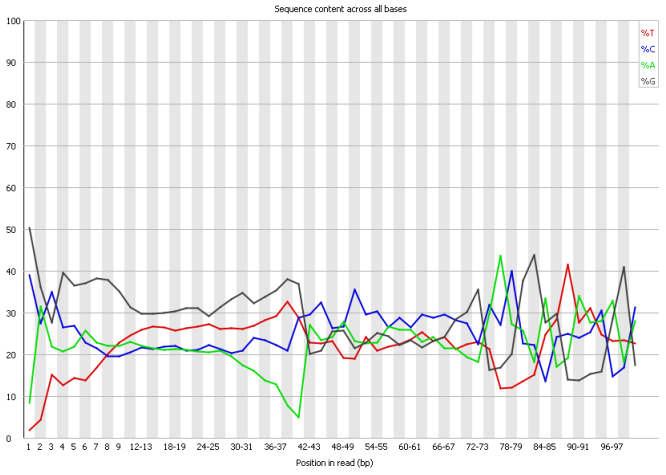

Figure 63: HSA NGS data. Plot of sequence content across all bases. Trimming of primer regions from 3' end.

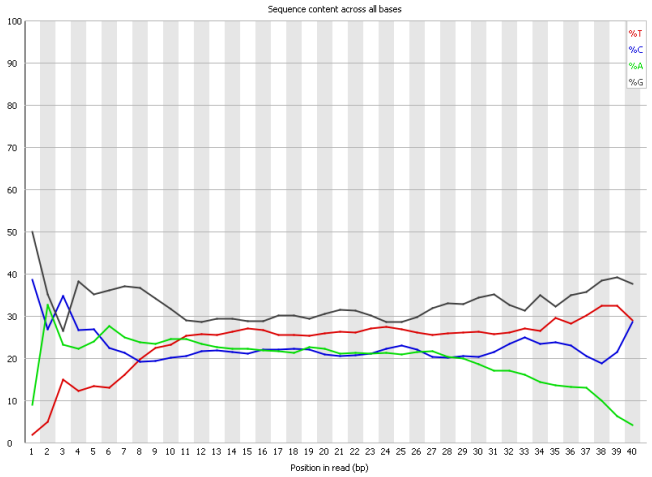

Figure 64: HSA NGS data. Plot of sequence content across all bases. Removal of all strands that are not 40 bases in length.

Figure 59 to Figure 64 plot the nucleotide we expect at each base position averaged out over the whole library. Theoretically we would expect bases before 32 and between 72 - 104 to have either a 100% or 0% nucleotide presence and as we are expecting more diversity within the random region, the nucleotide amount per position should be less polar. What is demonstrated in the original unmodified data (Figure 59) is that mutated strands affect this distribution. Upon removal of the reverse strands (Figure 60) and in particular the homogenous strands (Figure 61) we see that the theoretical nucleotide distribution takes shape. Of note in Figure 61 is that the forward prime region is more defined than the reverse prime region. While looking at the distribution of over represented Illumina adopter primers, it was noted that most occurred towards the end of the read. All strands were ligated to the Illumina adaptors but short mutated strands which ligated to them may not have been removed from the data. This results in the reverse prime region being more heterogeneous than would be expected.

Noting overall duplication levels, we should observe the figures in Table 2 which records total duplicate count, along with total sequence count. As is evident from Table 2, we have a low amount of duplicates once mutated strands are removed. This is not unexpected as a relatively low number of affinity cycles were performed in the SELEX process. While there is a relatively low amount of complete duplicates, many more may hold similar structures or just vary by a few bases.

Stage	Duplicates (%)	Total Sequences	Duplicate Sequences
Original	25.15	6368505	1601679.008
Reverse Remove	36.82	3760924	1384772.217
Homo Remove	9.19	2146048	197221.8112
5' Primer Remove	7.39	2146048	158592.9472
3' Primer Remove	9.88	2146048	212029.5424
Only 40	1.54	1198028	18449.6312

Table 2: Amount of duplicate sequences as a proportion of complete sequences over various stages of NGS data cleanup.

3.5.1.2 Cutadapt data

Clipping of both the forward and reverse strands produced that allowed a further look into the distribution and quality of data.

Cutting of the 5' primer adaptor sequence CATGACCTAGTAGTAAGCATCCGCTGGTTGAC demonstrated that a region of 32 bases was removed in 2,005,810 of the strands. This represents 93.47% of the strands at this stage. The distribution of the removal of bases can be observed in Figure 65. As is observed a comparatively low number of regions that weren't 32 bases in length were removed. The next two most significant number of base regions removed was 54,736 that were 31 in length and 9,940 that were 33 bases in length. This removal of strands that were not identical to the input sequence is due to cutadapt searching for not just identical regions but similar regions. The 31 and 33 base length regions would have a removed and additional base respectively within the known adaptor region.

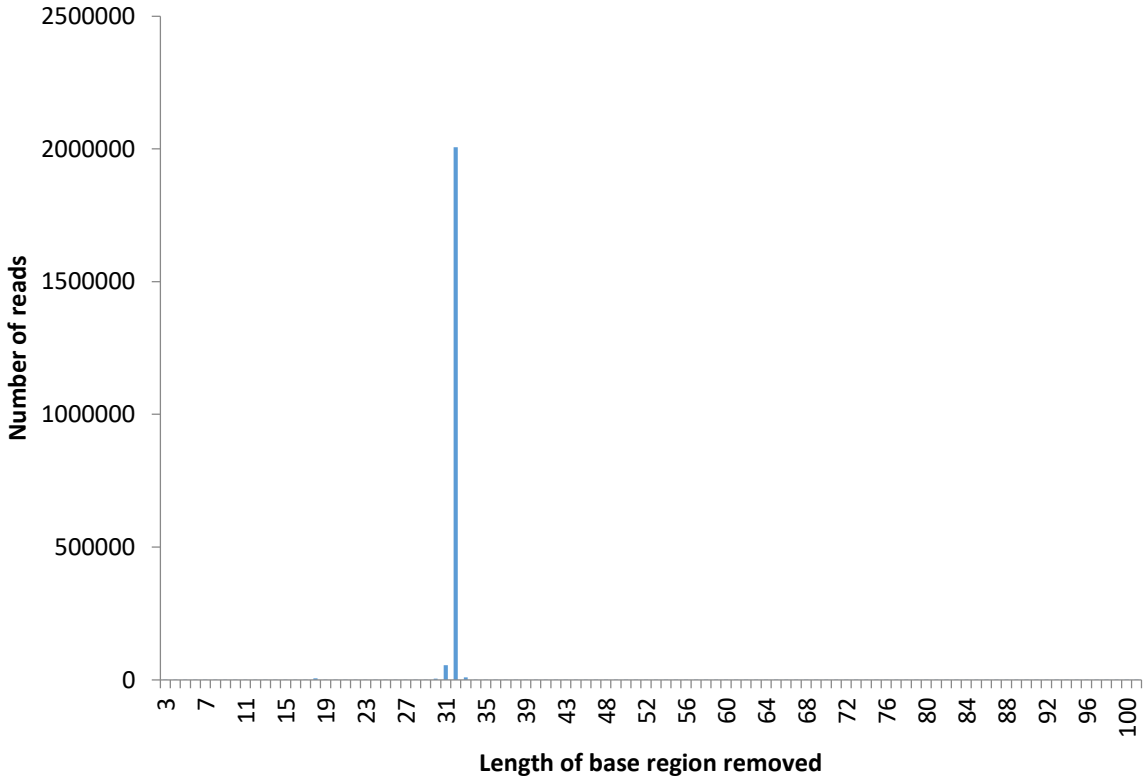

Figure 65: Number of bases removed against number of reads they were removed from. Plotted for the 5' clipped aptamer library.

Removal of the adaptor region from the 3' end resulted in a less defined peak around 32 bases. Cutting of the 3' primer adaptor sequence GATCTTGGACCCTGCGAACGATCATCTGAATC demonstrated that a region of 29 bases was removed in 1,250,497 of the strands. This represents 58.27% of the strands available. While a region of the expected 32 bases was removed in 16,844 cases (0.78%). This 3 base removal was demonstrated by the FastQC data which observed 101 bases were present instead of the expected 104. This change in peak bases removed and a wider distribution of bases removed (Figure 66) than from the 5' prime region is expected based on the FastQC data (Figure 56).

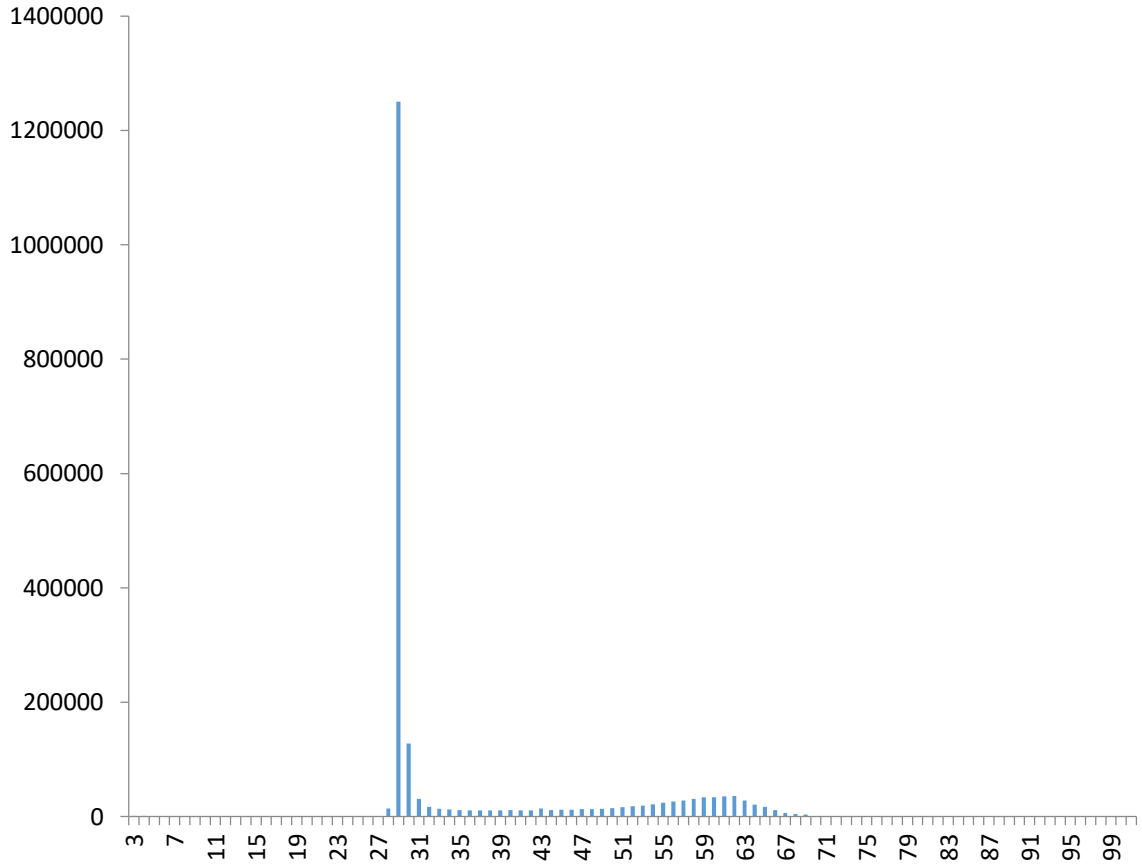

Figure 66: Number of bases removed against number of reads they were removed from. Plotted for the 3' clipped aptamer library.

3.5.1.3 MAFFT and Clustal Omega (HSA)

After cleanup of the data, it was analysed by various software packages to determine which aptamer sequences could be potential binders.

When the HSA SELEX aptamers were first selected, no aptamer specific software existed. A few packages were trialled but eventually MAFFT and Clustal Omega were chosen to select aptamers. Both are normally utilised for a variety of genomic applications (168,169,184–186). All alignments generated were viewed in JalView.

Both MAFFT and Clustal Omega aim to align strands into groups of similar sequences, often referred to as families. These clusters of similar sequences can form family trees and can be mapped and observed by the use of Jalview.

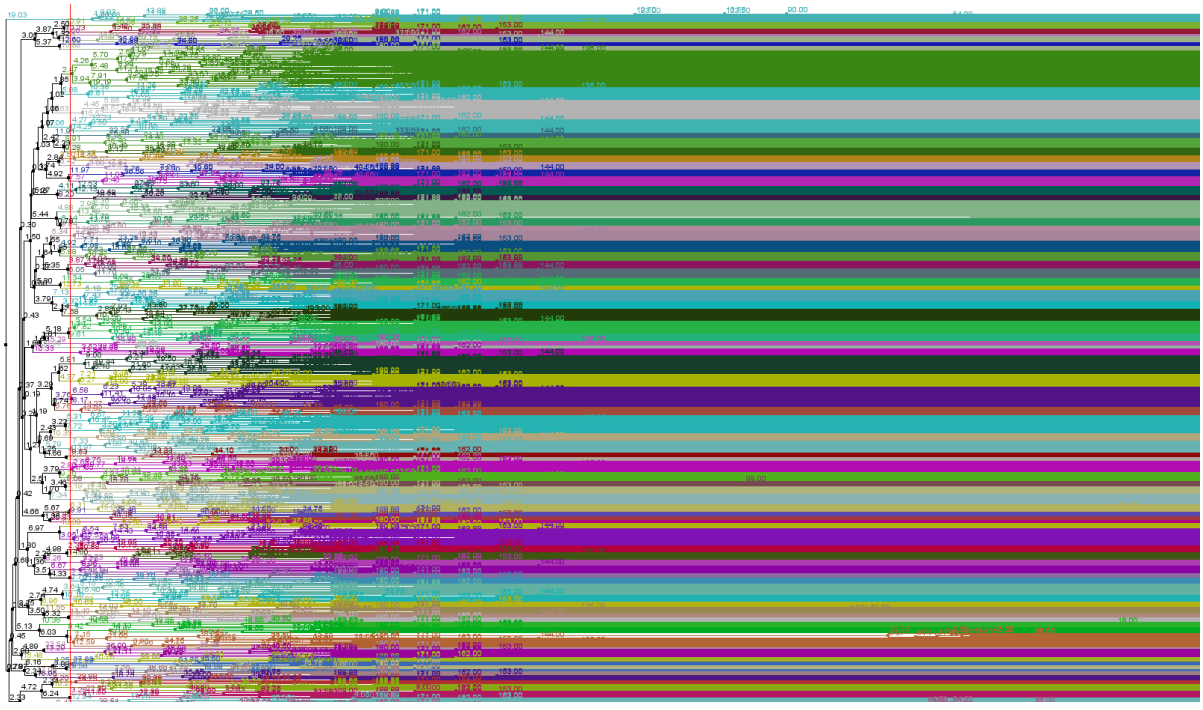

Figure 67: Overview of a selection of aptamers that have been aligned with MAFFT. A low threshold has been selected and as such aptamers are grouped in loosely related families

Within Jalview, thresholds were altered between more loosely or closely related family trees. This is represented by Figure 67 and Figure 68. Both represent an extremely small selection of the entire library as it is not possible to display it in its entirety, however, we are still observing thousands of

sequences. Here we have used a low threshold so aptamers are grouped into relatively loose families. This means several nucleotides may be different but overall sequences are similar. Compare this to Figure 68 where a high threshold has been utilised, here only identical sequences are grouped together. When we look deeper into these interactions we see Figure 69. Here we can see more clearly the groups that are generated from the MAFFT or Clustal Omega Data analysis.

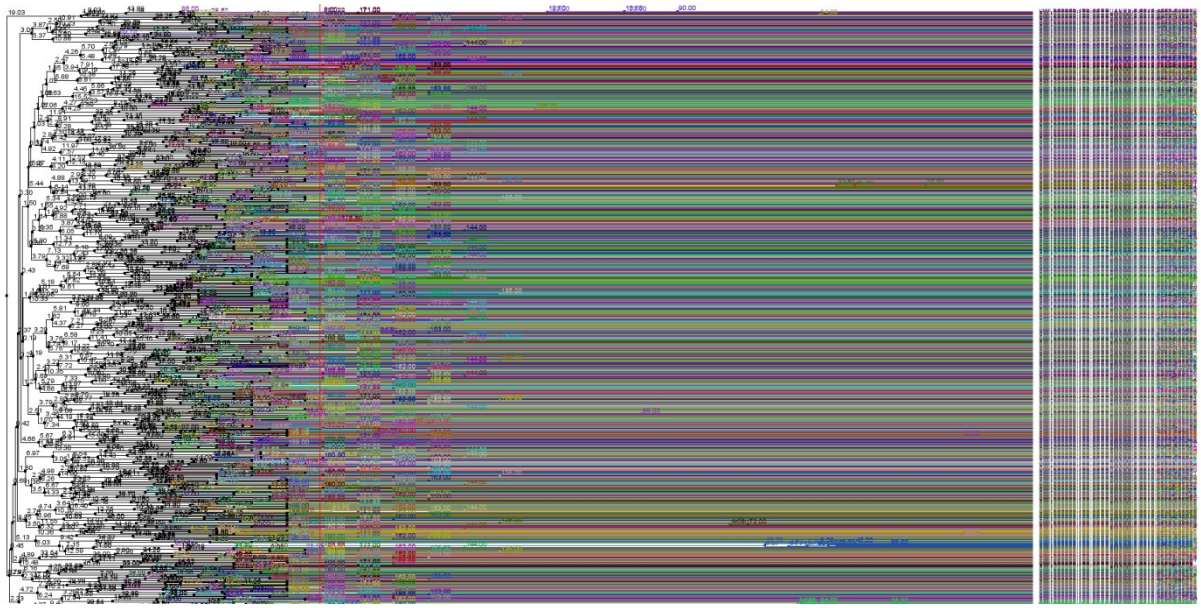

Figure 68: Overview of a selection of aptamers that have been aligned with MAFFT. A high threshold has been selected and as such aptamers are grouped in closely related families

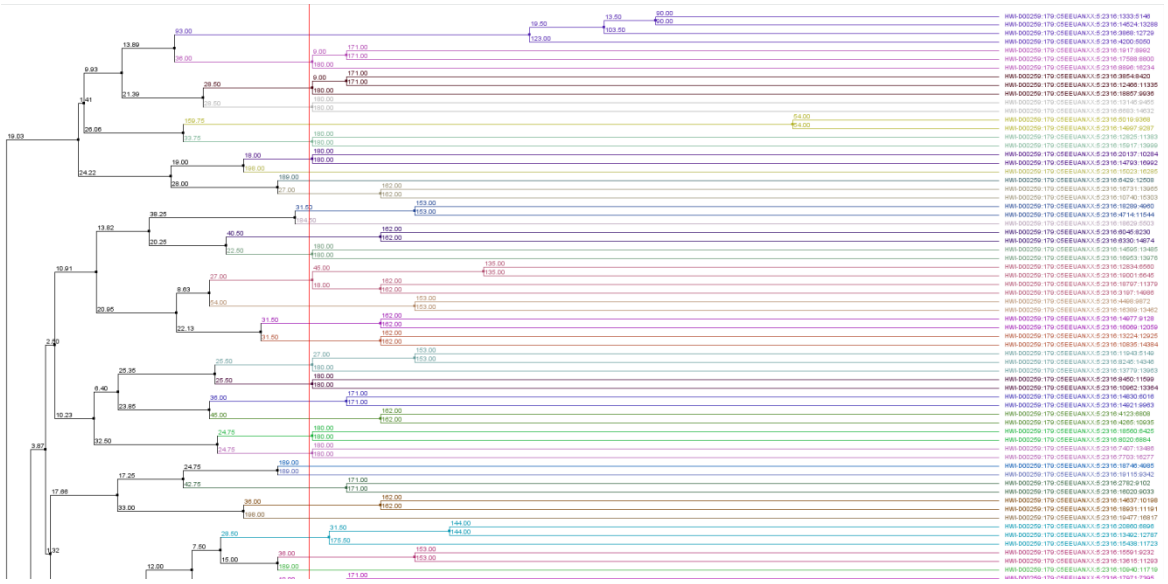

Figure 69: Overview of a small selection of aptamers that have been aligned with MAFFT. A high threshold has been selected and as such aptamers are grouped in closely related families

Thresholds were set extremely high so only almost identical sequences were analysed. The main roadblock in using MAFFT, Clustal Omega and Jalview was computational power. MAFFT and Clustal Omega could take from several hours to a few day to analyse a multi gigabit data set depending on the requirements of the analyse. Data was analysed using both the Imperial College bioinformatics server which is a 16 core setup with 128GB of RAM and a Desktop PC with a 4 core setup and 8 Gb RAM. Problems also arose when trying to view the data within Jalview as the program works within a virtual environment and RAM limitations are present often limiting the amount of data that could be viewed simultaneously.

Although Clustal Omega was trialled, MAFFT was eventually chosen for the analysis due to tis ability to work on larger data sets at a much greater speed. Once an array of aptamers were selected they were manually checked for mutations and inconsistencies like reduced or increased random region sizes, primer-primer annealing and reverse strands. Eventually 26 aptamers were selected (an additional aptamer was selected later with FASTAptamer). These aptamer were:

Table 3: HSA aptamers selected by MAFFT analysis by utilisation of Method 1 (Section 2.2.5.2). Reverse primer region shown in blue was added back post data analysis; this was to enable the binding of a complimentary strand in ELONA and electrochemistry experiments.

Aptamer 1	AGCCACGGGCGACAACTTATGCAACAGGAGCACCACCTGGATCTTGGACCCTGCGAA
Aptamer 2	GAGGGGCAATGGGATTGGCCTTGCTCGTTTGTGAGTTTCGATCTTGGACCCTGCGAA
Aptamer 3	GATGTTCTGGCGCTACTTACTAAATATCGGCCTGTCATGGATCTTGGACCCTGCGAA
Aptamer 4	GCACAGTGTTAACGTGGATGGCTTCTGTGTGGGCAGCCCGATCTTGGACCCTGCGAA
Aptamer 5	CCCGTGGAATTTGCGGTCGTGCTATGATCGACCACCCTGGATCTTGGACCCTGCGAA
Aptamer 6	GATCGGAAGAGCACACGTCTGAACTCCAGTCACACAGTGGATCTTGGACCCTGCGAA
Aptamer 7	GCGCAAGGACAAATTGTTCAAGAGCCCCGACTGTGATTAGATCTTGGACCCTGCGAA
Aptamer 8	GAATTGGGCGCAATAGTATGAGGATGACTTAGGCTCGGTGATCTTGGACCCTGCGAA

Aptamer 9	GCGGGATTATGTGTGAACGTGGCGGGCCGTGGACTTGTGGATCTTGGACCCTGCGAA
Aptamer 10	GCGCGAGAAACGATGTGTTCGGGAACGCGGGGCGGTGGTGATCTTGGACCCTGCGAA
Aptamer 11	GCAGAACGGCAGCATTGGAAGCGTGGGTTTTGTGTAACGGATCTTGGACCCTGCGAA
Aptamer 12	CGCATAGGACGGGTGTATGGATTTACTTTCGTCATGTTGGATCTTGGACCCTGCGAA
Aptamer 13	CACGGCCTGCAGATGTTGTGTATGGTCCGACCGTTGGTGGATCTTGGACCCTGCGAA
Aptamer 14	GAATTCAGATGATCGTTCGCAGGGTCCAAGATCCACAGTGATCTTGGACCCTGCGAA
Aptamer 15	CACACACATTATGTTGCACGTGTAACTGGTATCGGTTGTGATCTTGGACCCTGCGAA
Aptamer 16	GTACAGGTAGCACCTACTATTAGTTGGTTTCCGTTCCTTGATCTTGGACCCTGCGAA
Aptamer 17	CACGGGGTGACTGTCTGCATACACGTATTTCTTGTCGGTGATCTTGGACCCTGCGAA
Aptamer 18	GCGCCGATGTAGGTGTGACAGAGCGCTCTGCTGGGGTGGGATCTTGGACCCTGCGAA
Aptamer 19	GGCAAAATGTACTGGATGTTGGCTGGAGGAGTGCGTGCGGATCTTGGACCCTGCGAA
Aptamer 20	GGGAACAGCACACCAAGGGGCAATCGTGTCATAGCGTCTGATCTTGGACCCTGCGAA
Aptamer 21	GCCAACATAGTGGAGACATCCAAGCTTTGGGCGGTTTGCGATCTTGGACCCTGCGAA
Aptamer 22	GGGACCCAACGTGGTATGGTTACTGTCTACGCGGCTCCAGATCTTGGACCCTGCGAA
Aptamer 23	GGTCGATGCGAATAGTATAGGAAGTTAGTTCATTCCTGTGATCTTGGACCCTGCGAA
Aptamer 24	TTTGATTTGCGGAGCCATGTAGAGACTGCTGGCCACAATGATCTTGGACCCTGCGAA
Aptamer 25	GGAGTGGCGGAATCGTTGTCCTGCTGTGCGGTCGGACGTGATCTTGGACCCTGCGAA
Aptamer 26	GGTCCGACGCTGCATATCCGGTTTTGTCAGGATATGGGGGATCTTGGACCCTGCGAA

All aptamers except aptamers 14 and 6 were present in approximately 0.1% of the library while aptamers 6 and 14 were present in 0.2% and 2.5% of the library, respectively. We can see duplicate sequences make up a very small component of the entire library. When comparing the overall duplication levels of the original data and the reverse removed original data to the final QC data (Table 2) we see that many of the duplicates were removed with the data processing indicating that they were mutations that were favoured by PCR but were not binders. This comparatively low levels of binders to PCR mutations indicate the importance of utilising NGS to elucidate binders from the background noise.

3.5.1.4 HSA FASTAptamer

Between sequencing of HSA aptamer library and GHSA aptamer library, the FASTAptamer software package was published by Alam, Chang and Burke(173). After analysis of GHSA data, it was decided to run the HSA data through the package to try and identify any additional aptamers. A slight modification to the data preparation was undertaken as described in the next section.

Strand 1 is the only strand that wasn't heavily mutated, the rest contain significant repeat adaptor sections (Table 4). As evidenced by Table 4, 19 out of the top 20 strands selected by fastaptamer were heavily mutated with random regions typically less than 5 bases in length and prime regions ligated in a forward-reverse-forward array. This further explains the double banding seen in the SELEX gels as these repeat primer regions would have also likely occurred at higher weights. Additionally this further highlights the need for good quality controls on data that is demonstrated to be of low quality. However, quality controls will never catch all bad data and manual checks are needed to ensure the right aptamers are selected.

Strand 1's random region is 41 bases and does not contain the last 4 bases of the reverse strand (AATC). Strand 1 was synthesised with the shortened reverse primer section and tested experimentally alongside the previously selected 26 aptamers as aptamer 27.

This data set contained 1312923 sequences of which 1287129 were unique. 25,794 strands were duplicates. This low level of duplicates would be extremely difficult to detect with cloning and sanger sequencing. The data for the first 20 reads is shown unedited below, where the first number is its rank, second is the count and the third is reads per million.

A different data cleanup processes was utilised and aptamers shorter than 40 and strands that contained Illumina primers were removed. The command line below is instructing fastx_clipper to both remove strands that are shorter than 40 bases and/or start with the illumina NGS primers. As Illumina leading oligos should have been removed at point of data collection, any aptamers that contain this were most likely ligated to short mutated strands. Where *-l 40* defined strands smaller than 40 bases to removed, *-C* defined any strands containing the Illumina primer to be removed and *-Q33* defined Illumina encoding.

fastx_clipper -a GATCGGAAGAGCG -l 40 -C -Q33 -i /location/Inputfile.fastq -o /location/Outputfile.fastq

Finally reverse strands were removed. The command line below is instructing fasx_clipper to remove any strands that start with the specified sequence, in this case that is the known bases of the 5' end of the reverse strand.

fastx_clipper -a GATTCAGATGATCGTTCGCAGGGTCCAAGATC -C -Q33 -i /location/Inputfile.fastq -o /location/Outputfile.fastq

Table 4: HSA aptamers selected by fastaptamer with a reduced quality control process. Red highlighted indicated forward prime region, blue indicates reverse prime region and black is random regions. First number is it's rank, second is the count and the third is reads per million.

>1-282-214.79 - **HSA Aptamer 27**
CATGACCTAGTAGTAAGCATCCGCTGGTTGACCACCTAGGGTATTGAGTGAAAGGTGGGGTGATTGTAGTTGCGATCTTGGACCCTGCGAACGATCATCTG
>2-186-141.67
CATGACCTAGTAGTAAGCATCCGCTGGTTGACGGGGGGGATCTTGGACCCTGCGAACGATCATCTGAATCCCATGACCTAGTAGTAAGCATCCGCTGGTTG
>3-142-108.16
CATGACCTAGTAGTAAGCATCCGCTGGTTGACGGGGGGATCTTGGACCCTGCGAACGATCATCTGAATCCCATGACCTAGTAGTAAGCATCCGCTGGTTGA

>4-139-105.87
CATGACCTAGTAGTAAGCATCCGCTGGTTGACGGGGGATCTTGGACCCTGCGAACGATCATCTGAATCCCAT GACCTAGTAGTAAGCATCCGCTGGTTGAC
>5-129-98.25
CATGACCTAGTAGTAAGCATCCGCTGGTTGACGGGGGGGATCTTGGACCCTGCGAACGATCATCTGAATCTC ATGACCTAGTAGTAAGCATCCGCTGGTTG
>6-119-90.64
CATGACCTAGTAGTAAGCATCCGCTGGTTGACGGCCGATCTTGGACCCTGCGAACGATCATCTGAATCCCAT GACCTAGTAGTAAGCATCCGCTGGTTGAC
>7-118-89.88
CATGACCTAGTAGTAAGCATCCGCTGGTTGACGGGGGATCTTGGACCCTGCGAACGATCATCTGAATCTCAT GACCTAGTAGTAAGCATCCGCTGGTTGAC
>8-96-73.12
CATGACCTAGTAGTAAGCATCCGCTGGTTGACGGGGGGGGATCTTGGACCCTGCGAACGATCATCTGAATCC CATGACCTAGTAGTAAGCATCCGCTGGTT
>9-87-66.26
CATGACCTAGTAGTAAGCATCCGCTGGTTGACGGGGGGATCTTGGACCCTGCGAACGATCATCTGAATCTCA TGACCTAGTAGTAAGCATCCGCTGGTTGA
>10-85-64.74
CATGACCTAGTAGTAAGCATCCGCTGGTTGACCCCCGATCTTGGACCCTGCGAACGATCATCTGAATCCCATG ACCTAGTAGTAAGCATCCGCTGGTTGAC
>11-81-61.69
CATGACCTAGTAGTAAGCATCCGCTGGTTGACGGCCGATCTTGGACCCTGCGAACGATCATCTGAATCTCAT GACCTAGTAGTAAGCATCCGCTGGTTGAC
>12-78-59.41
CATGACCTAGTAGTAAGCATCCGCTGGTTGACGGGCGATCTTGGACCCTGCGAACGATCATCTGAATCCCAT GACCTAGTAGTAAGCATCCGCTGGTTGAC
>13-68-51.79
CATGACCTAGTAGTAAGCATCCGCTGGTTGACGGGGGGGGATCTTGGACCCTGCGAACGATCATCTGAATCT CATGACCTAGTAGTAAGCATCCGCTGGTT
>14-59-44.94
CATGACCTAGTAGTAAGCATCCGCTGGTTGACGGGCGATCTTGGACCCTGCGAACGATCATCTGAATCTCAT GACCTAGTAGTAAGCATCCGCTGGTTGAC
>15-57-43.41
CATGACCTAGTAGTAAGCATCCGCTGGTTGACCCCGATCTTGGACCCTGCGAACGATCATCTGAATCCCATGA CCTAGTAGTAAGCATCCGCTGGTTGACG
>16-55-41.89
CATGACCTAGTAGTAAGCATCCGCTGGTTGACGGCGATCTTGGACCCTGCGAACGATCATCTGAATCCCATG ACCTAGTAGTAAGCATCCGCTGGTTGACC
>17-54-41.13
CATGACCTAGTAGTAAGCATCCGCTGGTTGACGGGGATCTTGGACCCTGCGAACGATCATCTGAATCCCATG ACCTAGTAGTAAGCATCCGCTGGTTGACG
>18-52-39.61
CATGACCTAGTAGTAAGCATCCGCTGGTTGACGGCGATCTTGGACCCTGCGAACGATCATCTGAATCCCATG ACCTAGTAGTAAGCATCCGCTGGTTGACG
>19-51-38.84
CATGACCTAGTAGTAAGCATCCGCTGGTTGACGCCGATCTTGGACCCTGCGAACGATCATCTGAATCCCATG ACCTAGTAGTAAGCATCCGCTGGTTGACG

>19-51-38.84
CATGACCTAGTAGTAAGCATCCGCTGGTTGACGCCCGATCTTGGACCCTGCGAACGATCATCTGAATCCCATG ACCTAGTAGTAAGCATCCGCTGGTTGAC

3.5.2 GHSA NGS Analysis

As previously highlighted the development of the Fastaptamer software package enabled significantly quicker data analysis for the GHSA NGS data. Herein we outline the process undertaken.

3.5.2.1 Cleanup of data

Before sequencing of the data can be performed, the data went through minor quality controls. The workflow for this can be found in the experimental Chapter 2.2.5.3.

Basic statistics

- Total sequences = 4484929
- Sequence length = 126
- 50 %GC
- Encoding : Sanger / Illumina 1.9
- Sequences flagged as poor quality = 0

At over 4 million sequences we have less than the 6 million sequences achieved from the HSA but still have an abundance of data far beyond what is achievable from cloning. Average sequence length is noted as 126 bases. Theoretically we expect the aptamers to be 104 bases in length and with HSA NGS we saw 101 bases. This 21% increase in length over what is predicted can be attributed to the addition of Illumina primers. Figure 70 demonstrates that from 102-104 bases the presence of Illumina apdators increases to 100% demonstrating that unlike the HSA data the Illumina primers were not removed from the dataset at the point of sequencing.

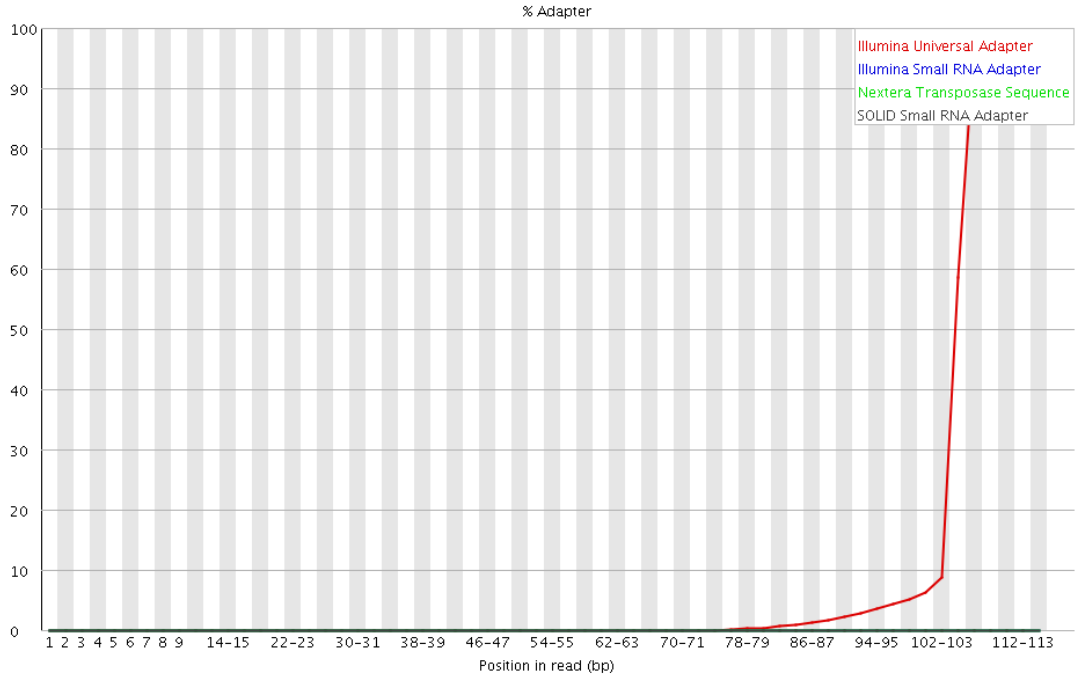

Figure 70: Plot of common adaptors within aptamer library.

Initial analysis of the unmodified NGS data demonstrates the higher quality associated with reduced SELEX rounds. Unlike the unmodified and reverse removed HSA data all base Phred scores are over 30 indicating a base call accuracy of above 99.9%(181,182) (Figure 71 and Figure 73). This change in Phred scores most likely relates to large regions within the HSA data set that had homogenous bases due to mutations arising from the large number of PCR rounds. These regions are difficult to read with accuracy due to overlapping signals.

Plotting the base content against position in the read we see the primer areas are well defined unlike the unmodified and reverse removed HSA data. The random region demonstrates no base preference at any point.

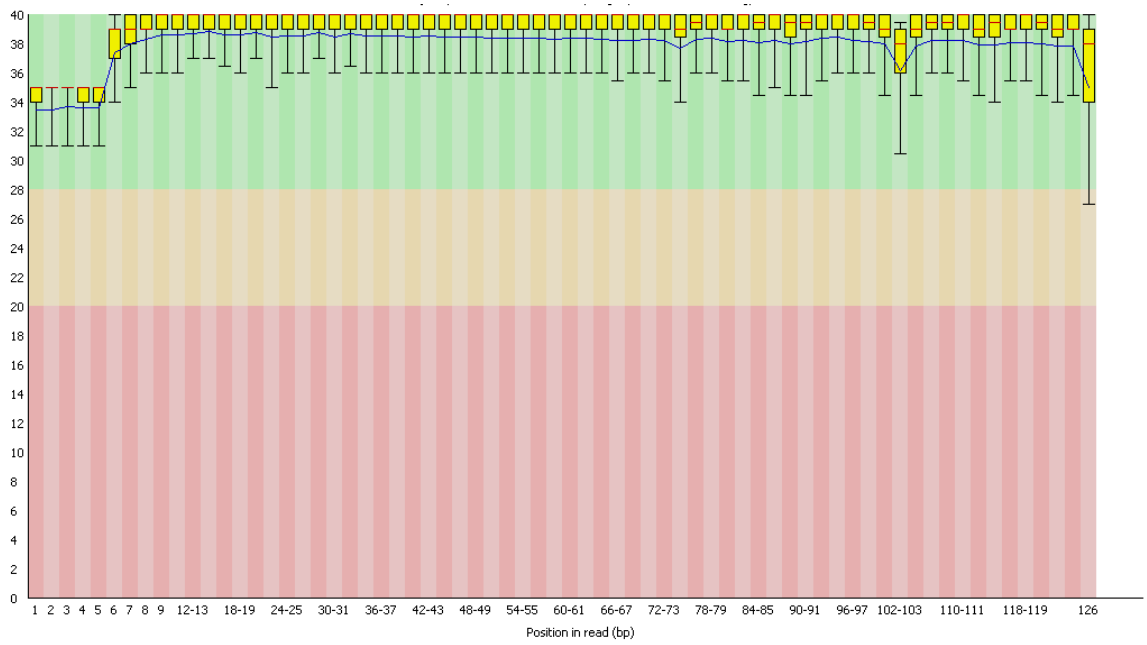

Figure 71: GHSA NGS data. Quality (Phred) scores against base position. Original unmodified GHSA NGS data.

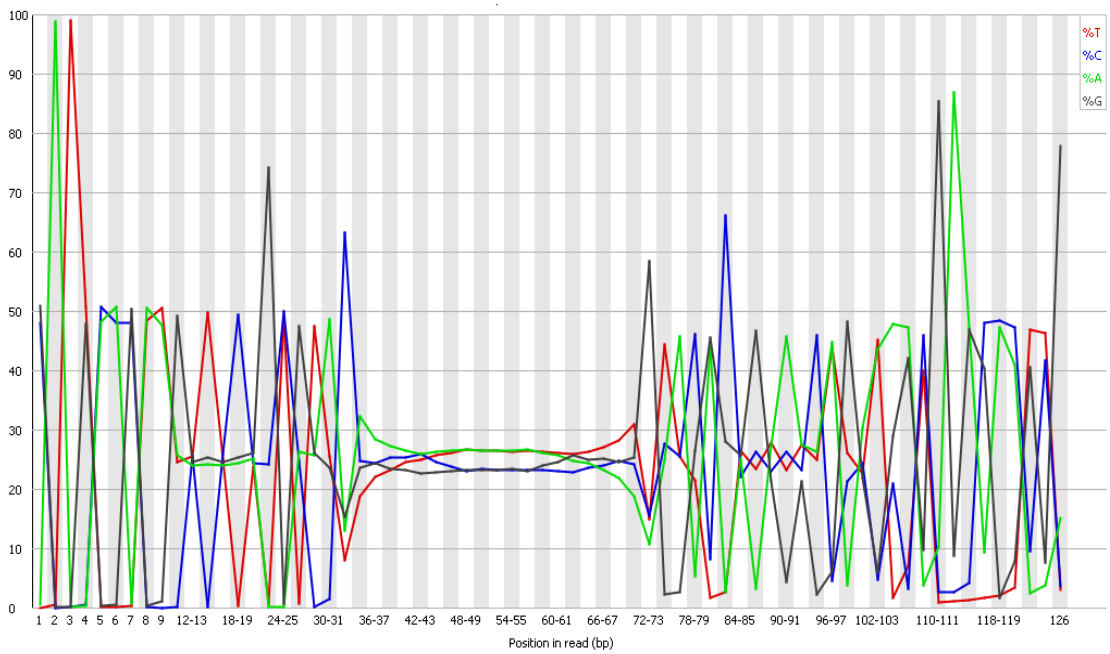

Figure 72: GHSA NGS data. Plot of sequence content across all bases. Original unmodified GHSA NGS data.

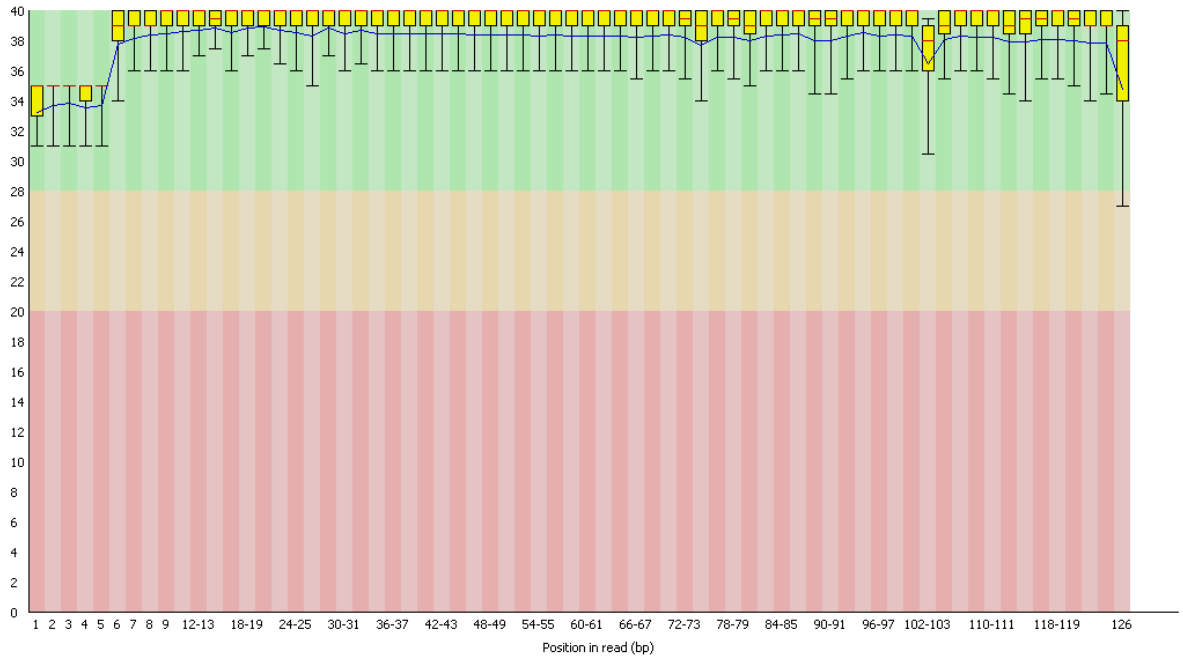

Figure 73: GHSA NGS data. Quality (Phred) scores against base position. Reverse strand removed.

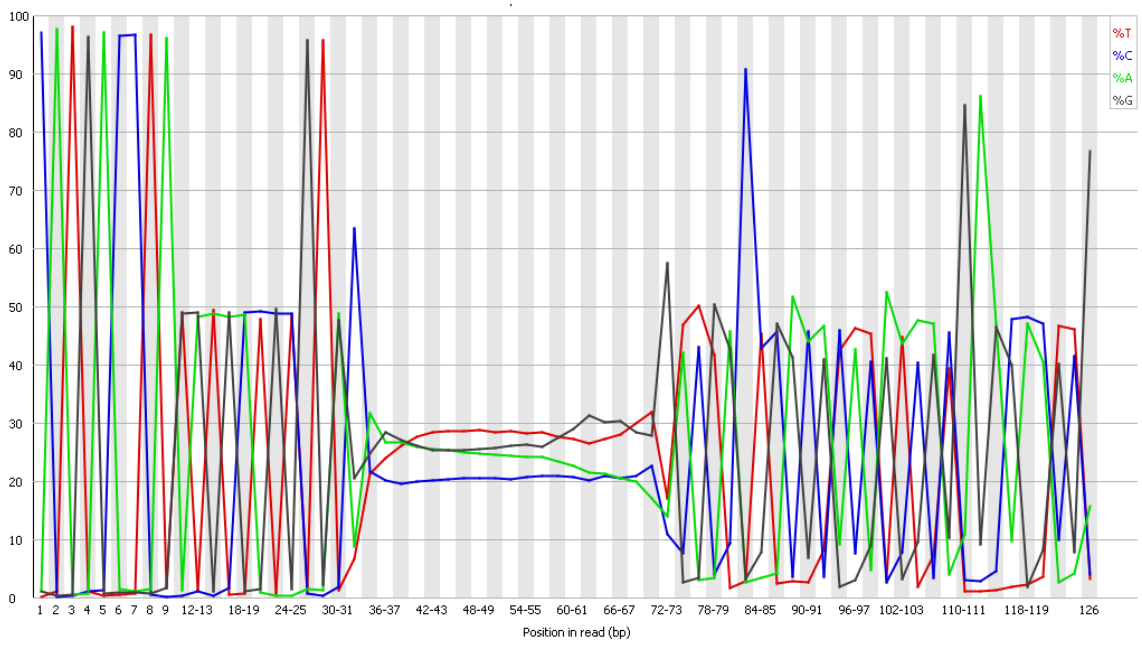

Figure 74: GHSA NGS data. Plot of sequence content across all bases. Reverse strand removed.

After initial analysis of the data, the reverse strands were removed by identifying the strands that started with the extended reverse primer (GATTCAGATGATCGTTCGCAGGGTCCAAGATC) and using FASTX Clipper/discard_seqs to remove them.

At this point it was decided to analyse the GHSA NGS data to try and determine some potential aptamers. This was undertaken as the library was relatively clean and removal of primer regions or excessive homogenous regions was not thought to be needed. Additionally the development and publication of the FASTAptamer software package by Alam, Chang and Burke (173) between the sequencing of the HSA and GHSA data allowed for a more aptamer tailored approach to the bioinformatics.

3.5.2.2 GHSA FASTAptamer

Majority of software packages for analysing vast DNA data sets focus on genomic information, as such custom solutions have to be utilised for aptamer selection from NGS data. However, the creation of the FASTAptamer software package enables a variety of aptamer specific operations including counting and ranking sequences, population comparison and fold enrichment calculations.

Code utilised:

perl fastaptamer_count –i /location/Inputfile.fastq –o/ location/Outputfile.fasta

The analysis of the data where the reverse strands were removed demonstrates that there were 2229465 total sequences, of which 2208890 were unique sequences meaning 20,575 were repeats. This low level of duplicates would be extremely difficult to detect with cloning and sanger sequencing. The data for the first 20 reads is shown unedited below, where the first number is it's rank, second is the count and the third is reads per million.

fastx_clipper removed significantly more than half of the aptamers but it was determined that the dataset still may have value. As such the top 15 strands based on abundance that showed the correct structure (primers in the correct positions and random region 40 $\pm$ 1 bases long) were

selected from the discard_seqs data and another 5 based on the same criteria were selected from the fastx_clipper data. This was done as there was a slight variation in the top aptamers with only one being the same across both data sets, to account for this variation aptamers from both data sets were included.

In the GHSA discard_seqs data (Table 5) we observe that the top twenty strands are heavily mutated with a combination of forward and reverse prime regions and additionally Illumina adaptors (TruSeq adaptor, Index 3). Here like the HSA data we see preference of amplification of PCR specific products and not just binders. When further studying the data it observed that binders present themselves between the top 50 and top 100. The 15 most frequent were selected and represent the first 15 sequences in Table 8.

TruSeq adaptor, Index 3:

5’ GATCGGAAGAGCACACGTCTGAACTCCAGTCACTTAGGCATCTCGTATGCCGTCTTCTGCTTG 3'

Region in green indicate areas that consistently appear within the top twenty strands

Table 5: GHSA aptamers selected by fastaptamer with only reverse strands removed using discard_seqs. Red highlighted indicated forward prime region, blue indicates reverse prime region, green indicated Illumina TruSeq adaptor and black is random regions. First number is it's rank, second is the count and the third is reads per million.

>1-253-113.48
CATGACCTAGTAGTAAGCATCCGCTGGTTGACGATCTTGGACCCTGCGAACGATCATCTGAATCAGATCGGA AGAGCACACGTCTGAACTCCAGTCACTAATGCGCATCTCGTATGCCGTCTTCTG
>2-66-29.60
CATGACCTAGTAGTAAGCATCCGCTGGTTGACGGATCTTGGACCCTGCGAACGATCATCTGAATCAGATCGG AAGAGCACACGTCTGAACTCCAGTCACTAATGCGCATCTCGTATGCCGTCTTCT
>3-34-15.25
CATGACCTAGTAGTAAGCATCCGCTGGTTGACTGATCTTGGACCCTGCGAACGATCATCTGAATCAGATCGG AAGAGCACACGTCTGAACTCCAGTCACTAATGCGCATCTCGTATGCCGTCTTCT

>4-27-12.11
CATGACCTAGTAGTAAGCATCCGCTGGTTGACCGATCTTGGACCCTGCGAACGATCATCTGAATCAGATCGG AAGAGCACACGTCTGAACTCCAGTCACTAATGCGCATCTCGTATGCCGTCTTCT
>5-20-8.97
ATTAAAGAGGAGAAATTAACCATGAAATACCTATTGCCTACGGCAGCCGCTGGCTTGCTGCTGCTGGCAGCT CAGCCGGCCATGGGCCTGATGCGTTGCAAACAGGATAGCGATTGCCTGGCGGGC
>6-19-8.52
CATGACCTAGTAGTAAGCATCCGCTGGTTGACTAGATCTTGGACCCTGCGAACGATCATCTGAATCAGATCG GAAGAGCACACGTCTGAACTCCAGTCACTAATGCGCATCTCGTATGCCGTCTTC
>7-17-7.63
CATGACCTAGTAGTAAGCATCCGCTGGTTGACGTGATCTTGGACCCTGCGAACGATCATCTGAATCAGATCG GAAGAGCACACGTCTGAACTCCAGTCACTAATGCGCATCTCGTATGCCGTCTTC
>8-15-6.73
CATGACCTAGTAGTAAGCATCCGCTGGTTGACGGGATCTTGGACCCTGCGAACGATCATCTGAATCAGATCG GAAGAGCACACGTCTGAACTCCAGTCACTAATGCGCATCTCGTATGCCGTCTTC
>9-13-5.83
CATGACCTAGTAGTAAGCATCCGCTGGTTGACCGGATCTTGGACCCTGCGAACGATCATCTGAATCAGATCG GAAGAGCACACGTCTGAACTCCAGTCACTAATGCGCATCTCGTATGCCGTCTTC
>10-12-5.38
CATGACCTAGTAGTAAGCATCCGCTGGTTGACCCGATCTTGGACCCTGCGAACGATCATCTGAATCAGATCG GAAGAGCACACGTCTGAACTCCAGTCACTAATGCGCATCTCGTATGCCGTCTTC
>11-11-4.93
CATGACCTAGTAGTAAGCATCCGCTGGTTGACTAGGATCTTGGACCCTGCGAACGATCATCTGAATCAGATC GGAAGAGCACACGTCTGAACTCCAGTCACTAATGCGCATCTCGTATGCCGTCTT
>11-11-4.93

CATGACCTAGTAGTAAGCATCCGCTGGTTGACGCTGATCTTGGACCCTGCGAACGATCATCTGAATCAGATC GGAAGAGCACACGTCTGAACTCCAGTCACTAATGCGCATCTCGTATGCCGTCTT
>11-11-4.93
CATGACCTAGTAGTAAGCATCCGCTGGTTGACGCGATCTTGGACCCTGCGAACGATCATCTGAATCAGATCG GAAGAGCACACGTCTGAACTCCAGTCACTAATGCGCATCTCGTATGCCGTCTTC
>14-10-4.49
CATGACCTAGTAGTAAGCATCCGCTGGTTGACCAGATCTTGGACCCTGCGAACGATCATCTGAATCAGATCG GAAGAGCACACGTCTGAACTCCAGTCACTAATGCGCATCTCGTATGCCGTCTTC
>15-9-4.04
CATGACCTAGTAGTAAGCATCCGCTGGTTGACACGATCTTGGACCCTGCGAACGATCATCTGAATCAGATCG GAAGAGCACACGTCTGAACTCCAGTCACTAATGCGCATCTCGTATGCCGTCTTC
>15-9-4.04
CATGACCTAGTAGTAAGCATCCGCTGGTTGACGTTGATCTTGGACCCTGCGAACGATCATCTGAATCAGATC GGAAGAGCACACGTCTGAACTCCAGTCACTAATGCGCATCTCGTATGCCGTCTT
>15-9-4.04
CATGACCTAGTAGTAAGCATCCGCTGGTTGACCATGATCTTGGACCCTGCGAACGATCATCTGAATCAGATC GGAAGAGCACACGTCTGAACTCCAGTCACTAATGCGCATCTCGTATGCCGTCTT
>18-8-3.59
CATGACCTAGTAGTAAGCATCCGCTGGTTGACGAGGATCTTGGACCCTGCGAACGATCATCTGAATCAGATC GGAAGAGCACACGTCTGAACTCCAGTCACTAATGCGCATCTCGTATGCCGTCTT
>18-8-3.59
CATGACCTAGTAGTAAGCATCCGCTGGTTGACACTGATCTTGGACCCTGCGAACGATCATCTGAATCAGATC GGAAGAGCACACGTCTGAACTCCAGTCACTAATGCGCATCTCGTATGCCGTCTT
>18-8-3.59
CATGACCTAGTAGTAAGCATCCGCTGGTTGACCGTGATCTTGGACCCTGCGAACGATCATCTGAATCAGATC

GGAAGAGCACACGTCTGAACTCCAGTCACTAATGCGCATCTCGTATGCCGTCTT

In the GHSA fastx_clipper data we observe a combination of mutations as before in the top twenty strands, however, we also locate five new potential aptamers in addition to one that was found before (GHSA Aptamer 4). The additional 5 were experimentally tested along with the other 15 from the discard_seqs data.

Table 6: GHSA aptamers selected by fastaptamer with only reverse strands removed using fastx_clipper. First number is it's rank, second is the count and the third is reads per million. Blue bases represent the reverse primer region.

>1-20-398.33
ATTAAAGAGGAGAAATTAACCATGAAATACCTATTGCCTACGGCAGCCGCTGGCTTGCTGCTGCTGGCAGCT CAGCCGGCCATGGGCCTGATGCGTTGCAAACAGGATAGCGATTGCCTGGCGGGC
>2-5-99.58
ATTAAAGAGGAGAAATTAACCATGAAATACCTATTGCCTACGGCAGCCGCTGGCTTGCTGCTGCTGGCAGCT CAGCCGGCCATGGGCCTGATGCGTTGCAAACAGGATAGCGATTGCCTGCGGGCA
>2-5-99.58
ATTAAAGAGGAGAAATTAACCATGAAATACCTATTGCCTACGGCAGCCGCTGGCTTGCTGCTGCTGGCAGCT CAGCCGGCCATGGGCCTGATGCGTTGCAAACAGGATAGCGATTGCCGGCGGGCA
>4-4-79.67
CGTACGCTACTGACTTTCGTTCTTGATCGATGAAAACATCCTTGGCAAATGCTTTCGCAGTAGTCCGTCTTTAA CAAATCCAAGAATTTCACCTCTGACAGTTAAATACGAATGCCCCCAACTATC
>5-3-59.75
GCCGCTTGCTGCGCCGCAGAACCAAGCGTATTCCCAAGTGTAAGACCAAGAGCACACGCTGCCCGCAGGCA ATCGCTATCCTGTTTGCAACGCATCAGGCCCATGGCCGGCTGAGCTGCCAGCAGC
>5-3-59.75
GCCGCTTGCTGCGCCGCAGAAACGAGAGTTACGGTATTTGTCAACACCCAGGCACACGCTGCCCGCCGGCAA TCGCTATCCTGTTTGCAACGCATCAGGCCCATGGCCGGCTGAGCTGCCAGCAGC
>5-3-59.75 - **GHSA aptamer 4**
CATGACCTAGTAGTAAGCATCCGCTGGTTGAC**GAACGGTCAGGTCAGTCGTTACGGTGTGTATTAGATGAT G**GATCTTGGACCCTGCGAACGATCATCTGAATCAGATCGGAAGAGCACACGTCTG
>5-3-59.75
ATTAAAGAGGAGAAATTAACCATGAAATACCTATTGCCTACGGCAGCCGCTGGCTTGCTGCTGCTGGCAGCT CAGCCGGCCATGGGCCTGATGCGTTGCAAACAGGTAGCGATTGCCTGGCGGGCA
>5-3-59.75
ATTAAAGAGGAGAAATTAACCATGAAATACCTATTGCCTACGGCAGCCGCTGGCTTGCTGCTGCTGGCAGCT CAGCCGGCCATGGGCCTGATGCGGTGCAAACAGGATAGCGATTGCCTGGCGGGC
>10-2-39.83 - **GHSA aptamer 16**
CATGACCTAGTAGTAAGCATCCGCTGGTTGAC**CGAGGGGGTGAAACTGTTTCCAGCAGGCCTGCTGTTCGT C**GATCTTGGACCCTGCGAACGATCATCAGATCGGAAGAGCACACGTCTGAACTCC
>10-2-39.83
CAATGACCTAGTAGTAAGCATCCGCTGGTTGACCAGTGAAAATTCCTAAAAGGACTGCGGATCTTGGACCCT GCGAACGATCATCTGAATCCCATGACCTAGTAGTAAGCATCCGCTGGTTGACGT
>10-2-39.83

GCCGCTTGCTGCGCCGCAGAAACGAACAACCCACAGGTACCAGTCGTAACCGCACACGCTGCCCGCCAGGC AATCGCATCCTGTTTGCAACGCATCAGGCCCATGGCCGGCTGAGCTGCCAGCAGC
>10-2-39.83 - **GHSA aptamer 17**
CATGACCTAGTAGTAAGCATCCGCTGGTTGAC**GGTCCTGCCGGAGGTCAGGACTTCGATGAACGTGAATCA G**GATCTTGGACCCTGCGAACGATCATCTGAATCAGATCGGAAGAGCACACGTCTG
>10-2-39.83 - **GHSA aptamer 18**
CATGACCTAGTAGTAAGCATCCGCTGGTTGAC**TAGCTTGAGGTCTCCGCGGAATGAGTTGGATCAAACCAG A**GATCTTGGACCCTGCGAACGATCATCTAGATCGGAAGAGCACACGTCTGAACTC
>10-2-39.83
GATCGTTCGCAGGGTCCAAGATCGTGCGACGCCCCCCATATTTACTAAACTTCTGACGAGGTGGTCAACCAG CGGATGCTTACTACTAGGTCATGAGATCGGAAGAGCACACGTCTGAACTCCAGT
>10-2-39.83 - **GHSA aptamer 19**
CATGACCTAGTAGTAAGCATCCGCTGGTTGAC**GCGTGCTGTTCCGGCTAGTATTCATATGTACGTGGAGGTT** GATCTTGGACCCTGCGAACGATCATCTGAATCAGATCGGAAGAGCACACGTCTG
>10-2-39.83
CCAAGATCCCAAACAATAAGTACAAGCGTTCAGTGGAGGGGATACTCCGTCAACCAGCGGATGCTTACTACT AGGTCATGAGATCGGAAGAGCACACGTCTGAACTCCAGTCACTAATGCGCATCT
>10-2-39.83 - **GHSA aptamer 20**
CATGACCTAGTAGTAAGCATCCGCTGGTTGAC**ACTCTGGAATTAAAAGGGAGGTGTCGGGGAGCGAGGTG GT**GATCTTGGACCCTGCGAACGATCATCTGAAGATCGGAAGAGCACACGTCTGAAC
>10-2-39.83
CATGACCTAGTAGTAAGCATCCGCTGGTTGACGAACTAACGTTAGAGGGATGGCAGCGACCGGTTCCTTGG ATCTTGGACCCTGCGAACGATCATCTGAACAGATCGGAAGAGCACACGTCTGAAC
>10-2-39.83
CATGACCTAGTAGTAAGCATCCGCTGGTTGACGGTGCTTGAGGATTTGTTAAGCGTACCCGACCCGTGAATA GATCTTGGACCTGCGAACGATCATCTGAATAGATCGGAAGAGCACACGTCTGAA

3.6 HSA and GHSA aptamers selected using NGS

3.6.1 HSA aptamers

Table 7: HSA aptamers selected from NGS analysis.

Aptamer 1	AGCCACGGGCGACAACTTATGCAACAGGAGCACCACCTGGATCTTGGACCCTGCGAA
Aptamer 2	GAGGGGCAATGGGATTGGCCTTGCTCGTTTGTGAGTTTCGATCTTGGACCCTGCGAA
Aptamer 3	GATGTTCTGGCGCTACTTACTAAATATCGGCCTGTCATGGATCTTGGACCCTGCGAA
Aptamer 4	GCACAGTGTTAACGTGGATGGCTTCTGTGTGGGCAGCCCGATCTTGGACCCTGCGAA
Aptamer 5	CCCGTGGAATTTGCGGTCGTGCTATGATCGACCACCCTGGATCTTGGACCCTGCGAA

Aptamer 6	GATCGGAAGAGCACACGTCTGAACTCCAGTCACACAGTGGATCTTGGACCCTGCGAA
Aptamer 7	GCGCAAGGACAAATTGTTCAAGAGCCCCGACTGTGATTAGATCTTGGACCCTGCGAA
Aptamer 8	GAATTGGGCGCAATAGTATGAGGATGACTTAGGCTCGGTGATCTTGGACCCTGCGAA
Aptamer 9	GCGGGATTATGTGTGAACGTGGCGGGCCGTGGACTTGTGGATCTTGGACCCTGCGAA
Aptamer 10	GCGCGAGAAACGATGTGTTCGGGAACGCGGGGCGGTGGTGATCTTGGACCCTGCGAA
Aptamer 11	GCAGAACGGCAGCATTGGAAGCGTGGGTTTTGTGTAACGGATCTTGGACCCTGCGAA
Aptamer 12	CGCATAGGACGGGTGTATGGATTTACTTTCGTCATGTTGGATCTTGGACCCTGCGAA
Aptamer 13	CACGGCCTGCAGATGTTGTGTATGGTCCGACCGTTGGTGGATCTTGGACCCTGCGAA
Aptamer 14	GAATTCAGATGATCGTTCGCAGGGTCCAAGATCCACAGTGATCTTGGACCCTGCGAA
Aptamer 15	CACACACATTATGTTGCACGTGTAACTGGTATCGGTTGTGATCTTGGACCCTGCGAA
Aptamer 16	GTACAGGTAGCACCTACTATTAGTTGGTTTCCGTTCCTTGATCTTGGACCCTGCGAA
Aptamer 17	CACGGGGTGACTGTCTGCATACACGTATTTCTTGTCGGTGATCTTGGACCCTGCGAA
Aptamer 18	GCGCCGATGTAGGTGTGACAGAGCGCTCTGCTGGGGTGGGATCTTGGACCCTGCGAA
Aptamer 19	GGCAAAATGTACTGGATGTTGGCTGGAGGAGTGCGTGCGGATCTTGGACCCTGCGAA
Aptamer 20	GGGAACAGCACACCAAGGGGCAATCGTGTCATAGCGTCTGATCTTGGACCCTGCGAA
Aptamer 21	GCCAACATAGTGGAGACATCCAAGCTTTGGGCGGTTTGCGATCTTGGACCCTGCGAA
Aptamer 22	GGGACCCAACGTGGTATGGTTACTGTCTACGCGGCTCCAGATCTTGGACCCTGCGAA
Aptamer 23	GGTCGATGCGAATAGTATAGGAAGTTAGTTCATTCCTGTGATCTTGGACCCTGCGAA
Aptamer 24	TTTGATTTGCGGAGCCATGTAGAGACTGCTGGCCACAATGATCTTGGACCCTGCGAA

Aptamer 25	GGAGTGGCGGAATCGTTGTCCTGCTGTGCGGTCGGACGTGATCTTGGACCCTGCGAA
Aptamer 26	GGTCCGACGCTGCATATCCGGTTTTGTCAGGATATGGGGGATCTTGGACCCTGCGAA
Aptamer 27*	CACCTAGGGTATTGAGTGAAAGGTGGGGTGATTGTAGTTGCGATCTTGGACCCTGCGAA

*Selected with FastAptamer after the initial 26 aptamers were selected using MAFT and ClustalO.

3.6.2 GHSA aptamers

Table 8: GHSA aptamers selected from NGS analysis.

Name	**Sequence**
GHSA aptamer 1	CGTCGGTTGAATTTTATGAAGGAAAGTGGGGAGACGGTGGATCTTGGACCCTGCGAA
GHSA aptamer 2	GCAGTGTGATCAATGATTTATTGATTGGAAACCGCATCAAGATCTTGGACCCTGCGAA
GHSA aptamer 3	AGGTTTAGACGGACGGCCCTTACGGACAATCAACAGCACGGATCTTGGACCCTGCGAA
GHSA aptamer 4	GAACGGTCAGGTCAGTCGTTACGGTGTGTATTAGATGATGGATCTTGGACCCTGCGAA
GHSA aptamer 5	CCCAGGGCGGACAGGATCTACGACTTTCCCGTGCTGATTAGATCTTGGACCCTGCGAA
GHSA aptamer 6	GGAAAGTCCTGACTTAGGCTAACATGCGTATCGAGCGTATGATCTTGGACCCTGCGAA
GHSA aptamer 7	TACCGACAGACAGGACCCCCGTCGGAGCAGTGGAGCCTCGGATCTTGGACCCTGCGAA
GHSA aptamer 8	ATGTTACCCAAGCGGCGTGGTATCACGTTTTATAGTGCATGATCTTGGACCCTGCGAA
GHSA aptamer 9	GGCAGTTAATGAGTGAATCGACAAGGTGCTAACATTAATCGATCTTGGACCCTGCGAA
GHSA aptamer 10	GAGGTAGAAGATATAGCTACCTTGTTTTTCTGGCGACTGTGATCTTGGACCCTGCGAA
GHSA aptamer 11	CGACTGATTCGCTACCCTGAATTGGGCAATAGTAGTGGCTGATCTTGGACCCTGCGAA
GHSA aptamer 12	CGGGATGTCGTGAAAGCGTCGAATATTTTGCGTAACGCTGGATCTTGGACCCTGCGAA

GHSA aptamer 13	CTACGGGTAATCATCATACGTTATAACGGTTGTATGTGCTGATCTTGGACCCTGCGAA
GHSA aptamer 14	GAGGTATGTGTATTCTCGTGGTGTGATTGTACCTATGAGAGATCTTGGACCCTGCGAA
GHSA aptamer 15	CAAGGATGGTCGTTGGGGTTAAGGACTGATCCCATAGATGGATCTTGGACCCTGCGAA
GHSA aptamer 16	CGAGGGGGTGAAACTGTTTCCAGCAGGCCTGCTGTTCGTCGATCTTGGACCCTGCGAA
GHSA aptamer 17	GGTCCTGCCGGAGGTCAGGACTTCGATGAACGTGAATCAGGATCTTGGACCCTGCGAA
GHSA aptamer 18	TAGCTTGAGGTCTCCGCGGAATGAGTTGGATCAAACCAGAGATCTTGGACCCTGCGAA
GHSA aptamer 19	GCGTGCTGTTCCGGCTAGTATTCATATGTACGTGGAGGTTGATCTTGGACCCTGCGAA
GHSA aptamer 20	ACTCTGGAATTAAAAGGGAGGTGTCGGGGAGCGAGGTGGTGATCTTGGACCCTGCGAA

Chapter 3.7

Results: ELONA (Enzyme Linked Oligonucleotide Assay)

3.7 ELONA (Enzyme Linked Oligonucleotide Assay)

Enzyme linked oligonucleotide assay is a powerful tool for analysing binding. It is based on ELISA, an enzyme linked antibody binding assay. The 27 aptamers generated from the HSA NGS and the 20 from the GHSA NGS were all tested against HSA, glycated HSA and IGG. The aptamers contained the 40 base random region and the original non extended 18 base forward primer region. This was done so a biotin forward primer could be hybridised. This biotin can then bind to the streptavidin - HRP, generating a signal under the addition of TMB. Initial experiments focused around determining the correct experimental protocol, particularly the type and amount of blocking agent used. Commonly ELONA or ELISA plates are blocked with BSA, this would cause non specific binding with the aptamer generated in SELEX as BSA has many structural and chemical similarities to HSA. Multiple blocking agents were trialled.

3.7.1 HSA ELONA

3.7.1.1 Initial testing of blocking conditions

HSA was immobilised on the Costar plates and all other steps were carried out as described in Chapter 2.3 except for aptamer incubation. This was done to determine the amount of non-specific binding of the SA-HRP to the well. Casein solutions above 1 per cent could not be tested as it would not dissolve in Binding Buffer. Four different samples per concentration were ran with each well being measured three times, this totalled 12 different measurements for each condition which were mean averaged. Standard deviation was calculated from all 12 measurements.

Variations between samples were a result of arbitrary incubation times with TMB. Originally wells were measured visually, future experiments set a time limit (5 minutes) on TMB incubation.

In Figure 75 we see there is a large variance between samples. Noblock produced lower background then some of the casein blocked wells. There was a slight improvement on background signal when washing with casein at every step after blocking. The absorbance reading is high across all casein and

synblock concentrations, normally a background reading of below 0.05 would be expected. The range of standard deviation involved makes it difficult to determine any statistical difference between the blocking agents. At this stage 0.1% casein was chosen based on references to literature; however doubts remained about its suitability. (187).

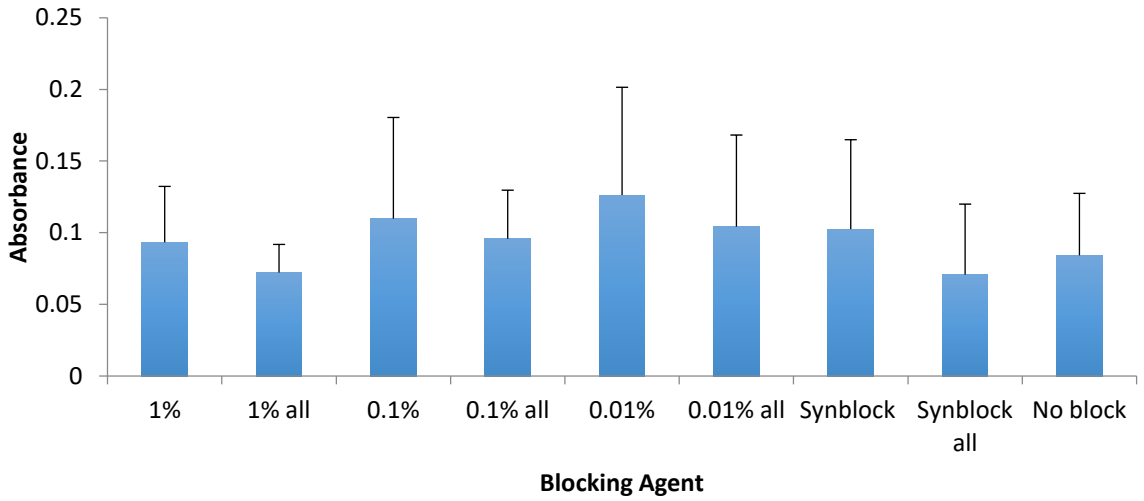

Figure 75:ELONA response of background signal to casein at 1%, 0.1% and 0.01%. Commercially purchased synthetic blocking agent was also tested. Each test was repeated in four wells and three absorbance measurements were taken per well. Standard deviation was determined from all twelve measurements. "all" refers to well that were washed after blocking with binding buffer plus casein instead of binding buffer alone.

All 26 aptamers from the initial HSA NGS analysis were tested along with an aptamer (Aptamer concentration for all aptamers was 1uM) from the literature (Figure 76) that has been shown to bind to advanced glycated (AGE) HSA (58) (Kd 1 µmol/l. 56 bases in length) . Procedure was carried out as in section 2.3.2. The biotin modified primer was also tested for binding. Each aptamer was tested in four wells across 2 plates, with each well measured 3 times, totaling 12 measurements, mean average is shown for each individual plate and the combined plates. Standard deviation for both plates was calculated from all 12 measurements.

A high background is observed and while individual plate standard deviations are small the range between the two plates is relatively large, this is reflected in the standard deviation for the mean average of the two plates. At this point it was hypothesised that the plate wasn't blocked effectively

and the high background signal was distorting the results. The three best performing aptamers were chosen from this data and trialled in a dose dependent study to further analyse the signals that were being observed. Plate 1 demonstrates a higher absorbance across all aptamers indicating a systematic error that could be related to slight differences in incubation times or protein stability between plates.

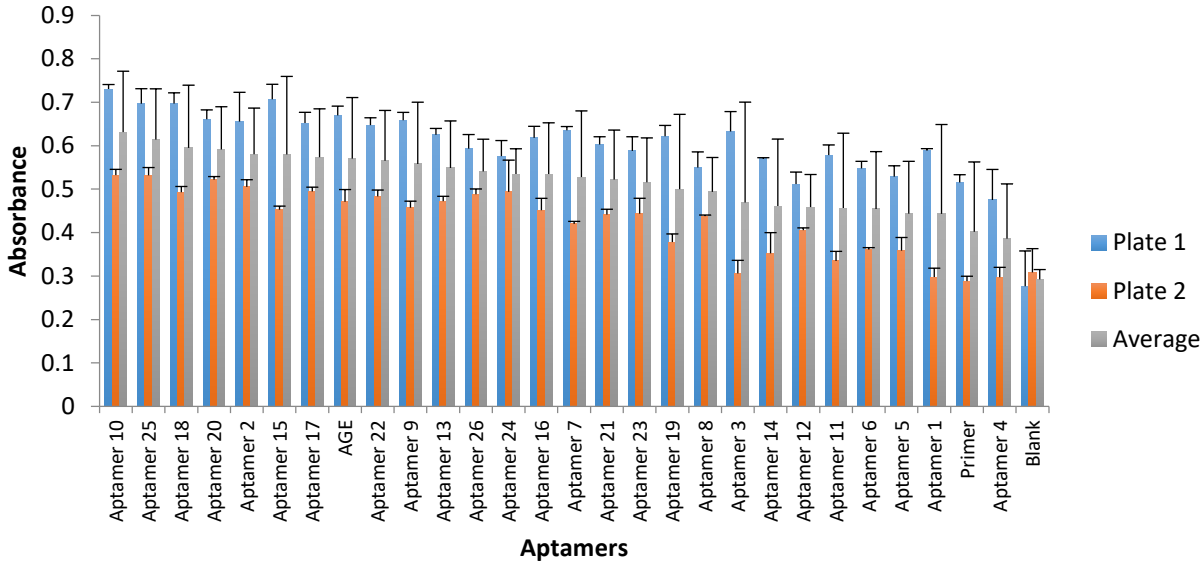

Figure 76: 26 HSA aptamers picked from initial analysis of HSA NGS data tested across two plates including a literature gHSA aptamer. HSA was immobilised at a concentration of 20ug/ml. Blocked with 0.1% casein. Each test was repeated in four wells and three absorbance measurements were taken per well. Standard deviation was determined from all twelve measurements. AGE = Advanced glycation end product aptamer.

Aptamers 10, 25 and 18 were chosen for further dose dependent experiments. Two experiments were run, one from 3nM to 10uM and then subsequently a separate test from 3nM to 100uM. Each concentration was tested across 3 wells with 3 measurements per well, totalling 9 measurements. A dose depended response is noted across both graphs (Figure 77 and Figure 78). In Figure 77 we observe between 300nM and 3uM the saturation of the absorbance and in some cases a reduction in the signal before a large jump at 10uM. While the trend below 1uM is less evident in Figure 78 we observe the same significant signal increase at 10uM for aptamers 18 and 25. As the range of the experiment for Figure 78 also goes further we see this trend continue, a significant signal increase is

seen at 30uM and 100uM. This double peak, initially at 300nM and then at 30uM could indicate a transition between specific binding and non-specific binding. While it could indicate the transition between two binding states it could also indicate a systematic error, for example pipetting inaccuracies, however, due to this occurring across multiple experiments I believe any systematic errors are minimised.

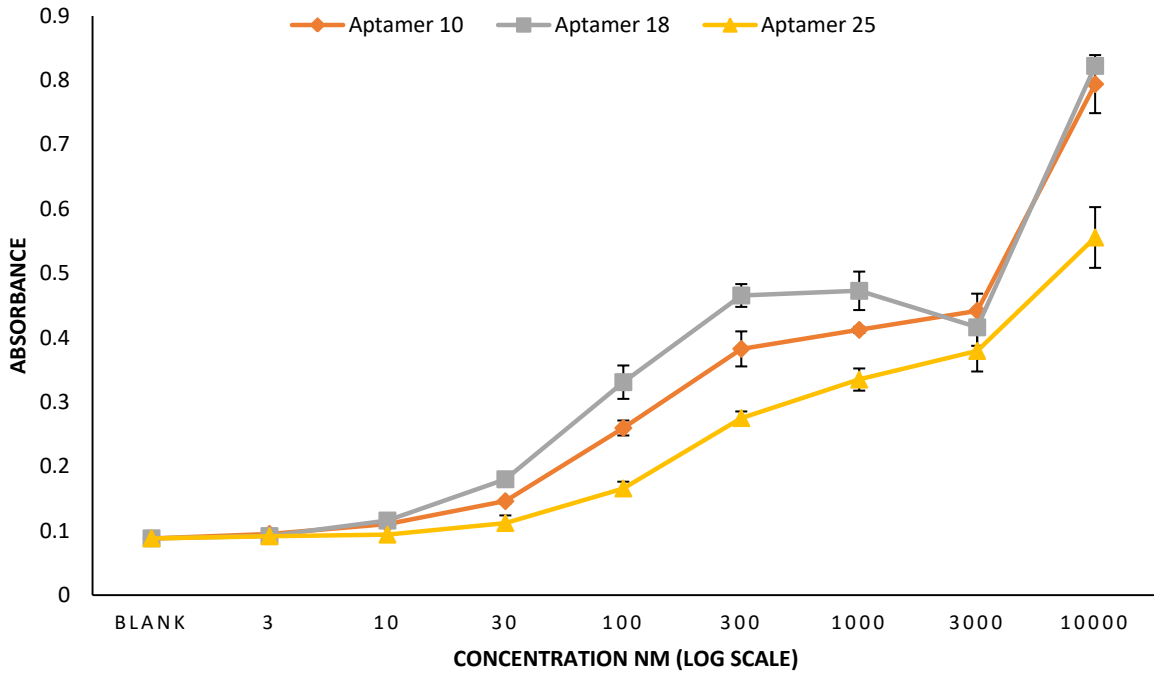

Figure 77: Dosage response of HSA aptamers 10, 18 and 25 from 3nM to 10uM. HSA was immobilised at a concentration of 20ug/ml. Blocked with 0.1% casein. Each aptamer test was repeated in three wells and three absorbance measurements were taken per well. Standard deviation was determined from all nine measurements.

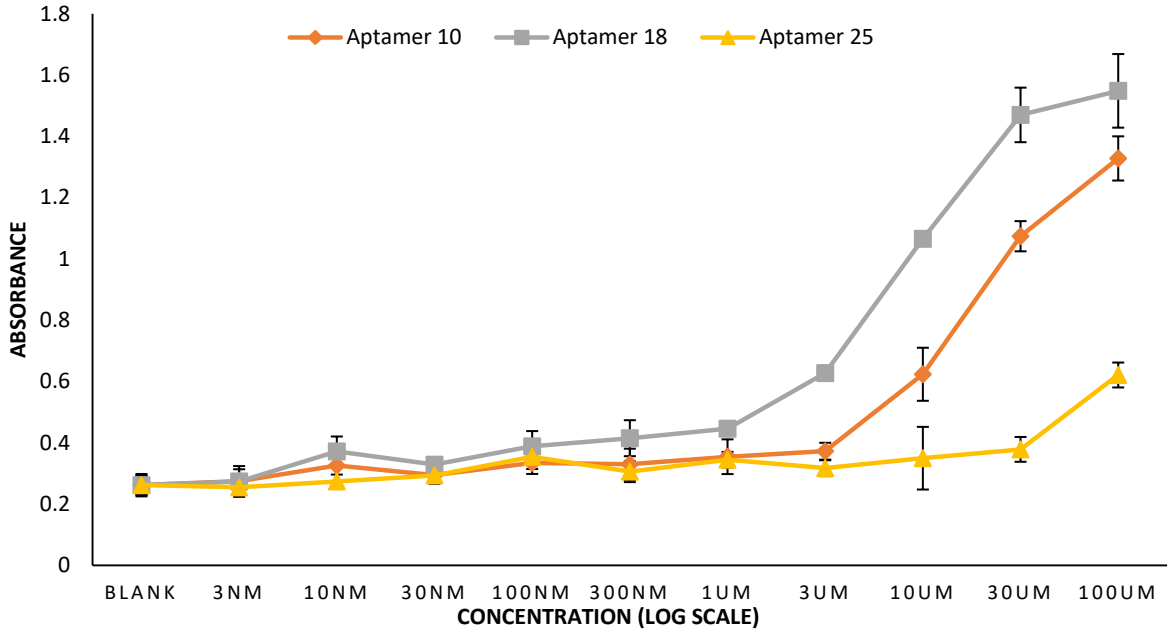

Figure 78: Dosage response of HSA aptamers 10, 18 and 25 from 3nM to 100uM. HSA was immobilised at a concentration of 20ug/ml. Blocked with 0.1% casein. Each aptamer test was repeated in three wells and three absorbance measurements were taken per well. Standard deviation was determined from all nine measurements.

3.7.1.2 Checking non-specific binding

To determine the specificity of binding, aptamers 10, 18 and 25 were tested against IgG, a highly abundant component of blood serum. Due to variations in IgG, this is an extremely complex sample to test against making it ideal in determining specific and non specific binding. Dose dependent response was recorded between 30nM and 30uM. Each concentration was repeated in two wells and three absorbance measurements were taken per well. Standard deviation is taken across all 6 measurements.

As can be observed in Figure 79 all three aptamers have a similar response to both HSA and IgG. This suggests that we are seeing non-specific binding of our aptamers to our target. The same aptamer solutions were utilised for both HSA and IgG resulting in almost no discrepancies between concentrations. As the responses are almost identical it was theorised that the response may not be related to either HSA or IgG but another factor like the casein.

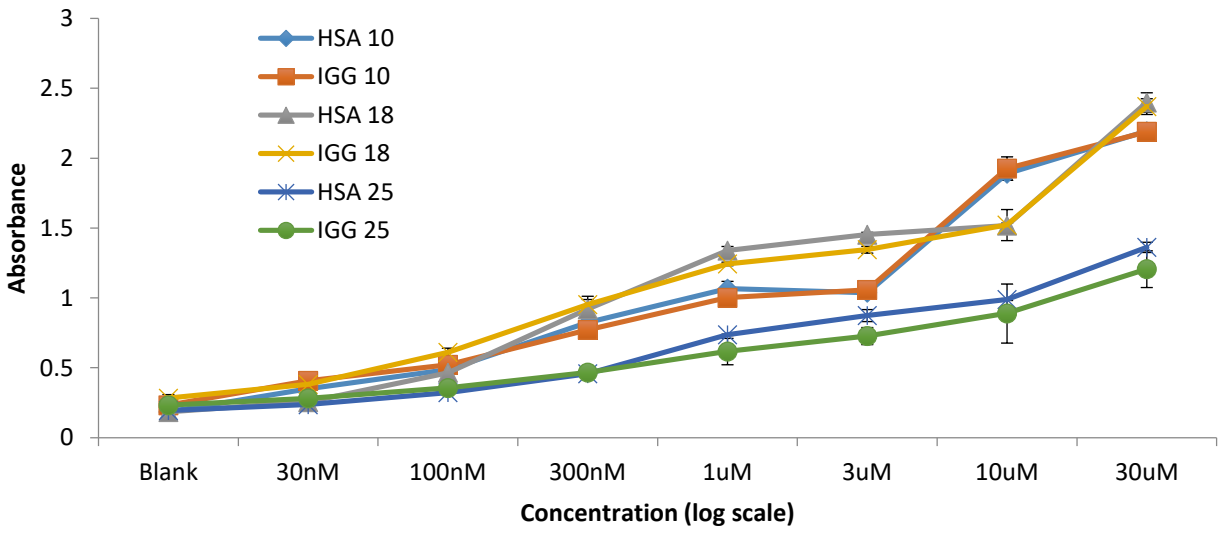

Figure 79: Response of HSA aptamers 10, 18 and 25 to HSA and IgG at a range of aptamer concentrations from 30nM to 30uM. HSA and IgG were immobilised at a concentration of 20ug/ml. Blocked with 0.1% casein. Each aptamer test was repeated in two wells and three absorbance measurements were taken per well. Standard deviation was determined from all six measurements.

The purity of casein is in question and it's possible that it could be contaminated with albumin, specifically lactalbumin. As the casein is added at a high concentration, the surface could be swamped with lactalbumin which would affect the signal.

Before looking into the potential casein problem all aptamers were tested against both IgG and HSA at an aptamer concentration of 1uM (Figure 80). Each aptamer tests was repeated in two wells and three absorbance measurements were taken per well.

We see that across the board that aptamers binding to HSA generate a more significant signal then to IgG. This difference can be more clearly observed in Figure 81 where aptamers 1, 3, 4 and 26 produce larger then a 1 absorbance unit response to HSA then IgG.

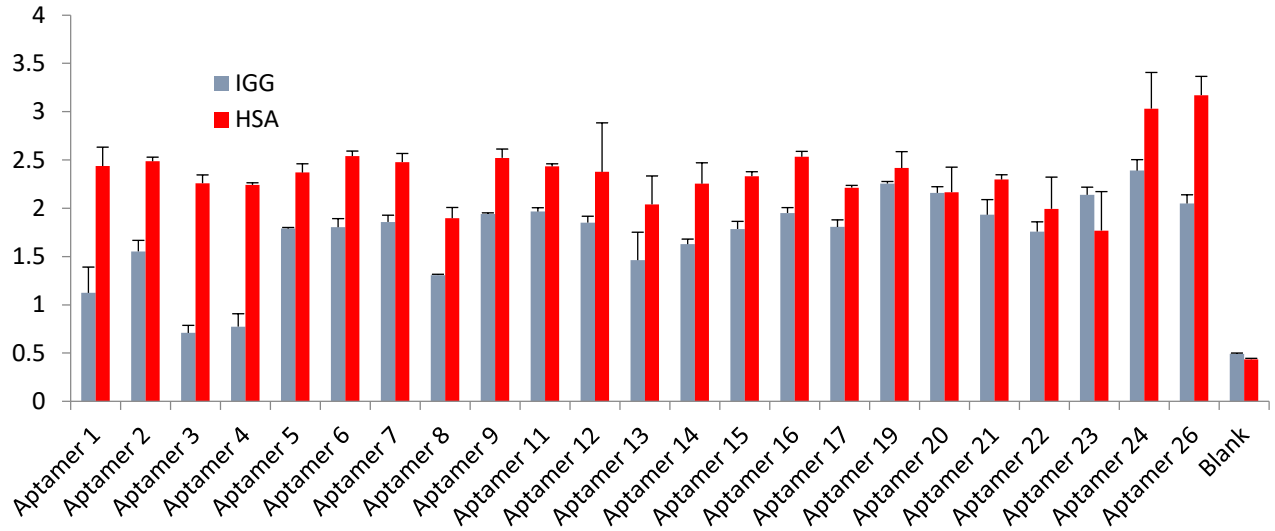

Figure 80: HSA aptamers tested against HSA and IgG at a concentration of 1uM. HSA and IgG were immobilised at a concentration of 20ug/ml. Blocked with 0.1% casein. HSA and IgG tested on separate plates. Each aptamer test was repeated in two wells and three absorbance measurements were taken per well. Standard deviation was determined from all six measurements.

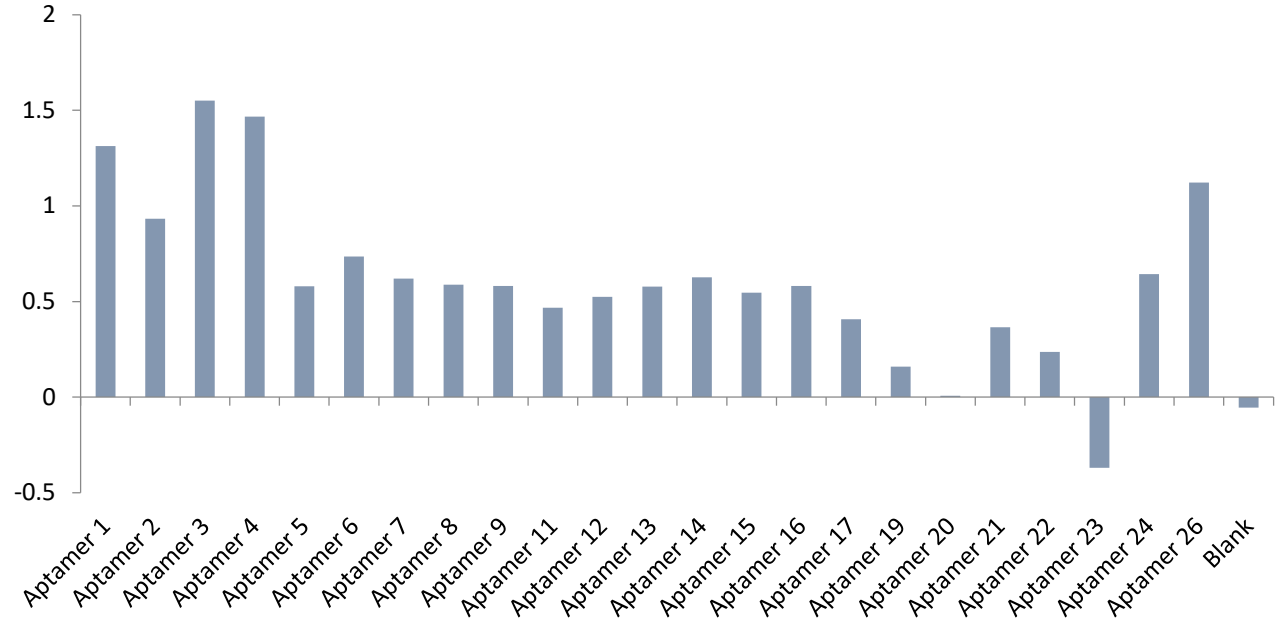

Figure 81: HSA aptamer response of HSA minus IgG at a concentration of 1uM. HSA and IgG were immobilised at a concentration of 20ug/ml. Blocked with 0.1% casein. HSA and IGG tested on separate plates. Each aptamer test was repeated in two wells and three absorbance measurements were taken per well. Standard deviation was determined from all six measurements.

After determining that aptamers 1,3,4 and 26 produced the greatest response with HSA over IgG, all four aptamers were tested for dose response.

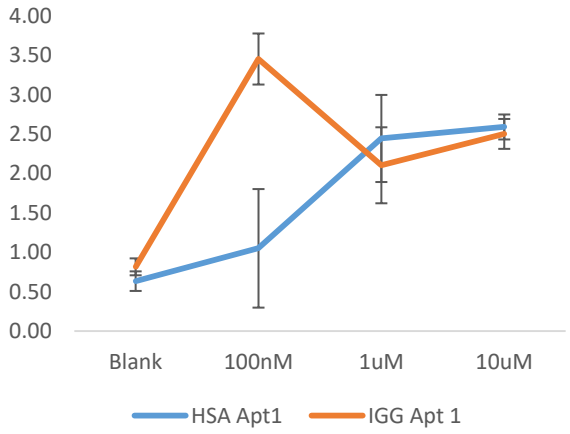

Figure 82: Dose response of HSA aptamer 1 to HSA and IgG. HSA and IgG were immobilised at a concentration of 20ug/ml. Blocked with 0.1% casein. Each concentration test was repeated in three wells and three absorbance measurements were taken per well. Standard deviation was determined from all nine measurements.

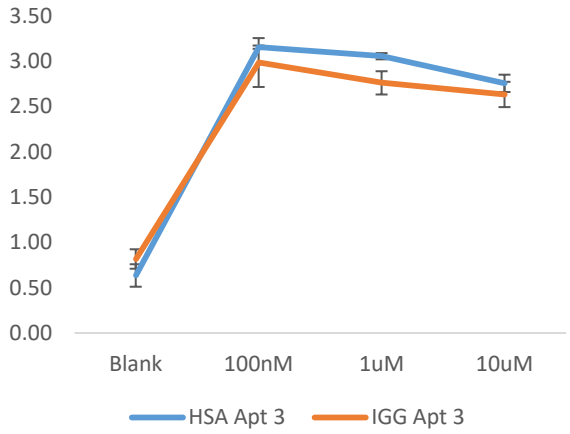

Figure 83: Dose response of HSA aptamer 3 to HSA and IgG. HSA and IgG were immobilised at a concentration of 20ug/ml. Blocked with 0.1% casein. Each concentration test was repeated in three wells and three absorbance measurements were taken per well. Standard deviation was determined from all nine measurements.

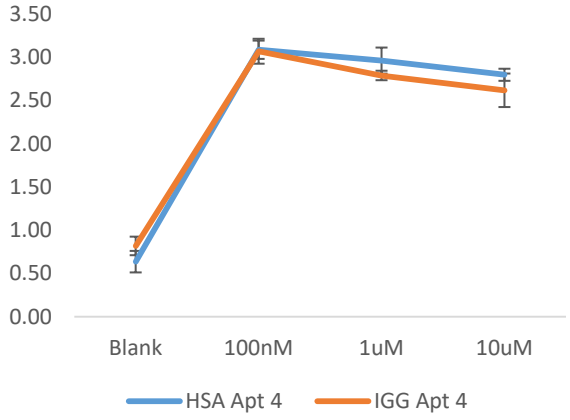

Figure 84: Dose response of HSA aptamer 4 to HSA and IGG. HSA and IgG were immobilised at a concentration of 20ug/ml. Blocked with 0.1% casein. Each concentration test was repeated in three wells and three absorbance measurements were taken per well. Standard deviation was determined from all nine measurements.

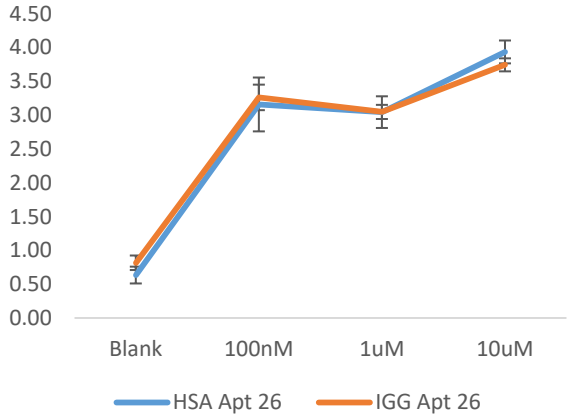

Figure 85: Dose response of HSA aptamer 26 to HSA and IGG. HSA and IgG were immobilised at a concentration of 20ug/ml. Blocked with 0.1% casein. Each concentration test was repeated in three wells and three absorbance measurements were taken per well. Standard deviation was determined from all nine measurements.

Figure 82 - Figure 85 demonstrates that in contrast to Figure 80 and Figure 81 the response of the aptamers to HSA is almost identical to that of IgG, except for a response at 100nM for aptamer 1. The conflicting data required a rerun of the experiment carried out in Figure 80 and Figure 81. This

data is shown in Figure 86 and Figure 87. Figure 86 shows a different trend to that shown in Figure 80 and Figure 81, where we generally see a larger IgG response across the board then HSA. However, it is noted that the backgrounds for both are particularly high, especially IgG which is substantially higher than HSA. When this background signal is removed, most aptamers demonstrate indistinguishable signals between HSA and IgG. This could be for a few reasons, the aptamers are not specific to HSA, the IgG has an affinity for denatured DNA in general (188) or the experimental setup is flawed, particularly in relation to the use of casein as a blocking agent. As casein is purified from milk, other contaminates may be present including lactate albumin. Due to the relative high concentration (compared to HSA or IgG) at which the casein is utilised, any signal generated from lactate albumin may be obscuring any HSA or IgG signal.

The binding of the aptamers to casein was trialled. In Figure 88 we observe that there is significant binding to casein across all aptamers. Interestingly both the literature aptamer AGEHSA and the primer also demonstrate a strong signal. This indicates significant non-specific binding; the decision was made to move away from Casein blocking.

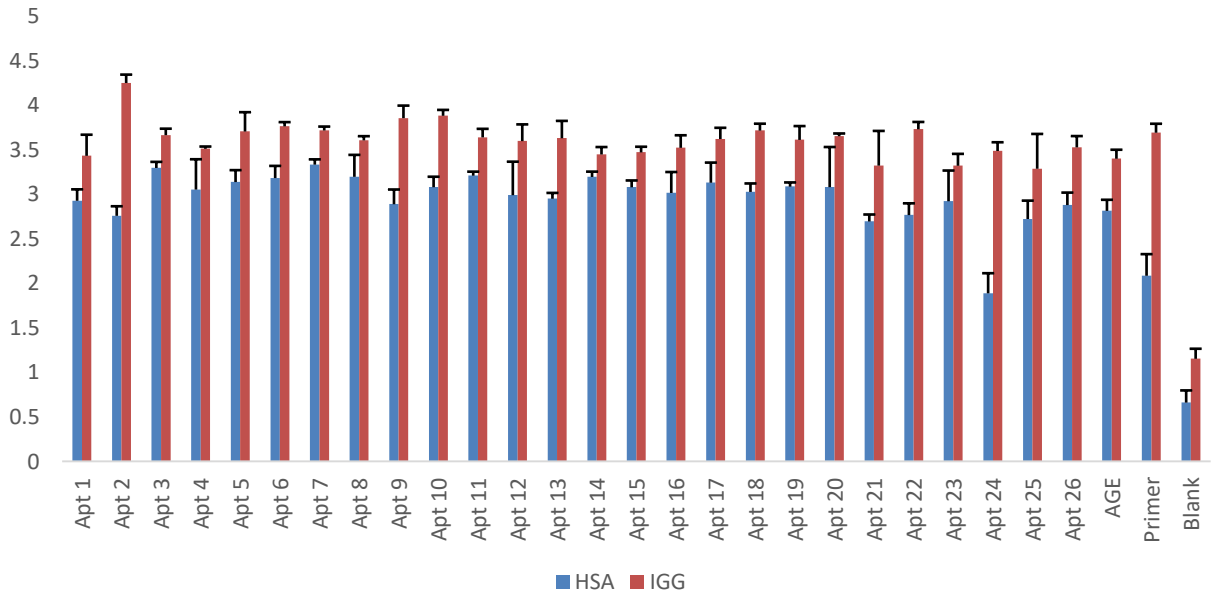

Figure 86: HSA aptamers tested against HSA and IGG at a concentration of 1uM. HSA and IGG were immobilised at a concentration of 20ug/ml. Blocked with 0.1% casein. HSA and IGG tested on separate plates. Each aptamer test was repeated in two wells and three absorbance measurements were taken per well. Standard deviation was determined from all six measurements.

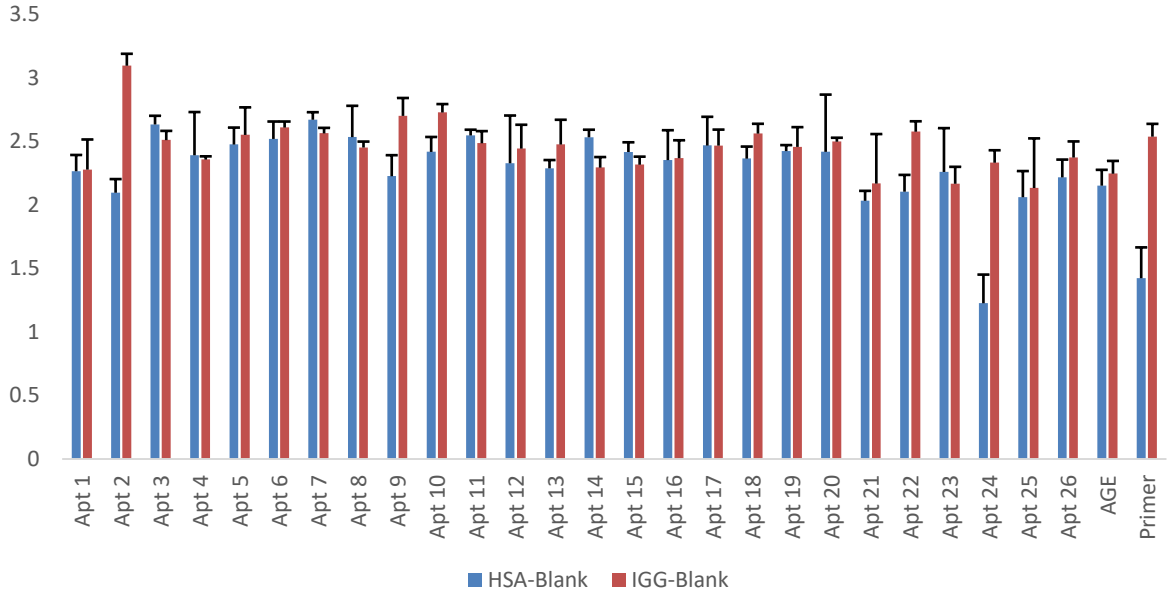

Figure 87: Difference in response of HSA aptamers tested against HSA and IgG at a concentration of 1uM standardised to background. HSA and IgG were immobilised at a concentration of 20ug/ml. Blocked with 0.1% casein. HSA and IgG tested on separate plates. Each aptamer test was repeated in two wells and three absorbance measurements were taken per well. Standard deviation was determined from all six measurements. AGE = Advanced glycation end product aptamer.

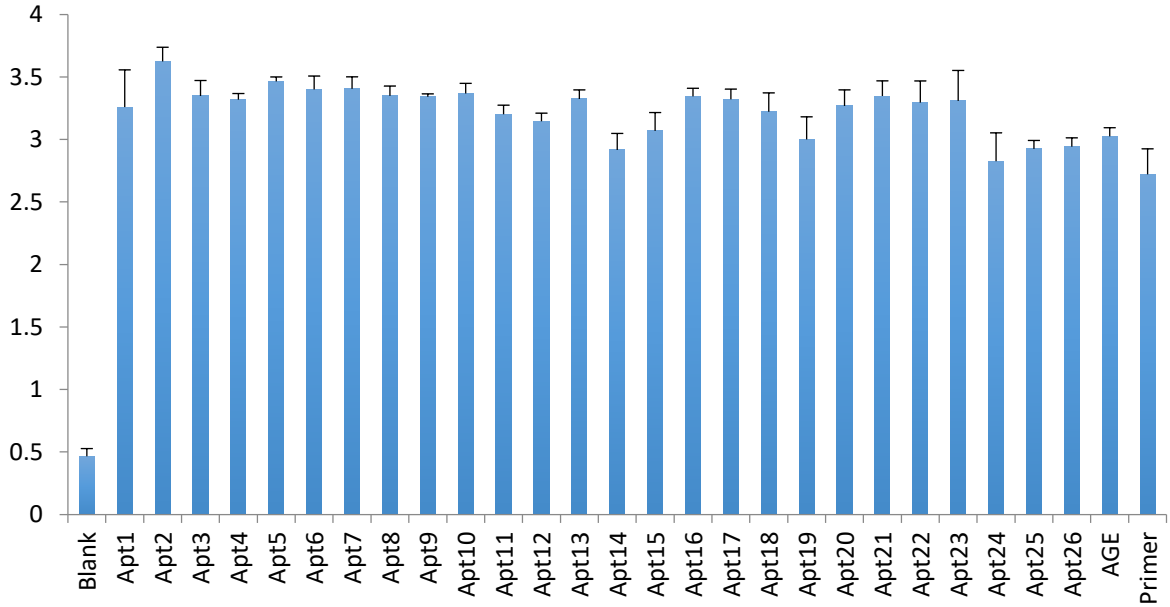

Figure 88: Binding of HSA aptamers to immobilised casein. Casein immobilised at a concentration of 0.01%. Aptamer concentrations were 1um. Each aptamer test was repeated in three wells and three absorbance measurements were taken per well. Standard deviation was determined from all six measurements. AGE = Advanced glycation end product aptamer.

A shift was made to synthetic blocking agents, there was less risk of contamination with albumin and literature demonstrated equal blocking to many protein blocking agents. Blocking was performed with SynBlock and all subsequent washing steps were carried out with binding buffer plus 0.05% Tween. SA-HRP incubation was also carried out in binding buffer with 0.05% Tween.

3.7.1.3 Specific binding of HSA aptamers

All 26 HSA selected aptamers plus the literature AGE HSA aptamer, a lysozyme aptamer and follicle-stimulating hormone (FSH) were tested against HSA, GHSA and IgG. An additional 27th aptamer was selected from further analysis of the NGS data by the package FastAptamer and experimentally tested. Aptamer concentrations were 1uM and protein concentrations were 20ug/ml. Unfortunately FSH was only able to be tested against IgG due to unforeseen limitations on available quantity. Figure 89 demonstrates the response of the aptamers against IgG using the synthetic blocker. Background signal as shown by Blank has decreased approximately 5 fold from casein blocked plates. FSH produces an extremely large signal compared to the rest of the aptamers, unfortunately due to the aforementioned limited supply, the response of this aptamer could not be observed against HSA and IgG.

To further probe the binding of aptamers, a comparison between HSA, IgG and GHSA binding is needed. Figure 90 compares the binding of the 27 selected aptamers, AGEHSA, Lyszozyme and primer against HSA, IgG and GHSA. Each aptamer/sample was tested across three wells except for blank measurements for HSA and IgG which were across six wells. Each well was spectroscopically measured 3 times.

Background signal as indicated by the blank wells is below 0.1 absorbance units for all three proteins with the mean average for each being 0.061 (HSA), 0.056 (GHSA) and 0.095 (IgG). Compared to the

last ran casein blocked experiment which had a background reading of 0.661 (HSA) and 1.153 (IgG) we see approximately a 10 fold reduction in background signal.

Unlike previous experiments, aptamer binding to glycated human serum albumin was tested. Pan specific aptamers (Bind to both HSA and GHSA) are preferable as total albumin count would be measured against glycated HSA in any potential device.

No aptamers demonstrate statistically similar binding to GHSA as they do to HSA, however, several aptamers demonstrate binding above IgG and of significant magnitude to be potentially useful as a pan specific aptamer to GHSA and HSA. Aptamers 9, 11, 12, 17, 19, 20 all demonstrate significant binding to GHSA while having relatively low IGG binding.

Primer binding is significantly below all other aptamer binding as is demonstrated by Figure 90. Aptamers demonstrated between 2.1 (Aptamer 10) and 15.8 (Aptamer 3) fold increase in absorbance signal with HSA over IgG. Mean increase in absorbance units of HSA signal over IgG is 5.6 $\pm$ 2.78. Standard deviation across aptamers was more than previously seen in casein experiments but within an acceptable range.

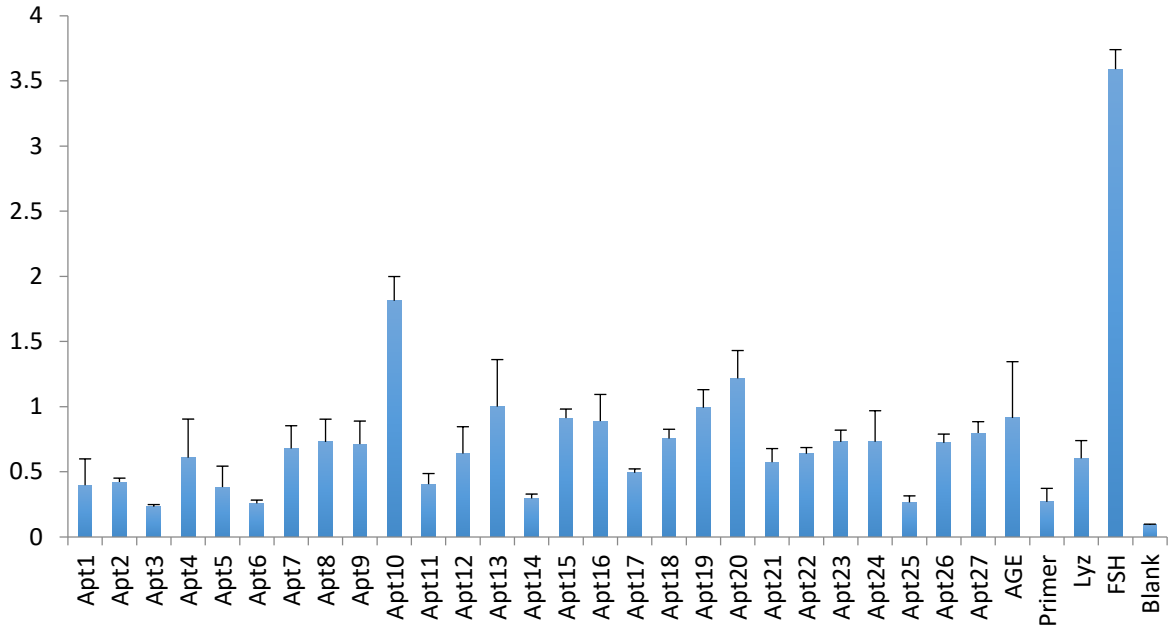

Figure 89: HSA aptamers tested against IgG at a concentration of 1uM. IgG was immobilised at a concentration of 20ug/ml. Blocked with Synblock and 0.05% Tween washing. Each aptamer test was repeated in three wells and three absorbance measurements were taken per well. Standard deviation was determined from all nine measurements. Lyz = lysozyme aptamer. FSH = Follicle-stimulating hormone aptamer. AGE = Advanced glycation end product aptamer.

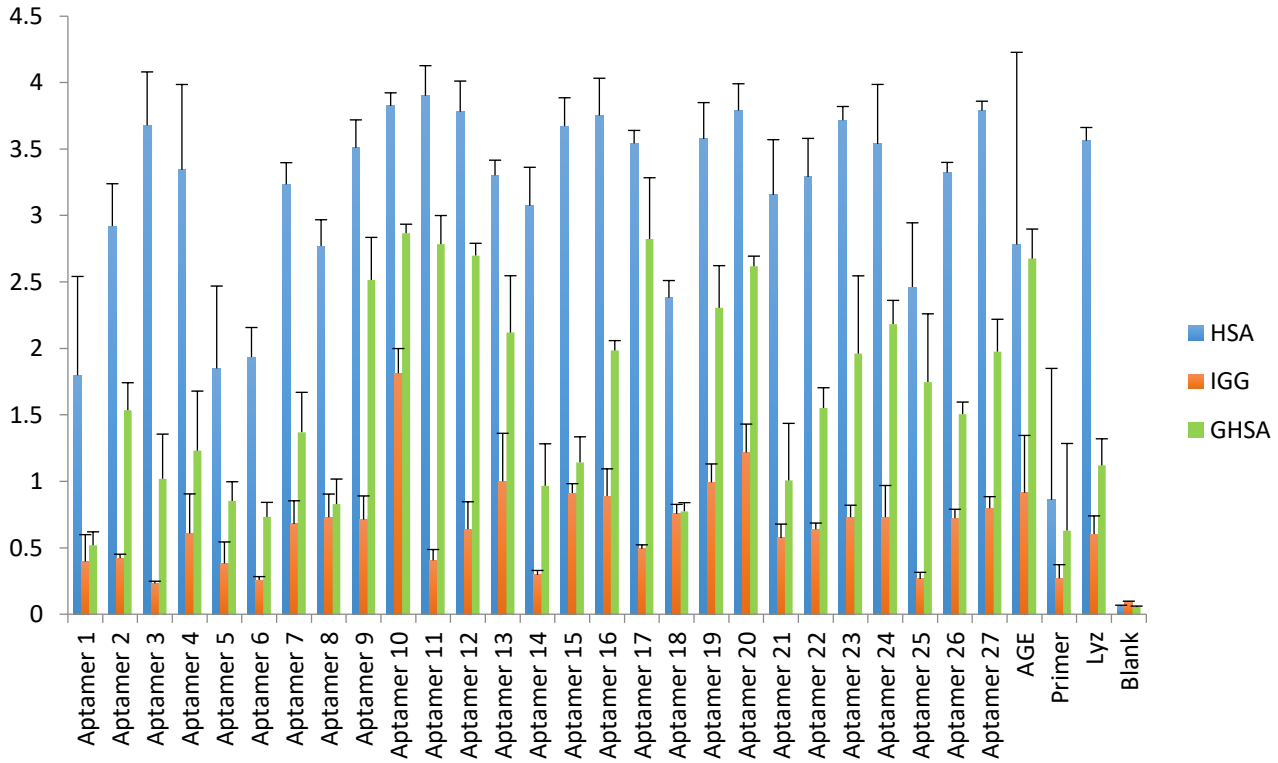

Figure 90: HSA aptamers binding to HSA, IgG, GHSA using synthetic blocking agent. Aptamer concentrations were 1uM and protein concentrations were 20ug/ml. Blocked with Synblock and 0.05% Tween washing. Each aptamer test was

repeated in three wells and three absorbance measurements were taken per well. Standard deviation was determined from all nine measurements. Lyz = lysozyme aptamer. AGE = Advanced glycation end product aptamer.

Absorbance signal from IGG was removed from the respective HSA signal and ordered according to difference as seen in Figure 91. From this 4 aptamers were chosen to test their dose response. Aptamers 3, 11, 17 and 27 were selected. All 4 aptamers were carefully selected for different characteristics. Aptamer 3 was selected as it demonstrated the largest difference between HSA and IgG absorbance while maintaining a significant difference in absorbance between HSA and GHSA, demonstrating an aptamer that could potentially be selective for HSA alone. Aptamers 11 and 17 were selected as they both exhibit significant differences in absorbance between HSA and IGG while having closer HSA and GSHA absorbance; thus indicating potential pan specific aptamers (bind to both GHSA and HSA). Finally, aptamer 27 was selected. In addition to demonstrating significant absorbance differences between HSA and GHSA/IGG, it was selected with a different NGS analytical technique (FASTAptamer) to the other aptamers and was the largest non mutated repeat sequence in this analysis group.

Lysozyme aptamer also produced a large absorbance signal when binding to HSA over IGG.

The response of each aptamer to HSA, IgG and GHSA was measured (Figure 92 -Figure 95). With all 4 aptamers we see a double peak, initially around 30nM and then 1uM/3uM before falling back down at 10uM. The 1st peak around 30nM is notably present in the HSA binding experiments for all 4 aptamers, while IGG binding across all 4 aptamers is significantly reduced. Aptamer 27 also demonstrates significant binding to GHSA at 30nM. Contrast this to absorbance demonstrated at 1uM and 3uM we similar response to HSA, GHSA and IgG for all aptamers before this drops off at 10uM.

It is possible that specific binding is observed at 30nM before competition at the surface causes steric hindrance at 100nM and 200nM. As the concentration increases non specific binding dominates which results in a large signal increase before once again steric hindrance effects dominate and limited aptamers are able to stably bind to the surface and are thus washed off. A reduction in surface protein from 20ug/ml could potentially allow for this specific zone to be extended. As previously discussed, this effect could also be a result of a systematic error like pipetting, however, as this effect was observed across multiple experiments which were all separately undertaken, carefully controlled and methodically carried out, it is believed these errors have been kept to a minimum. At this stage it was determined that progression to electrochemistry would be beneficial as some of the effects being observed could be ELONA specific.

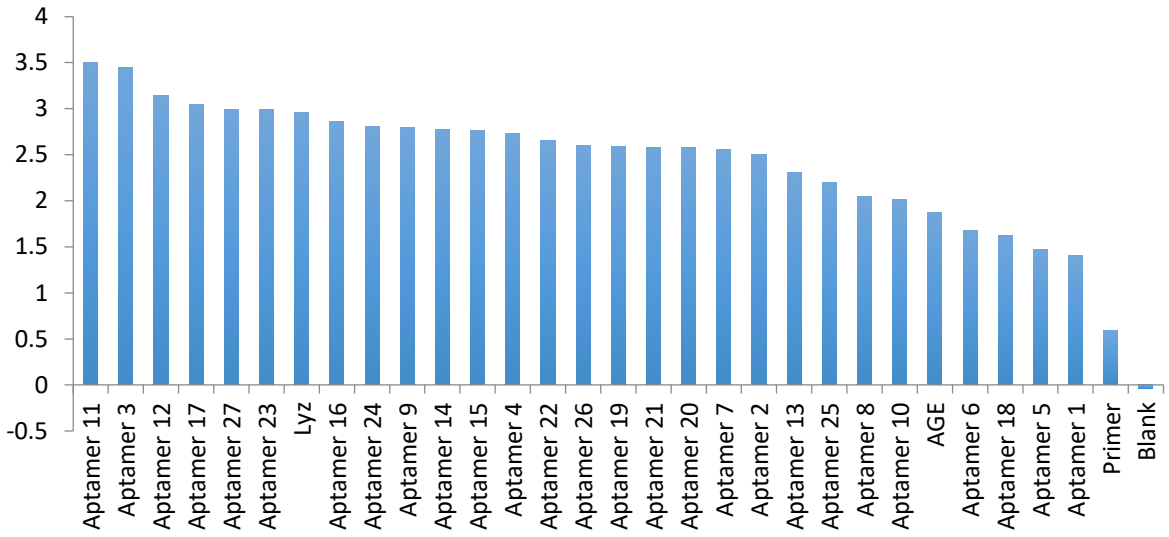

Figure 91: HSA aptamer binding to HSA minus IGG binding. Aptamer concentrations were 1uM and protein concentrations were 20ug/ml. Blocked with Synblock and 0.05% Tween washing. Each aptamer test was repeated in three wells and three absorbance measurements were taken per well. Standard deviation was determined from all nine measurements. Lyz = lysozyme aptamer. AGE = Advanced glycation end product aptamer.

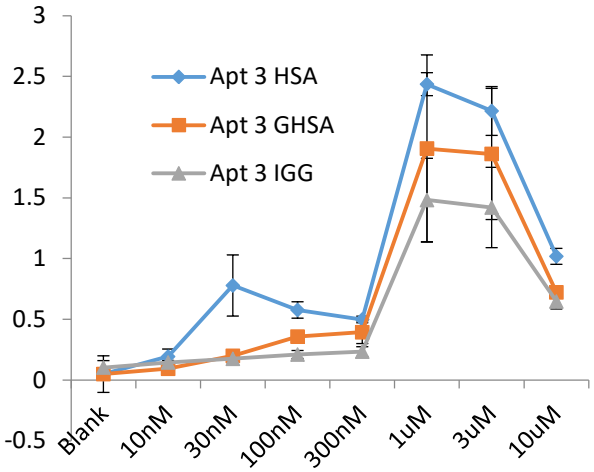

Figure 92: Dose response of HSA aptamer 3 to HSA, GHSA and IGG. HSA, GHSA and IGG were immobilised at a concentration of 20ug/ml. Blocked with Synblock and 0.05% Tween washing. Each concentration test was repeated in three wells and three absorbance measurements were taken per well. Standard deviation was determined from all nine measurements.

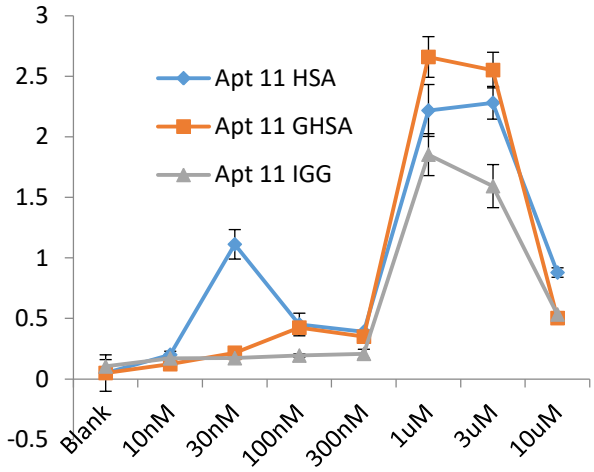

Figure 93: Dose response of HSA aptamer 11 to HSA, GHSA and IGG. HSA, GHSA and IGG were immobilised at a concentration of 20ug/ml. Blocked with Synblock and 0.05% Tween washing. Each concentration test was repeated in three wells and three absorbance measurements were taken per well. Standard deviation was determined from all nine measurements.

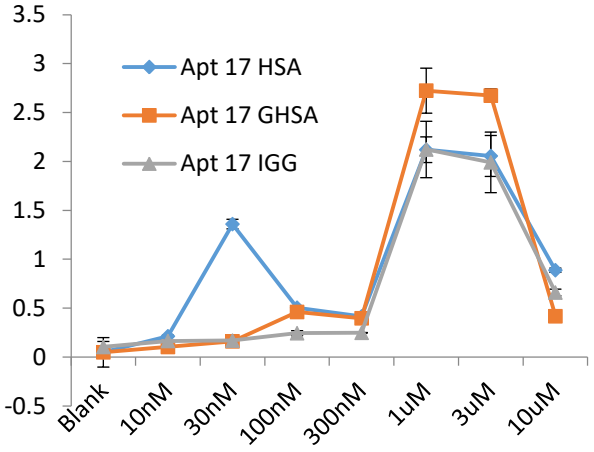

Figure 94: Dose response of HSA aptamer 17 to HSA, GHSA and IGG. HSA, GHSA and IGG were immobilised at a concentration of 20ug/ml. Blocked with Synblock and 0.05% Tween washing. Each concentration test was repeated in three wells and three absorbance measurements were taken per well. Standard deviation was determined from all nine measurements.

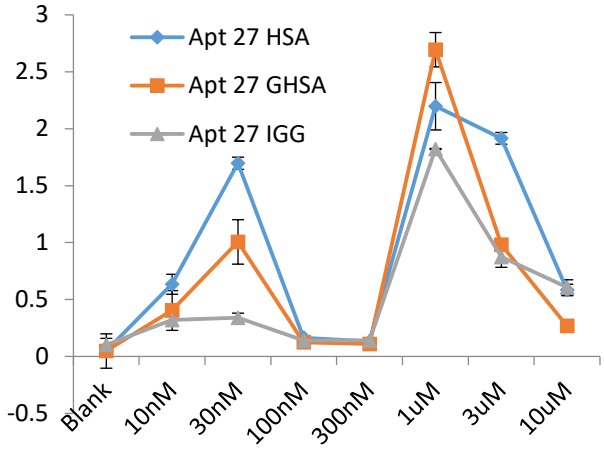

Figure 95: Dose response of HSA aptamer 27 to HSA, GHSA and IGG. HSA, GHSA and IGG were immobilised at a concentration of 20ug/ml. Blocked with Synblock and 0.05% Tween washing. Each concentration test was repeated in three wells and three absorbance measurements were taken per well. Standard deviation was determined from all nine measurements.

3.7.2 ELONA GHSA

Once the NGS analysis was completed for the GHSA SELEX aptamers, they were tested for binding with ELONA. Using what was learnt throughout the HSA ELONA testing process, GHSA plates were blocked with Synblock and all subsequent blocking steps were carried out with binding buffer plus 0.05% Tween. SA-HRP incubation was carried out in binding buffer with 0.05% Tween. The 20 aptamers selected from the NGS analysis along with both the literature AGE HSA aptamer and lysozyme aptamer were tested against glycated HSA and non glycated HSA. Aptamer concentration was 1uM and protein incubation concentration was 20ug/ml.

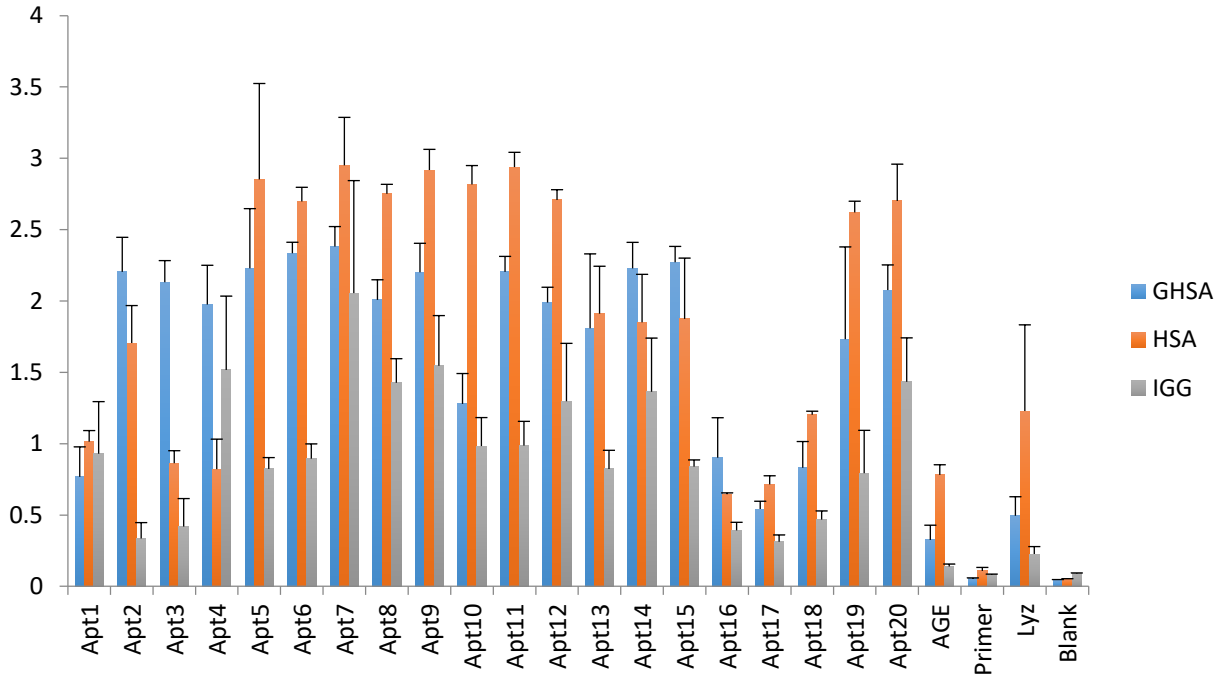

Figure 96: GHSA aptamers binding to HSA, IGG, GHSA using synthetic blocking agent. Aptamer concentrations were 1uM and protein concentrations were 20ug/ml. Blocked with Synblock and 0.05% Tween washing. Each aptamer test was repeated in three wells and three absorbance measurements were taken per well. Standard deviation was determined from all nine measurements. Lyz = lysozyme aptamer. AGE = Advanced glycation end product aptamer.

Two aptamers demonstrated a strong absorbance in the GHSA arm, while showing much lower HSA absorbance. These were aptamers were chosen to further test, specifically their dose response against GHSA, HSA and IGG. They were tested alongside aptamer 17 which demonstrated the lowest

absorbance across all three proteins and aptamer 15 which had very similar absorbance between HSA and GHSA. The absorbance responses are seen in Figure 97 -Figure 100.

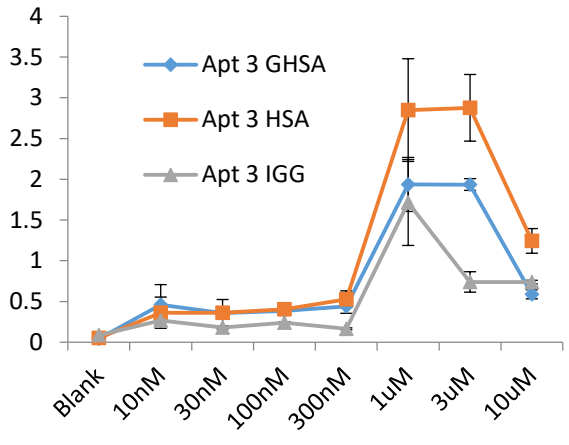

Figure 97: Dose response of GHSA aptamer 3 to HSA, GHSA and IGG. HSA, GHSA and IGG were immobilised at a concentration of 20ug/ml. Blocked with Synblock and 0.05% Tween washing. Each concentration test was repeated in three wells and three absorbance measurements were taken per well. Standard deviation was determined from all nine measurements.

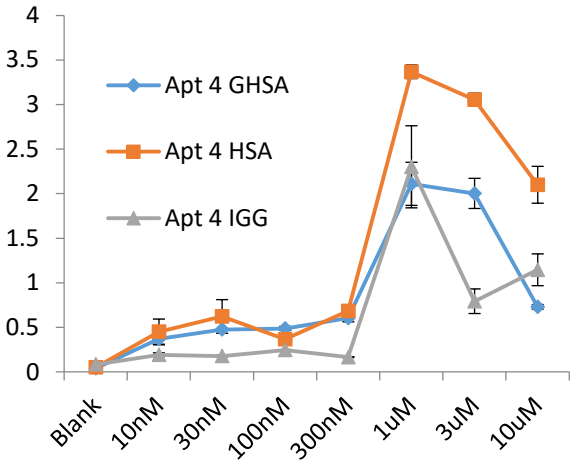

Figure 98: Dose response of HSA aptamer 4 to HSA, GHSA and IGG. HSA, GHSA and IGG were immobilised at a concentration of 20ug/ml. Blocked with Synblock and 0.05% Tween washing. Each concentration test was repeated in three wells and three absorbance measurements were taken per well. Standard deviation was determined from all nine measurements.

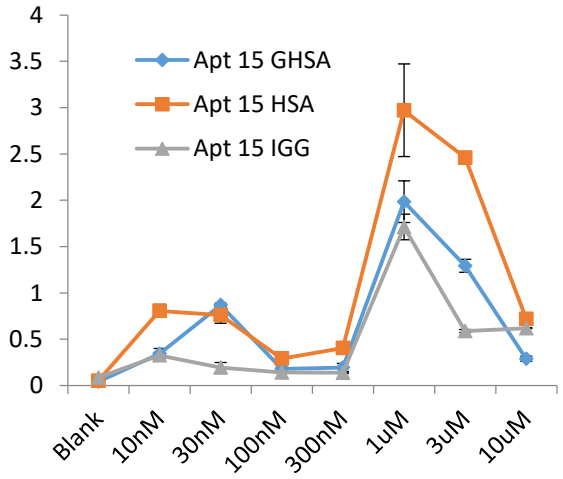

Figure 99: Dose response of HSA aptamer 15 to HSA, GHSA and IGG. HSA, GHSA and IGG were immobilised at a concentration of 20ug/ml. Blocked with Synblock and 0.05% Tween washing. Each concentration test was repeated in three wells and three absorbance measurements were taken per well. Standard deviation was determined from all nine measurements.

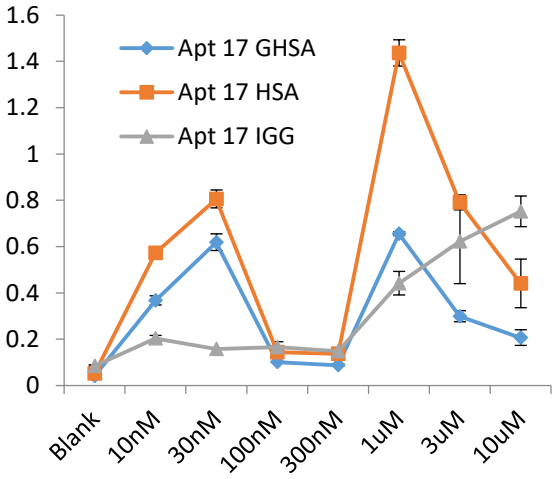

Figure 100: Dose response of HSA aptamer 17 to HSA, GHSA and IGG. HSA, GHSA and IGG were immobilised at a concentration of 20ug/ml. Blocked with Synblock and 0.05% Tween washing. Each concentration test was repeated in three wells and three absorbance measurements were taken per well. Standard deviation was determined from all nine measurements.

A similar response was observed by the GHSA aptamers to that seen with the HSA aptamers. Peaks for all four aptamers were seen at 1uM before falling significantly back down at 10uM. The exception for this was the IgG response for aptamers 15 and 17. The response of aptamers 15 and 17 when compared with the other aptamers including the HSA aptamers further reinforces the theory that the absorbance response we are seeing above 1uM is indicative of a non specific response. There is minimal IgG absorbance for aptamer 15 and 17 between 10nM and 300nM but we see a gradual increase up through 1uM, 3uM and 10uM. Whether this is attributable to a specific or non-specific response is difficult to determine, however, the gradual increase of the IgG as the HSA and GSHA absorbance falls away alludes to a specific response. Rubin et al have shown that IgG from normal human serum shows actively to denatured DNA (ssDNA), specifically that a small fraction of IGG has the capability to bind denatured DNA; this could explain the observed signal (188).

Aptamers 3, 4 and 15 demonstrate very similar magnitudes of absorbance indicating the same effect is being observed across all three, that of a non specific response. The lower magnitude of response for aptamer 17 across all three proteins and a more gradual IGG response may indicate a different operating concentration.

Chapter 3.8

Results: Electrochemistry

3.8 Electrochemistry

Testing of the selected aptamers with Electrochemistry was undertaken. Utilisation of electrochemistry as an analytical method was undertaken for two reasons. First any patient or clinician focused device needs to be a simple and cheap as possible. Electrochemistry allows for a scalability and cheap production of devices that is not always possible with other detection systems like ELONA. Secondly, additional information from aptamer binding is needed from another system. ELONA while a powerful technique relies on the immobilisation of protein which is unrealistic in a clinical environment. Electrochemical devices can be constructed from a range of materials and involve various sensing mechanisms. It was decided to utilise gold disk electrodes over other materials and electrode types. While carbon screen printed electrodes are commonly used in glucose electrode systems, surface roughness and more difficult surface chemistry in relations to aptamers make them a difficult choice. Gold disk electrodes are reusable and as such allow for a limited form of consistency between experiments.

3.8.1 Preparation and cleaning of electrodes

Before utilisation of aptamers within an electrochemical system the gold electrodes need to be cleaned and checked for quality of response. Gold electrodes are manually and electrochemically cleaned as described in Chapter 2.4.4. The electrochemical graph typical for a clean electrode is shown in Figure 101. It shows the removal and formation of gold oxide as demonstrated by a reduction peak seen at 0.9V and 3 oxidation peaks seen between 1.2V and 1.3V, however, the three peaks can often be observed as a single or double peak

Next the clean gold electrodes were tested with cyclic voltammetry utilising solution free ferrocene carboxylic acid in binding buffer (PBS 10mM + $MgCl_2$ 10mM pH7.4) (Figure 102). While a different response is expected with surface bound redox probe, the solution free response will be able to inform us about the quality of the electrode. Oxidation peaks between 0.35V and 0.38 were observed at concentrations of ferrocene carboxylic acid from 100uM to 10mM. Reduction peaks

were observed between 0.26 and 0.29 over the same range. The shape and amount of peak separation represent as a reversible system as expected with ferrocene carboxylic acid. This demonstrates that the cleaned gold electrodes are suitable for electrochemical testing. Multiple methods can be utilised to generate an electrochemical signal from aptamer binding (Chapter 1.4). It was decided to utilise a surface immobilised aptamer covalently attached to a redox probe. This is advantageous over other techniques as once the electrode is prepared it is ready to use and it doesn't require the addition of any redox probe or other solution in the measurement step. However, one potential major disadvantage is associated with the aptamer structure. If it doesn't change structure upon binding then minimal or no signal will be observed.

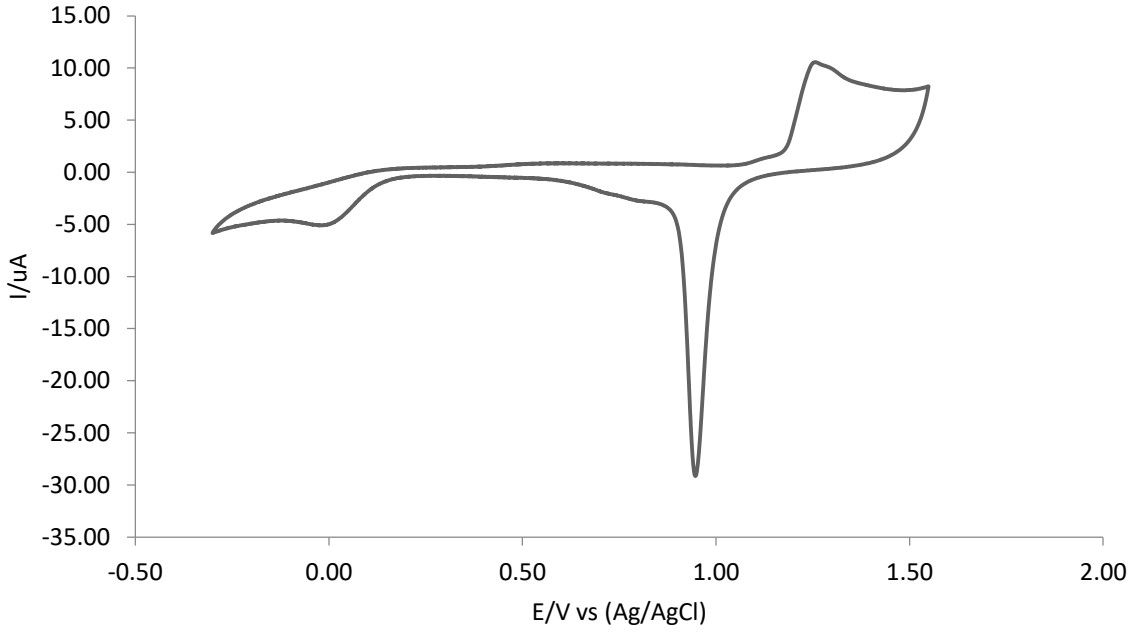

Figure 101: Cyclic Voltammetry cleaning of gold electrode in 0.5M H_2SO_4. Scan range -0.3V to 1.55V. Scan rate =0.1Vs^{-1}. Step/Interval = 0.001V. Changed H_2SO_4 solution when curve no longer progressing, typically between 10 and 20 cycles. Cycled until reached above curve. Typically between 30 and 40 scans required to reach the typical curve seen above.

3.8.2 Cyclic Voltammetry of HSA binding

Selected aptamer was extended with an 18 base region that is complementary to a thiol modified 18 base primer. The aptamer strand contained an amine group at the 5' end which was modified with ferrocene carboxylic acid utilising NHS/EDC chemistry (as described in Chapter 2.4.6). Aptamer and

primer strands were then hybridised together before immobilisation onto a gold electrode. Primer contained a thiol group at the 5' end which allowed for its immobilisation onto a gold electrode.

Aptamers 3, 4 and 11 were chosen based on the response from Figure 90. All three demonstrated a strong response over IGG, while 3 and 4 also demonstrated a strong response over GHSA. Aptamer 11's similar response between HSA and GHSA allows for a comparison.

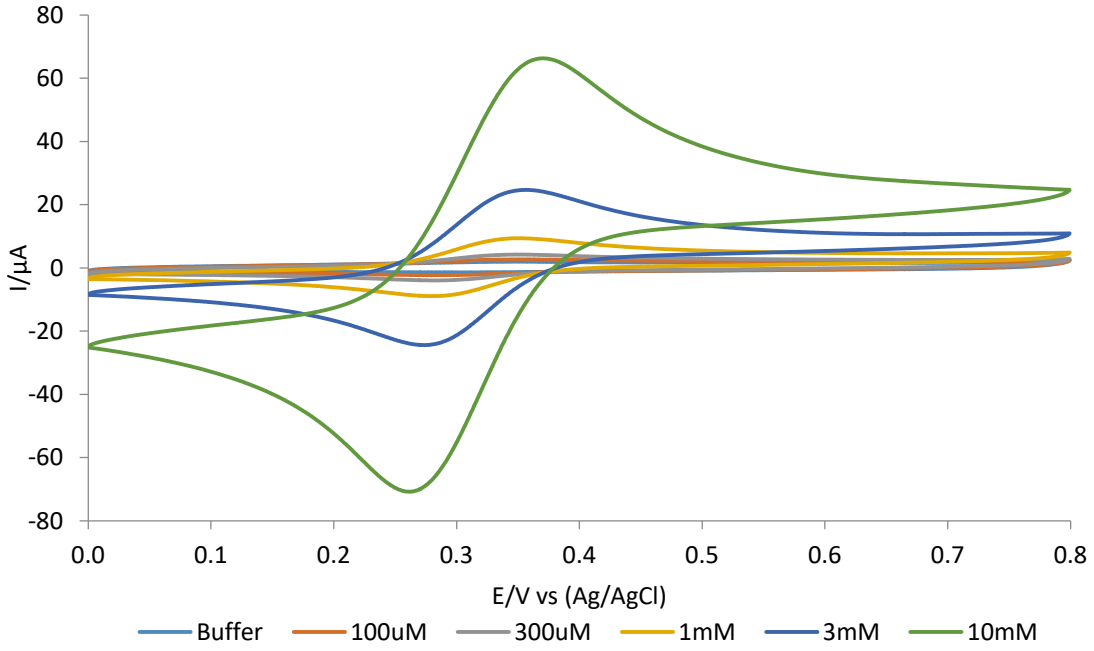

Figure 102: **Cyclic Voltammetry of buffer and 100uM,300uM,1mM,3mM and 10mM Ferrocenecarboxylic acid concentrations. Utilised gold disk electrode that has been mechanically and electrochemically cleaned. Gold electrode was not modified. Binding buffer was utilised as measurement solution. Voltage scanned between 0V and 0.8V. Scan rate =0.5Vs^{-1}. Step/interval =0.001V.**

The response of aptamers 3, 4 and 11 were tested across 4 different electrodes utilising cyclic voltammetry. We see oxidation peaks around 0.3V and small but noticeable variations in current upon addition of HSA with most of the sensors utilised.

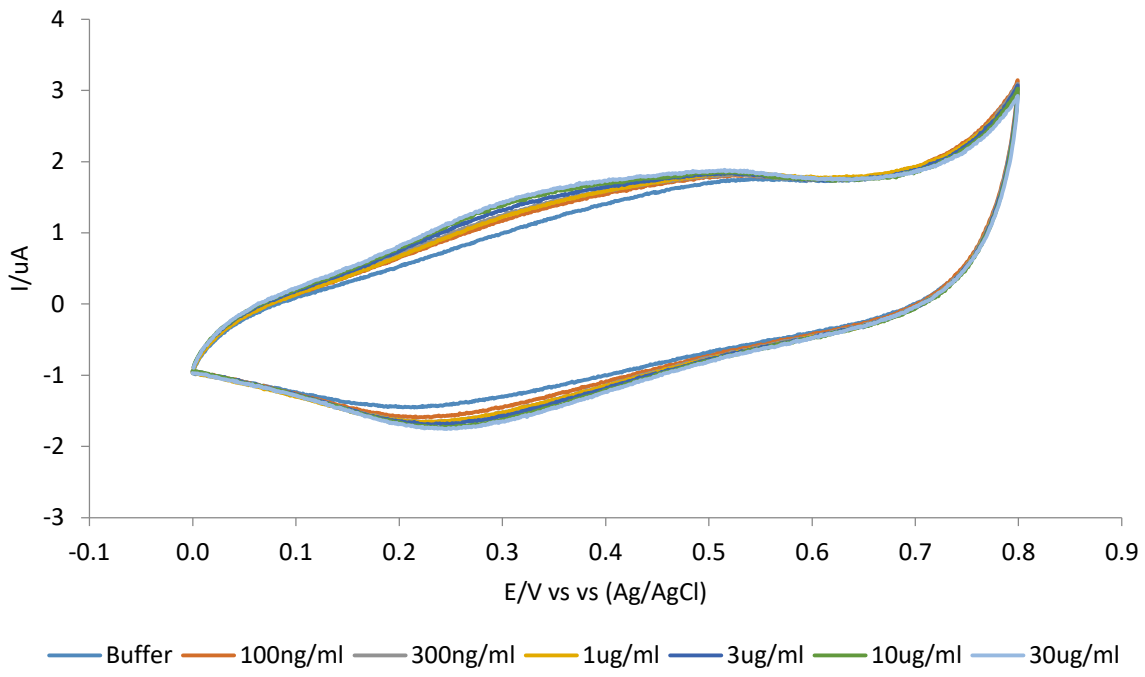

Figure 103: Electrode 2 HSA Aptamer 3 tested against various concentrations of HSA. Fully prepared sensor but no FC attached to the aptamer. Binding buffer was utilised as measurement solution. Voltage scanned between 0V and 0.8V. Scan rate =0.5Vs-1. Step/interval =0.001V.

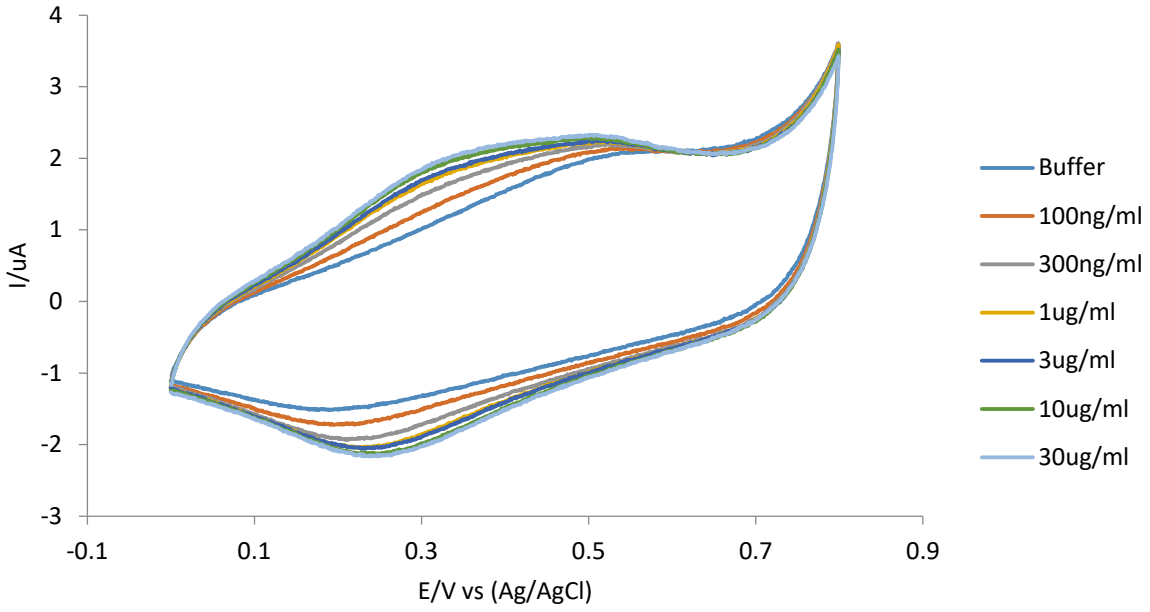

Figure 104: Electrode 3 HSA Aptamer 3 tested against various concentrations of HSA. Binding buffer was utilised as measurement solution. Voltage scanned between 0V and 0.8V. Scan rate =0.5Vs-1. Step/interval =0.001V.

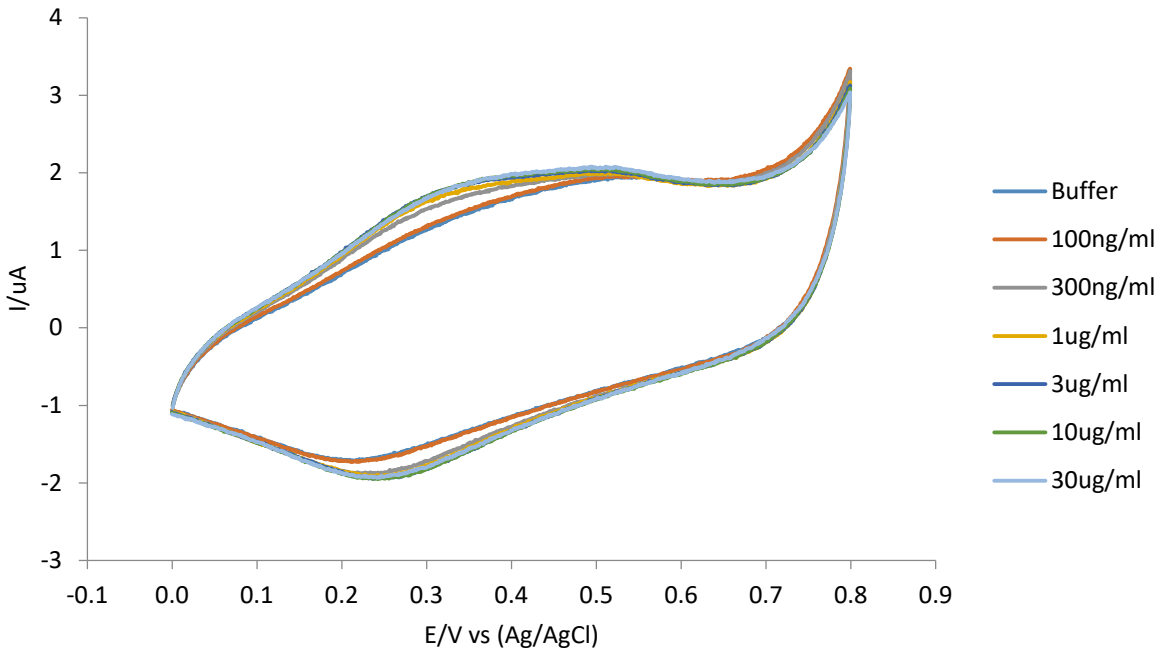

Figure 105: Electrode 4 with HSA aptamer 3. Tested against various concentrations of HSA. Binding buffer was utilised as measurement solution. Voltage scanned between 0V and 0.8V. Scan rate =0.5Vs-1. Step/interval =0.001V.

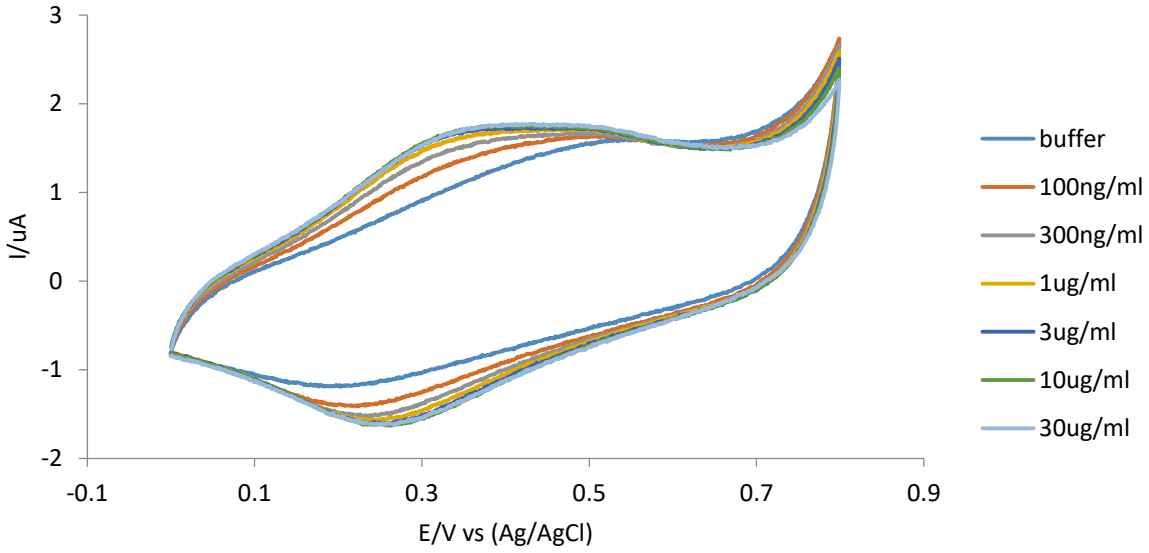

Figure 106 : Electrode 6 Aptamer 11 tested against varying concentrations of HSA. Binding buffer was utilised as measurement solution. Voltage scanned between 0V and 0.8V. Scan rate =0.5Vs-1. Step/interval =0.001V.

Figure 107 shows the variations in current at 0.3V across 4 sensors. We see that the three electrodes modified with ferrocene carboxylic acid aptamers generate a greater signal than aptamer without ferrocene. However, the expected signal difference is lower than one would expect and could indicate problems, specifically the attachment of the ferrocene carboxylic acid may not be efficient.

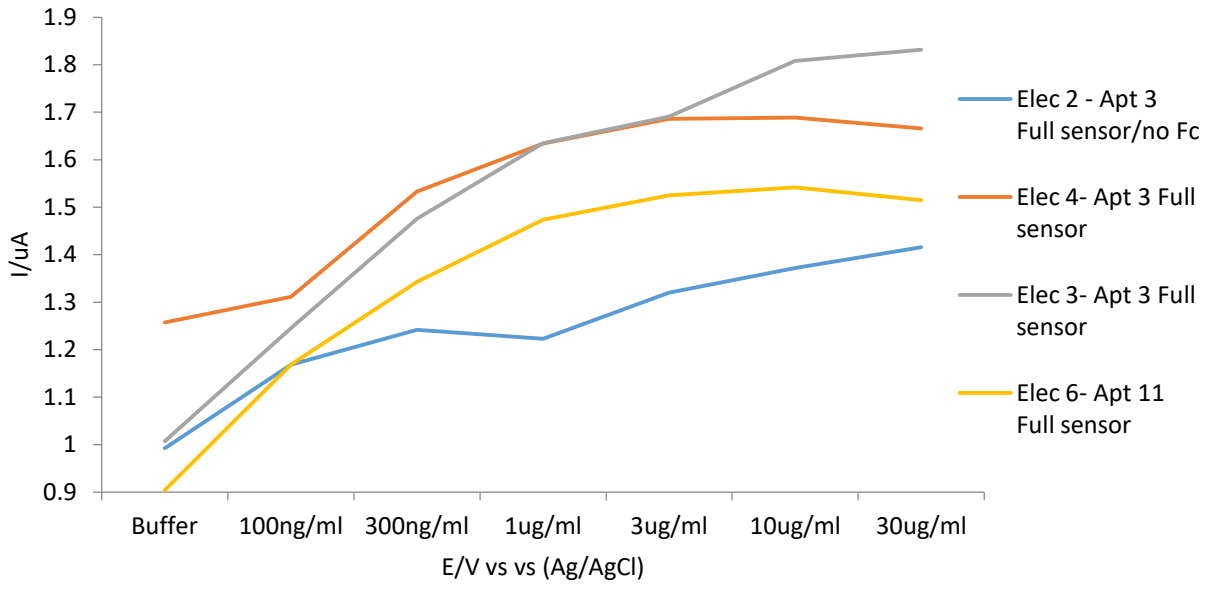

Figure 107: Comparison of CV aptamer response against HSA at 0.3V across 4 different electrodes. Binding buffer was utilised as measurement solution.

3.8.3 Testing different concentrations of immobilised aptamers

Aptamer surface concentration can effect binding of protein. Solution free aptamer concentration was tested at 10uM and 0.1uM. 2 electrodes were tested per concentration and compared with previously tested sensors. Aptamer 11 was chosen as the reference aptamer. Unfortunately due to problems with the electrode utilised in one test, results were not comparable. Only one aptamer incubated in 1uM aptamer was able to be compared. High levels of noise can also be noticed. It was later determined that this was due to an intermittent problem within the Ivium compactstat. Later experiments were carried out with Gamray Ref600 Potentiostat. Due to background noise it is

difficult to determine between concentrations but a clear distinction can be made between baseline and HSA concentration in all cases.

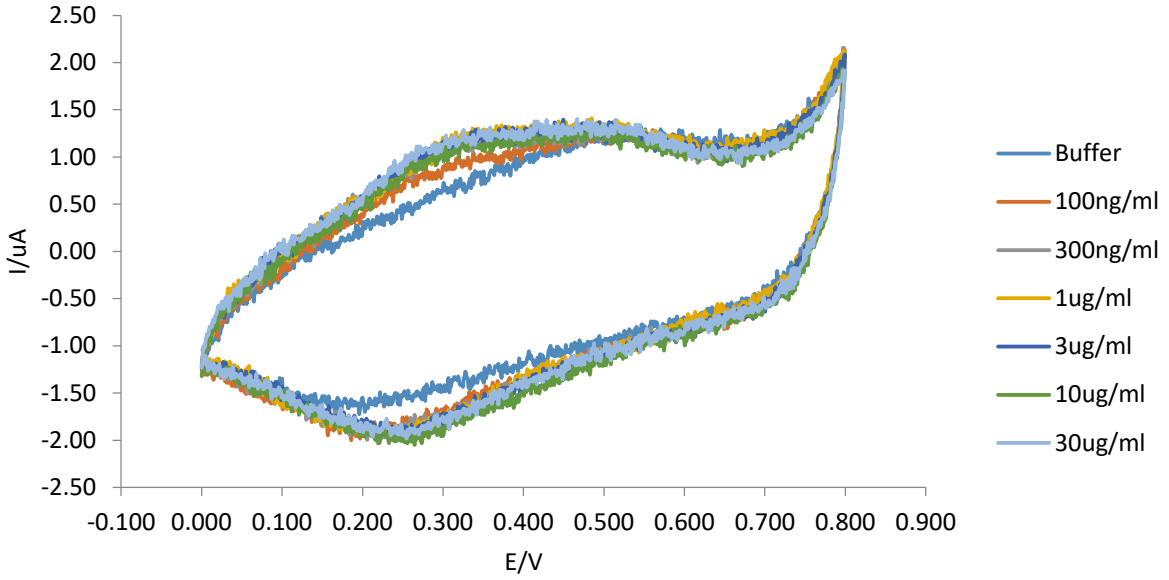

Figure 108: Electrode 1 aptamer 11 10uM - testing against various HSA concentrations. Binding buffer was utilised as measurement solution. Voltage scanned between 0V and 0.8V. Scan rate =0.5Vs-1. Step/interval =0.001V.

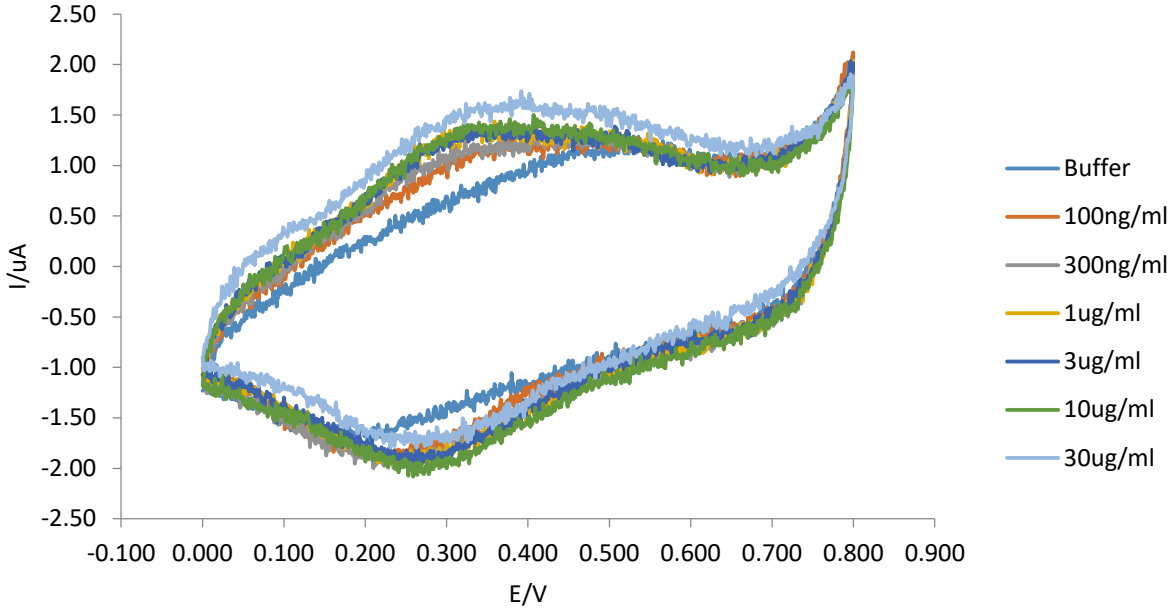

Figure 109: Electrode 6 0.1uM Aptamer 11. Tested against HSA. Binding buffer was utilised as measurement solution. Voltage scanned between 0V and 0.8V. Scan rate =0.5Vs-1. Step/interval =0.001V.

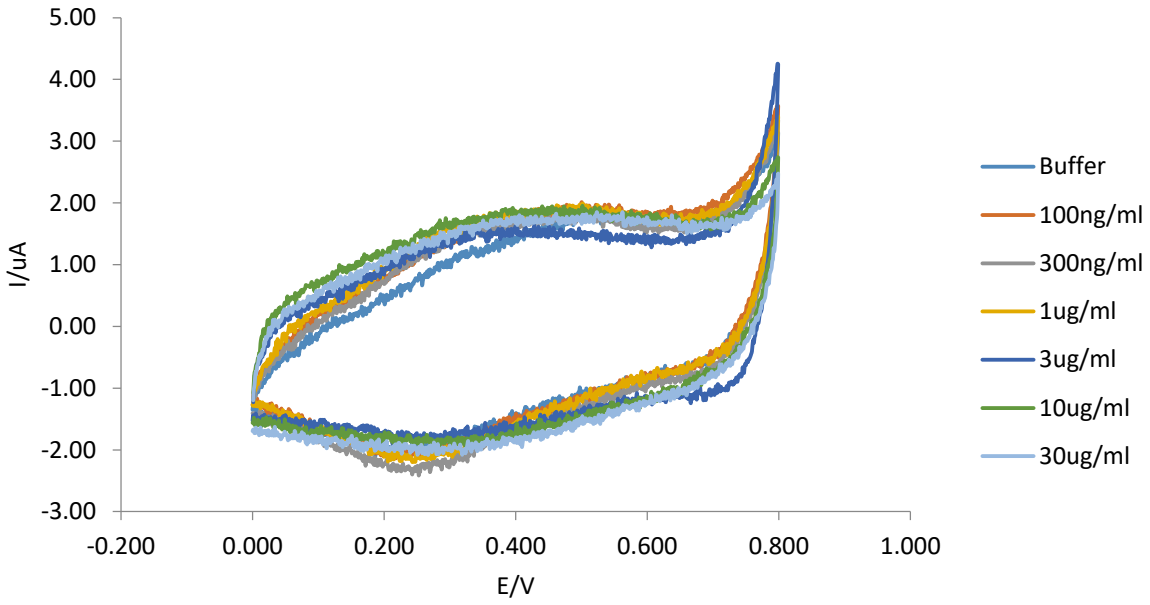

Figure 110: Electrode 2 10uM aptamer 11. Tested against HSA. Binding buffer was utilised as measurement solution. Voltage scanned between 0V and 0.8V. Scan rate =0.5Vs-1. Step/interval =0.001V.

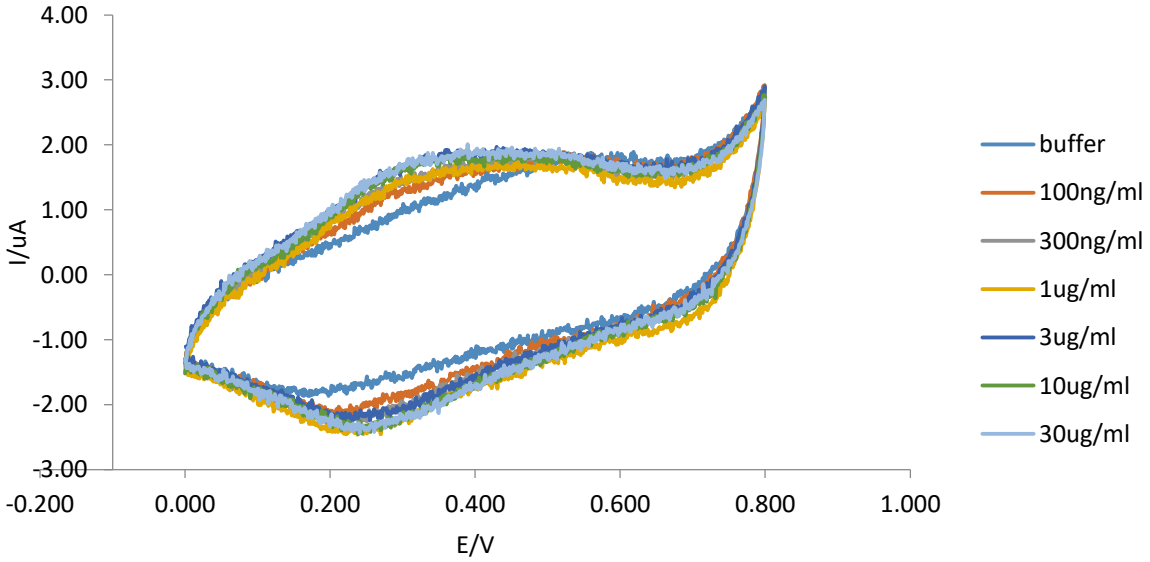

Figure 111: Electrode 4 0.1uM aptamer 11. Tested against HSA. Binding buffer was utilised as measurement solution. Voltage scanned between 0V and 0.8V. Scan rate =0.5Vs-1. Step/interval =0.001V.

The response across electrodes, aptamer and HSA concentration were compared at 0.3V (Figure 112).

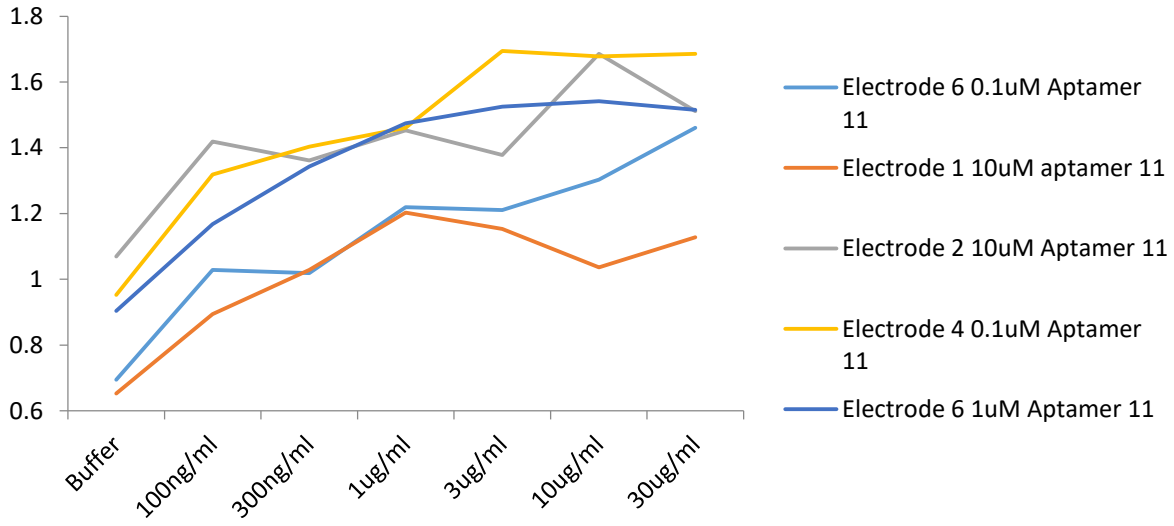

Figure 112: Comparison of CV aptamer response at 0.3V across 5 electrodes with aptamer 11. Binding buffer was utilised as measurement solution.

3.8.4 CV comparison of binding to HSA, GHSA and IGG

Binding to GHSA and IGG was additionally compared to HSA for aptamer 11. No discernible difference could be observed between binding of HSA, GHSA and IGG (Figure 113 and Figure 114) even once differences in background signal were normalised. As detectable differences in signal have been observed in the ELONA data, this could be a result of the limitations of the CV technique. As such a more sensitive technique to changes in redox potential was tested in the next section.

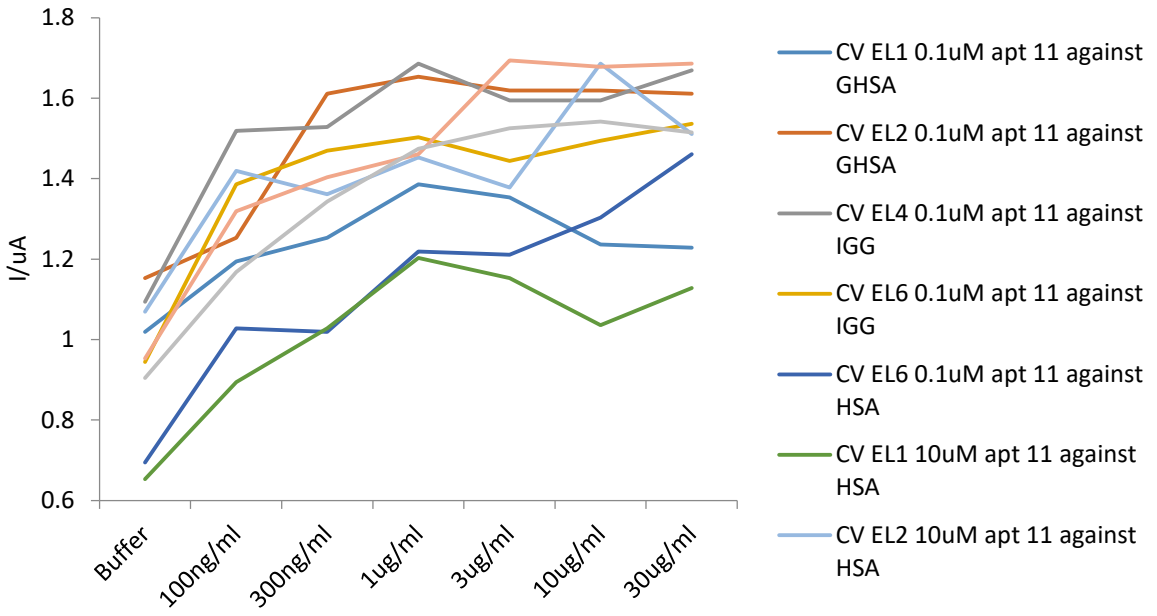

Figure 113: Comparison of CV aptamer response at 0.3V across 7 electrodes with aptamer 11. Binding buffer was utilised as measurement solution. Tested against HSA, GHSA and IGG.

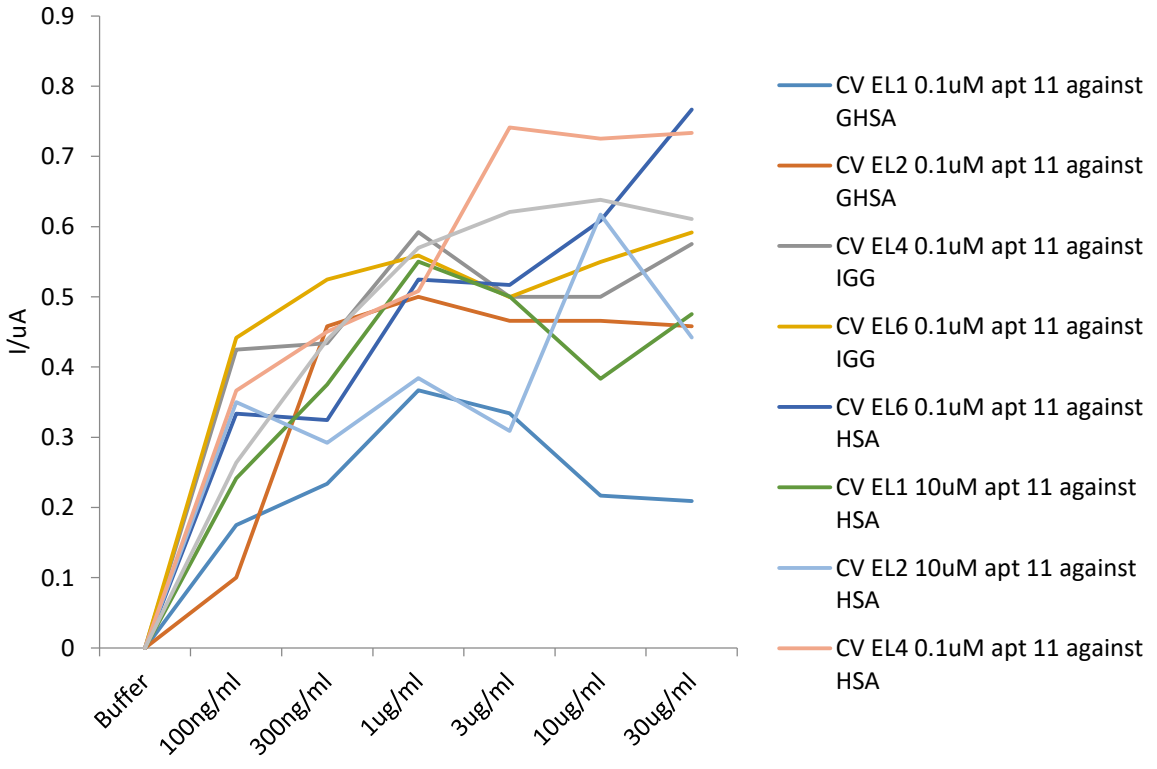

Figure 114: Background removed comparison of CV aptamer response at 0.3V across 7 electrodes with aptamer 11. Binding buffer was utilised as measurement solution. Tested against HSA, GHSA and IGG.

3.8.5 Square wave voltammetry of HSA binding

Square wave voltammetry (SWV) has better sensitivity over cyclic voltammetry to changes in redox current (Chapter 1.5). All 4 sensors previously tested against HSA with varying concentrations of immobilised aptamer were simultaneously tested utilising SWV alongside CV measurements. Unfortunately SWV data from Electrode 1 was corrupted so could not be observed. We see distinct signal differences between baseline measurements and addition of HSA across all concentrations for 0.1uM aptamer (Figure 115-Figure 116).

With 10uM aptamer we see a similar response in signal at baseline, 100 ng/ul, 300 ng/ul, 1 ug/ml and 3 ug/ml. At the higher concentrations of 10 ug/ml and 30 ug/ml we see a distinct current increase (Figure 117).This indicates that a higher aptamer concentration may decrease sensitivity, if we compare baseline at 0.3V of the 10uM aptamer electrode to the 1 uM, we observe that the 1 uM electrodes have a baseline around 1.5 uA, while the 10 uM electrode is close to 4 uA. This could indicate that the higher surface concentration of FCA at the higher aptamer concentration generate an increased background current. It could result in any structural changes (and the resulting current change) from aptamer HSA binding not being detected at lower HSA concentrations.

Across the 0.1uM aptamer sensors we see initially a large increase in current at 100ng/ul which then saturates at higher concentrations. This is evident when comparing the response at 0.3V at each concentration as can be seen in Figure 118. We see similar current increases for both sensors before reaching a plateau. The similarity of response of both sensors at this stage is a good indicator that the electrode and sensor preparation are consistent.

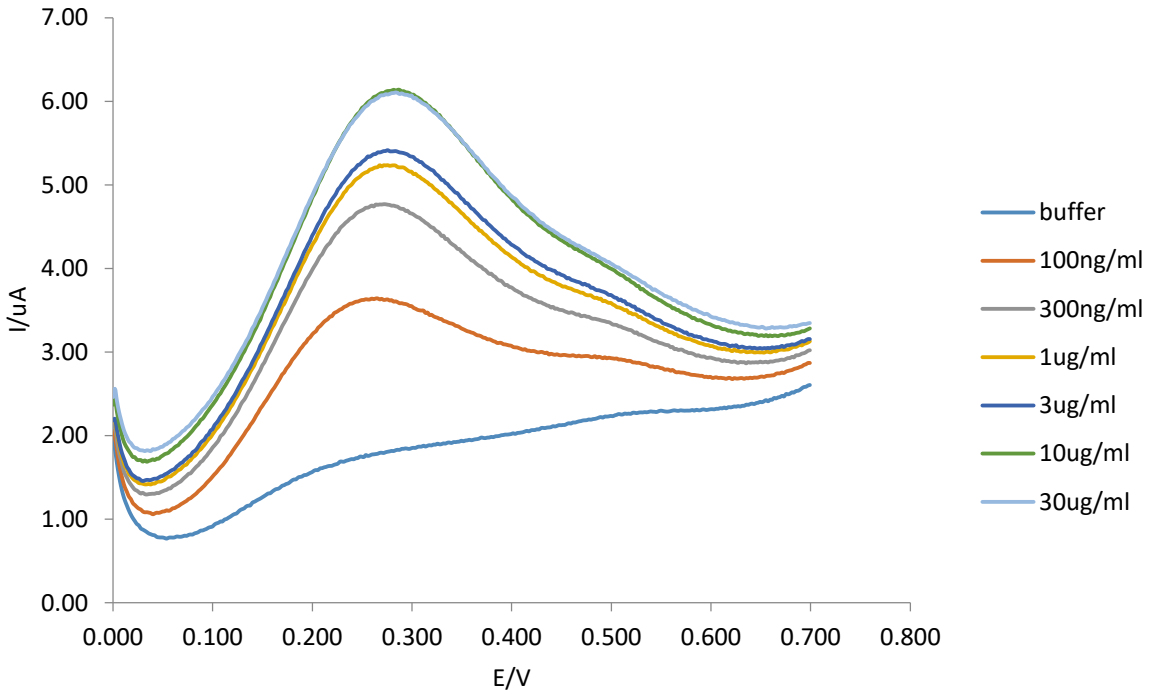

Figure 115: SWV, Electrode 4, aptamer 11 (0.1uM). Tested against HSA. Binding buffer was utilised as measurement solution. Range between 0 and 0.7V. Step size: 2mV. Frequency: 100Hz. Pulse Size 50mV.

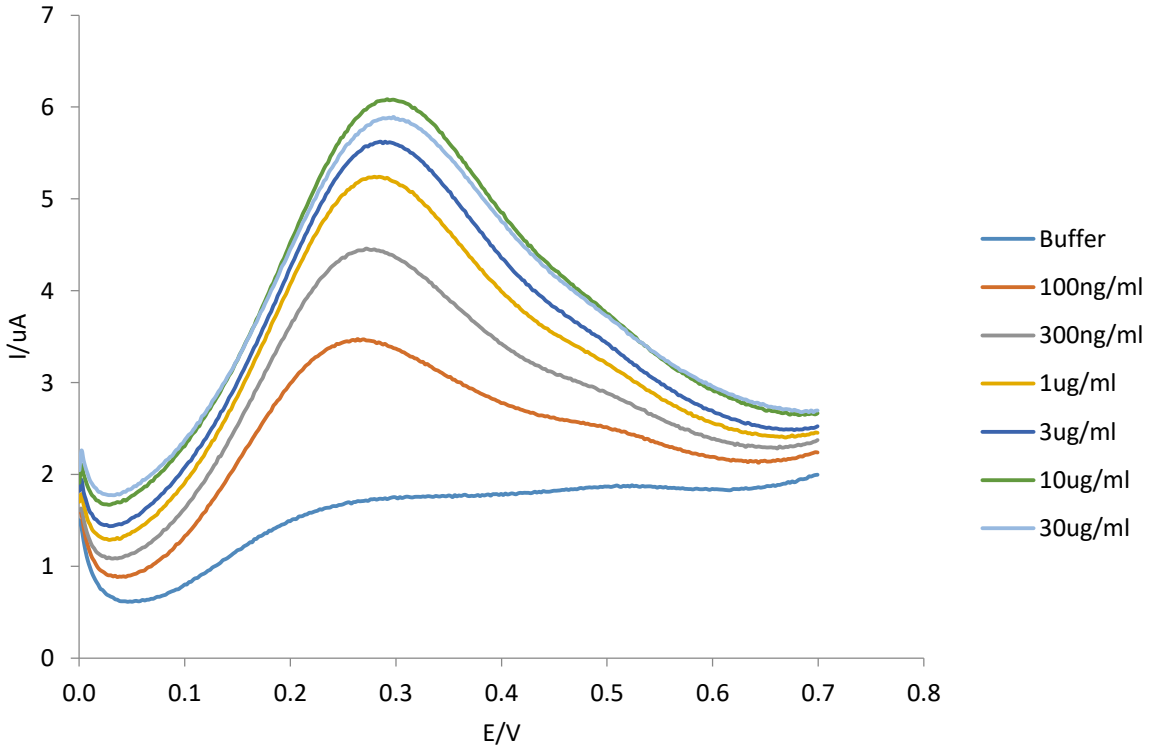

Figure 116: SWV, Electrode 6, aptamer 11 (0.1uM). Tested against HSA. Binding buffer was utilised as measurement solution. Range between 0 and 0.7V. Step size: 2mV. Frequency: 100Hz. Pulse Size 50mV.

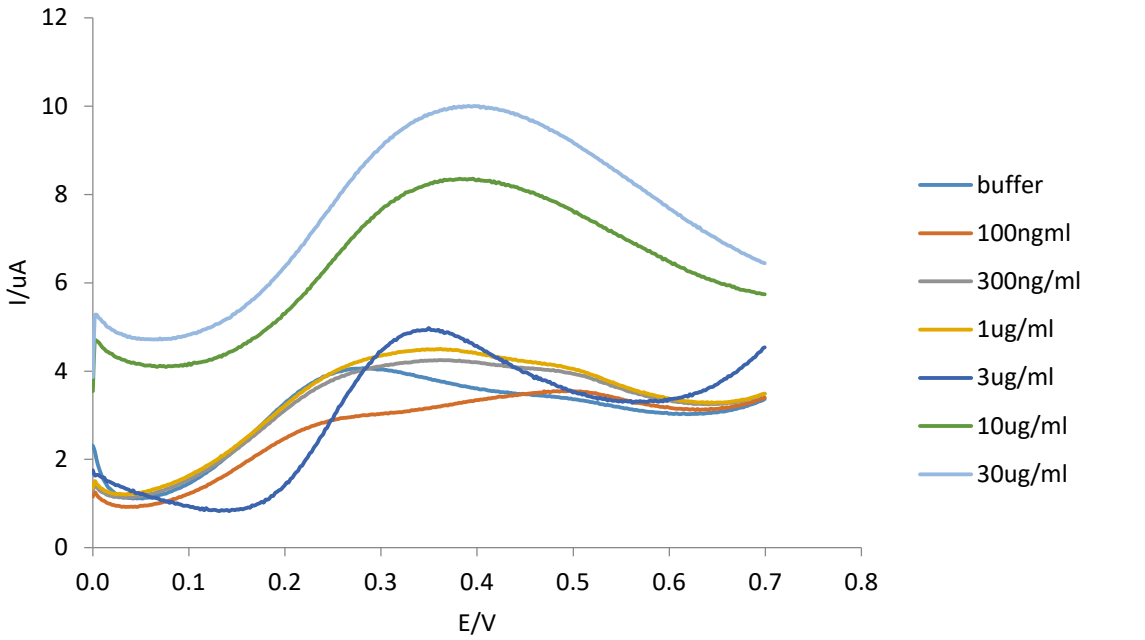

Figure 117: SWV, Electrode 2, aptamer 11 (10uM).Tested against HSA. Binding buffer was utilised as measurement solution. Range between 0 and 0.7V. Step size: 2mV. Frequency: 100Hz. Pulse Size 50mV.

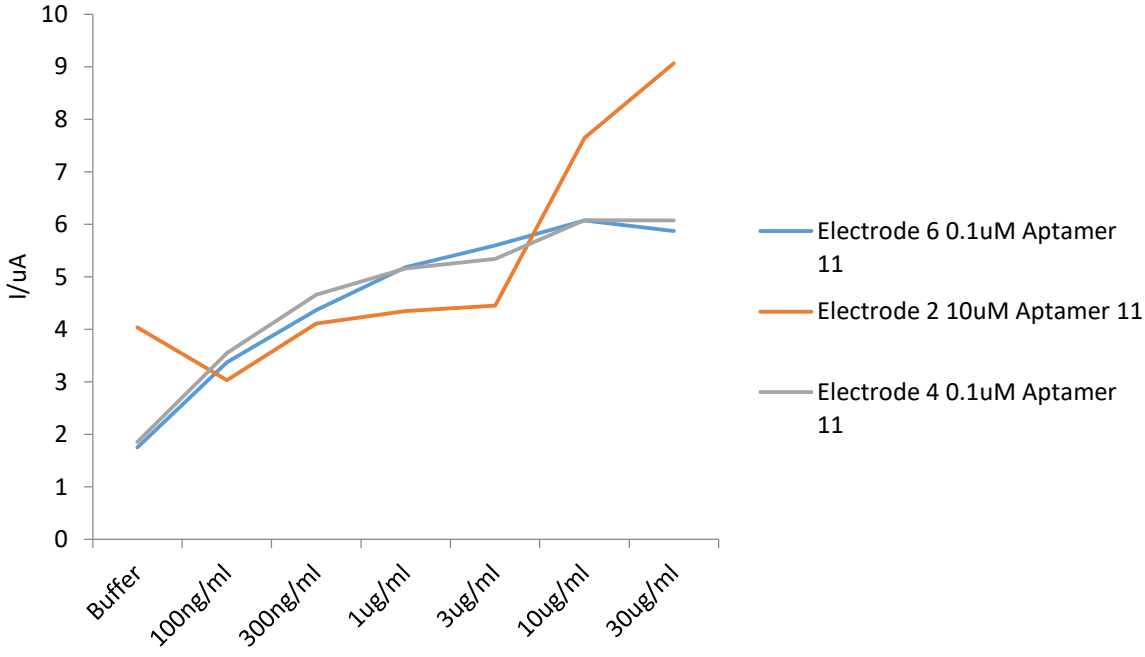

Figure 118: Comparison of SWV aptamer response at 0.3V across 3 electrodes with aptamer 11. Binding buffer was utilised as measurement solution.

3.8.6 SWV comparison of binding to HSA,GSHA and IGG.

Aptamer 11 was tested against IGG and GHSA to determine the dose response of it to other analytes. A similar response to HSA is observed, however the magnitude of response is not as significant as with HSA. From background buffer to 30ug/ml the two 0.1 uM aptamer 11 HSA sensors increased 4.218 uA (Figure 115) and 4.119 uA (Figure 116), while the 10 uM aptamer 11 increased 5.030uA (Figure 117). Comparatively two 0.1 uM aptamer 11 sensors increased 3.271 uA (Figure 119) and 3.566 uA (Figure 120) when incubated with GHSA, while two 0.1 uM aptamer 11 sensors increased 2.629 uA (Figure 121) and 2.344 uA (Figure 122) when incubated with IGG. Mean increase in 0.1 uM aptamer 11 response was 67.65% for HSA over IGG and 21.94% over GHSA. Considering that HSA concentration in vivo is considerably higher than GHSA or IgG, the difference if measuring a patient's blood sample may be substantially more. Comparative response at 0.3V is demonstrated in Figure 123 and Figure 124.

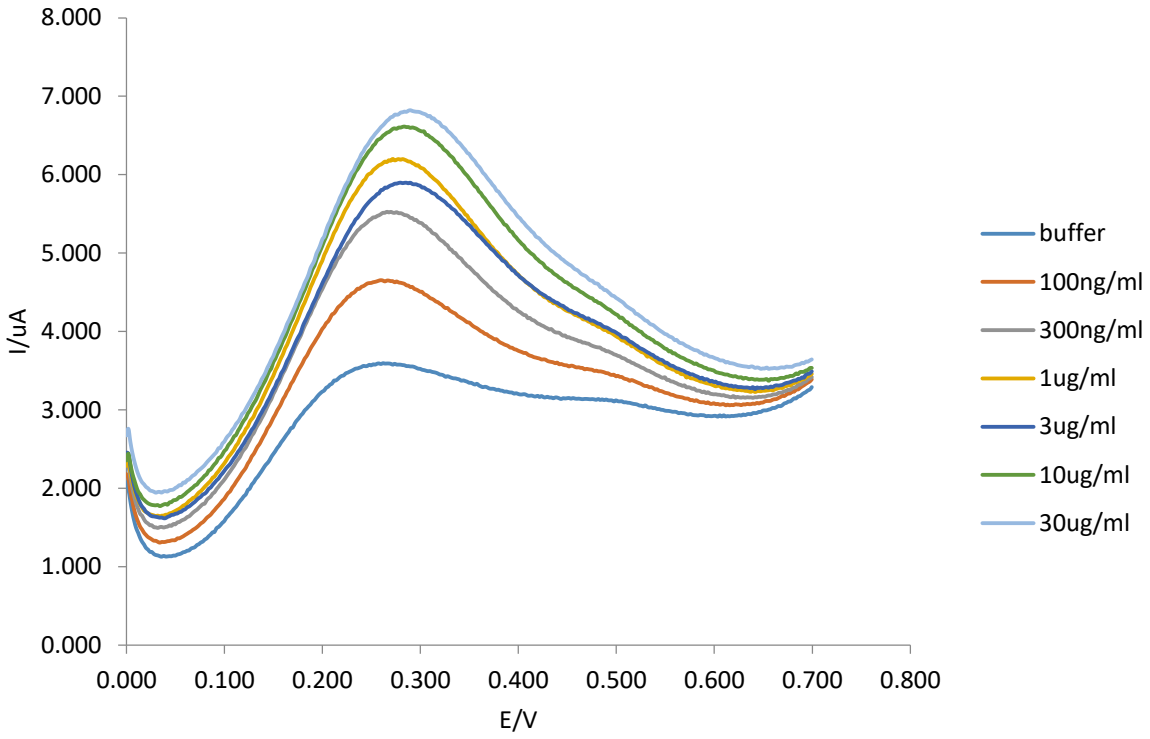

Figure 119: SWV, Electrode 2, aptamer 11 (0.1uM). Tested against GHSA. Binding buffer was utilised as measurement solution. Range between 0 and 0.7V. Step size: 2mV. Frequency: 100Hz. Pulse Size 50mV.

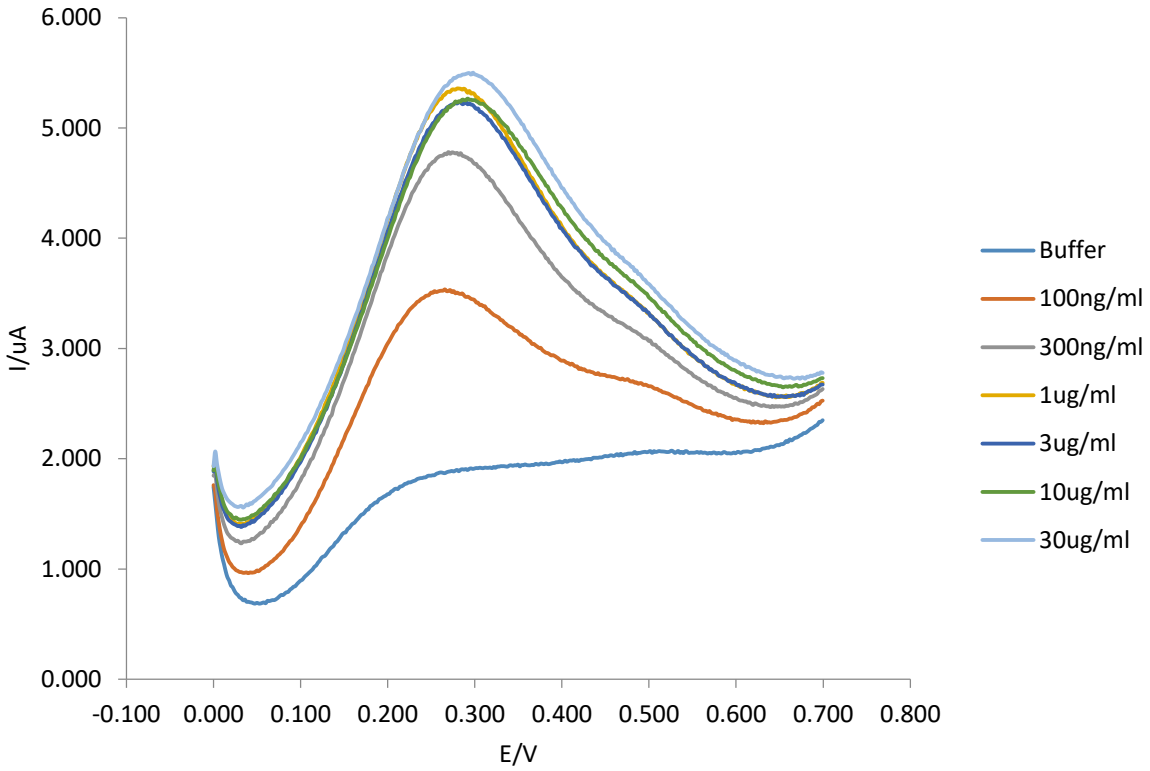

Figure 120: SWV Electrode 1, aptamer 11 (0.1uM). Tested against GHSA. Binding buffer was utilised as measurement solution. Range between 0 and 0.7V. Step size: 2mV. Frequency: 100Hz. Pulse Size 50mV.

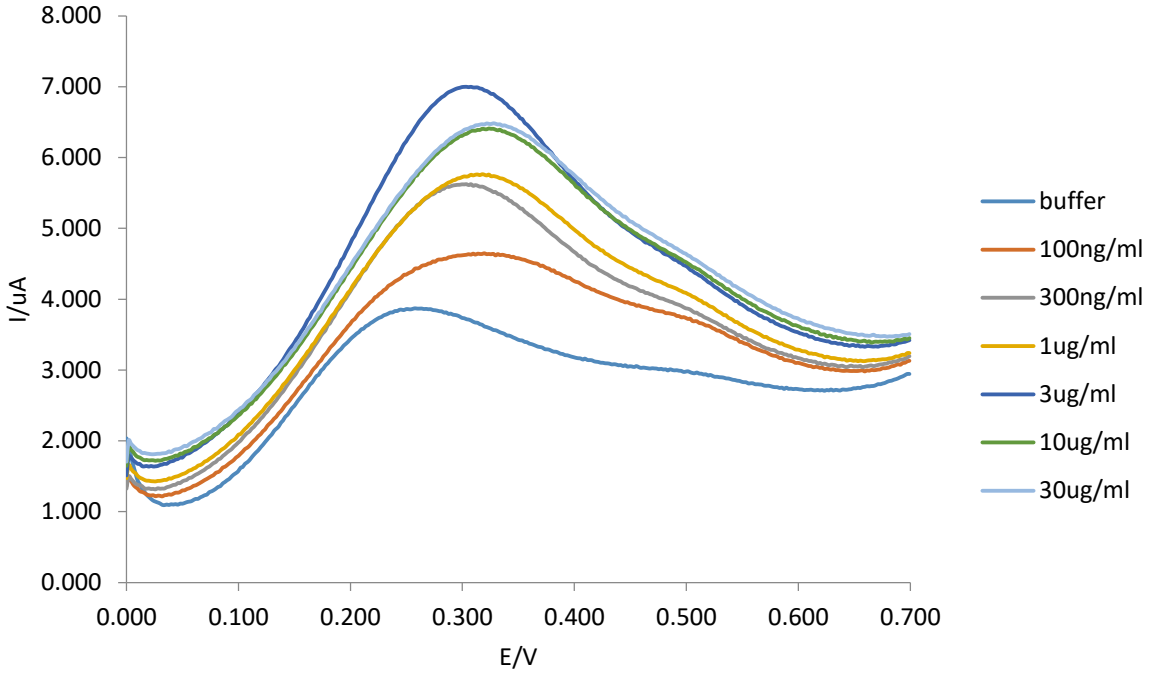

Figure 121: SWV, Electrode 4, aptamer 11 (0.1uM). Tested against IGG. Binding buffer was utilised as measurement solution. Range between 0 and 0.7V. Step size: 2mV. Frequency: 100Hz. Pulse Size 50mV.

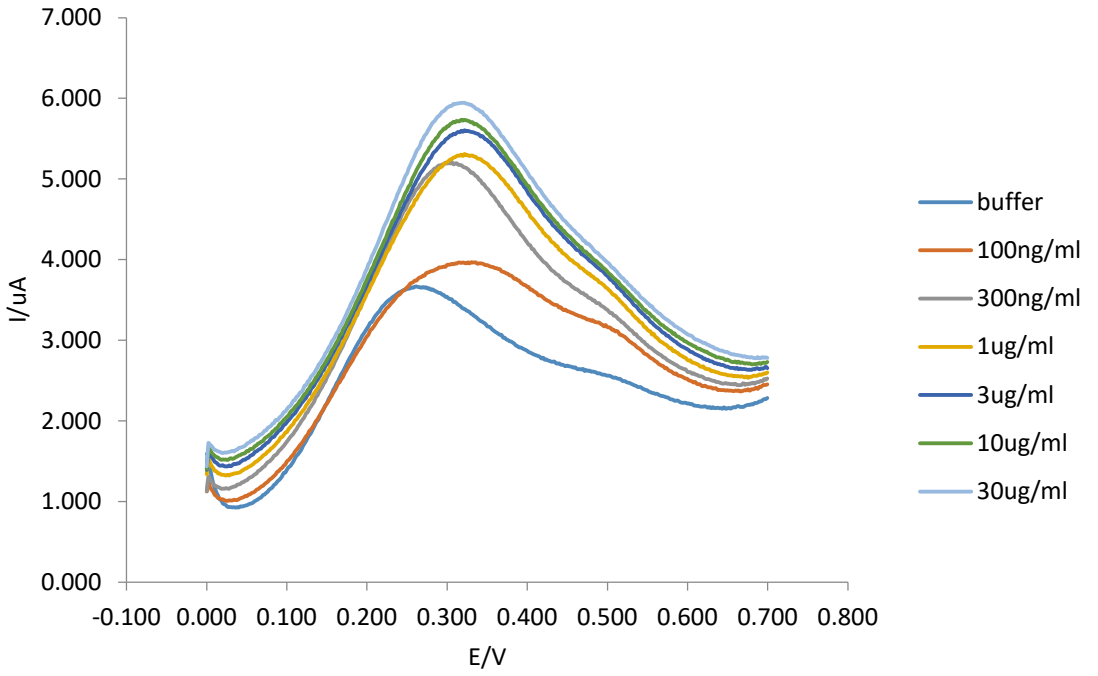

Figure 122: SWV, Electrode 6, aptamer 11 (0.1uM).Tested against IGG. Binding buffer was utilised as measurement solution. Range between 0 and 0.7V. Step size: 2mV. Frequency: 100Hz. Pulse Size 50mV.

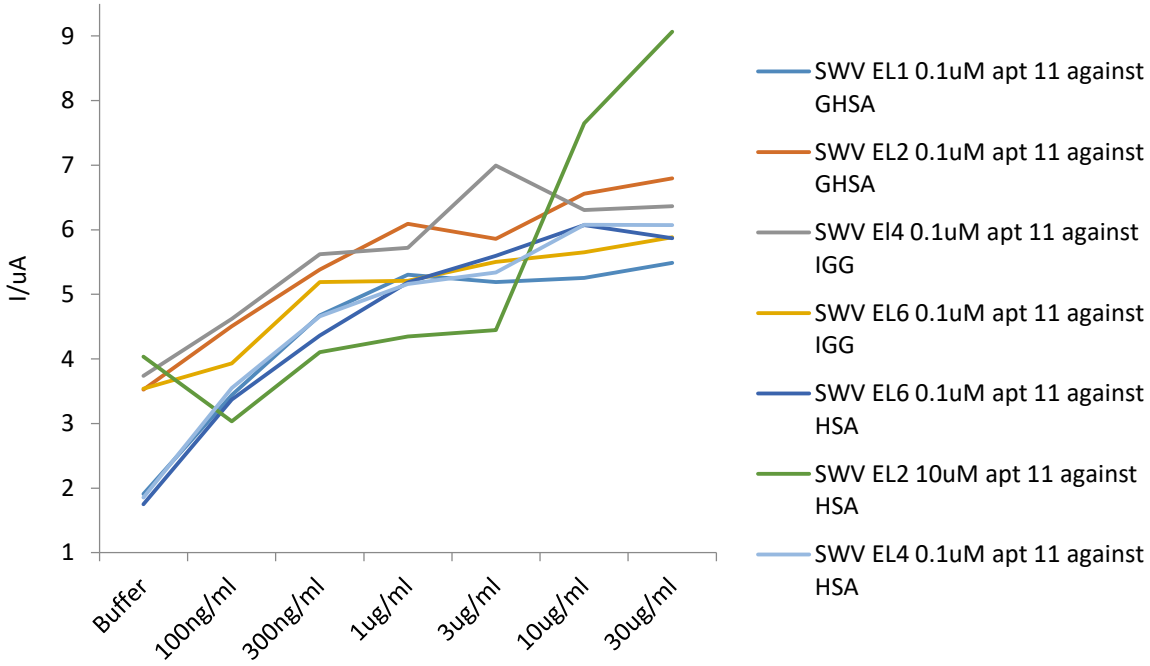

Figure 123: Comparison of SWV aptamer response at 0.3V across 7 electrodes with aptamer 11. Binding buffer was utilised as measurement solution. Tested against HSA, GHSA and IGG.

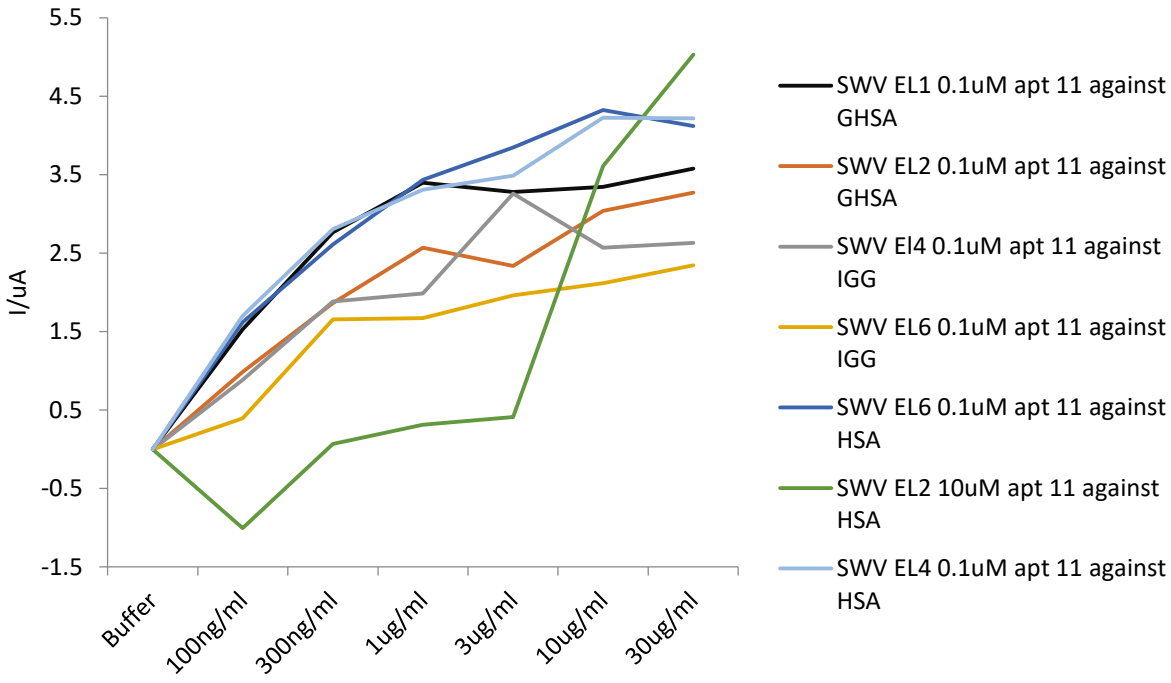

Figure 124: Background removed comparison of SWV aptamer response at 0.3V across 7 electrodes with aptamer 11. Binding buffer was utilised as measurement solution. Tested against HSA, GHSA and IGG.

Chapter 3.9

Results: Aptamers selected

3.9 Aptamers selected

6.4 million HSA and 4.5 million GHSA single strands of DNA were sequenced by NGS following the SELEX process. Of these sequences, 27 potential HSA aptamers and 20 potential GHSA aptamers were selected from the sequenced libraries using a variety of NSG analytical techniques. These were tested with ELONA to determine which could selectively bind to HSA and GHSA. Based on an array of 96 well assays, 4 HSA aptamers (HSA aptamers 3, 11, 17 and 27) and 4 GHSA aptamers (GSHA aptamers 3, 4, 15 and 17) were tested for dose dependent responses.

Based on the ELONA data, HSA aptamers 3, 4 and 11 were tested utilising CV, while HSA aptamer 11 was further investigated with SWV. HSA aptamer 11 at 0.1uM demonstrated a dose dependent response to HSA between 100 ng/ml and 30ug/ml. The positive electrochemical response of HSA aptamer 11 alongside the promising ELONA data makes HGA aptamer 11 an ideal primary candidate for further development, although data would appear to suggest it would more suitable in measuring HSA concentration alone and not total HSA/GHSA concentration. Aptamer 27 also could be further developed as its ability to selectively bind GHSA and HSA while showing limited IGG binding potentially make it an ideal pan specific aptamer that could measure total glycated and non glycated HSA. While HSA aptamers 3, 4 and 17 demonstrated promise in their ability to selectively bind HSA. GSHA aptamers 17 and 15 demonstrated the ability to potentially act as a pan specific aptamer that could measure total HSA/GHSA concentration. While GHSA aptamers 3 and 4 could be utilised to measure specific GSHA concentration. Although, the utilisation of ELONA and electrochemistry to measure aptamer binding has been demonstrated, the utility of aptamers mean other techniques can be easily trialled and tested now the aptamer sequences are known.

The selection and testing of aptamers for HSA and GHSA has produced an array of aptamers that hold promise and are suitable for further testing in a point of care system. The potential of measuring HSA/GHSA, a biomarker that responds quicker to changes in glucose then HbA1c and has been shown to be better indicator of glycemic status in certain patient groups mean future

development towards a point of care device could have a marked benefit to patient care. The aptamers selected and generated in this thesis could provide an easy and cost effective means to measure HSA/GSHA at point of care.

Chapter 4

Conclusions

4 Conclusions

The generation, sequencing, selection, testing and prototyping of aptamers for both HSA and GHSA has been performed within this thesis. For the first time an array of HSA and GHSA binders have been selected. The ability to measure changes in human serum albumin glycation at point of care could prove extremely useful in diabetes management. Glycated human serum albumin as evidenced by the growing literature is demonstrating that it is at least equal to HbA1c and in many cases a better glycemic marker, particular in patients with chronic kidney disease, a well known result of diabetes. While new enzymatic HSA tests have entered the market in the last decade, they still really on lab centric testing involving skilled labour, this is both costly and time consuming. With increasing concern about ballooning global healthcare costs more pressure will be placed on both providers to reduce their outgoings. The idea of a aptamer based electrochemical sensor was built from the ground up to address these needs. Aptamers have been selected against numerous proteins and analytes since they were introduced by Tuerk and Gold (74). While the SELEX process is both time intensive and often problematic it can produce a range of potential aptamers that can be tested cheaply. The ability to synthesise aptamers to a high quality and be able to readily modify them is one of their main advantages compared to antibodies which are costly, difficult to modify and often suffer from batch to batch variations.

The strength of the response for the majority of HSA aptamers is clear from both ELONA and Electrochemistry, however, the degree of selective binding demonstrated contrasting results between the two techniques. All aptamers at 1uM concentration when tested with ELONA demonstrated a specific response over IGG. At lower concentrations, below 30nM HSA aptamers 3, 11 and 17 selectively bind HSA over GHSA or IGG, while aptamer 27 selectively binds HSA and GSHA over IGG indicating it could potentially be an ideal pan specific aptamer.

Aptamer 11 which was tested against HSA utilising electrochemistry, while no discernible difference in signal could be detected between HSA, GSHA and IGG with CV, utilisation of the more sensitive

SWV demonstrated that the signals could be separated. A mean difference in signal of 68% was observed of HSA over IGG binding and 22% over GHSA. As HSA concentration in vivo is considerably higher than GHSA or IGG, the difference if measuring a patient's blood sample may be substantially more.

An array of GHSA aptamers were selected, utilising ELONA the majority demonstrated statistically significant binding over IGG. While GHSA aptamers 3 and 4 demonstrated significant binding over HSA, the majority demonstrated comparable binding to HSA. This highlights the difficulty in selecting an aptamer that is selective only to the modified protein.

4.1 SELEX (Systematic evolution of ligands by exponential enrichment)

SELEX for HSA was time intensive and difficult. Eleven successful SELEX rounds were performed for the generation of HSA aptamers out of a total of 22 partial or full rounds. A main attraction of SELEX is its applicability to a wide array of targets, equally this can also be one of its negatives as protocols between targets can differ drastically and tailoring of the process can take time. Problems with excessive mutations, low or no amplification, buffers, aptamer loss, high salt concentrations and inefficient PCR were highlighted.

Mutations in the PCR cycles were a constant concern as they would affect the final library composition. Preferential amplification of these mutations could hide any potential binders as they would be more numerous. Two key mutations were seen frequently, broadening of the bands and the creation of ladder like products. Band broadening often arose from unsuitable PCR mixes. As this was dependent on aptamer library concentration from the affinity purification step, suitable concentrations had to be continually trialled. Ladder like products have often been ignored in the literature but a study by Tolle et al (179) demonstrated potential solutions to this problem. Particular effort was undertaken in the GHSA SELEX process to reduce these ladder effects, removal of the elongation step (72^0C) appeared to delay the onset of these products but not eradicate them.

Little or no amplification was a consistent problem in the early stages of the HSA process. Changes to affinity purification, DNA cleanup and precipitation and PCR conditions were all trialled in order to determine the most effective protocol. Due to the low concentration of aptamer, concerns about loss of DNA in any cleanup process were had. Tests were undertaken to determine the effect PD-10 and NAP-5/25 columns had on DNA and salt concentrations, salt removal was found to be vital for effective PCR amplification.

SELEX is both highly technical and involves significant know how especially relating to the aptamer library and target of choice. As such the selection of aptamers for glycated human serum albumin was significantly faster as both the library and protein, although glycated had been utilised previously. In the selection of GHSA aptamers, reductions in PCR cycles were introduced to minimise mutations. The subsequent NGS data of both libraries demonstrated that GHSA was of much higher quality as a result of this reduction in PCR cycles. Only 8 successful SELEX rounds (14 were performed in total) were performed to select the aptamers, this would not be possible if cloning instead of next generation sequencing was utilised as cloning only allows for a sampling of a small percentage of the total aptamer pool.

4.2 NGS (Next generation sequencing)

Unlike traditional sanger sequencing that is performed on clones, NGS allows for the entire library of aptamers to be sequenced. A high number of SELEX rounds, often between 12-18 rounds are needed to ensure binding aptamers are sequenced by cloning/sanger. While this will ensure enrichment of certain aptamers in the library they may not be the ones that demonstrate the most effective binding. Instead they may be a result of preferential PCR amplifications as some DNA sequences may be amplified more effectively than others, regardless of how well they bind to the target. The ability to sequence the entire library with NGS allows for the removal of mutated and unwanted strands, along with the identification of numerically low but potentially important aptamers.

Initial work on analysing the data set from the HSA sequencing relied on custom combinations of software packages that were not designed for SELEX analysis. The cleanup and analysis of the data relied on the software package FastQC to determining quickly the effects certain data manipulations had on its quality. 6.4 million aptamers were reduced down to 1.2 million aptamers through various quality control steps including removal of reverse strands, strands with large homogenous regions of bases and selection of strands that met the length criteria. Based on FastQC metrics an improvement in the quality of the dataset was observed through the quality processes. 36.82% of the forward strand library contained duplicates, however after various aforementioned quality controls this was reduced to 1.54% indicating an abundance of mutations in the initial data. This 1.54% represented approximately 18 thousand strands. Additionally a reduction in quality of the data was consistently observed at the 3' end of the forward strand library but this effect was shown to be minimised through the quality control process.

Finally utilising MAFFT, 25 HSA aptamers were selected with an additional aptamer selected from a later analysis with the FASTAptamer software package. The FASTAptamer software package was not available at the time of the initial data analysis. MAFFT and FASTAptamer demonstrated that even after quality control processes significant number of mutated strands remained. Particular repeat primer regions (e.g. forward-reverse-forward), a phenomenon that was theorised while undertaking the SELEX process.

The GHSA data was of a higher quality then the HSA data as evidenced by the FastQC analysis of both the unmodified and reverse strand removed data. This can probably be attributed to the reduction in PCR cycles in the GHSA SELEX process compared with the HSA process. 20 aptamers were selected from the FASTAptamer data, with 15 from the discard_seqs reverse removed data and 5 from the fastx_clipper data. Similar to the HSA data we once again observed significant mutations, however, these also included the addition of Illumina adaptors which were not readily observed in

the HSA data. We see further evidence of the careful balance needed between increased SELEX rounds that could lead to better aptamer amplification but also increased mutations.

4.3 ELONA (Enzyme linked oligonucleotide assay)

ELONA based on the well known technique ELISA is extremely useful in probing the binding capabilities of aptamers. The low cost of aptamers and HSA, plus the ability to run multiple experiments in parallel due to the well format of ELONA makes it ideal for testing multiple aptamers in multiple conditions. While initial problems with blocking, mainly due the selection of casein as a blocking agent hid some of the relevant signals. Latter experiments utilising synthetic blocker demonstrated the benefit of utilising ELONA to determine aptamer binding .

BSA is commonly utilised to block ELONA plates, obviously the similarities between it and HSA meant it was unable to be utilised in these experiments. Various blocking techniques were trialled and casein was selected to block the plates against non-specific binding. Casein is a well known and an effective blocking agent, however, across an array of trials it generated inconsistent data. It was theorised that the samples could be contaminated with lactate albumin that could be masking any HSA signal.

A synthetic blocking agent was utilised in place of casein and enabled the generation of more consistent data. HSA aptamers demonstrated between 2.1 and 15.8 fold increase in absorbance signal over IGG, a common component of blood plasma. Additionally multiple aptamers demonstrated impressive binding to GSHA, while others showed selectivity against the protein. A range of aptamers were tested for dose dependent response. Most generated similar responses to HSA, GSHA and IGG at protein concentrations of 1uM and above. While HSA aptamers 3, 11 and 17 all demonstrated a specific response to HSA at lower concentrations around 30nM. HSA aptamer 27 demonstrated a specific response to HSA and GHSA above IGG at these lower concentrations. A double peak effect can be observed in all cases. An initial peak around 30nM is theorised to be specific in nature followed by a trough between 100nM and 300nM where increase concentrations

generates steric hindrance. A further peak at 1uM is potentially non-specific in nature as all proteins generate a response. This peak then reduces at 10uM as non-specific interactions find it more difficult to bind to the aptamers in a more competitive and saturated environment.

GSHA aptamers generally demonstrate higher absorbance across all aptamers to HSA and GHSA then to IGG. Aptamers 2 and 3 demonstrate statistically higher significant binding to GHSA then HSA. However, most aptamers have a larger absorbance response to HSA then GHSA which is unexpected. There are a few potential reasons for this, firstly not enough SELEX rounds may have been performed. In an aim to reduce both the amount of PCR related mutations and to reduce the preferential enrichment of aptamers that weren't specific to the target protein; SELEX rounds and particularly the number of PCR rounds was kept to a minimum. This may seem counterintuitive as increased SELEX rounds allow for the enrichment of binders, however, it can also enable the enrichment of non binders. This can occur as certain aptamers may have low affinity to the target protein but may have a particular sequence which means they are preferentially enriched in the PCR process. If aptamers are being cloned and then sequenced a significant number of SELEX rounds need to be performed to ensure binders appear due to the relatively small number of clones (often below 50) often utilised. NGS on the other hand allows for all aptamers which were in the SELEX process to be sequenced allowing for lower enriched sequences to be extracted before PCR mutations and enrichments heavily effect the final pool.

Alternatively many HSA and GHSA absorbencies for an individual aptamer show a similar absorbance to each other when taking into account for the region of error defined by the standard deviation. Suggesting that binding to both is similar. This could indicate that binding is either stronger or more prevalent to HSA sites that are similar between both. As glycated sites are relatively small in comparison to the whole HSA protein, finding binding to these sites utilising a whole GHSA protein is extremely difficult even with counter selection rounds that aim to remove HSA specific aptamers.

Additionally a third possibility is that due to the variety of glycation sites on the HSA molecule, there will be various distributions of glycation sites across the HSA molecule. Aptamers may only be specific to a few if not just one of these sites. If these sites are not present on all GHSA proteins then they won't bind.

When studying the dose response of the aptamer we see GHSA aptamer 15 and 17 demonstrating a specific response over IGG. Additionally we see the double peak response that is evident with the HSA aptamers.

4.4 Electrochemistry

Electrochemistry was utilised to test the response of immobilised aptamers to HSA, GSHA and IGG. A range of HSA aptamers demonstrate a typical dose response to HSA utilising both CV and SWV. Utilising CV we are unable to detect noticeable difference in HSA aptamer binding between HSA, GHSA and IGG. However, utilising the more sensitive SWV, a 68% increase in signal with HSA over IGG and a 22% increase in signal over GHSA is observed. An aptamer that measures both HSA and GSHA concentrations would be beneficial in measure overall HSA concentration. As actual serum concentrations of IGG would be significantly lower this difference could potentially be more significant in real samples.

4.5 Future Work

While considerable progress has been carried out in selecting and characterising HSA and GSHA aptamers, further work could still be carried out to further define the aptamers and develop a prototype sensing system.

Further work could include:

- Characterisation of GHSA electrochemistry response
- Further characterisation of HSA electrochemistry response

- Characterisation of aptamer structures and adaption of aptamers if needed for signal generation.
- Testing of aptamers using ELONA and Electrochemistry in complex medium
- Testing of aptamers in patient samples
- Further data analysis of NGS data utilising other techniques to see if further binding aptamers exist.

References

References

1. World Health Organization. Global Report on Diabetes. 2016;88. Available from: http://apps.who.int/iris/bitstream/10665/204871/1/9789241565257_eng.pdf

2. Clark LC, Lyons C. Electrode systems for continuous monitoring in cardiovascular surgery. Ann N Y Acad Sci [Internet]. 1962;102(1):29–45. Available from: http://onlinelibrary.wiley.com/doi/10.1111/j.1749-6632.1962.tb13623.x/full%5Cnhttp://doi.wiley.com/10.1111/j.1749-6632.1962.tb13623.x

3. Goldstein DE, Little RR, Lorenz RA, Malone JI, Nathan D, Peterson CM, et al. Tests of Glycemia in Diabetes. Diabetes Care. 2004;27(7):1761–73.

4. Munshi MN, Segal AR, Slyne C, Samur AA, Brooks KM, Horton ES. Shortfalls of the use of HbA1C-derived eAG in older adults with diabetes. Diabetes Res Clin Pract [Internet]. 2015;110(1):60–5. Available from: http://dx.doi.org/10.1016/j.diabres.2015.07.012

5. Sacks DB, Bruns DE, Goldstein DE, Maclaren NK, McDonald JM, Parrott M. Guidelines and recommendations for laboratory analysis in the diagnosis and management of diabetes mellitus. Clin Chem [Internet]. 2002;48(3):436–72. Available from: http://www.ncbi.nlm.nih.gov/entrez/query.fcgi?cmd=Retrieve&db=PubMed&dopt=Citation&list_uids=11861436

6. Nagayama H, Inaba M, Okabe R, Emoto M, Ishimura E, Okazaki S, et al. Glycated albumin as an improved indicator of glycemic control in hemodialysis patients with type 2 diabetes based on fasting plasma glucose and oral glucose tolerance test. Biomed Pharmacother [Internet]. 2009 Mar [cited 2012 Mar 11];63(3):236–40. Available from: http://www.ncbi.nlm.nih.gov/pubmed/18538530

7. Diabetes UK. Facts and stats [Internet]. 2015. Available from: https://ezp.lib.unimelb.edu.au/login?url=https://search.ebscohost.com/login.aspx?direct=true&db=s3h&AN=SPHS-1036820&site=eds-live

8. Association BD. Diabetes in the UK. 1996.

9. Health and Social Care Information Centre. Prescribing for Diabetes, England 2005-06 to 2012-13 [Internet]. 2013. Available from: http://www.hscic.gov.uk/catalogue/PUB11422/pres-diab-eng-2005-2013-rep.pdf

10. International Diabetes Federation. IDF Diabetes Atlas,Sixth Edition. 2013.

11. Health and Social Care Information Centre. National Diabetes Audit 2012-2013 Report 1: Care

Processes & Treatment Targets [Internet]. 2014. Available from: http://www.hscic.gov.uk/catalogue/PUB14970

12. Scottish Diabetes Survey Monitoring Group. Scottish Diabetes Survey 2013 [Internet]. NHS Scotland. 2013. Available from: http://www.diabetesinscotland.org.uk/Publications/SDS2013.pdf

13. Ehtisham S, Barrett TG, Shaw NJ. Type 2 diabetes mellitus in UK children--an emerging problem. Diabet Med [Internet]. 2000;17(12):867–71. Available from: http://www.ncbi.nlm.nih.gov/pubmed/11168330

14. Naranjo D, Hessler DM, Deol R, Chesla C a. Health and Psychosocial Outcomes in U.S. Adult Patients with Diabetes from Diverse Ethnicities. Curr Diab Rep [Internet]. 2012;12(6):729–38. Available from: http://link.springer.com/10.1007/s11892-012-0319-y

15. Public Health England. Adult obesity and type 2 diabetes About Public Health England. 2014.

16. Ng M, Fleming T, Robinson M, Thomson B, Graetz N, Margono C, et al. Global, regional, and national prevalence of overweight and obesity in children and adults during 1980–2013: a systematic analysis for the Global Burden of Disease Study 2013. Lancet [Internet]. 2014;384(9945):766–81. Available from: http://linkinghub.elsevier.com/retrieve/pii/S0140673614604608

17. Morrish NJ, Stevens LK, Fuller JH, Keen H. Mortality and causes of death in the WHO multinational study of vascular disease in diabetes. Diabetes. 2001;44:14–21.

18. Ceriello A, Colagiuri S, Gerich J, Tuomilehto J. Guideline for management of postmeal glucose [Internet]. Vol. 18, Nutr Metab Cardiovasc Dis. 2008. S17-33 p. Available from: http://www.ncbi.nlm.nih.gov/entrez/query.fcgi?cmd=Retrieve&db=PubMed&dopt=Citation&list_uids=18501571

19. Diabetes.co.uk. Blood Sugar Level Ranges [Internet]. [cited 2016 Sep 3]. Available from: http://www.diabetes.co.uk/diabetes_care/blood-sugar-level-ranges.html

20. NICE. Type 2 diabetes in adults. Nice Inf public [Internet]. 2015;(December):1–57. Available from: https://www.nice.org.uk/guidance/ng28

21. NICE. Preventing excess weight gain. Nice Guid [Internet]. 2015;(March). Available from: https://www.nice.org.uk/guidance/ng7

22. Tirone TA, Brunicardi FC. Overview of glucose regulation. World J Surg. 2001;25(4):461–7.

23. Sun Y-M, Su Y, Li J, Wang L-F. Recent advances in understanding the biochemical and molecular mechanism of diabetic nephropathy. Biochem Biophys Res Commun [Internet]. 2013;433(4):359–61. Available from: http://linkinghub.elsevier.com/retrieve/pii/S0006291X13004762

24. Kim SS, Kim JH, Kim IJ. Current Challenges in Diabetic Nephropathy: Early Diagnosis and Ways to Improve Outcomes. Endocrinol Metab (Seoul, Korea) [Internet]. 2016;245–53. Available from: http://www.ncbi.nlm.nih.gov/pubmed/27246284

25. Volpe M, Battistoni A, Savoia C, Tocci G. Understanding and treating hypertension in diabetic populations. Cardiovasc Diagn Ther. 2015;5(5):353–63.

26. Kovacic JC, Castellano JM, Farkouh ME, Fuster V. The relationships between cardiovascular disease and diabetes: Focus on pathogenesis. Endocrinol Metab Clin North Am. 2014;43(1):41–57.

27. Jia WZ, Wang K, Xia XH. Elimination of electrochemical interferences in glucose biosensors. TrAC - Trends Anal Chem [Internet]. 2010;29(4):306–18. Available from: http://dx.doi.org/10.1016/j.trac.2010.01.006

28. Wang J. Electrochemical glucose biosensors. Chem Rev [Internet]. 2008 Feb;108(2):814–25. Available from: http://www.ncbi.nlm.nih.gov/pubmed/18154363

29. Heller A, Feldman B. Electrochemical glucose sensors and their applications in diabetes management. Chem Rev [Internet]. 2008 Jul;108(7):2482–505. Available from: http://www.ncbi.nlm.nih.gov/pubmed/18465900

30. Cass AEG, Davis G, Francis GD, Hill HAO, Aston WJ, Higgins IJ, et al. Ferrocene-mediated enzyme electrode for amperometric determination of glucose. Anal Chem [Internet]. 1984;56(4):667–71. Available from: http://pubs.acs.org/doi/abs/10.1021/ac00268a018%5Cnpapers3://publication/doi/10.1021/ac00268a018

31. Zheng C-M, Ma W-Y, Wu C-C, Lu K-C. Glycated albumin in diabetic patients with chronic kidney disease. Clin Chim Acta [Internet]. 2012 Oct 9 [cited 2012 Aug 10];413(19–20):1555–61. Available from: http://www.ncbi.nlm.nih.gov/pubmed/22579765

32. Anguizola J, Matsuda R, Barnaby OS, Hoy KS, Wa C, DeBolt E, et al. Review: Glycation of human serum albumin. Clin Chim Acta [Internet]. 2013 Oct 21 [cited 2014 Jan 6];425:64–76. Available from: http://www.ncbi.nlm.nih.gov/pubmed/23891854

33. Guerin-Dubourg a, Catan a, Bourdon E, Rondeau P. Structural modifications of human albumin in diabetes. Diabetes Metab [Internet]. 2012 Apr [cited 2012 May 9];38(2):171–8. Available from: http://www.ncbi.nlm.nih.gov/pubmed/22349032

34. Inaba M, Okuno S, Kumeda Y, Yamada S, Imanishi Y, Tabata T, et al. Glycated albumin is a better glycemic indicator than glycated hemoglobin values in hemodialysis patients with diabetes: effect of anemia and erythropoietin injection. J Am Soc Nephrol [Internet]. 2007 Mar [cited 2013 Jan 30];18(3):896–903. Available from: http://www.ncbi.nlm.nih.gov/pubmed/17267743

35. Bor M V, Bor P, Cevik C. Serum fructosamine and fructosamine-albumin ratio as screening tests for gestational diabetes mellitus. Arch Gynecol Obstet [Internet]. 1999 Jan;262(3–4):105–11. Available from: http://www.ncbi.nlm.nih.gov/pubmed/10326628

36. Cohen MP. Clinical, pathophysiological and structure/function consequences of modification of albumin by Amadori-glucose adducts. Biochim Biophys Acta [Internet]. 2013 Dec [cited 2013 Dec 10];1830(12):5480–5. Available from: http://www.ncbi.nlm.nih.gov/pubmed/23624335

37. Sany D, Elshahawy Y, Anwar W. Glycated albumin versus glycated hemoglobin as glycemic indicator in hemodialysis patients with diabetes mellitus: variables that influence. Saudi J Kidney Dis Transpl [Internet]. 2013;24(2):260–73. Available from: http://www.sjkdt.org/temp/SaudiJKidneyDisTranspl242260-6464221_175722.pdf%5Cnhttp://www.ncbi.nlm.nih.gov/pubmed/23538348

38. Rondeau P, Bourdon E. The glycation of albumin: structural and functional impacts. Biochimie [Internet]. 2011 Apr [cited 2012 Aug 8];93(4):645–58. Available from: http://www.ncbi.nlm.nih.gov/pubmed/21167901

39. Roohk HV, Zaidi AR. A review of glycated albumin as an intermediate glycation index for controlling diabetes. J Diabetes Sci Technol [Internet]. 2008 Nov;2(6):1114–21. Available from: http://www.pubmedcentral.nih.gov/articlerender.fcgi?artid=2769832&tool=pmcentrez&rendertype=abstract

40. Shaklai N, Garlick RL, Bunn HF. Nonenzymatic glycosylation of human serum albumin alters its conformation and function. J Biol Chem [Internet]. 1984 Mar 25;259(6):3812–7. Available from: http://www.ncbi.nlm.nih.gov/pubmed/6706980

41. Nakajou K, Watanabe H, Kragh-Hansen U, Maruyama T, Otagiri M. The effect of glycation on the structure, function and biological fate of human serum albumin as revealed by recombinant mutants. Biochim Biophys Acta - Gen Subj. 2003;1623(2–3):88–97.

42. Kisugi R, Kouzuma T, Yamamoto T, Akizuki S, Miyamoto H, Someya Y, et al. Structural and glycation site changes of albumin in diabetic patient with very high glycated albumin. Clin Chim Acta. 2007;382(1–2):59–64.

43. Evans TW. Review article: albumin as a drug--biological effects of albumin unrelated to oncotic pressure. Aliment Pharmacol Ther. 2002;16 Suppl 5:6–11.

44. Otagiri M. A molecular functional study on the interactions of drugs with plasma proteins. Drug Metab Pharmacokinet [Internet]. 2005;20(5):309–23. Available from: http://www.ncbi.nlm.nih.gov/pubmed/16272748

45. Kim KJ, Lee B-W. The roles of glycated albumin as intermediate glycation index and pathogenic protein. Diabetes Metab J [Internet]. 2012 Apr;36(2):98–107. Available from: http://www.pubmedcentral.nih.gov/articlerender.fcgi?artid=3335903&tool=pmcentrez&rendertype=abstract

46. Sudlow G, Birkett DJ, Wade D. The Characterization of Two Specific Drug Binding Sites on Human Serum. Mol Pharmacol. 1975;11:824–32.

47. Sudlow G, Birkett DJ, Wade D. Further Characterization of Specific Drug Binding Sites on Human Serum Albumin. Mol Pharmacol. 1976;12:1052–61.

48. Yang, J., and Hage DS. Characterization of the binding and chiral separation of o- and Ltryptophan on a high-performance immobilized human serum albumin column. J Chromatogr. 1993;645:241–50.

49. Oettl K, Stauber RE. Physiological and pathological changes in the redox state of human serum albumin critically influence its binding properties. Br J Pharmacol [Internet]. 2007;151(5):580–90. Available from: http://www.pubmedcentral.nih.gov/articlerender.fcgi?artid=2013999&tool=pmcentrez&rendertype=abstract

50. Taverna M, Marie A-L, Mira J-P, Guidet B. Specific antioxidant properties of human serum albumin. Ann Intensive Care [Internet]. 2013;3(1):4. Available from: http://www.pubmedcentral.nih.gov/articlerender.fcgi?artid=3577569&tool=pmcentrez&rendertype=abstract

51. Sattarahmady N, Moosavi-Movahedi A, Habibi-Rezaei M. A Biophysical Comparison of Human Serum Albumin to be Glycated In Vivo and In Vitro. J Med Biochem [Internet]. 2011 Jan 1 [cited 2013 Aug 22];30(1):5–10. Available from: http://www.degruyter.com/view/j/jomb.2011.30.issue-1/v10011-010-0026-7/v10011-010-0026-7.xml

52. Garlick RL, Mazer S. The Principal Site of Nonenzymatic Glycosylation of Human Serum Albumin in Vivo. J Biol Chem. 1983;258(10):6142–6.

53. Iberg N, Fluckiger R. Nonenzymatic glycosylation of albumin in vivo. Identification of multiple glycosylated sites. J Biol Chem. 1986;261(29):13542–5.

54. Ahmed N, Dobler D, Dean M, Thornalley PJ. Peptide mapping identifies hotspot site of modification in human serum albumin by methylglyoxal involved in ligand binding and esterase activity. J Biol Chem. 2005;280(7):5724–32.

55. Zeng J, Davies MJ. Evidence for the formation of adducts and S-(carboxymethyl)cysteine on reaction of alpha-dicarbonyl compounds with thiol groups on amino acids, peptides, and proteins. Chem Res Toxicol [Internet]. 2005;18(8):1232–41. Available from: http://dx.doi.org/10.1021/tx050074u

56. Bourdon E, Blache D. The Importance of Proteins in Defence Against Oxidation. Antioxid Redox Signal. 2001;3(2):293–311.

57. Cohen M. Intervention strategies to prevent pathogenetic effects of glycated albumin. Arch Biochem Biophys [Internet]. 2003 Nov 1 [cited 2011 Dec 14];419(1):25–30. Available from: http://linkinghub.elsevier.com/retrieve/pii/S0003986103004375

58. Higashimoto Y, Yamagishi S, Nakamura K, Matsui T, Takeuchi M, Noguchi M, et al. In vitro selection of DNA aptamers that block toxic effects of AGE on cultured retinal pericytes. Microvasc Res [Internet]. 2007 Jul [cited 2012 Aug 3];74(1):65–9. Available from: http://www.ncbi.nlm.nih.gov/pubmed/17493639

59. Davis WA, Bruce DG, Davis TME. Does self-monitoring of blood glucose improve outcome in type 2 diabetes? The Fremantle Diabetes Study. Diabetologia. 2007;50(3):510–5.

60. Welschen LMC, Bloemendal E, Nijpels G, Dekker JM, Heine RJ, Stalman WAB, et al. Self-Monitoring of Blood Glucose in Patients With Type 2 Diabetes Who Are Not Using Insulin. Diabetes Care [Internet]. 2005;28(6):1510–7. Available from: http://care.diabetesjournals.org/content/28/6/1510.short

61. Gerrald KR, Malone RM, Shilliday BB. Clinical Benefit of Self-Monitoring of Blood Glucose Is Uncertain for Non-Insulin-Treated Patients With Type 2 Diabetes. Clin Diabetes [Internet]. 2010;28(3):121–3. Available from: http://clinical.diabetesjournals.org/content/28/3/121.full

62. Klonoff DC. Benefits and limitations of self-monitoring of blood glucose. J Diabetes Sci Technol [Internet]. 2007;1(1):130–2. Available from: http://www.pubmedcentral.nih.gov/articlerender.fcgi?artid=2769614&tool=pmcentrez&rendertype=abstract

63. Stratton IM. Association of glycaemia with macrovascular and microvascular complications of type 2 diabetes (UKPDS 35): prospective observational study. Bmj [Internet]. 2000;321(7258):405–12. Available from: http://www.bmj.com/content/321/7258/405?linkType=FULL&ck=nck&resid=321/7258/405&journalCode=bmj

64. Freedman BI, Shenoy RN, Planer J a, Clay KD, Shihabi ZK, Burkart JM, et al. Comparison of glycated albumin and hemoglobin A1c concentrations in diabetic subjects on peritoneal and hemodialysis. Perit Dial Int [Internet]. 2010 [cited 2014 Jul 15];30(1):72–9. Available from: http://www.ncbi.nlm.nih.gov/pubmed/20056983

65. Peacock TP, Shihabi ZK, Bleyer a J, Dolbare EL, Byers JR, Knovich M a, et al. Comparison of glycated albumin and hemoglobin A(1c) levels in diabetic subjects on hemodialysis. Kidney Int [Internet]. 2008 May [cited 2014 Jul 18];73(9):1062–8. Available from: http://www.ncbi.nlm.nih.gov/pubmed/18288102

66. Baker JR, Zyzak D V., Thoroe SR, Baynes JW. Chemistry of the fructosamine assay: D-glucosone is the product of oxidation of Amadori compounds. Clin Chem. 1994;40(10):1950–5.

67. Cohen MP, Hud E. Measurement of plasma glycoalbumin levels with a monoclonal antibody based ELISA. J Immunol Methods. 1989;122(2):279–83.

68. Paroni R, Ceriotti F, Galanello R, Battista Leoni G, Panico A, Scurati E, et al. Performance characteristics and clinical utility of an enzymatic method for the measurement of glycated albumin in plasma. Clin Biochem. 2007;40(18):1398–405.

69. Kohzuma T, Koga M. Lucica GA-L glycated albumin assay kit: a new diagnostic test for diabetes mellitus. Mol Diagn Ther [Internet]. 2010;14(1):49–51. Available from: http://eutils.ncbi.nlm.nih.gov/entrez/eutils/elink.fcgi?dbfrom=pubmed&id=20121290&retmo

de=ref&cmd=prlinks%5Cnpapers3://publication/doi/10.2165/11317390-000000000-00000

70. Kouzuma T, Uemastu Y, Usami T, Imamura S. Study of glycated amino acid elimination reaction for an improved enzymatic glycated albumin measurement method. Clin Chim Acta. 2004;346(2):135–43.

71. Montagnana M, Paleari R, Danese E, Salvagno GL, Lippi G, Guidi GC, et al. Evaluation of biological variation of glycated albumin (GA) and fructosamine in healthy subjects. Clin Chim Acta [Internet]. 2013 Aug 23 [cited 2013 Aug 19];423:1–4. Available from: http://www.ncbi.nlm.nih.gov/pubmed/23588063

72. Freedman BI, Shenoy RN, Planer JA, Clay KD, Shihabi ZK, Burkart JM, et al. Comparison of glycated albumin and hemoglobin A1c concentrations in diabetic subjects on peritoneal and hemodialysis. Perit Dial Int. 2010;30(1):72–9.

73. Kim J-K, Park JT, Oh HJ, Yoo DE, Kim SJ, Han SH, et al. Estimating average glucose levels from glycated albumin in patients with end-stage renal disease. Yonsei Med J [Internet]. 2012 May;53(3):578–86. Available from: http://www.pubmedcentral.nih.gov/articlerender.fcgi?artid=3343437&tool=pmcentrez&rendertype=abstract

74. Tuerk C, Gold L. Systematic Evolution of Ligands by Exponential Enrichment : RNA Ligands to Bacteriophage T4 DNA Polymerase. Science (80-). 1990;249:505–10.

75. Ellington AD, Szostak JW. In vitro selection of RNA molecules that bind specific ligands. Nature. 1990;346:818–22.

76. Carlson R. The changing economics of DNA synthesis. Nat Biotechnol [Internet]. 2009;27(12):1091–4. Available from: http://dx.doi.org/10.1038/nbt1209-1091

77. Gopinath SCB. Methods developed for SELEX. Anal Bioanal Chem [Internet]. 2007 Jan [cited 2012 Jul 31];387(1):171–82. Available from: http://www.ncbi.nlm.nih.gov/pubmed/17072603

78. Stoltenburg R, Reinemann C, Strehlitz B. SELEX--a (r)evolutionary method to generate high-affinity nucleic acid ligands. Biomol Eng [Internet]. 2007 Oct [cited 2012 Jul 16];24(4):381–403. Available from: http://www.ncbi.nlm.nih.gov/pubmed/17627883

79. Nieuwlandt D. In Vitro Selection of Functional Nucleic Acid Sequences. Currrent Issues Mol Biol. 2000;2(1):9–16.

80. Sampson T. Aptamers and SELEX: the technology. World Pat Inf [Internet]. 2003;25(2):123–9.

Available from: http://www.sciencedirect.com/science/article/B6V5D-488VWN9-1/2/a1197758e43da48df980513622977d51

81. NIH. National Human Genome Research Institute [Internet]. Available from: https://www.genome.gov/27541954/dna-sequencing-costs-data/

82. Přistoupil T. M, Kramlová M. Microchromatographic separation of ribonucleic acids from proteins on nitrocellulose membranes. J Chromatogr A [Internet]. 1968;32:769–70. Available from: http://www.sciencedirect.com/science/article/pii/S0021967301805653

83. Yoshida Y, Sakai N, Masuda H, Furuichi M, Nishikawa F, Nishikawa S, et al. Rabbit antibody detection with RNA aptamers. Anal Biochem [Internet]. 2008 Apr 15 [cited 2011 Oct 22];375(2):217–22. Available from: http://www.ncbi.nlm.nih.gov/pubmed/18252191

84. Sando S, Ogawa A, Nishi T, Hayami M, Aoyama Y. In vitro selection of RNA aptamer against Escherichia coli release factor 1. Bioorg Med Chem Lett [Internet]. 2007;17(5):1216–20. Available from: http://www.sciencedirect.com/science/article/B6TF9-4MHX7F8-6/2/14240d5f1ac78d00645228920239c657

85. Klussmann S. The Aptamer Handbook: Functional Oligonucleotides and Their applications. Klussmann S, editor. Wiley-VCH. 2006.

86. Tombelli S, Minunni M, Mascini M. Analytical applications of aptamers. Biosens Bioelectron [Internet]. 2005 Jun 15 [cited 2011 Jul 26];20(12):2424–34. Available from: http://www.ncbi.nlm.nih.gov/pubmed/15854817

87. Huizenga DE, Szostak JW. A DNA aptamer that binds adenosine and ATP. Biochemistry [Internet]. 1995 Jan 17;34(2):656–65. Available from: http://www.ncbi.nlm.nih.gov/pubmed/7819261

88. Acimovic JM, Stanimirovic BD, Mandic LM. The role of the thiol group in protein modification with methylglyoxal. J Serbian Chem Soc. 2009;74(8–9):867–83.

89. Huang YC, Ge B, Sen D, Yu H-Z. Immobilized DNA switches as electronic sensors for picomolar detection of plasma proteins. J Am Chem Soc [Internet]. 2008 Jun 25;130(25):8023–9. Available from: http://www.ncbi.nlm.nih.gov/pubmed/18517197

90. Xiao Y, Lubin A a, Heeger AJ, Plaxco KW. Label-free electronic detection of thrombin in blood serum by using an aptamer-based sensor. Angew Chem Int Ed Engl [Internet]. 2005 Aug 26 [cited 2011 Aug 22];44(34):5456–9. Available from: http://www.ncbi.nlm.nih.gov/pubmed/16044476

91. Hianik T, Ostatna V, Sonlajtnerova M, Grman I. Influence of ionic strength, pH and aptamer configuration for binding affinity to thrombin. Bioelectrochemistry [Internet]. 2007;70(1):127–33. Available from: http://www.sciencedirect.com/science/article/B6W72-4JNF072-4/2/8a1c2ea12f5312726380364afa192ded

92. Mir M, Vreeke M, Katakis I. Different strategies to develop an electrochemical thrombin aptasensor. Electrochem commun [Internet]. 2006 Mar [cited 2011 Sep 15];8(3):505–11. Available from: http://linkinghub.elsevier.com/retrieve/pii/S1388248106000075

93. Tan ESQ, Wivanius R, Toh C-S. Heterogeneous and Homogeneous Aptamer-Based Electrochemical Sensors for Thrombin. Electroanalysis [Internet]. 2009 Mar [cited 2012 Jan 31];21(6):749–54. Available from: http://doi.wiley.com/10.1002/elan.200804473

94. Hansen J a, Wang J, Kawde A-N, Xiang Y, Gothelf K V, Collins G. Quantum-dot/aptamer-based ultrasensitive multi-analyte electrochemical biosensor. J Am Chem Soc [Internet]. 2006 Feb 22;128(7):2228–9. Available from: http://www.ncbi.nlm.nih.gov/pubmed/16478173

95. Liu X, Li Y, Zheng J, Zhang J, Sheng Q. Carbon nanotube-enhanced electrochemical aptasensor for the detection of thrombin. Talanta [Internet]. 2010 Jun 15 [cited 2013 Oct 14];81(4–5):1619–24. Available from: http://www.ncbi.nlm.nih.gov/pubmed/20441948

96. Wang J, Wang F, Dong S. Methylene blue as an indicator for sensitive electrochemical detection of adenosine based on aptamer switch. J Electroanal Chem [Internet]. 2009 Feb 15 [cited 2011 Aug 21];626(1–2):1–5. Available from: http://linkinghub.elsevier.com/retrieve/pii/S0022072808003264

97. Wu Z-S, Guo M-M, Zhang S-B, Chen C-R, Jiang J-H, Shen G-L, et al. Reusable electrochemical sensing platform for highly sensitive detection of small molecules based on structure-switching signaling aptamers. Anal Chem [Internet]. 2007 Apr 1;79(7):2933–9. Available from: http://www.ncbi.nlm.nih.gov/pubmed/17338505

98. Kerman K, Ozkan D, Kara P, Meric B, Gooding JJ, Ozsoz M. Voltammetric determination of DNA hybridization using methylene blue and self-assembled alkanethiol monolayer on gold electrodes. Anal Chim Acta. 2002;462:39–47.

99. Xiao Y, Piorek BD, Plaxco KW, Heeger AJ. A reagentless signal-on architecture for electronic, aptamer-based sensors via target-induced strand displacement. J Am Chem Soc [Internet]. 2005 Dec 28;127(51):17990–1. Available from: http://www.ncbi.nlm.nih.gov/pubmed/16366535

100. Chen Q, Tang W, Wang D, Wu X, Li N, Liu F. Amplified QCM-D biosensor for protein based on aptamer-functionalized gold nanoparticles. Biosens Bioelectron [Internet]. 2010 Oct 15 [cited 2013 Oct 23];26(2):575–9. Available from: http://www.ncbi.nlm.nih.gov/pubmed/20692147

101. White RJ, Phares N, Lubin A a, Xiao Y, Plaxco KW. Optimization of electrochemical aptamer-based sensors via optimization of probe packing density and surface chemistry. Langmuir [Internet]. 2008 Sep 16;24(18):10513–8. Available from: http://www.pubmedcentral.nih.gov/articlerender.fcgi?artid=2674396&tool=pmcentrez&rendertype=abstract

102. Fan C, Plaxco KW, Heeger AJ. Electrochemical interrogation of conformational changes as a reagentless method for the sequence-specific detection of DNA. Proc Natl Acad Sci U S A [Internet]. 2003 Aug 5;100(16):9134–7. Available from: http://www.pubmedcentral.nih.gov/articlerender.fcgi?artid=170884&tool=pmcentrez&rendertype=abstract

103. Ferapontova EE, Olsen EM, Gothelf K V. An RNA Aptamer-Based Electrochemical Biosensor for Detection of Theophylline in Serum. J Am Chem Soc [Internet]. 2008;130(13):4256–8. Available from: http://dx.doi.org/10.1021/ja711326b

104. Radi A-E, Acero Sánchez JL, Baldrich E, O'Sullivan CK. Reagentless, reusable, ultrasensitive electrochemical molecular beacon aptasensor. J Am Chem Soc [Internet]. 2006 Jan 11;128(1):117–24. Available from: http://www.ncbi.nlm.nih.gov/pubmed/16390138

105. Ferapontova EE, Gothelf K V. Effect of serum on an RNA aptamer-based electrochemical sensor for theophylline. Langmuir [Internet]. 2009 Apr 21 [cited 2011 Aug 25];25(8):4279–83. Available from: http://www.ncbi.nlm.nih.gov/pubmed/19301828

106. Lai RY, Plaxco KW, Heeger AJ. Aptamer-Based Electrochemical Detection of Picomolar Platelet-Derived Growth Factor Directly in Blood Serum. Anal Chem. 2007;79(1):229–33.

107. Baker BR, Lai RY, Wood MS, Doctor EH, Heeger AJ, Plaxco KW. An electronic, aptamer-based small-molecule sensor for the rapid, label-free detection of cocaine in adulterated samples and biological fluids. J Am Chem Soc [Internet]. 2006 Mar 15;128(10):3138–9. Available from: http://www.ncbi.nlm.nih.gov/pubmed/16522082

108. Vicens MC, Sen A, Vanderlaan A, Drake TJ, Tan W. Investigation of Molecular Beacon Aptamer-Based Bioassay for Platelet-Derived Growth Factor Detection. ChemBioChem [Internet]. 2005;6(5):900–7. Available from: http://dx.doi.org/10.1002/cbic.200400308

109. Ferapontova EE, Gothelf KV. Optimization of the Electrochemical RNA-Aptamer Based Biosensor for Theophylline by Using a Methylene Blue Redox Label. Electroanalysis [Internet]. 2009 Jun [cited 2011 Aug 20];21(11):1261–6. Available from: http://doi.wiley.com/10.1002/elan.200804558

110. Stojanovic MN, de Prada P, Landry DW. Aptamer-based folding fluorescent sensor for cocaine. J Am Chem Soc [Internet]. 2001 May 30;123(21):4928–31. Available from: http://www.ncbi.nlm.nih.gov/pubmed/11457319

111. Rodriguez MC, Kawde A-N, Wang J. Aptamer biosensor for label-free impedance spectroscopy detection of proteins based on recognition-induced switching of the surface charge. Chem Commun (Camb) [Internet]. 2005 Sep 14 [cited 2011 Aug 22];(34):4267–9. Available from: http://www.ncbi.nlm.nih.gov/pubmed/16113717

112. Lee J a, Hwang S, Kwak J, Park S Il, Lee SS, Lee K-C. An electrochemical impedance biosensor with aptamer-modified pyrolyzed carbon electrode for label-free protein detection. Sensors Actuators B Chem [Internet]. 2008 Jan [cited 2011 Sep 15];129(1):372–9. Available from: http://linkinghub.elsevier.com/retrieve/pii/S0925400507006545

113. Li L, Zhao H, Chen Z, Mu X, Guo L. Aptamer biosensor for label-free square-wave voltammetry detection of angiogenin. Biosens Bioelectron [Internet]. 2011 Dec 15 [cited 2011 Dec 7];30(1):261–6. Available from: http://www.ncbi.nlm.nih.gov/pubmed/22018671

114. Hayat A, Haider W, Rolland M, Marty J-L. Electrochemical grafting of long spacer arms of hexamethyldiamine on a screen printed carbon electrode surface: application in target induced ochratoxin A electrochemical aptasensor. Analyst [Internet]. 2013 May 21 [cited 2013 Oct 25];138(10):2951–7. Available from: http://www.ncbi.nlm.nih.gov/pubmed/23535890

115. Wetter LR, Deutsch HF. Immunological Studies On Egg White Proteins : IV . Immunochemical And Physical Studies Of Lysozyme. J Biol Chem. 1951;192:237–42.

116. Cheng AKH, Ge B, Yu H-Z. Aptamer-based biosensors for label-free voltammetric detection of lysozyme. Anal Chem [Internet]. 2007 Jul 15;79(14):5158–64. Available from: http://www.ncbi.nlm.nih.gov/pubmed/17566977

117. Cox JC, Ellington a D. Automated selection of anti-protein aptamers. Bioorg Med Chem [Internet]. 2001 Oct;9(10):2525–31. Available from: http://www.ncbi.nlm.nih.gov/pubmed/11557339

118. Li X, Shen L, Zhang D, Qi H, Gao Q, Ma F, et al. Electrochemical impedance spectroscopy for study of aptamer-thrombin interfacial interactions. Biosens Bioelectron [Internet]. 2008 Jun 15 [cited 2013 Oct 14];23(11):1624–30. Available from: http://www.ncbi.nlm.nih.gov/pubmed/18339536

119. Tasset DM, Kubik MF, Steiner W. Oligonucleotide inhibitors of human thrombin that bind distinct epitopes. J Mol Biol [Internet]. 1997 Oct 10;272(5):688–98. Available from: http://www.ncbi.nlm.nih.gov/pubmed/9368651

120. Oliver NS, Toumazou C, Cass AEG, Johnston DG. Glucose sensors : a review of current and emerging technology. Diabet Med. 2009;26:197–210.

121. Deng K, Xiang Y, Zhang L, Chen Q, Fu W. An aptamer-based biosensing platform for highly sensitive detection of platelet-derived growth factor via enzyme-mediated direct electrochemistry. Anal Chim Acta [Internet]. 2013 Jan 8 [cited 2013 Oct 22];759:61–5. Available from: http://www.ncbi.nlm.nih.gov/pubmed/23260677

122. Ikebukuro K, Kiyohara C, Sode K. Novel electrochemical sensor system for protein using the aptamers in sandwich manner. Biosens Bioelectron [Internet]. 2005 Apr 15 [cited 2011 Jul 14];20(10):2168–72. Available from: http://www.ncbi.nlm.nih.gov/pubmed/15741093

123. Lu Y, Li X, Zhang L, Yu P, Su L, Mao L. Aptamer-based electrochemical sensors with aptamer-complementary DNA oligonucleotides as probe. Anal Chem [Internet]. 2008 Mar 15;80(6):1883–90. Available from: http://www.ncbi.nlm.nih.gov/pubmed/18290636

124. Li B, Du Y, Wei H, Dong S. Reusable, label-free electrochemical aptasensor for sensitive detection of small molecules. Chem Commun (Camb) [Internet]. 2007 Sep 28 [cited 2011 Aug 22];(36):3780–2. Available from: http://www.ncbi.nlm.nih.gov/pubmed/17851626

125. Chakraborty B, Jiang Z, Li Y, Yu H-Z. Rational design and performance testing of aptamer-based electrochemical biosensors for adenosine. J Electroanal Chem [Internet]. 2009 Oct 15 [cited 2011 Sep 28];635(2):75–82. Available from: http://linkinghub.elsevier.com/retrieve/pii/S0022072809002903

126. Mabbott GA. An introduction to cyclic voltammetry. J Chem Educ [Internet]. 1983;60:697. Available from: http://dx.doi.org/10.1021/ed060p697

127. Kissinger PT, Heineman WR. Cyclic voltammetry. J Chem Educ [Internet]. 1983;60:702. Available from: http://pubs.acs.org/doi/abs/10.1021/ed060p702

128. Bard AJ, Faulkner LR. Electrochemcial Methods: Fundamentals and Applications. Vol. 677,

Analytica chimica acta. 2001.

129. Osteryoung JG, Osteryoung RA. Square Wave Voltammetry. Anal Chem [Internet]. 1985;57:101A–110A. Available from: http://dx.doi.org/10.1021/ac00279a789

130. Macdonald DD. Characterizing electrochemical systems in the frequency domain. Electrochim Acta. 1998 Jan;43(1–2):87–107.

131. Engvall E, Perlmann P. Enzyme-linked immunosorbent assay (ELISA) quantitative assay of immunoglobulin G. Immunochemistry [Internet]. 1971 Sep [cited 2015 Jan 30];8(9):871–4. Available from: http://www.sciencedirect.com/science/article/pii/001927917190454X

132. W.Drolet D, Moon-McDermott L, Romig TS. An enzyme-linked oligonucleotide assay. Nat Biotechnol. 1996;14:1021–5.

133. Kuo T-C, Lee P-C, Tsai C-W, Chen W-Y. Salt bridge exchange binding mechanism between streptavidin and its DNA aptamer--thermodynamics and spectroscopic evidences. J Mol Recognit [Internet]. 2013 Mar [cited 2013 Oct 25];26(3):149–59. Available from: http://www.ncbi.nlm.nih.gov/pubmed/23345105

134. Kanakaraj I, Chen W-H, Poongavanam M, Dhamane S, Stagg LJ, Ladbury JE, et al. Biophysical characterization of VEGF-aHt DNA aptamer interactions. Int J Biol Macromol [Internet]. 2013 Jun [cited 2013 Oct 25];57:69–75. Available from: http://www.ncbi.nlm.nih.gov/pubmed/23470436

135. Potty ASR, Kourentzi K, Fang H, Schuck P, Willson RC. Biophysical characterization of DNA and RNA aptamer interactions with hen egg lysozyme. Int J Biol Macromol [Internet]. 2011 Apr 1 [cited 2013 Oct 25];48(3):392–7. Available from: http://www.ncbi.nlm.nih.gov/pubmed/21167858

136. Neves M a D, Reinstein O, Saad M, Johnson PE. Defining the secondary structural requirements of a cocaine-binding aptamer by a thermodynamic and mutation study. Biophys Chem [Internet]. 2010 Dec [cited 2013 Oct 25];153(1):9–16. Available from: http://www.ncbi.nlm.nih.gov/pubmed/21035241

137. Potty ASR, Kourentzi K, Fang H, Jackson GW, Zhang X, Legge GB, et al. Biophysical characterization of DNA aptamer interactions with vascular endothelial growth factor. Biopolymers [Internet]. 2009 Feb [cited 2013 Oct 25];91(2):145–56. Available from: http://www.ncbi.nlm.nih.gov/pubmed/19025993

138. Lin P-H, Yen S-L, Lin M-S, Chang Y, Louis SR, Higuchi A, et al. Microcalorimetrics studies of the

thermodynamics and binding mechanism between L-tyrosinamide and aptamer. J Phys Chem B [Internet]. 2008 May 29;112(21):6665–73. Available from: http://www.ncbi.nlm.nih.gov/pubmed/18457441

139. Hamaguchi N, Ellington a, Stanton M. Aptamer beacons for the direct detection of proteins. Anal Biochem [Internet]. 2001 Jul 15 [cited 2013 Oct 24];294(2):126–31. Available from: http://www.ncbi.nlm.nih.gov/pubmed/11444807

140. He X, Li Z, Jia X, Wang K, Yin J. A highly selective sandwich-type FRET assay for ATP detection based on silica coated photon upconverting nanoparticles and split aptamer. Talanta [Internet]. 2013 Jul 15 [cited 2013 Oct 25];111:105–10. Available from: http://www.ncbi.nlm.nih.gov/pubmed/23622532

141. Zhou Z-M, Yu Y, Zhao Y-D. A new strategy for the detection of adenosine triphosphate by aptamer/quantum dot biosensor based on chemiluminescence resonance energy transfer. Analyst [Internet]. 2012 Sep 21 [cited 2013 Oct 25];137(18):4262–6. Available from: http://www.ncbi.nlm.nih.gov/pubmed/22832507

142. Li W, Yang X, Wang K, Tan W, Li H, Ma C. FRET-based aptamer probe for rapid angiogenin detection. Talanta [Internet]. 2008 May 15 [cited 2011 Jul 29];75(3):770–4. Available from: http://www.ncbi.nlm.nih.gov/pubmed/18585145

143. Lin F, Yin B, Li C, Deng J, Fan X, Yi Y, et al. Fluorescence resonance energy transfer aptasensor for platelet-derived growth factor detection based on upconversion nanoparticles in 30% blood serum. Anal Methods [Internet]. 2013 [cited 2013 Oct 25];5(3):699. Available from: http://xlink.rsc.org/?DOI=c2ay25519g

144. Li W, Wang K, Tan W, Ma C, Yang X. Aptamer-based analysis of angiogenin by fluorescence anisotropy. Analyst [Internet]. 2007 Feb [cited 2011 Jul 18];132(2):107–13. Available from: http://www.ncbi.nlm.nih.gov/pubmed/17260069

145. Zou M, Chen Y, Xu X, Huang H, Liu F, Li N. The homogeneous fluorescence anisotropic sensing of salivary lysozyme using the 6-carboxyfluorescein-labeled DNA aptamer. Biosens Bioelectron [Internet]. 2012 Feb 15 [cited 2013 Oct 23];32(1):148–54. Available from: http://www.ncbi.nlm.nih.gov/pubmed/22217604

146. Kang K, Sachan A, Nilsen-Hamilton M, Shrotriya P. Aptamer functionalized microcantilever sensors for cocaine detection. Langmuir [Internet]. 2011 Dec 6;27(23):14696–702. Available from: http://www.ncbi.nlm.nih.gov/pubmed/21875108

147. Perrier S, Ravelet C, Guieu V, Fize J, Roy B, Perigaud C, et al. Rationally designed aptamer-based fluorescence polarization sensor dedicated to the small target analysis. Biosens Bioelectron [Internet]. 2010 Mar 15 [cited 2013 Oct 25];25(7):1652–7. Available from: http://www.ncbi.nlm.nih.gov/pubmed/20034782

148. Fang X, Cao Z, Beck T, Tan W. Molecular aptamer for real-time oncoprotein platelet-derived growth factor monitoring by fluorescence anisotropy. Anal Chem [Internet]. 2001 Dec 1;73(23):5752–7. Available from: http://www.ncbi.nlm.nih.gov/pubmed/11774917

149. McCauley TG, Hamaguchi N, Stanton M. Aptamer-based biosensor arrays for detection and quantification of biological macromolecules. Anal Biochem [Internet]. 2003;319(2):244–50. Available from: http://www.sciencedirect.com/science/article/B6W9V-48WJNJ3-5/2/c1b294a9270a8a383998299aef511304

150. Deng T, Li J, Zhang L-L, Jiang J-H, Chen J-N, Shen G-L, et al. A sensitive fluorescence anisotropy method for the direct detection of cancer cells in whole blood based on aptamer-conjugated near-infrared fluorescent nanoparticles. Biosens Bioelectron [Internet]. 2010 Mar 15 [cited 2013 Oct 25];25(7):1587–91. Available from: http://www.ncbi.nlm.nih.gov/pubmed/20022484

151. Nagai Y, Carbajal JD, White JH, Sladek R, Grutter P, Lennox RB. An electrochemically controlled microcantilever biosensor. Langmuir [Internet]. 2013 Aug 13;29(32):9951–7. Available from: http://www.ncbi.nlm.nih.gov/pubmed/23841706

152. Zhai L, Wang T, Kang K, Zhao Y, Shrotriya P, Nilsen-hamilton M. An RNA Aptamer-Based Microcantilever Sensor To Detect the Inflammatory Marker, Mouse Lipocalin-2. Anal Chem. 2012;84:8763–70.

153. Hou H, Bai X, Xing C, Gu N, Zhang B, Tang J. Aptamer-based cantilever array sensors for oxytetracycline detection. Anal Chem [Internet]. 2013 Feb 19;85(4):2010–4. Available from: http://www.ncbi.nlm.nih.gov/pubmed/23350586

154. Hwang KS, Lee S-M, Eom K, Lee JH, Lee Y-S, Park JH, et al. Nanomechanical microcantilever operated in vibration modes with use of RNA aptamer as receptor molecules for label-free detection of HCV helicase. Biosens Bioelectron [Internet]. 2007 Nov 30 [cited 2013 Oct 23];23(4):459–65. Available from: http://www.ncbi.nlm.nih.gov/pubmed/17616386

155. Savran C a, Knudsen SM, Ellington AD, Manalis SR. Micromechanical detection of proteins using aptamer-based receptor molecules. Anal Chem [Internet]. 2004 Jun 1;76(11):3194–8.

Available from: http://www.ncbi.nlm.nih.gov/pubmed/15167801

156. Liu J, Wang C, Jiang Y, Hu Y, Li J, Yang S, et al. Graphene Signal Amplification for Sensitive and Real-Time Fluorescence Anisotropy Detection of Small Molecules. Anal Chem. 2013;85:1424–30.

157. Zhang J, Tian J, He Y, Chen S, Jiang Y, Zhao Y, et al. Protein-binding aptamer assisted signal amplification for the detection of influenza A (H1N1) DNA sequences based on quantum dot fluorescence polarization analysis. Analyst [Internet]. 2013 Sep 7 [cited 2013 Oct 26];138(17):4722–7. Available from: http://www.ncbi.nlm.nih.gov/pubmed/23826611

158. Zhu Z, Ravelet C, Perrier S, Guieu V, Fiore E, Peyrin E. Single-stranded DNA binding protein-assisted fluorescence polarization aptamer assay for detection of small molecules. Anal Chem [Internet]. 2012 Aug 21;84(16):7203–11. Available from: http://www.ncbi.nlm.nih.gov/pubmed/22793528

159. Arlett JL, Myers EB, Roukes ML. Comparative advantages of mechanical biosensors. Nat Nanotechnol [Internet]. 2011 Apr [cited 2011 Jul 6];6(4):203–15. Available from: http://www.ncbi.nlm.nih.gov/pubmed/21441911

160. Liss M, Petersen B, Wolf H, Prohaska E. An aptamer-based quartz crystal protein biosensor. Anal Chem [Internet]. 2002 Sep 1;74(17):4488–95. Available from: http://www.ncbi.nlm.nih.gov/pubmed/12236360

161. Buttry D a., Ward MD. Measurement of interfacial processes at electrode surfaces with the electrochemical quartz crystal microbalance. Chem Rev [Internet]. 1992 Sep;92(6):1355–79. Available from: http://pubs.acs.org/doi/abs/10.1021/cr00014a006

162. Dong Z-M, Zhao G-C. A theophylline quartz crystal microbalance biosensor based on recognition of RNA aptamer and amplification of signal. Analyst [Internet]. 2013 Apr 21 [cited 2013 Oct 23];138(8):2456–62. Available from: http://www.ncbi.nlm.nih.gov/pubmed/23467569

163. Pan Y, Guo M, Nie Z, Huang Y, Pan C, Zeng K, et al. Selective collection and detection of leukemia cells on a magnet-quartz crystal microbalance system using aptamer-conjugated magnetic beads. Biosens Bioelectron [Internet]. 2010 Mar 15 [cited 2013 Oct 23];25(7):1609–14. Available from: http://www.ncbi.nlm.nih.gov/pubmed/20031387

164. Nutiu R, Li Y. Structure-switching signaling aptamers. J Am Chem Soc [Internet]. 2003 Apr 23;125(16):4771–8. Available from: http://www.ncbi.nlm.nih.gov/pubmed/22724553

165. Lee M, Walt DR. A Fiber-Optic Microarray Biosensor Using Aptamers as Receptors. Anal Biochem [Internet]. 2000;282(1):142–6. Available from: http://www.sciencedirect.com/science/article/B6W9V-45FK56V-BF/2/77d0a808a314d95b48eafd063ff27dec

166. Kong L, Xu J, Xu Y, Xiang Y, Yuan R, Chai Y. A universal and label-free aptasensor for fluorescent detection of ATP and thrombin based on SYBR Green I dye. Biosens Bioelectron [Internet]. 2013 Apr 15 [cited 2013 Oct 24];42:193–7. Available from: http://www.ncbi.nlm.nih.gov/pubmed/23202351

167. Zeng X, Zhang X, Yang W, Jia H, Li Y. Fluorescence detection of adenosine triphosphate through an aptamer-molecular beacon multiple probe. Anal Biochem [Internet]. 2012 May 1 [cited 2013 Oct 25];424(1):8–11. Available from: http://www.ncbi.nlm.nih.gov/pubmed/22369893

168. Sievers F, Wilm A, Dineen D, Gibson TJ, Karplus K, Li W, et al. Fast, scalable generation of high-quality protein multiple sequence alignments using Clustal Omega. Mol Syst Biol [Internet]. 2011;7(1):539–539. Available from: http://msb.embopress.org/cgi/doi/10.1038/msb.2011.75

169. Katoh K, Misawa K, Kuma K, Miyata T. MAFFT : a novel method for rapid multiple sequence alignment based on fast Fourier transform. 2002;30(14):3059–66.

170. Andrews S. FastQC: A Quality Control Tool For High Throughput Sequence Data [Internet]. 2010. Available from: http://www.bioinformatics.babraham.ac.uk/projects/fastqc/

171. Waterhouse AM, Procter JB, Martin DMA, Clamp M, Barton GJ. Jalview Version 2--a multiple sequence alignment editor and analysis workbench. Bioinformatics [Internet]. 2009;25(9):1189–91. Available from: http://bioinformatics.oxfordjournals.org/cgi/doi/10.1093/bioinformatics/btp033

172. FASTX - Toolkit [Internet]. Available from: http://hannonlab.cshl.edu/fastx_toolkit/

173. Alam KK, Chang JL, Burke DH. FASTAptamer: A Bioinformatic Toolkit for High-throughput Sequence Analysis of Combinatorial Selections. Mol Ther Acids [Internet]. 2015;4(August 2014):e230. Available from: http://www.pubmedcentral.nih.gov/articlerender.fcgi?artid=4354339&tool=pmcentrez&rendertype=abstract

174. Martin M. Cutadapt removes adapter sequences from high-throughput sequencing reads.

EMBnet.journal. 2011;17(1):10–2.

175. Han D, Kim Y-R, Oh J-W, Kim TH, Mahajan RK, Kim JS, et al. A regenerative electrochemical sensor based on oligonucleotide for the selective determination of mercury(ii). Analyst [Internet]. 2009;134(9):1857. Available from: http://xlink.rsc.org/?DOI=b908457f

176. Ma W, Ying Y-L, Qin L-X, Gu Z, Zhou H, Li D-W, et al. Investigating electron-transfer processes using a biomimetic hybrid bilayer membrane system. Nat Protoc [Internet]. 2013;8(3):439–50. Available from: http://www.nature.com/doifinder/10.1038/nprot.2013.007

177. Hermanson GT. Zero-Length Crosslinkers. In: Bioconjugate Techniques. 2013. p. 259–66.

178. Hu J, Yu Y, Brooks JC, Godwin L a, Somasundaram S, Torabinejad F, et al. A reusable electrochemical proximity assay for highly selective, real-time protein quantitation in biological matrices. J Am Chem Soc [Internet]. 2014 Jun 11;136(23):8467–74. Available from: http://www.ncbi.nlm.nih.gov/pubmed/24827871

179. Tolle F, Wilke J, Wengel J, Mayer G. By-Product Formation in Repetitive PCR Amplification of DNA Libraries during SELEX. PLoS One [Internet]. 2014;9(12):e114693. Available from: http://dx.plos.org/10.1371/journal.pone.0114693

180. Fuller CW, Middendorf LR, Benner S a, Church GM, Harris T, Huang X, et al. The challenges of sequencing by synthesis. Nat Biotechnol [Internet]. 2009;27(11):1013–23. Available from: http://www.ncbi.nlm.nih.gov/pubmed/19898456

181. Illumina. Quality Scores for Next-Generation Sequencing. Http://ResIlluminaCom/Documents/Products/Technotes/Technote_Q-ScoresPdf. 2011;1–2.

182. Illumina. Understanding Illumina Quality Scores. Tech Note Informatics. :1–2.

183. Ledergerber C, Dessimoz C. Base-calling for next-generation sequencing platforms. Brief Bioinform. 2011;12(5):489–97.

184. Katoh K, Standley DM. MAFFT multiple sequence alignment software version 7: improvements in performance and usability. Mol Biol Evol [Internet]. 2013 Apr [cited 2014 Jul 13];30(4):772–80. Available from: http://www.pubmedcentral.nih.gov/articlerender.fcgi?artid=3603318&tool=pmcentrez&rendertype=abstract

185. Katoh K, Toh H. PartTree: an algorithm to build an approximate tree from a large number of unaligned sequences. Bioinformatics [Internet]. 2007 Mar 1 [cited 2014 Oct 29];23(3):372–4.

Available from: http://www.ncbi.nlm.nih.gov/pubmed/17118958

186. Katoh K, Asimenos G, Toh H. Bioinformatics for DNA Sequence Analysis. Posada D, editor. 2009 [cited 2014 Jul 12];537. Available from: http://link.springer.com/10.1007/978-1-59745-251-9

187. Vogt R V., Phillips DL, Omar Henderson L, Whitfield W, Spierto FW. Quantitative differences among various proteins as blocking agents for ELISA microtiter plates. J Immunol Methods [Internet]. 1987 Jun;101(1):43–50. Available from: http://linkinghub.elsevier.com/retrieve/pii/0022175987902146

188. Rubin RL, Carr RI. Anti-DNA Activity of IgG F (ab')2 from Normal Human Serum. J Immunol. 1979;122:1604–7.